The role of MSK1 in homeostatic plasticity from *in vitro* to *in vivo*

Sandrine Wauters

A thesis submitted for the degree of Doctor of Philosophy

University of Warwick

School of Life Sciences

September 2013

Table of contents

List of figures

List of tables

Acknowledgements

It is with my great pleasure that I acknowledge and thank those people who have helped me throughout these past four years;

Firstly, I would like to thank both Professor Bruno Frenguelli and Dr. Sonia Corrêa, my two supervisors who have helped me endlessly with the support and guidance I needed. I have learnt many neuroscience techniques which I know will shape my future career in science. I am also thankful for the grant Dr. Sonia Corrêa received in collaboration with São Paulo University which gave me an opportunity to travel to Brazil and experience a different culture in and outside the lab. I learnt many skills all under the guidance and hospitality of Professor Luis da Silva who I also thank deeply.

Secondly there are two colleagues who helped me enormously throughout my research who are Dr. Ján Lopatář and Holly Baum. Ján trained me in the theoretical and practical field of electrophysiology. He never gave up on me and supported me right until the end, as a colleague and as a friend. Holly Baum was always there for me, especially during the difficult times. She is an excellent scientist who is always willing to put everyone else before herself. She was my rock throughout my PhD and I wish her every success in the future.

Thirdly there is my family, my parents who have always loved, supported and protected me. They have always encouraged me to work hard and follow my dreams. My three younger brothers don't even realise how much they help me by just being there to give me a hug when I need. And finally my partner, James, who has stuck by me through everything and has always, supported and cared for me throughout my studies. I am very lucky to have such a wonderful family.

There are current and past members of both Frenguelli's and Corrêa's lab which have played an important part in my progress in science as well as building strong friendships. My friends from home were also always incredibly supportive.

Work from Stephanie von Kutsleben whose data is presented in Figure 5.11, Dr. Jürgen Muller and Holly Baum for the help with the BiFC experiments shown in Figure 6.8 and 6.9 as well as Professor Luis da Silva from São Paulo University and his lab members. I want to thank my committee members, Dr. Mark Wall, Professor Colin Robinson and Dr. Corinne Smith for their advice and guidance. There was also my GSK supervisor, Alastair D Reith who gave a helping hand and support when needed.

Last but not least, this work would have not been possible without the financial support of my two funding bodies, the BBSRC/GSK case studentship as well as BBSRC/FAPESP for my final research year which allowed me to do an exchange at São Paulo University for 3 weeks.

Declaration

I hereby declare that all work in this thesis was carried out and written by myself, under the supervision of Professor Bruno Frenguelli and Dr. Sonia Corrêa, with the exception of;

1. The work carried out by Stephanie von Kutsleben, summarised in Figure 5.11, which contributed to her final year undergraduate dissertation.
2. Figures 3.8 and 3.9 were carried out by authors mentioned in the paper listed below (Correa et al., 2012) (also see Appendix 1). Figure 3.8 B is published in this paper but was carried out by myself.
3. The design and manufacturing of the BiFC constructs used in Figures 6.8 and 6.9 was carried out by Dr. Jürgen Muller and his lab member, Holly Baum.
4. Figure 6.8 was carried out in São Paulo University by a collaborator Professor Luis da Silva and his group including Yunan Costa Januario and Dr. Luciana Almeida.
5. Table 6.1 illustrates some of the protein hits from Mass spectrometry analysis which was carried out by Bristol University Mass Spectrometry services.
6. The work carried out by Kirsty Martin from the University of Dundee (supervised by our collaborator Dr. Simon Arthur) carried out the experiments in Figure 5.3. She did the Q-PCR and analysis of the data from the samples used in our lab which I extracted.

Correa SAL, Hunter CJ, Palygin O, Wauters SC, Martin KJ, McKenzie C, McKelvey K, Morris RGM, Pankratov Y, Arthur JSC, Frenguelli BG (2012) MSK1 Regulates Homeostatic and Experience-Dependent Synaptic Plasticity. Journal of Neuroscience 32:13039-13051.

None of the work in this thesis has been submitted for any previous degree. All sources of information are acknowledged in the form of references.

Sandrine Wauters

September 2013

Summary

Synaptic plasticity is the ability of neuronal synapses to strength and weaken from a set threshold determined by previous 'experience' thus representing a cellular basis for learning and memory. There are different forms of synaptic plasticity including Hebbian, homeostatic synaptic scaling as well as experience-dependent plasticity such as when animals are exposed to environmental enrichment (EE). Small protrusions which receive excitatory inputs known as dendritic spines are able to change morphology which has also been linked to trafficking of glutamate AMPA receptors (AMPAR) in response to neuronal activity.

Brain-derived neurotrophic factor (BDNF) is a neutrophin involved in regulating both transcription and translation during synaptic plasticity. A plasticity-related gene, activity-regulated cytoskeleton-associated protein (Arc) controls the endocytosis of AMPAR nonetheless downstream signalling pathways are still largely unknown. The nuclear kinase, mitogen-and stress-activated protein kinase 1 (MSK1) regulates gene transcription in a BDNF-dependent manner. Thus we wanted to investigate whether MSK1 plays a role in regulating Arc expression in response to BDNF-induced synaptic plasticity.

In order to test this hypothesis we used MSK1 kinase dead (MSK1 KD) transgenic mouse which had an inactivating knock-in mutation in the MSK1 N-terminus kinase domain. Dissociated hippocampal neurones were cultured from MSK1 KD and wild-type (WT) mice and stimulated with BDNF to monitor Arc protein expression. MSK1 KD neurones showed a delayed response in BDNF-induced Arc upregulation. Interestingly in the presence of tetrodotoxin (TTX) which reduces BDNF levels, MSK1 KD mice failed to show homeostatic scaling of synaptic transmission, Arc expression and spine morphological changes *in vitro.* After measuring the same parameters, EE-induced plasticity was unaffected in MSK1 KD adult mice but this may be a reflection of the experimental protocol used highlighted in the literature. The link between Arc and the cytoskeleton is unfamiliar and thus our finding of a novel interacting partner associated with clathrin-mediated endocytosis will carve out innovative mechanisms involved in synaptic plasticity.

MSK1 acts an important homeostat during TTX-induced up-scaling of Arc protein and may influence structural effects on spine morphology. However MSK1 may more of a local homeostat rather than generalised as its role in BDNF or experience-dependent stimulation was not as clear. Arc is an important synaptic mediator and thus linking it to the cytoskeleton could bridge the gap in understanding the mechanisms underlying learning and memory.

List of Abbreviations

Abbreviation	Full form
µA	Microampere
µM	Micromolar
µm	Micrometer
aa	Amino acid
aCSF	Artificial cerebrospinal fluid
ADF	Actin-depolymerising factor
AGC	cAMP-dependent protein kinase/protein kinase G/protein kinase C
AKT	Serine threonine kinase or protein kinase B
AMPAR	α-amino-3-hydroxy-5-methyl-4-iso-xazolepropionic acid receptor
ANOVA	Analysis of variance
AP	Adaptor protein
AP180	Adpator protein-180
AP-2	Adaptor protein 2
APP	Amyloid precursor protein
APS	Ammonium persulphate
Arc	Activity-regulated cytoskeleton-associated protein/activity-regulated gene 3.1 (Arg3.1)
Arp2/3	Actin related protein 2/3 complex
AS	Antisense
Aβ	β-amyloid
BAR	Bin-Amphiphysin-Rvs
BCA	Bicinchoninic acid Protein assay
BDNF	Brain-derived neurotrophic factor
Bic	Bicuculline
Brd-U	Bromodeoxyuridine
BSA	Bovine serum albumin
CA	Cornu ammonis
Ca^{2+}	Calcium
$CaCl_2$	Calcium chloride
CALM	Clathrin assembly lymphoid myeloid leukaemia
CaMK	Calcium/calmodulin-dependent protein kinase

CaMKII	$Ca^{2+/}$Calmodulin-dependent protein kinase II
CaMKK	Calcium/calmodulin-dependent protein kinase kinase
CaN	Calcineurin
CBP	CREB binding protein
CCV	Clathrin-coated vesicles
CHC	Clathrin-heavy chain
ChIP	Chromatin immunoprecipitation
CLC	Clathrin-light chain
CLS	Coffin-Lowry syndrome
CNS	Central nervous system
CO_2	Carbon dioxide
CRE	cAMP response element
CREB	Cyclic AMP response element-binding protein
CT	C-terminus
CT KD	C-terminus kinase domain
DFG	Aspartate -Phenylalanine -Glycine
DG	Dentate gyrus
dH_2O	Distilled water
DHPG	3,5-Dihydroxyphenylglycine
DIV	Days *in vitro*
DMEM	Dulbecco's modified eagle medium
DMSO	Dimethyl sulfoxide
DNA	Deoxyribonucleic acid
DNase	Deoxyribonuclease
DTT	Dithiothreitol
Dyn	Dynamin 2
E	Endosome
EC	Entorhinal cortex
ECL	Enhanced Chemiluminescence
EDTA	Ethylenediaminetetraacetic acid
EE	Environmental enrichment
EEA1	Early endosome antigen 1
eGFP	Enhanced green fluorescent protein
Elk1	E-26-like protein 1

E-LTP	Early LTP
End	Endophilin 3
ER	Endoplasmic reticulum
ERK	Extracellular signal-regulated kinase
ES	Embryonic stem
EZ	Endocytic zones
F	Fimbria
F-actin	Filamentous actin
fEPSP	Field excitatory postsynaptic potential
FRAP	Fluorescence recovery after photobleach
FV	Fibre volley
g	Gravitational force
GABA	γ-aminobutyric acid
GAP	GTPase ativating proteins
GAPDH	Glyceraldehyde 3-phosphate dehydrogenase
GEF	Guanine nucleotide exchange factor
GFP	Green fluorescent protein
GluA2L	GluA2 with long CT domain
GRIP1	Glutamate receptor interacting protein 1
GTPase	Hydrolyse guanosine triphosphate
H	Hours
H3	Histone H3
H3	Histone H3
HAT	Histone acetyltransferase
HBSS	Hank's buffered salt solution
HCL	Hydrochloric acid
HEPES	4-(2-Hydroxyethyl) piperazine-1-ethanesulfonic acid
HFS	High-frequency stimulation
HS	Horse serum
Hz	Hertz
I/O	Input/Output
ICC	Immunocytochemistry
IEG	Immediate-early gene
iGluR	Ionotropic receptor

IKKα	Ikappa B kinase α
IP	Immunoprecipitated
IPI	Interpulse interval
IVC	Individually ventilated cages
KCL	Potassium chloride
KD	Kinase dead
kDa	Kilodaltons
KO	Knock out
KS	Kolmogorov-Smirnov
L	Leucine
LB	Lysogeny Broth
LFS	Low-frequency stimulation
L-LTP	Late LTP
LPA	Lysophosphatidic acid
LTD	Long-term depression
LTP	Long-term potentiation
M	Molar
MAPK	Mitogen-activated protein kinase
MEF	Mouse embryo fibroblast
MEF2	Myocyte enhancer factor 2
MEK	Mitogen-activated protein kinase kinase
mEPSC	Miniature excitatory postsynaptic currents
Mg^{2+}	Magnesium
$MgCl_2$	Magnesium chloride
mGlus	Metabotropic glutamate receptors
$MgSO_4$	Magnesium sulphate
mins	Minutes
mM	Millimolar
ms	Milliseconds
MSK	Mitogen-and stress-activated protein kinase
mV	Millivolts
N- Cadherin	Neuronal- Cadherin
Na_3VO4	Sodium orthovanadate
$Na_4P_2O_7$	Sodium pyrophosphate tetrabasic

NaCl	Sodium chloride
NaF	Sodium azide
NaH_2PO_4	Sodium dihydrogen phosphate
$NaHCO_3$	Sodium bicarbonate
NaN_3	Sodium azide
NaOH	Sodium hydroxide
NFT	Neurofibrillary tangles
NGF	Nerve growth factor
NIH	National Institutes of Health
NMDAR	N-methyl-D-aspartic acid receptor
NSF	N-ethylmaleimide-sensitive factor
NT	N-terminus
NT	Neurotransmitter
NT KD	N-terminus kinase domain
NT-3	Neurotrophin-3
NT-4	Neurotrophin-4
O_2	Oxygen
ORF	Open reading frame
P	Postnatal day
P	Phosphorylated
PAGE	Polyacrylamide gel electrophoresis
PAK	A-p21-activated kinase
PBS	Phosphate buffer solution
PC12	Pheochromocytoma 12
PDZ	Postsynaptic density protein-95, disc-large tumour suppressor protein, zonula occludens-1
PFA	Paraformaldehyde
pHluorin	pH-sensitive GFP variant
Phospho	Phosphorylated
PI3K	Phosphoinositide 3-kinase
PICK1	Protein interacting with C-kinase 1
PIP_2	Phosphatidylinositol-4,5-bisphosphate
PIP_3	Phosphatidylinositol-4,5-triphosphate
PIX	PAK interacting exchange factor

PKA	Protein kinase A
PKC	Protein kinase C
PLCγ	Phospholipase Cγ
PP	Paired pulse
PSD	Postsynaptic density
Q	Glutamine
Q/R	Glutamine/Arginine
Q-PCR	Quantitative -polymerase chain reaction
RA	Retinoic acid
RARα	Retinoic acid receptor
Ras	Rat sarcoma protein
RNA	Ribonucleic acid
rRNA	Ribosomal ribonucleic acid
RSK	Ribosomal S6 kinase
RT	Room temperature
S	Serine
SAP 97	Synapse-associated protein 97
SARE	Synaptic activity-responsive element
SC	Schaffer collateral
SDS	Sodium dodecyl sulphate
SDS-PAGE	Sodium dodecyl sulphate polyacrylamide gel electrophoresis
SEM	Standard error of mean
SEP	Sepereclipticphluorin
SFK	Src family kinase
SH	Standard housing
Shc	SH2-containing collagen-related protein
SOC	Super-optima broth with catabolite repression
SRE	Serum response element
SRF	Serum response factor
Sub	Subiculum
SUMO	Small ubiquitin-like modifier
T	Threonine
TARP	Transmembrane AMPAR regulatory protein
TBS	Theta burst stimulation

TD	Terminal domain
TEMED	N,N,N′,N′-Tetramethylethylenediamine
T-LTP	Tetanus LTP
TNFα	Tumor necrosis factor α
TPA	12-O-Tetradecanoyl-phorbol-13-acetate
Tris	2-Amino-2-(hydroxymethyl)-1,3-propanediol
TrkB	Tropomyosin receptor kinase B
TSA	Trichostatin
TTX	Tetrodotoxin
UTR	Untranslated region
VDCC	Voltage-dependent calcium channel
WT	Wild-type
Y	Tyrosine
YFP	Yellow fluorescent protein
ZLF	Zeste-like factor
ZLF-RE	Zest-like factor response element
Φ	Hydrophobic amino acid

Chapter 1.

Introduction

1.1 The Hippocampus

1.1.1 The structure and circuitry

The hippocampus is a beautifully designed structure located in the medial temporal lobe of the brain (Figure 1.1A). The structure is conserved across phylogeny and was named by Julius Caesar Aranzi in 1587, due to its striking structural similarity when dissected from a human brain to a sea horse, the genus name for which is *Hippocampi*. There are two hippocampi in the brain one located in the left hemisphere and the other in the right hemisphere forming part of the limbic system.

The hippocampus is organised into principal cell layers together with highly structured laminar distribution of many of its inputs thus creating a model system for neurobiological research (Andersen, 2007; Neves et al., 2008) (Figure 1.1B). The major source of synaptic input into the hippocampus originates from the entorhinal cortex (EC) through the perforant pathway. The dentate gyrus (DG) harbours oval-shaped cell bodied granule cells projecting their mossy fibres axons onto CA3 pyramidal cells. This signal can then be relayed to the CA1 pyramidal cells via the Schaffer collateral (SC) pathway or via the commissural pathway coming from the fimbria to the CA1 cells (Figure 1.1C). These afferent axons will form synapses along the CA1 pyramidal cell dendrites (Figure 1.1 (B) pink box). The efferent fibres signal from the CA1 pyramidal cells into the EC, either directly or via the Subiculum (Sub).

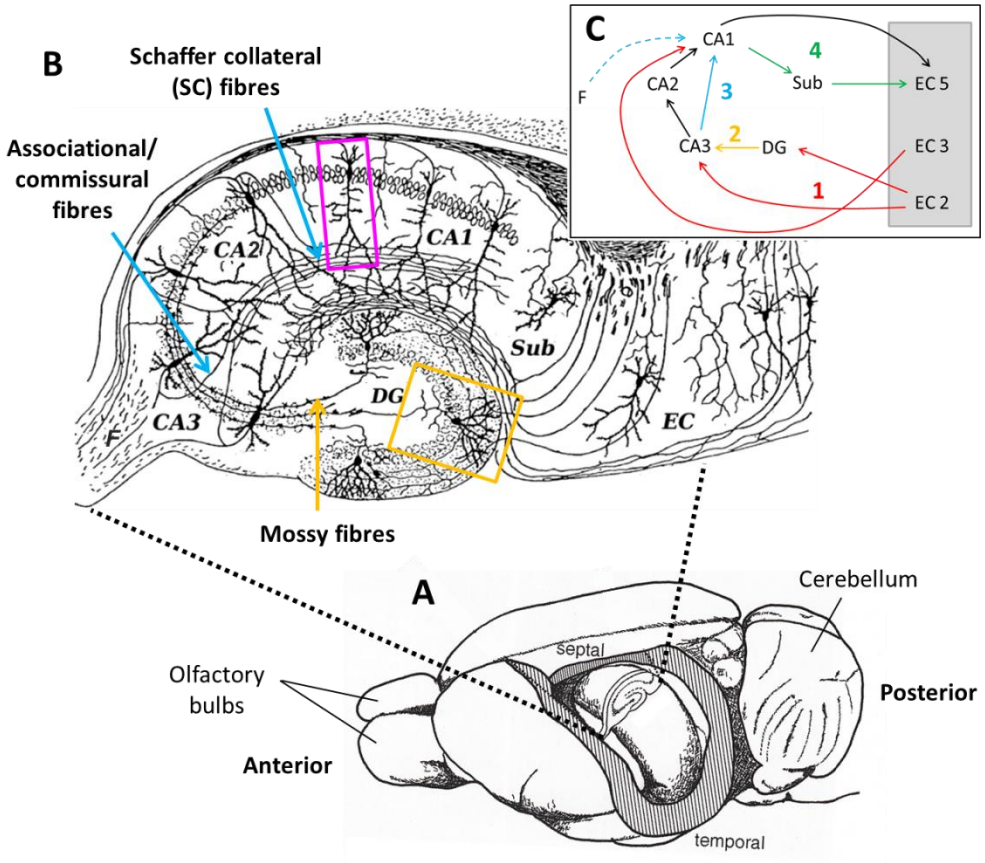

Figure 1.1; A representative figure showing the hippocampus' localisation in a rat brain and a histological image of the organisation of the neurones and their communicative pathways. (A) *A line drawing representing the structure of the brain highlighting the location of the hippocampus. The hippocampus is located in the medial temporal lobe. The septal and temporal regions of the hippocampus are labelled as well the as the anterior and posterior ends of the brain. A transverse section across the hippocampus has been enlarged to show the circuitry and structure (Andersen, 2007).* ***(B)*** *A histological sketch based on Camillo Golgi staining technique representing the structure and organisation of the hippocampal neurones. There are different cell layers found in the hippocampus, the main pyramidal cell layers are CA1-3 regions and there is the dentate gyrus (DG) shown on the diagram. The fimbria (F) contains myelinated fibres which can project into the CA regions. As for the entorhinal cortex (EC) there are different layers of cells which communicate with different regions of the CA regions where the subiculum (Sub) relays the output to the EC from the CA1 pyramidal cells. The Schaffer collateral fibres originate from the CA3 pyramidal cells which project their axons onto the CA1 pyramidal cells (pink box). The commissural fibres come from the fimbria and project onto the CA1 axons and the associational fibres project onto the CA3 axons. The DG contains granule cells (orange box) which project out mossy fibre axons onto CA3 pyramidal neurones. [Adapted from; (Ramón y Cajal, 1909)* ***(C)*** *A basic diagram of the neuronal connectivity in the hippocampus. The red arrows (1) represent perforant pathway to the DG or to the CA3 which is the major source of neuronal input. The orange arrow (2) presents the mossy fibre pathway where the granule cells' axons project to the CA3. The solid blue arrow (3) represents the Schaffer collateral axons and the dotted blue line (3) presents the Commissural fibres where both these axons form the Schaffer/Commissural pathway. The Temporoammonic pathway is the CA1-Sub-EC pathway (4) which forms the*

principal output from the hippocampus. However this pathway is not uni-directional. [EC; Entorhinal cortex, Sub; Subicuclum, DG; Dentate gyrus, F; Fimbria; CA; Cornu ammonis] Adapted from;(Ramón y Cajal, 1909; Neves et al., 2008)

1.1.2 The characteristics of the different hippocampal cell types

The most well characterised type of neurone in the brain is the excitatory pyramidal neurone which can be found in the hippocampus as well as other areas of the brain, such as neocortex. In the hippocampus, pyramidal cells are found in the CA1, CA2 and the CA3 regions. They have a triangular shaped cell body with dendrites sprouting from both the apical and basal region of the cell body (Figure 1.2). These dendrites are appendages which extend from the neuronal cell body in order to form a synaptic connection with a neighbouring neuronal axon. Axons conduct electrical impulses away from the cell body and determine the targets of the output signal (Purves et al., 2012). Dendrites on the other hand can define the inputs received which is influenced by the complexity of dendritic branching (Purves et al., 2012). Dendrites are 'plastic' in nature allowing morphological alterations, which has been shown to regulate changes in synaptic connections (Tavosanis, 2011). Pyramidal cells are studded with thousands of spines along their dendrites. These spines are small protrusions which form active synapses with presynaptic boutons. The synapse between the Schaffer collaterals and the apical dendrites of the CA1 pyramidal cells has been extensively studied and characterised as an excitatory neuronal connection driven by the excitatory neurotransmitter, glutamate (Kerchner and Nicoll, 2008).

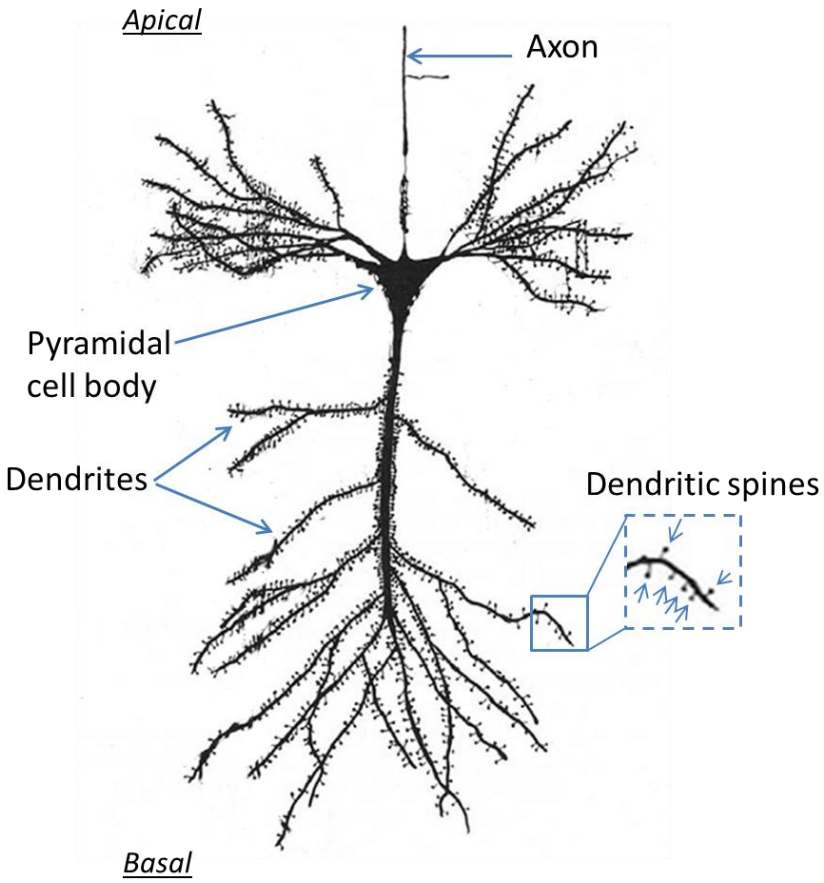

Figure 1.2; A representative schematic diagram of a CA1 pyramidal cell. *The pyramidal shaped cell body has an axon projecting away from the cell body. The dendrites are sprouting from the apical and basal area of the neurone. The basal dendritic branching is more extensive when compared to the apical region. The dendrites are studded with spines highlighted in the blue box as small protruding compartments. The location of this cell is shown in the pink box in Figure 1.1B. [Figure adapted from; (DeFelipe, 2011)]*

The CA1 pyramidal neurones will receive both inhibitory and excitatory inputs from presynaptic neurones. The inhibitory input can be delivered by another cell type found in the hippocampus called interneurones. These interneurones form connections between other neurones e.g. pyramidal cells, by projecting their small axons and releasing their primary inhibitory neurotransmitter, γ-aminobutyric acid (GABA) onto their targets. Their morphological structure comprises of a small round cell body with protruding dendrites radiating from cell body. However they are a heterogeneous population of neurones with many sub-classes which differ in structure and location across the hippocampus (Ascoli et al., 2008).

A region specific neuronal cell type known as granule cells are found in the DG. These cells give rise to axons which innervate other hippocampal regions (e.g. CA3) (Andersen, 2007). They harbour a small elliptical cell body with projecting dendrites originating from a single branching dendritic tree, extending out into the molecular layer of the DG (Figure 1.1, orange box). These dendrites are also covered in dendritic spines like the pyramidal cells. These cells can receive inhibitory and excitatory inputs and conduct principally glutamatergic excitatory outputs through their mossy fibres. However in the literature it appears that the mossy fibres synapses release both inhibitory GABA and excitatory glutamatergic neurotransmitters (Beltran and Gutierrez, 2012).

The hippocampus is made up of many neuronal cell types of which a few are discussed above. However there is another important non-neuronal cell type known as glial cells which are at a 3 to 1 ratio with neurones (Purves et al., 2012). These glial cells which are star-shaped and have protruding processes. However there are different classes of glial cells which carry different functions and structures as well as expression in different locations. These include astrocytes which are mainly restricted to the central nervous system (i.e. the brain and the spinal cord). Their main function is to maintain a balanced ionic and chemical environment for neuronal signalling. Their extending processes are unique in that they are able to ensheath surrounding neuronal synapses (Purves et al., 2012). These glial processes do not function like neuronal dendrites as they are not as prominent as they are in neurones, they don't carry nerve impulses nor do they have spines. However the ability of glial processes to ensheath a neuronal synapse allows them to sense neuronal activity and respond to neuronal inputs through intracellular calcium signalling (Haydon, 2001). It has also been shown that neurones respond to glial calcium waves by elevating their intracellular calcium and increasing their electrical activity via glutamate receptor channels (Hassinger et al., 1995). These characteristics have lead neuroscientists to elucidate that glial cells part-take in neuronal synaptic transmission in the brain.

1.1.3 The function of the hippocampus

The hippocampus is involved in consolidating information for short and long term memory as well as spatial navigation (Andersen, 2007). The importance of the hippocampus in memory consolidation was first discovered through patient HM who underwent a bilateral media temporal-lobe excision, i.e. a surgery removing both his hippocampi, in order to relieve his severe epilepsy. However patient HM suffered severe memory deficits following his operation. He was unable to form new memories about experienced events (e.g. episodic memories) also known as anterograde amnesia (Scoville and Milner, 1957). As well as suffering from partial retrograde amnesia meaning he was unable to remember things before the surgery but could still remember childhood memories. These symptoms gave neuroscientists an insight to the role of the hippocampus in memory formation and consolidation (Andersen, 2007).

The role of the hippocampus in spatial navigation was first hypothesised where the hippocampus could act as a 'neuronal map' representing different locations in an environment (Eichenbaum and Cohen, 2001). This was later confirmed when hippocampal neurones were seen to fire bursts of action potentials in relation to certain locations, like a neuronal map (O'Keefe and Dostrovs, 1971). These cells were referred to as 'place cells' which acted like a spatial 'storage' system. Evidence in the literature has shown that lesions in the hippocampus can affect spatial memory such as dorsal hippocampal lesion in rodents substantially impaired spatial learning, even though only 40% of the hippocampal volume was excised (Moser et al., 1993). Spatial learning can be tested using 'The Morris water maze' which involves placing a mouse or rat in a small pool of water which contains an escape hidden platform a few millimetres below the water surface. Visual cues are placed in the eye line of the rodent and various parameters are recorded whilst the subject swims to find the escape (Morris et al., 1982).

An age-related disease known as Alzheimer's disease affects the hippocampus from early stages of the disease. The neuropathological traits have been described by Braak who characterised the stages of the disease according to the pattern of toxic neurofibrillary tangles (NFT) observed across the limbic area of the brain (Braak and Braak, 1991). Interestingly the early stages of the disease (Stages 1-2) shows NFT deposits in the trans-entorhinal region of the brain, which is located between

association cortices and the hippocampus. This is an important area involved in integrating the information and learning and memory processes. By stage 3-4 of the neurological disease the CA1 pyramidal cells of the subiculum start to develop NFT (Braak and Braak, 1991). Studies have shown that these neuropathological effects observed throughout the Braak Stages are related to a decline in memory in the suffering patients (Grober et al., 1999). This demonstrates once more the importance of the hippocampus in learning and memory processes.

1.2 An overview of synaptic plasticity

Synaptic plasticity refers to the ability of neurones to be able to modulate their synaptic strength according to changes in neuronal activity (Hughes, 1958; Bliss and Lomo, 1973; Bliss and Collingridge, 1993). There are short term forms of synaptic plasticity which can last from milliseconds to a few minutes and long term forms which can last from minutes to hours. These longer forms of synaptic plasticity have been thought to underlie learning and memory and therefore have been a focus of interest to many neuroscientists.

In terms of long term synaptic plasticity there are two well characterised forms known as long-term potentiation (LTP) and long-term depression (LTD) (Figure 1.3), which is the strengthening and weakening of neuronal synapses from a set level determined by previous 'experience' thus representing a cellular basis for learning and memory (Bliss and Collingridge, 1993; Malinow and Malenka, 2002; Nicoll, 2003; Collingridge et al., 2004; Malenka and Bear, 2004). These are called Hebbian forms of synaptic plasticity where the name 'Hebbian' comes from Donald Hebb who first postulated that synaptic plasticity entails an increase in synaptic efficacy arising from when a postsynaptic cell received repeated and persistent stimulation. Synaptic plasticity was later characterised to be associative, rapidly induced and input specific (Malenka, 2003).

There are a few mechanisms involved during synaptic plasticity including **(A)** glutamate AMPAR (α-amino-3-hydroxy-5-methyl-4-iso-xazolepropionic acid receptor) trafficking (Section 1.3.1), **(B)** morphological changes in dendritic spines (Section 1.3.2) and **(C)** diverse range of intracellular signalling pathways which are all discussed below (Section 1.3.3).

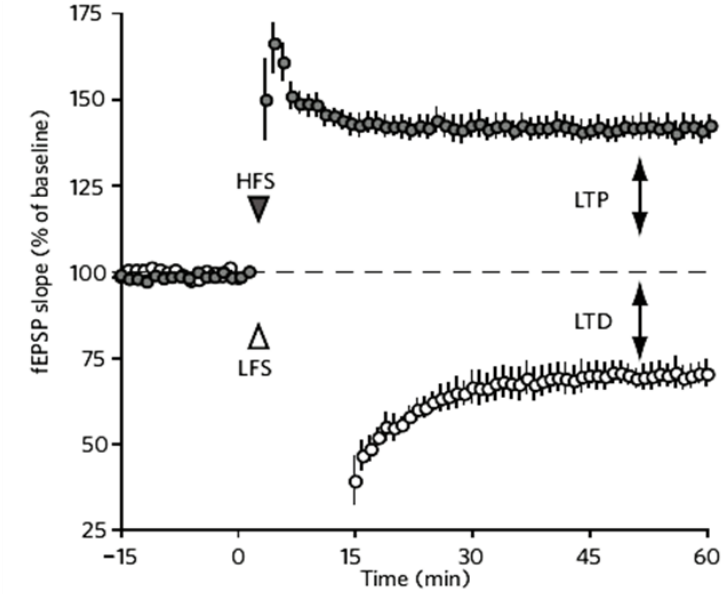

Figure 1.3; A schematic representation of LTP and LTD. *An example of a typical electrophysiological experiment obtained from recording from the CA1 region of the hippocampus. The experiments represent an electrophysiological recording for basal synaptic transmission before and after high-frequency stimulation (HFS)-induced LTP and low-frequency stimulation (LFS)-LTD. The average field excitatory postsynaptic potential (fEPSP) slope is plotted as % of baseline against time.[Adapted from (Fleming and England, 2010)]*

1.3 Mechanisms underlying synaptic plasticity

1.3.1 (A) The trafficking of glutamate AMPA receptors

1.3.1.1 Overview of glutamate receptors

Glutamate receptors are transmembrane receptors that support the majority of excitatory synaptic transmission in the mammalian central nervous system (CNS). There are two classes of glutamate receptors, the ionotropic receptors (iGluR) and the metabotropic glutamate receptors (mGlu). The AMPAR, kainate receptor and NMDAR (N-methyl-D-aspartic acid receptor) are iGluR and mediate fast excitatory synaptic transmission, the majority of which is via the AMPAR. These are ligand-gated ion channels which are permeable to cations. NMDA receptors are heterotetramers consisting of two obligatory NR1 subunits, which bind the co-agonists glycine or D-serine and two of four possible glutamate-binding NR2 subunits: NR2A, NR2B, NR2C, and NR2D (Li and Tsien, 2009). There is also a related gene family of NR3 A and B subunits which do not seem to have a role in the

hippocampus (Andersen, 2007). NMDA receptors have unique properties compared to AMPAR and kainate receptors; one of these is that magnesium (Mg^{2+}) ions block the ionophore in a voltage-dependent manner. Thus the receptor-mediated ion influx only occurs upon neuronal depolarisation. Depolarisation occurs in response to a neuronal stimulus that induces the influx of sodium ions and efflux of potassium ions. The mGlus, of which there are 3 classes, Groups I, II, III, are G-protein-coupled receptors and modulate the activity of iGluR. The Group I receptors (mGlu1 and mGlu5) are generally localised postsynaptically and are coupled to G-proteins as well as second messenger cascades (Gladding et al., 2009).

1.3.1.2 Characteristics of AMPA receptors and their organisation at the postsynaptic density (PSD)

The AMPAR subunit composition plays an important role in determining ionic permeability as well as subunit specific phosphorylation at target residues which can promote downstream protein interactions and kinase signalling cascades. These all contribute to the trafficking of the receptors during constitutive recycling as well as during different forms of synaptic plasticity.

AMPAR are tetrameric complexes of four homologous subunits known as GluA1 to GluA4. Each of these subunits share 68-74% amino acid identity at the protein level and will combine together to form different stoichiometries as distinct receptor subtypes (Song and Huganir, 2002). Each subunit consists of an extracellular N-terminus (NT) tail joined by four transmembrane domains and an intracellular C-terminus (CT) tail (Figure 1.4A). Heteromeric AMPAR containing the GluA2 subunit is impermeable to calcium (Ca^{2+}). The kinetics of the AMPAR such as ion permeability is determined by the Q/R editing domain in the first intracellular loop shown in Figure 1.4A (Fleming and England, 2010; Anggono and Huganir, 2012). Interestingly the receptor subunit composition is variable depending on the cell type, brain region and development. For example the main AMPAR subtype expressed by hippocampal pyramidal cells is either GluA1/2 or GluA2/3 heteromers (Wenthold et al., 1996).

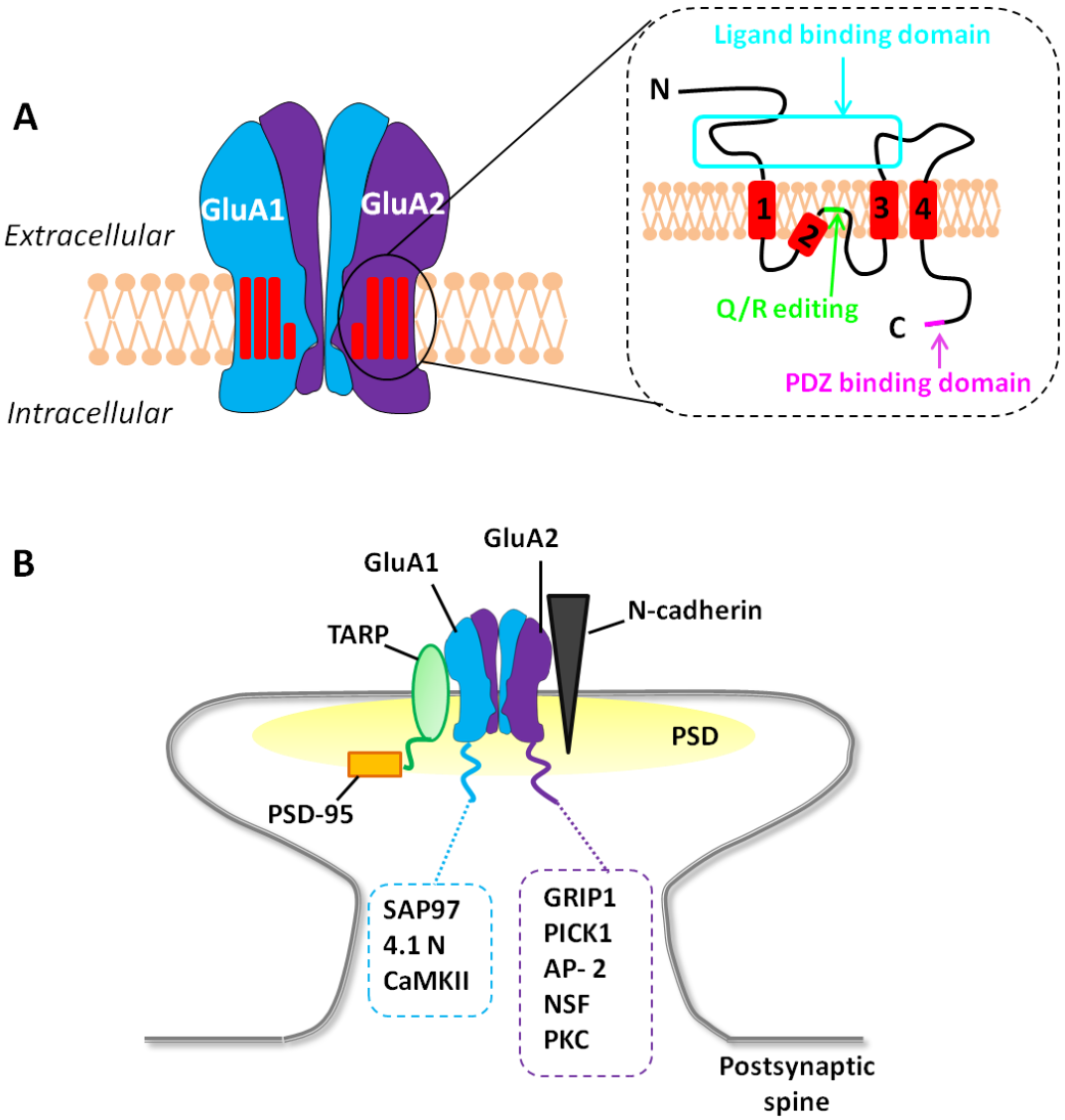

Figure 1.4; A schematic representation of the structure of an AMPAR. (A) *AMPAR are tetrameric complexes which form an ionotropic channel. In this particular case a GluA1/2 heteromeric AMPAR is represented. Each subunit is composed of four TM labelled 1-4. The TM2 forms a re-entrant membrane loop that lines the ion channel which is thought to determine ion permeability. This occurs through the Q/R (glutamine/arginine) editing region (green) which involves the editing of a glutamine codon to a arginine codon in the ion channel pore region of GluA2 which subsequently regulates calcium permeability (Shepherd and Huganir, 2007). The NT loop exposed extracellularly is important in receptor assembly as well as retaining the ligand binding domain (blue box). The CT tail is very important as it contains several binding sites for interacting proteins, including the PDZ-binding motif at the end of the CT tail (pink)* ***(B)*** *In the postsynaptic spine head, the postsynaptic density (PSD) harbours a high concentration of proteins which include AMPAR (GluA1/2), transmembrane AMPAR regulatory proteins (TARP) such as stargarzin and N-cadherin. AMPAR and TARP interact at the PSD allowing the binding to PSD-95. Whilst the N-cadherin may be interacting with GluA2 acting as a cell adhesion molecule located in the PSD. Upon neuronal stimulation a chain of intracellular signalling reactions will be induced involving proteins which interact with the CT tail of each AMPAR subunit. Protein kinases can also be activated and phosphorylate specific residues found along the CT tail. Some of the many proteins and kinases are shown in the boxes below the GluA1 and GluA2 subunits and are*

*explained in the text. [PDZ; **P**ostsynaptic density protein-95, **d**isc-large tumour suppressor protein, **z**onula occludens-1, TM; Transmembrane domains, NT; N-terminus, CT; C-terminus SAP 97; Synaptic associated protein 97 kDa, 4. 1 N; Neuron- specific protein 4.1 , GRIP1; Glutamate receptor interacting protein 1, PICK1; Protein interacting with C-kinase 1 , NSF; N-ethylmaleimide-sensitive factor, CaMKII; $Ca^{2+/}$Calmodulin-Dependent Protein Kinase II, PKC; Protein kinase C, AP- 2; Adaptor protein 2 ; TARP; Transmembrane AMPAR regulatory proteins, PSD; Postsynaptic density]*

1.3.1.2.1 Stabilisation at the postsynaptic density

There is a family of transmembrane AMPAR regulatory proteins (TARP) known as stargazin-related proteins which have been implicated in AMPAR function (Tomita et al., 2003; Yamazaki et al., 2004). TARP has been shown to play a role in multiple AMPAR functions ranging from facilitating the export of the AMPAR from the endoplasmic reticulum (ER) to trafficking them to the plasma membrane where it is inserted extrasynaptically. AMPAR are assembled and associate with TARP in the ER which allows the AMPA-TARP complex to be exported out of the ER and trafficked to the extrasynaptic plasma membrane (Ziff, 2007). The TARP, stargazin is concentrated at the synapse by its CT PDZ binding site which binds with the synaptic scaffolding protein PSD-95. This process is thought to anchor the AMPAR in the PSD (Figure 1.4B) (Bredt and Nicoll, 2003). Consistent with this, when PSD-95 is overexpressed it selectively enhances AMPAR-mediated synaptic transmission and occludes LTP (Stein et al., 2003; Ehrlich and Malinow, 2004). Interestingly TARP are specific to AMPAR themselves but do not show subunit specificity (Ziff, 2007).

There are other proteins found at the PSD which enable AMPAR to be anchored and stabilised. For example N-cadherin is a trans-synaptic cell adhesion molecular which has been shown to regulate activity-mediated stabilisation of spines in hippocampal neurones (Arikkath, 2010). A study showed that a dominant negative N-cadherin mutant transfected in CA1 neurones, prevented the activity-dependent stabilisation of new spines as well as the accumulation of PSD-95 at the synapses (Mendez et al., 2010). Interestingly, Sheng's group elucidated that the N-terminus of GluA2 interacts with N-cadherin which influences morphological changes of the postsynaptic spine. The molecular mechanism has not been fully described but it is thought that the presence of GluA2 enhances N-cadherin synaptic localisation

leading to intracellular signalling events affecting actin dynamics (Passafaro et al., 2003).

1.3.1.2.2 Characterisation of AMPA receptor C-terminus tail and their interacting proteins

Each glutamate receptor subtype has a unique C-terminus (CT) tail which can interact with specific cytoplasmic proteins. One of the well characterised interacting domains found in the cytoplasmic proteins is the PDZ domain either in a single or multiple motifs. This ~80 amino acid binding motif in the interacting protein will bind to a specific region at the end of the CT tail (Sheng and Sala, 2001). The CT tail is longer and homologous in subunits GluA1, GluA4 and GluA2L (GluA2 with long CT domain) which is an alternative splice variant of GluA2. Alternatively the prominent GluA2 variant with a short CT domain, GluA3 subunit and GluA4c cerebellum-specific splice isoform all have homologous short CT (Hollmann and Heinemann, 1994).

The actin cytoskeleton can influence AMPAR expression during different forms of synaptic plasticity such as LTP and LTD. When there is an increase in polymerised actin filaments (F-actin) there is a higher surface AMPAR expression (Allison et al., 1998). Therefore actin depolymerisation enhances the removal of AMPAR from the PSD. The regulation of the actin cytoskeleton has been shown to be influenced by certain AMPAR-interacting proteins some of which are shown in Figure 1.4B. For example 4.1 N protein contains a spectrin-binding/actin-binding domain which interacts with the CT of GluA1 which in turn regulates the surface GluA1 expression (Shen et al., 2000).

Type I PDZ-binding motif expressed by SAP 97 (synapse-associated protein 97), has been found to interact with the GluA1 CT whilst the type II PDZ domain of glutamate receptor interacting protein 1 (GRIP1) and protein interacting with C-kinase 1 (PICK1) allows them to bind to GluA2 subunit. Other interacting proteins N-ethylmaleimide-sensitive factor (NSF) and adaptor protein 2 (AP-2) can bind to either GluA1 and/or GluA2 subunit via non-PDZ domains. The direct binding between these interacting proteins and AMPAR can target the receptors for endocytosis, exocytosis or degradation which can determine their functional output. For example AP-2 is a multimeric complex comprising of 4 subunits, α, β, σ and μ where the μ subunit binds to the GluA2 CT (Lee et al., 2002) which overlaps with

the binding site of another interacting protein known as *N*-thylmaleimide-sensitive factor (NSF). The interaction between AP-2 and GluA2 appears to be important in hippocampal NMDA-induced LTD where AMPAR are internalised (Lee et al., 2002; Kastning et al., 2007). Controversially, a recent paper used a single-cell molecular replacement strategy to replace all endogenous AMPA receptors with transfected subunits and showed that the GluA1 CT was not required for LTP in mouse CA1 hippocampal pyramidal neurons (Granger et al., 2013).

1.3.1.3 AMPA receptor trafficking during synaptic plasticity

In hippocampal neurones it appears that 80% of the AMPAR dependent synaptic transmission is mediated by GluA1/2 AMPAR heteromers (Lu et al., 2009). These subunits have also been shown to be trafficked during different forms of synaptic plasticity which influences neuronal synaptic output (Contractor and Heinemann, 2002; Shepherd and Huganir, 2007; Hanley, 2008; Wang et al., 2012).

There is an increase in surface AMPAR when synaptic transmission is potentiated during LTP or a decrease in surface AMPAR expression when transmission is depressed during LTD (Figure 1.5). A mechanism which influences AMPAR trafficking is the phosphorylation status of the CT which is modulated by a range of protein kinases. For example an important kinase which phosphorylates GluA1 CT at serine (S) residue 831 is $Ca^{2+/}$Calmodulin-dependent protein kinase II (CaMKII) which has been shown to increase GluA1 phosphorylation levels after LTP induction (Barria et al., 1997a; Barria et al., 1997b). This increased phosphorylation status at S831 enhances the single-channel conductance of the GluA1 subunit suggesting that this phosphorylation might in part mediate potentiation of synaptic transmission during LTP (Benke et al., 1998; Derkach et al., 1999). The balance between phosphorylation and dephosphorylation of AMPAR subunits has been proposed to modulate synaptic activity. A working model could include the activity-dependent phosphorylation of GluA1 which would deliver the receptors to the synapse during LTP, whereas the dephosphorylation of GluA1 would signal for internalisation and thus LTD. In contrast, when GluA2 subunit is phosphorylated this leads to internalisation and its dephosphorylation allows the receptors to be retained in the synapse (Henley et al., 2011).

1.3.1.3.1 Mechanisms involved during AMPA receptor trafficking

Receptors undergo constitutive cycles of endocytosis/exocytosis which means that internalised receptors (endocytosis) are recycled back to the plasma membrane (exocytosis). This dynamic system can also be modulated during LTP and LTD thus altering AMPAR surface expression (Figure 1.5). For example, LTD has been suggested to involve the internalisation of AMPAR by endocytosis thus reducing the number of surface receptors at the synapse in cultured hippocampal neurones and CA1 hippocampal slices (Beattie et al., 2000; Man et al., 2000). As oppose to LTP where an insertion of additional AMPAR by exocytosis occurs to increase AMPAR expression (Lledo et al., 1998; Lu et al., 2001). The system seems to be more elaborate than researchers first thought as there are complex intracellular trafficking pathways implicated in endosomal sorting.

Figure 1.5 summarises the endosomal sorting; where receptor recycling occurs in many cell types including neurones where membrane bounded receptors are internalised into endocytotic vesicles known as early endosomes. The endocytosed receptors are then either targeted to the recycling endosome or to the late endosome. The receptors which are sorted via the recycling endosome are re-inserted into the plasma membrane. As opposed to those who are trafficked to the late endosomes for degradation via lysosomes (Hanley, 2010). AMPAR were found to co-localise with these intracellular membrane compartments. Immunocytochemical staining used against early endosome markers such as early endosome antigen 1 (EEA1), Rab5, transferin receptor and Rab4 in live hippocampal neurones, co-localised with AMPAR (Ehlers, 2000). AMPAR also co-localised with synataxin-13, a recycling endosome marker and as well as Lamp1, a late-endosome/lysosome maker which was visualised in hippocampal neurones (Lee et al., 2004).

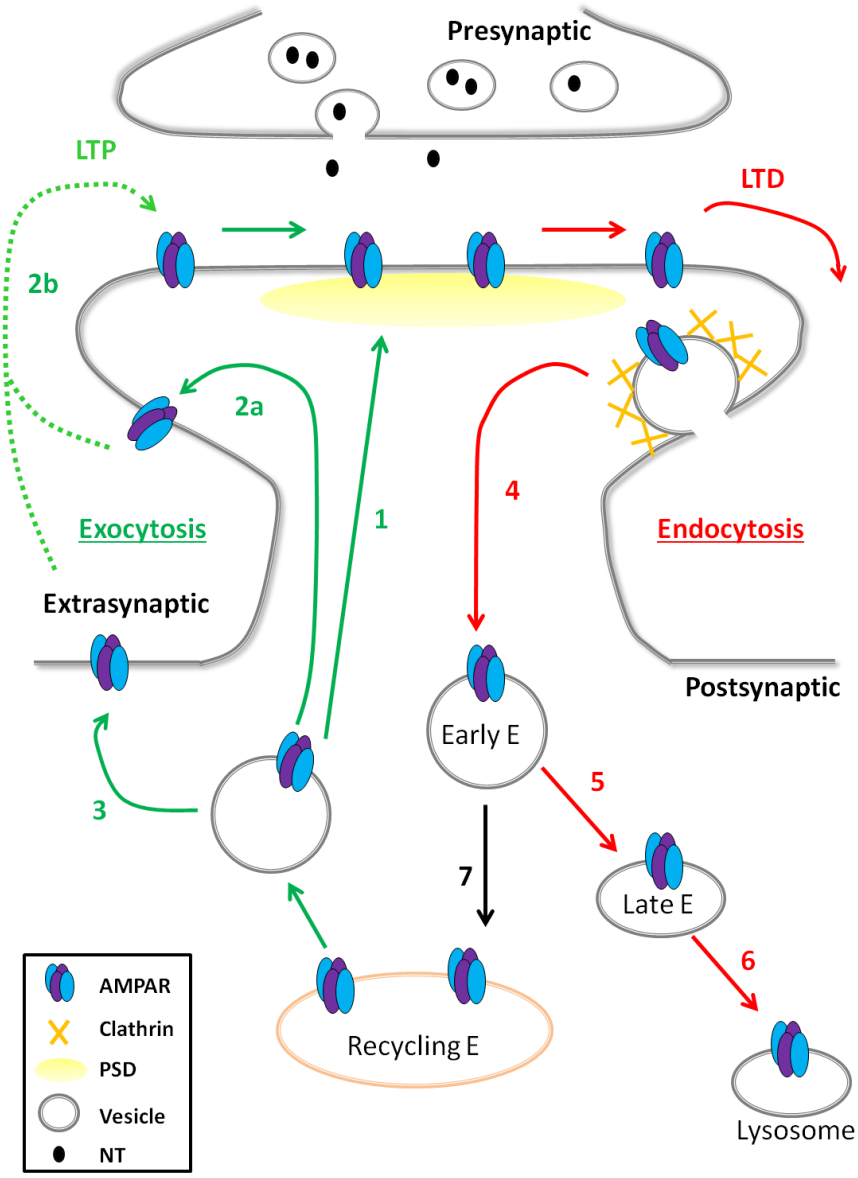

Figure 1.5 A diagram demonstrating a simplified mechanism of both exocytosis and endocytosis of AMPAR at a synapse. *At a synapse there is a presynaptic terminal which releases neurotransmitters across the synaptic cleft which act on the postsynaptic terminal. AMPAR can undergo exocytosis at the postsynaptic terminal (green arrows) where the receptors are inserted from the either* ***(1)*** *directly into the postsynaptic density (PSD)* ***(2a, b)*** *adjacent to but outside the PSD or* ***(3)*** *along the dendritic shaft (e.g. extrasynaptically). The dotted green lines represent AMPAR lateral diffusion to the PSD. This will increase the number of AMPAR in the surface membrane and thus increasing synaptic transmission leading to LTP. The opposite trafficking mechanism is endocytosis of AMPAR which involves receptors being internalised from the PSD (red arrow) by clathrin-mediated endocytosis* ***(4)****. These internalised receptors form the early endosome (E) where they can be sorted via two different pathways. The first is via the late endosome* ***(5)*** *which then leads to receptor degradation via lysosomes* ***(6)****. Or the AMPAR can be recycled back into the plasma membrane via the recycling endosome pathway* ***(7)****. [PSD; Postsynaptic density, NT; Neurotransmitter, LTP; Long-term potentiation, LTD; Long-term depression, AMPAR; α-amino-3-hydroxy-5-methyl-4-iso-xazolepropionic acid receptor, E; Endosome [Adapted from (Shepherd and Huganir, 2007; Hanley, 2008)].*

1.3.1.3.2 The trafficking of AMPA receptors using endocytosis

Under LTD-like conditions there is a reduction in surface AMPAR at synapses in dissociated hippocampal neurones which could account for a depression of synaptic transmission characterised by LTD (Carroll et al., 1999a). In addition, this internalisation of AMPAR was shown to be regulated by clathrin-mediated endocytosis because the intracellular perfusion of peptides targeted to interfere with endocytosis blocked the induction of LTD in both the hippocampus and cerebellum (Man et al., 2000; Wang and Linden, 2000).

Following endocytosis, the fate of the internalised receptor also plays an important role. For example after chemically inducing NMDA-dependent LTD in hippocampal neurones, the endocytosed AMPAR were diverted from the recycling endosome to the late endosome/lysosome (Lee et al., 2004). The early endosome marker, Rab5 has been shown to be an important regulator of early endosome function. This was shown in a study where a dominant negative mutant was expressed in CA1 hippocampal neurones which blocked low-frequency induced LTD but not the constitutive AMPAR trafficking. Therefore the role of Rab5 appears to be specific to LTD-induced stimulation (Brown et al., 2005).

The proteins which interact with the C-terminus (CT) tail of AMPAR have also been shown to play a role in deciding the fate of the internalised receptor from the early endosomal state. For example the protein PICK1 which binds with GluA2 CT tail plays a role in vesicle trafficking during NMDA-dependent GluA2 internalisation. A study used pH-sensitive GFP variant (pHluorin) tagged to the N-terminus of GluA2 to monitor its trafficking in response to NMDA stimulation in hippocampal neurones (Lin and Huganir, 2007). Using fluorescence recovery after photobleach (FRAP), it was observed that pHluorin-GluA2 was recycled back to cell surface following NMDA application. However when PICK1 was absent, NMDA-dependent GluA2 endocytosis was normal but there were increased levels of GluA2 recycling. This suggests that PICK1 restricts AMPAR recycling (Lin and Huganir, 2007).

Clathrin-mediated endocytosis is one of the main mechanisms which internalises plasma membrane proteins (Jung and Haucke, 2007). Clathrin is a protein which has a three-legged structure consisting of three heavy and three light chains. When clathrin is polymerised it forms a lattice which coats cytoplasmic

vesicles, also known as clathrin-coated vesicles (CCV), allowing intracellular trafficking of target proteins (Brodsky et al., 2001). The location of clathrin-mediated endocytosis occurs at endocytic zones (EZ) in dendritic spines adjacent to the PSD, which was visualised using GFP-tagged clathrin expressed in hippocampal neurones, (Blanpied et al., 2002). The formation of CCV requires recruitment of a range of clathrin binding proteins which aid the assembly and disassembly of the coated vesicles. For example AP180 (adaptor protein 180)/CALM (clathrin assembly lymphoid myeloid leukaemia) is a neuronal adaptor protein which can bind to both phosphatidylinositol-4,5-bisphosphate (PIP_2) at the plasma membrane at the same time as binding to clathrin. This indicates that AP180 could serve to tether clathrin to the membrane to allow nucleation of clathrin lattices (Ford et al., 2001). Interestingly, a group found that AP180 also binds to a crucial adaptor protein known as adaptor protein-2 (AP-2), independent of clathrin interaction. Furthermore, this AP180-AP-2 complex is more efficient at assembling clathrin under physiological conditions than is either protein alone (Hao et al., 1999). Another protein which has been shown to be a component of the endocytotic machinery is Stonin 2. This protein interacts with certain endocytotic machinery proteins including an indirect interaction with AP-2 (Martina et al., 2001).

Adaptor protein-2 (AP-2) is a large protein complex composed of four subunits, α, β2, μ2 and σ2. Each of the two large (approx. 100 kDa) α and β2 subunits consists of an N-terminal domain (called the trunk or head) and a globular C-terminal domain (called the appendage or ear), which are connected by a flexible hinge (Pearse et al., 2000). AP-2 is particularly important in AMPAR trafficking because it binds to GluA2 CT domain under conditions favouring clathrin-mediated receptor internalisation (Lee et al., 2002). The formation of clathrin-coated pits involves membrane invagination which is traditionally thought to be triggered by the recruitment of AP-2 to the plasma membrane. The AP-2 complex conjoins the endocytotic clathrin scaffold to PIP_2-containing membranes and transmembrane protein cargo via endocytic motifs present in the cargo's cytoplasmic tails (Ohno et al., 1995; Honing et al., 2005). The subunits which bind directly to the motifs on the cargo are the μ2 and the σ2 and the indirect interactions occur using the appendage domains to bind accessory adaptor proteins (Collins et al., 2002; Kelly et al., 2008). Interestingly, a conformational change occurs in the AP-2 complex where binding of endocytic motifs to the μ2 and σ2 subunits are blocked by parts of the β2 subunit

referred to as its 'locked' form. Following the conformational change the μ2 C terminus relocates subsequently exposing both cargo-binding sites as the μ2 linker becomes helical and binds back onto the complex (Jackson et al., 2010). The β2 subunit is important for the interaction with clathrin via two binding sites, one at a clathrin box motif in the hinge region and the other on a site in the ear domain (Owen et al., 2000). The other large subunit, α2 binds to the plasma membrane as well as endocytotic proteins such as amphiphysin and AP180 (Mousavi et al., 2004).

Clathrin is recruited to the plasma membrane by AP-2 and other accessory adaptor proteins where it is polymerised allowing coat assembly to occur (McMahon and Boucrot, 2011). The formation of free CCV involves the stabilisation of the curvature and displacement to the edge of the membrane. This process involves three proteins, two of which are enzymes; dynamin, a GTPase (hydrolyse guanosine triphosphate), endophilin, and lastly amphiphysin. Amphiphysin has two forms of which amphiphysin 1 is highly expressed in the brain. It has a binding domain for both clathrin and α2 whilst it also contains a proline-rich motif which binds endophilin (Zhang and Zelhof, 2002). However it can also bind to dynamin via its C terminal SH3 domain which is thought to be key in linking dynamin and the clathrin coat (Wigge and McMahon, 1998). It has been suggested that amphiphysin recruits dynamin to the coated vesicle where it associates with PIP_2 at the neck where the GTPase activity of dynamin causes vesicle scission (Takei et al., 1999). The importance of the role of dynamin in clathrin-mediated endocytosis was demonstrated when a dominant negative form of dynamin was overexpressed in cultured hippocampal neurones which subsequently attenuated AMPAR endocytosis (Carroll et al., 1999b). Finally endophilin binds to dynamin via its SH3 domain. It may act as a downstream effector to dynamin by modifiying lipid composition of the neck. In Drosophila, the absence of endophilin significantly impairs endocytosis in neuromuscular junctions and in synapses of the central nervous system (Guichet et al., 2002; Verstreken et al., 2002).

1.3.1.3.3 The trafficking of AMPA receptors using exocytosis

AMPAR can be exocytosed via different routes but the exact location of insertion remains a subject of debate. The three main possibilities are either AMPAR

insertion directly into the postsynaptic density (PSD), adjacent to but outside the PSD or along the dendritic shaft (e.g. extrasynaptically) (Figure 1.5, 1-3).

The exocytosis of AMPAR directly in the PSD has been published by a few groups. One of which demonstrated using electron microscopy analysis that the insertion was mediated by a component of the exocyst complex in hippocampal slices (Gerges et al., 2006). However the fact that the PSD is a highly and densely packed area of proteins makes it seem less likely that exocytosis of AMPAR would occur in this fashion due to the physical hindrance (Hanley, 2008). The insertion of AMPAR within or very close to the spine has been shown after imaging sepererecliptic phluorin (SEP) tagged N terminus-GluA1 in hippocampal slices using the two photon microscopy during spine-specific stimulation (Patterson et al., 2010). However there has also been evidence of exocytosis of AMPAR occuring extrasynaptically. The SEP-GluA1 construct was transfected in rat dissociated hippocampal neurones and visualised along the dendritic shaft using epifluorescence microscopy (Yudowski et al., 2007). These receptors are thought to undergo lateral diffusion in order to reach the synapse where they will be anchored in the postsynaptic density (PSD) (Shepherd and Huganir, 2007; Henley et al., 2011). However the receptors found closer to the vicinity of the PSD are commonly retained in intracellular vesicular pools and brought to the cell surface by cytoskeleton-associated motors, such as kinesin and/or dynein and calcium sensitive-Myosin Vb (Matsuzaki et al., 2004; Park et al., 2004; Henley et al., 2011). Exocytosis of AMPAR is a constitutive as well as activity-induced process in which intracellular pools are directed to multiple sites in the neuronal cell membrane (Henley et al., 2011).

During LTP, additional AMPAR are inserted into the synaptic plasma membrane which has been visualised using GFP (green fluorescent protein)-tagged AMPAR constructs overexpressed in hippocampal slices and their expression was monitored following neuronal stimulation (Song and Huganir, 2002; Perestenko et al., 2003; Lee et al., 2009). For example upon LTP-inducing stimuli a rapid recruitment of AMPAR at the synapse was observed in dissociated hippocampal and cortical neurones (Liao et al., 2001; Lu et al., 2001). Furthermore the increase in synaptic transmission induced by LTP correlates with increased AMPAR expression (Malinow and Malenka, 2002; Song and Huganir, 2002) as well as increased polymerised filamentous actin (F-actin) (Fukazawa et al., 2003). The importance of

F-actin polymerisation during LTP was also shown when an actin polymerisation inhibitor, latrunculin A impaired late phase LTP in the dentate gyrus (Fukazawa et al., 2003).

The fate of AMPAR during exocytosis was shown in hippocampal neurones where the GluA1 AMPAR inserted into the plasma membrane in response to LTP-inducing stimuli originated from the plasma membrane. This suggests that LTP expressed AMPAR have gone through the recycling endosomal sorting pathway (Park et al., 2004). If the recycling pathway is disrupted using dominant negative mutants of recycling endosome proteins such as Rab11, LPT-induced AMPAR trafficking is blocked (Park et al., 2004). Interestingly the LTP-induced increase in AMPAR expression are maintained in position by an increase in insertion of proteins referred to as 'slot proteins', such as PSD-95 and TARP, into the plasma membrane (Shi et al., 2001; Lisman and Raghavachari, 2006).

1.3.2 (B) Structural changes in dendritic spines

1.3.2.1 Dendritic spines

Dendritic spines are small actin-rich protrusions that form the postsynaptic part of most excitatory synapses and are major sites of information processing (Figure 1. 2). These small micrometre structures are located along neuronal dendrites of certain cell types, such as excitatory pyramidal neurones. They were first discovered and visualised by Cajal in 1888 (Ramon y Cajal, 1888; Ramón y Cajal, 1909; Garcia-Lopez et al., 2007) using the Golgi staining system which impregnate neurones with potassium dichromate and silver nitrate.

Their morphological traits are as follows; they have a ‘neck’ which protrudes from the dendritic shaft followed by a ‘head’ at the tip of the spine which retains the postsynaptic density (PSD) (Figure 1. 6). The PSD is the protein-rich active zone of the spine which contains all the machinery required for synaptic transmission. It anchors and clusters glutamate receptors as well as concentrating adhesion, signalling and scaffolding proteins which are required to regulate the actin cytoskeleton and therefore the structure of the spine (Sheng and Hoogenraad, 2007).

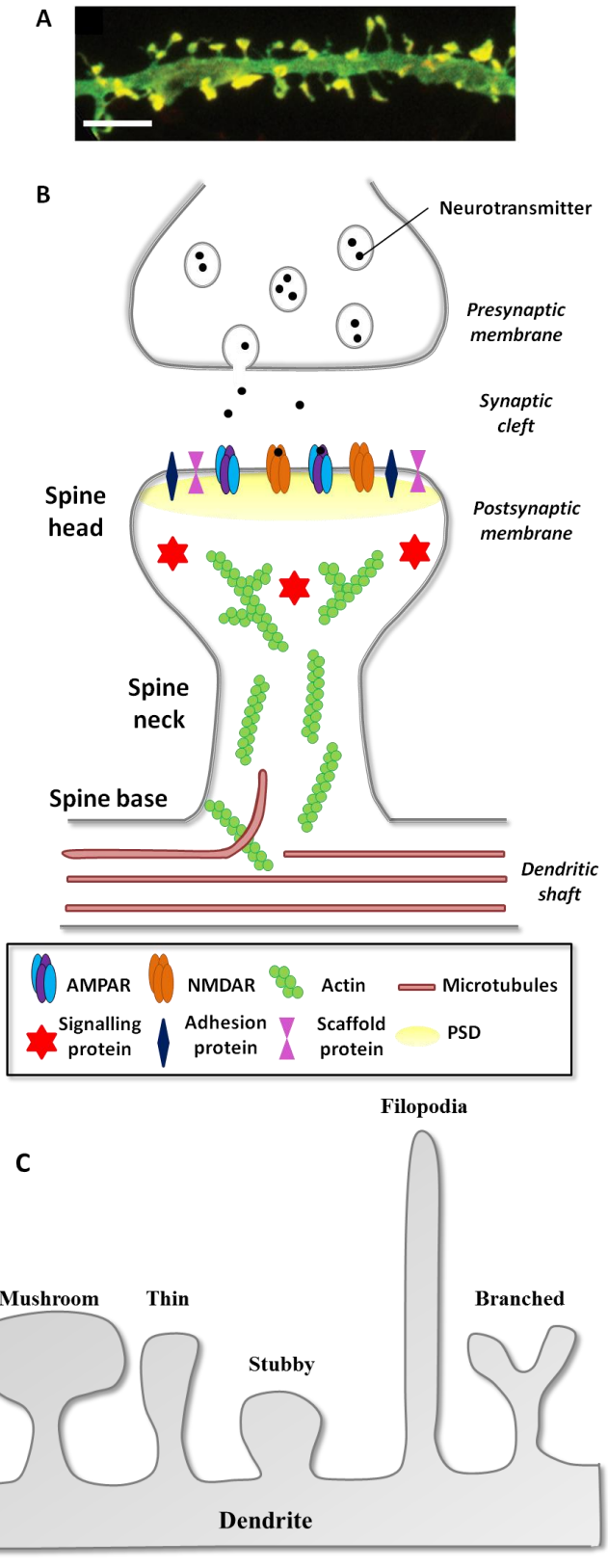

Figure 1.6 A figure representing the structure of dendritic spines and the different classifications. ***(A)*** *An image taken from (Hotulainen and Hoogenraad, 2010) showing the dendritic spine morphology (green) and the localisation of F-actin which was stained in red in cultured hippocampal neurones. The yellow is the merged red and green panels showing that actin is located at the spines. Scale bar; 5 µm.* ***(B)*** *A schematic representation of the organisation of a dendritic spine. A*

presynaptic membrane will form a synapse with the postsynaptic membrane. The presynaptic membrane contains the neurotransmitter vesicles. Upon neuronal activation, an action potential is elicited which induces an influx of calcium ions which allows the vesicles to fuse with the membrane to release neurotransmitters into the synaptic cleft. In the postsynaptic membrane, at the spines head there is the PSD which clusters and anchors glutamate receptors (e.g. AMPAR and NMDAR), as well as scaffolding proteins and adhesion proteins. The spine also contains actin filaments which regulate the morphological structure of the spine. The actin network is spread in the spines base, constricted in the neck and branches in the spine head. The spine is also filled with signalling molecules which regulate the actin dynamics. The dendrites have microtubules running down their shaft which allows the transport of proteins to and from the cell body and spine. In mature spines the microtubules are dynamic and move into the spine neck ***(C)*** *This figure demonstrates the range of spine morphologies. Mushroom shaped spines have a large head and narrow neck. Thin spines have a smaller head and a narrow neck and stubby spines show no constriction between the head and the attached to the shaft. Immature filopodia spines have extended necks without an obvious head. A branched spine has two heads which have originated from the same point along the dendritic shaft. [AMPAR; α-amino-3-hydroxy-5-methyl-4-iso-xazolepropionic acid receptor, NMDAR; N-methyl-D-aspartic acid receptor, PSD; Postsynaptic density]*

Spines occur at a density of around 1-10 spines per µm of dendrite length (Sorra and Harris, 2000) and can vary from 0.001 μm^3 volume to 1 μm^3 and 0.2 µm to 2 µm in length (Hotulainen and Hoogenraad, 2010). There is a diverse range of different spine morphologies which have been classified according to their relative neck and head size (Peters and Kaiserma, 1970). There are three main categories of spines (Figure 1.6 C); thin, filopodia-like structures (‘thin’), short without a well-defined spine neck (‘stubby’) and large bulbous head spines (‘mushroom’). There are also two sub categories which include spines with long and thin necks with a small head (‘filopodia’). The filopodia spines are categorised as immature and sometimes does not contain a PSD. The last category are spines with a shared neck but branches into two separate heads (‘branched’) (Bourne and Harris, 2008).

1.3.2.2 Molecular mechanisms involved in the regulation of the actin cytoskeleton in dendritic spines

Spine morphology is regulated by actin polymerisation which is associated with different forms of synaptic plasticity. For example, new spines and the enlargement of existing spines will occur in response to LTP-inducing stimuli (Matsuzaki et al., 2004; Nagerl et al., 2004; Okamoto et al., 2004). In contrast, LTD

is associated with shrinkage and/or retraction of spines (Zhou et al., 2004). The mechanism influencing spine morphology involves a shift in actin equilibrium. LTP is associated with a shift towards F-actin (filamentous actin) where actin is polymerised into a filmentous form allowing the enlargment of spine head and thus the recruitment of more AMPAR to the cell surface. In this case a protein known as profilin, promotes actin polymerisation and the Arp2/3 complex induces nucleation of new actin filaments causing them to branch (Okamoto et al., 2004). In contrast, during LTD a shift in actin equilbrium occurs favoring a monomeric G-actin (globular actin) state resulting in spine loss or shrinkage. This may involve a actin severing protein known as ADF (actin depolymerizing factor)/cofilin (Zhou et al., 2004).

This dynamic regulation of actin is controlled by many intracellular proteins, ranging from molecular motor proteins, actin binding proteins, GTPases, MAPK as well as adhesion and scaffolding proteins (Tada and Sheng, 2006). All of which are largely concentrated in the dendritic spine. For example, the motor protein mysoin VI has been found to be enriched in PSD preparations and thought to regulate spine morphology. This has been highlighted in a study carried out in mice lacking myosin V1 in which their hippocampal neurones exhibited abnormally short spines and reduced synapse number (Osterweil et al., 2005). The protein, cortactin has been shown to play an important role in spine morphology as it binds to F-actin. It is also an activator of the Arp2/3 complex which interacts with the PSD scaffolding protein, Shank, thus concentrating it in the spines. Using short- interfering RNA to knockdown cortactin in hippocampal neurones showed a reduction of dendritic spines. As oppose to when cortactin was over expressed the dendritic spines were elongated (Hering and Sheng, 2003).

There are families of GTPases which actively regulate the actin cytoskeleton through different signalling pathways. The Rho family (e.g. RhoA, Rac1 and Cdc42) have a profound influence on dendritic and spine morphogenesis (Newey et al., 2005). For example the introduction of a constitutively active RhoA construct in pyramidal neurones from cultured murine coritcal and hippocampal slices, reduced spine density and length, indicating that RhoA has a negative effect on spine formation and morphology (Tashiro et al., 2000). On the other hand, when Rho was inhibited using a C3 exoenzyme, an increase in density and length of spines was observed (Tashiro et al., 2000). As these GTPases clearly effect dendritic and spine

structure, they have subsequently been associated with mental retardation diseases (Newey et al., 2005). Upstream to the Rho family of GTPases are guanine nucleotide exchange factors (GEF) and GTPase activating proteins (GAP) which appear to regulate Rho GTPases postsynaptically. For example, Rac can be locally activated in the dendritic spines by a GEF known as PIX (a-p21-activated kinase [PAK] interacting exchange factor) shown using FRET in hippocampal culture (Zhang et al., 2005). A newly identified GEF for Rho family GTPases, GEFT, is expressed across the brain and has been shown to cause dendritic spine enlargement thought to be Rac and Cdc42-PAK dependent (Bryan et al., 2004).

A member of another family of GTPase, the Ras family, known as Rap1 has been implicated in regulating AMPAR trafficking by inducing the removal of receptors from the synaptic membrane (Zhu et al., 2005). Rap1 is also associated with activating spine lengthening and thinning in response to NMDA activation, consistent with a reduction in AMPAR surface expression (Xie et al., 2005; Zhu et al., 2005). It appears that Rap1 regulates the removal of GluA2/3 AMPAR in an p38 MAPK dependent manner during LTD (Zhu et al., 2002; Zhu et al., 2005). Opposing a closely related GTPase, Ras appears to promote LTP by regulating the insertion of GluA1 and GluA2L into the synaptic membrane via ERK1/2 MAPK (Zhu et al., 2005).

The scaffolding protein, Shank, can also regulate spine morphology presumably by recruiting interacting proteins to postsynaptic sites (Sheng and Kim, 2000). Using RNA interference to knockdown Shank in hippocampal neurones, there was a reduction in spine density. Astonishingly when Shank was overexpressed in cerebellar neurones which are normally non-spiny, there was an appearance of functional dendritic spines (Roussignol et al., 2005). Another protein known as N-cadherin, an adhesion molecule localised at the PSD has been shown to be important during depolarisation-induced spine enlargement (Okamura et al., 2004). Cadherin's activity depends on the cytoplasmic catenins to link cadherin to the actin cytoskeleton. For example β-catenin is recruited to the spines and cadherin by tyrosine dephosphorylation e.g. receptor tyrosine phosphatase which are required for spine and synapse development, shown in cultured rat hippocampal neurones (Dunah et al., 2005). This study also showed that the role of β-catenin linked the morphology and functional changes in the synapses as it complexes with AMPAR.

1.3.2.3 Dendritic spines during development

During early development there are striking changes in spine morphology and density. During synaptogenesis where neurones are forming synapses, small protrusions start to emerge from the dendritic shaft known as filopodia spines (Fiala et al., 1998). These filopodia spines are longer than other spines as they can reach up to 10 µm long in early development allowing them to seek to form nascent synapses with axons or other axonal filopodia. They are also highly motile and 'plastic' as they are able to extend and retract within 10 minutes which was visualised using time lapse fluorescent microscopy (Dailey and Smith, 1996). During development there are significant changes in spine density where the number of spines doubles from postnatal day (P) 1 to P15 in CA1 pyramidal cells (Harris et al., 1992). The distribution of spines also changes, where the number and length of filopodia spines decrease. Therefore more mature and stable spines with reduced motility are present later on in development.

The molecular mechanism behind these dynamic changes has been principally attributed to the actin cytoskeleton. For example, in mature spines the majority of branched F-actin is focused in the spine head which can increase the spine volume (Korobova and Svitkina, 2010). The dynamics of branching actin filaments is highly regulated and supported by other proteins concentrated in the dendritic spine. These include the actin related protein 2/3 complex (Arp2/3) which is the main nucleator of F-actin filaments i.e. controls the branching mechanism, as well as its activators (Goley and Welch, 2006) and ADF (actin-depolymerising factor)/cofilin which induces actin depolymerisation (Hotulainen et al., 2005).

So far it is clear that dendritic spines are dynamic and 'plastic' structures which are tightly regulated during development exhibiting morphological changes potentially linking to their function. I*n vivo* experiments showed that if one eye of a mouse was deprived of visual stimulation (e.g. monocular deprivation) during the critical period of development, the spine density in the binocular zone of the visual cortex was reduced and the motility of the spines was increased (Mataga et al., 2004; Oray et al., 2004). Morphological changes *in vivo* occur when inhibiting sensory input into visual cortex (e.g. dark rearing of animals) spine density is reduced but spine head width is increased when compared to the light reared animals (Wallace and Bear, 2004).

1.3.2.4 Functional role of dendritic spines

Changes in dendritic spine morphology have been shown to regulate neuronal synaptic output (Yuste and Bonhoeffer, 2001). Furthermore it is thought that structural alterations of spines play an important role in synaptic plasticity (Okamoto et al., 2004; Tada and Sheng, 2006; Cingolani et al., 2008). During LTP, neuronal transmission is increased leading to enlargement of pre-existing spines or the synthesis of new spines which is controlled by the actin cytoskeleton (Engert and Bonhoeffer, 1999; Maletic-Savatic et al., 1999). This was shown in CA1 neurones where a dense concentration of F-actin was found in the spines following theta burst stimulation (TBS)-induced LTP (Okamoto et al., 2004; Lynch et al., 2007). In contrast, LTD promotes smaller headed-spines which contribute to weak or silent connections.

Interestingly the large mushroom-shaped spines found after exposure to LTP-inducing conditions have been referred to as 'memory' spines as they are more stable, as opposed to the small and thin spines which appear to be more plastic and therefore called 'learning' spines. The strength of the synapse has been related to the trafficking of AMPAR in the PSD of the spine head. Following LTP these larger spines will harbour increased levels of a AMPAR which may contribute to the potentiation of synaptic transmission (Shi et al., 1999).

1.3.3 (C) Molecular signalling mechanisms during synaptic plasticity

LTP can be induced by high-frequency stimulation (HFS) which will increase glutamate release, while the coincident depolarisation relieves the Mg^{2+} block of the NMDA receptor. This causes an influx of calcium ions through the NMDA channel thus inducing an intracellular signalling cascade. The rapid rise in intracellular calcium triggers the activation of several enzymes which are important in the induction of LTP (Purves et al., 2012). One of these enzymes is the calcium dependent protein kinase II (CaMKII) which phosphorylates the GluA1 CT tail triggering the insertion of the AMPAR into the synapse (Sweatt, 1999; Minichiello, 2009). α-CaMKII knock out (KO) mice were deficient in their ability to produce LTP but some slices from these mutant mice showed normal LTP which was later shown to be due to the upregulation of the β isoform (Silva et al., 1992; Hinds et al., 1998).

Further to this study another transgenic mouse was created where CaMKII had a point mutation at threonine 286 (T286) which inactivated the ability of CaMKII to autophosphorylate. These mice were unable to undergo NMDA-dependent LTP as well as abolished spatial learning in the Morris water maze test (Giese et al., 1998). The later stage of LTP has been shown to involve local dendritic protein synthesis and nuclear transcription (Sutton and Schuman, 2006). There are three phases to long lasting-LTP and according to David Sweatt, the first is known as short term potentiation which is independent of kinase activity for its induction or expression and lasts up to 30-45 minutes. The second phase is called early LTP (E-LTP) which starts around 30 minutes or less after stimulation and is over 2-3 hours later. This process is dependent on persistent protein kinase activation. The final stage, late LTP (L-LTP) can last for many hours and is dependent on gene expression (Sweatt, 1999). In each of these phases there are tailored signalling cascades for the induction, maintenance and expression of LTP. The signalling mechanisms involved are protein kinases such as protein kinase A (PKA), CaMKIV and extracellular signal-regulated kinase (ERK) which signal to the nucleus to activate transcription factors such as cyclic AMP response element‑binding protein (CREB) which regulate the gene transcription of proteins required for the maintenance of LTP (Thomas and Huganir, 2004).

1.4 Another form of synaptic plasticity; Homeostatic scaling

1.4.1 Overview of homeostatic scaling

Homeostatic plasticity is a mechanism by which a neuronal population maintains their synaptic activity within physiological equilibrium. Neurones can sense and adjust their neuronal output in response to perturbations in synaptic activity. This is especially important for Hebbian plasticity as it functions as a positive feedback process therefore allowing potentially unconstrained/'runaway' excitation or quiescence of synapses. In order to stabilise this unconstrained activity within a neuronal network a homeostatic mechanism is fundamental to bring neuronal firing rates into equilibrium (Turrigiano, 2008). This process is also known as synaptic scaling where a neurone/population of neurones senses changes in synaptic activity and consequently alter their own properties (e.g. synapse number or

strength) in order to stabilise their activity (Turrigiano and Nelson, 2004; Turrigiano, 2008; Siddoway et al., 2013).

Chronic inhibition of synaptic activity using tetrodotoxin (TTX), a voltage gated sodium channel blocker in neuronal culture causes an increase in amplitude of miniature excitatory postsynaptic currents (mEPSC), known as up-scaling (OBrien et al., 1998; Turrigiano et al., 1998; Thiagarajan et al., 2005; Shepherd et al., 2006; Ibata et al., 2008; Turrigiano, 2008) (Figure 1.7). A mEPSC is the postsynaptic response to the spontaneous release of an individual vesicle containing neurotransmitter. So a change in mEPSC amplitude is generally interpreted as a change in receptor number or conductance at the postsynaptic membrane. Conversely, one way of inducing down-scaling is when GABA (γ-aminobutyric acid)-mediated inhibition (e.g. bicuculline or picrotoxin, $GABA_A$ receptor antagonists) is inhibited causing a reduction in amplitude of mEPSC (Lissin et al., 1998) (Figure 1.7). Homeostatic scaling has been studied *in vivo* in the visual cortex either through dark rearing or injecting TTX into the eye where there was an increase in synaptic activity within the visual cortex (Hubel and Wiesel, 1970; Maffei and Turrigiano, 2008; Pozo and Goda, 2010). Similarly exposure to an enriched environment thus stimulating different sensory and motor stimuli will induce experience-dependent scaling and thus altering neuronal morphological properties (Rosenzweig et al., 1978; Bennett et al., 1996; Pinaud et al., 2001b; Faherty et al., 2003; Chotiner et al., 2010).

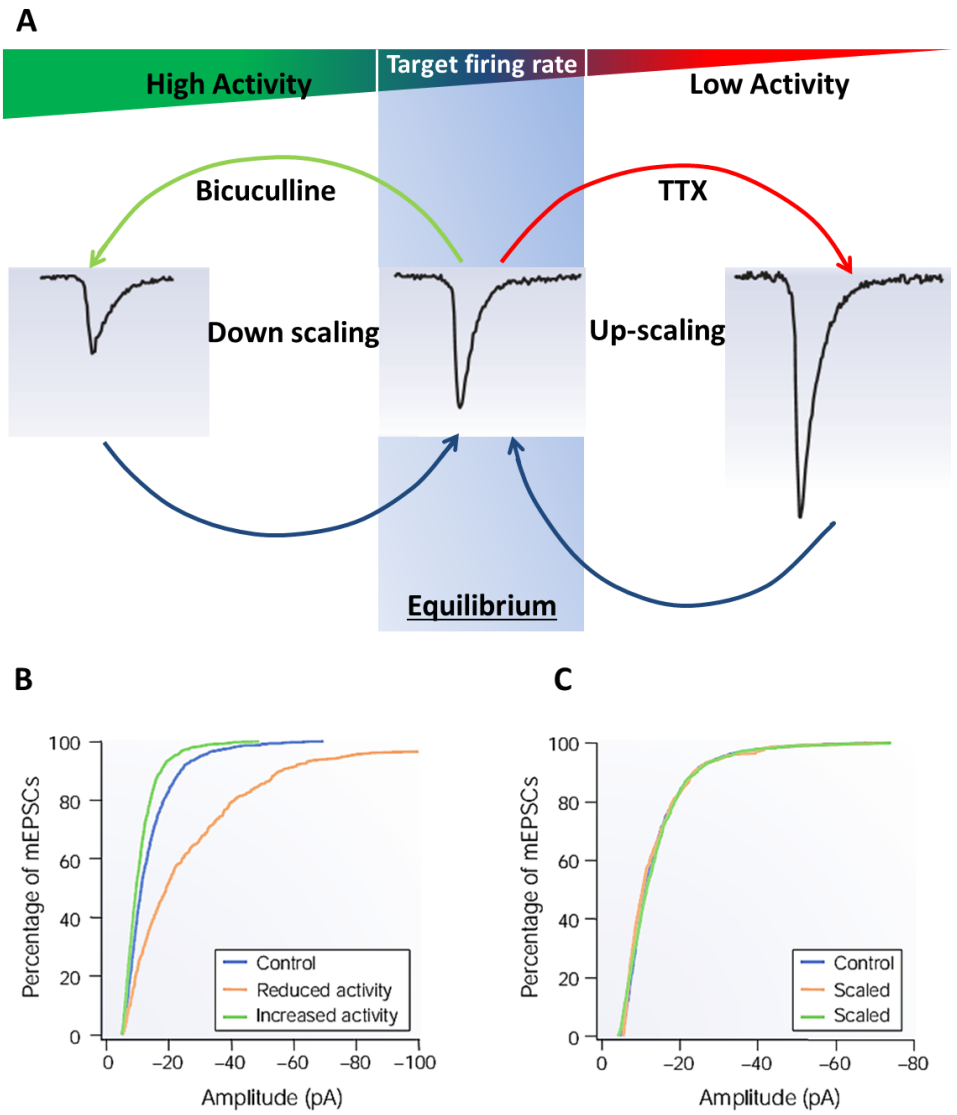

Figure 1.7; Homeostatic scaling model. (A) *Homeostatic model for stabilising firing rates through regulating synaptic drive. When an individual neurone increases its firing rate (e.g. in the presence of Bicuculline, green arrow) above equilibrium firing rate, homeostasis will reduce the strength of inputs (blue arrow) back to target firing rate (blue box). The same principle applies to when a neurone declines in firing rate below the threshold (e.g. in the presence of TTX, red arrow), the input strength is increased (blue arrow)* ***(B)*** *and* ***(C)*** *represent mEPSC recordings. To study the changes in neuronal synaptic transmission in response to altered activity it is necessary to measure mEPSC* ***(B)*** *An increase in activity (Bicuculline) induces a reduction in mEPSC amplitude within cortical pyramidal neurones and a decrease in activity (TTX) shows the opposite effect. The graphs represent cumulative histogram of mEPSC amplitudes, where a reduction of activity (red trace) increases the distribution of larger mEPSC amplitudes i.e. up-scaling. As for an increase in activity (green trace), mEPSC amplitudes decrease where the trace shifts to the left, i.e. down -scaling.* ***(C)*** *The graph shows that the mEPSC have 'scaled' to control physiological values in response to either TTX or Bicuculline i.e. homeostatic scaling.[TTX; Tetrodotoxin, mEPSC; Miniature excitatory postsynaptic currents] [Adapted from (Turrigiano and Nelson, 2004)].*

1.4.2 AMPAR trafficking and signalling during homeostatic scaling

Homeostatic scaling of excitatory synapses have also been attributed to bidirectional AMPAR trafficking indicating a postsynaptic effect (Figure 1.8) but there is also some evidence of a presynaptic role (Turrigiano and Nelson, 2004; Wang et al., 2012).

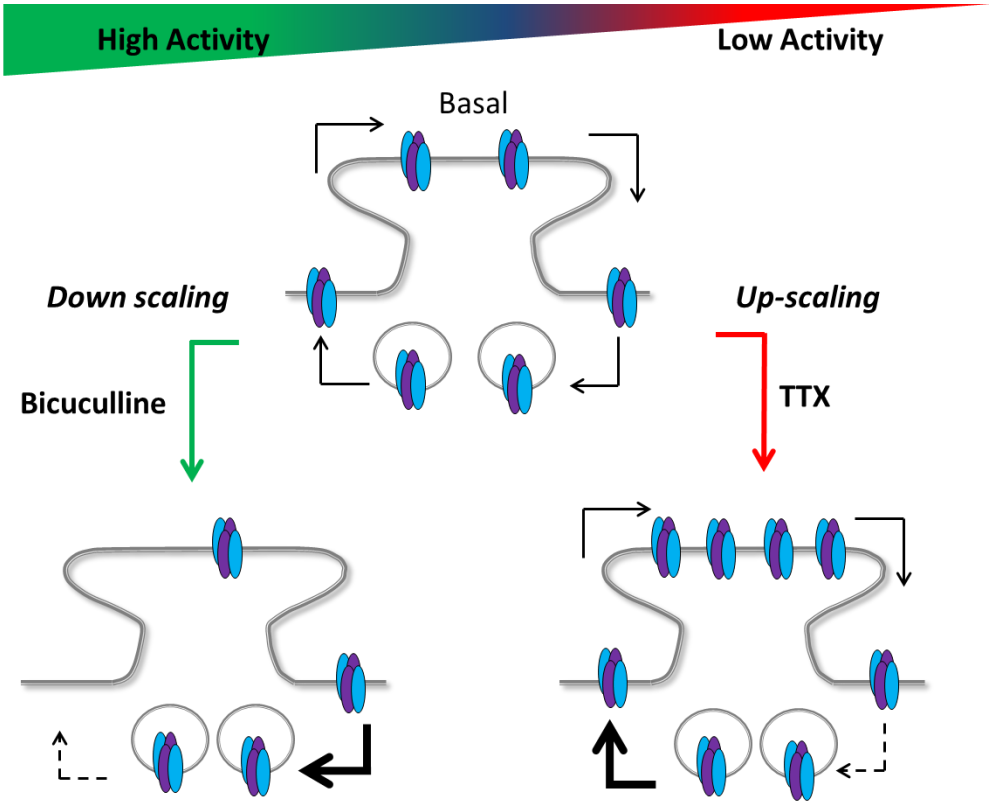

Figure 1.8 Homeostatic bi-directional regulation of AMPAR trafficking*. Under basal conditions, constitutive receptor trafficking occurs. However when a neuronal population is incubated with a $GABA_A$ antagonist, e.g. bicuculline for 1-2 days the number of surface AMPAR is reduced because the rate of insertion is decreased (dotted line) or the rate of internalisation is increased (thick arrow). In contrast when neurones are faced with synaptic deprivation via TTX-incubation where the rate of insertion is increased (bold arrow) or the rate of internalisation is decreased (dotted line) therefore increasing surface AMPAR expression.[TTX; Tetrodotoxin]*

Recent studies demonstrate different surface AMPAR expression through N-terminus AMPAR immunocytochemistry and by tracking fluorescently-tagged AMPAR subunits (Wierenga et al., 2005; Hou et al., 2008; Ibata et al., 2008). Exposure of neurones to TTX demonstrates an increase in surface AMPAR subunits as well as an increase in mEPSC amplitude (Figure 1.7 and 1.8). In the literature there appear to be discrepancies between trafficking of different AMPAR subunits e.g. GluA1 versus GluA2, which may reflect different brain regions examined, the methodology used or developmental stage of the neurones (Turrigiano, 2008; Pozo

and Goda, 2010). AMPAR composition is important especially as it dictates whether the receptor is calcium permeable or impermeable for example the GluA2 subunit confers calcium impermeability (Anggono and Huganir, 2012). It is important that neurones maintain appropriately low cytoplasmic levels of calcium under basal levels of stimulation (Isaac et al., 2007). Therefore trafficking of different AMPAR subunits could affect transient changes in AMPAR-mediated calcium influx which could subsequently affect downstream calcium signalling pathways induced during homeostatic scaling.

Several research groups have shown an increase in GluA2 subunit after incubating cortical neurones with TTX (Ibata et al., 2008; Gainey et al., 2009). On the other hand, an increase in GluA1 surface receptors was observed in TTX-treated hippocampal neurones (Hou et al., 2008). Both demonstrated an increase in mEPSC amplitude (Shepherd et al., 2006). The site of trafficking of GluA2-lacking AMPAR has recently been shown to expand from the synapse to extrasynaptically and somatically located in CA1 pyramidal neurones (Soares et al., 2013). The controversy of subunit-specific trafficking during scaling has been highlighted further in a recent study showing that scaling can recruit any AMPAR regardless of their subunit composition. This was shown in GluA1, GluA2, GluA3 and Glu4 KO hippocampal neurones which were still able to scale accordingly (Altimimi and Stellwagen, 2013). These opposing observations leads us to ask ourselves, is there a general or localised homeostatic mechanism?

The molecular profile of this upregulation of GluA1 surface receptor expression during chronic synaptic deprivation is still not clear (Turrigiano, 2008). There have been several proposed scaling mechanisms involving; retinoic acid (RA) production and activation of its receptor, RARα which mediate the increase in GluA1 synthesis and accumulation during TTX (Aoto et al., 2008), β3 integrins which regulate AMPAR surface expression (Cingolani et al., 2008), PICK1 regulates pool size of intracellular receptors (Anggono et al., 2011) and PSD-95 and 93 have been shown to stabilised AMPAR at synaptic sites (Sun and Turrigiano, 2011; Turrigiano, 2012). PICK1 is thought to regulate GluA2 specific trafficking by restricting its recycling (Lin and Huganir, 2007), which is also required for LTP expression (Terashima et al., 2008). A recent paper has shown that PICK1 also participates in homeostatic scaling in regulating AMPAR composition and abundance (Anggono et al., 2011). They found that TTX-treated hippocampal neurones demonstrated

reduced levels of PICK1 protein which correlated with accumulation of surface AMPAR. Furthermore, electrophysiological recordings of AMPAR-mediated mEPSC showed that TTX-induced scaling is occulded in PICK1 KO mice/PICK1 knockdown neurones due to altered subunit composisiton and abnormal trafficking of GluA2-containing AMPAR.

Another three scaling mechanisms proposed was calcium (Ca^{2+}) signalling (Tanaka et al., 2008), BDNF (brain-derived neurotrophic factor) signalling and the release of tumor necrosis factor α (TNFα) from astrocytes. The first supposed mechanism involves Ca^{2+} signalling via L-type calcium channels, reduced activation of calcium/calmodulin-dependent protein kinase kinase (CaMKK) and CaMKIV as well as a derepression of a 'scaling factor' gene (Turrigiano, 2008). In parallel, the neurotrophin, BDNF appears to have a role in the early (<24 hours) TTX -induced synaptic scaling, which is unlikely to involve L-type calcium channels (Rutherford et al., 1998; McCutchen et al., 2002). This process involves a reduction in BDNF release and thus TrkB receptor activation during TTX-induced up-scaling ultimately increasing surface GluA1 expression (OBrien et al., 1998). The third suggested mechanism involves protracted role for TNFα release from astrocytes after 48 hours of TTX incubation (Stellwagen and Malenka, 2006).

1.5 Brain-derived neurotrophic factor (BDNF)

1.5.1 BDNF, TrkB receptors and signalling cascades

BDNF is a secreted neurotrophin which is part of growth factor family. Neurotrophins are important in neuronal survival, differentiation and development. The highest expression levels in the mammalian brain is localised in the hippocampus, including neurones and glial cells (Murer et al., 2001). BDNF is secreted in an activity-dependent manner as either a precursor known as pro-BDNF or in a mature form (Chao and Bothwell, 2002; Ibanez, 2002). The pro-BDNF will bind with a high affinity to p75NTR receptor as opposed to the mature form which binds to the tyrosine kinase known as tropomyosin receptor kinase B (TrkB) (Fayard et al., 2005) which also binds other neurotrophins such as neurotrophin-4 (NT-4) and -3 (NT-3) (Chao and Bothwell, 2002; Huang and Reichardt, 2003; Lessmann and Brigadski, 2009).

TrkB dimerises upon ligand binding followed by autophosphorylation of tyrosine residues found in the intracellular receptor kinase domain (Minichiello, 2009). There are distinct pathways which are triggered upon BDNF binding to TrkB, these include phosphoinositide 3-kinase (PI3K), phospholipase Cγ1 (PLCγ1) and MAPK (mitogen-activated protein kinase) (Huang and Reichardt, 2003) (Figure 1.9). A very elegant study was carried out to depict these TrkB-dependent pathways which involved mutating specific tyrosine resides in the kinase receptor domain of the TrkB receptor. Using this technique it was shown that tyrosine residue 515 recruited the adaptor protein, SH2-containing collagen-related proteins (Shc) which induced Ras (Rat sarcoma protein)/MAPK and the PI3K signalling pathways (Figure 1.9). The PLCγ signalling pathway was dependent on the phosphorylation of another tyrosine residue, 816 (Minichiello et al., 2002). The phosphorylation of other tyrosine residues at 705/706 via SFK (Src family kinase) was shown to activate TrkB receptor. Upon BDNF-activation of TrkB receptor the SFK is phosphorylated which then phosphorylates the Y705/706 in a feedback mechanism (Huang and McNamara, 2010).

The BDNF-TrkB induced intracellular signalling pathways will regulate both gene transcription as well as protein synthesis (Figure 1.9). The binding to TrkB has been attributed to the BDNF-dependent synaptic effects observed. When hippocampal neurones were exposed to BDNF, the expression of surface TrkB receptor increased within seconds (Haapasalo et al., 2002). This has been speculated to selectively modulate active synapses (Nagappan and Lu, 2005). The three main functions of BDNF are either a presynaptic effect on the rate of neurotransmitter release, increasing the phosphorylation of NMDA receptor subunits, NR1 and NR2B and up-regulating the expression and phosphorylation of AMPAR (Tyler et al., 2002) all of which lead to enhanced synaptic transmission.

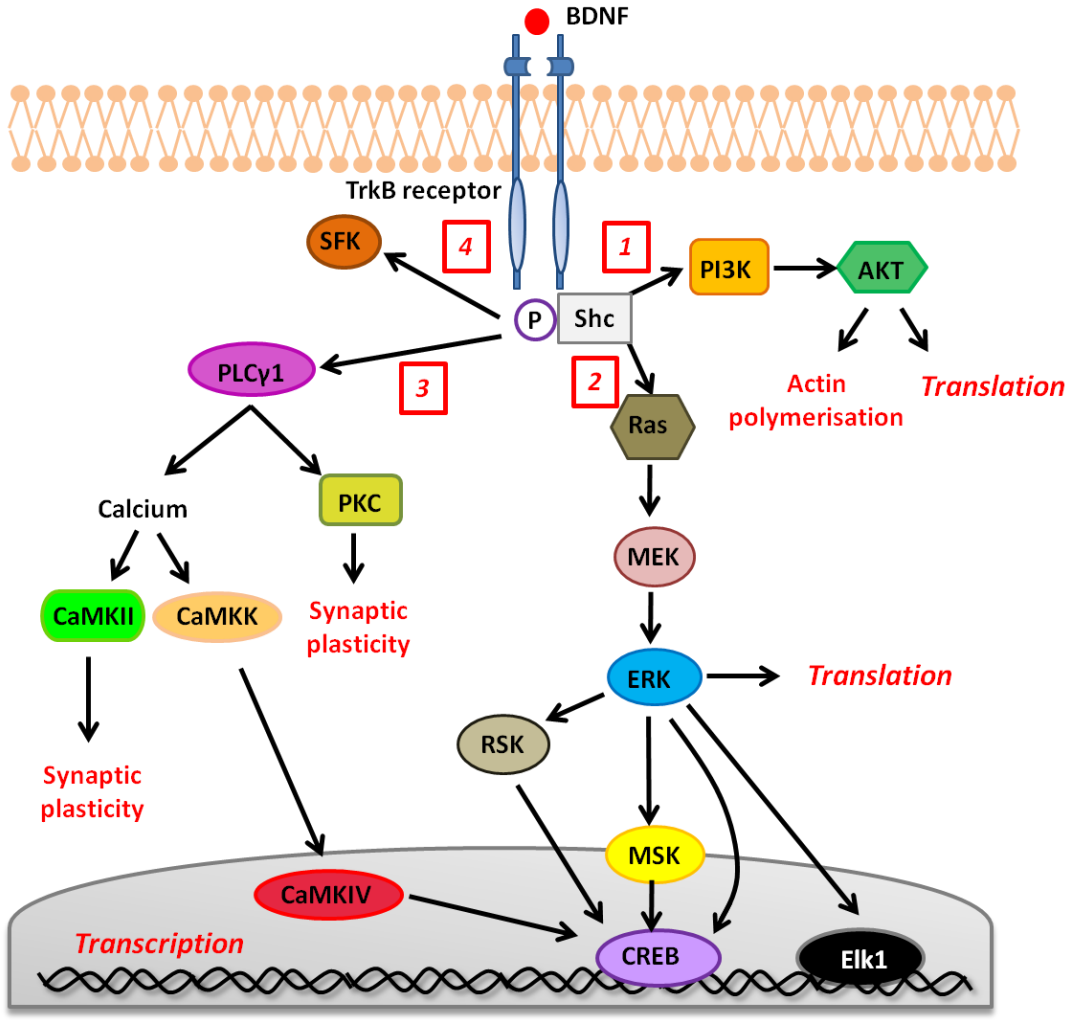

Figure 1.9; A highly simplified version of the intracellular signalling cascades induced by the binding of BDNF to TrkB receptor. *The TrkB receptor autophosphorylates via intracellular tyrosine kinase domains upon BDNF binding. There are three main signalling cascades that are induced;* ***(1)*** *PI3K,* ***(2)*** *Ras-MAPK* ***(3)*** *PLCγ1 via both CaMK and PKC. The fourth pathway involves the phosphorylation of SFK* ***(4)****.* ***(1)*** *When tyrosine residue 515 is phosphorylated on the CT tail of TrkB receptor, adaptor proteins are recruited including Shc, allowing the activation of PI3K. Subsequent activation of AKT induces downstream signalling molecules to regulate actin polymerisation and protein translation.* ***(2)*** *Another pathway involving the phosphorylation of the same tyrosine 515 residue along with the adaptor protein recruitment, Shc, but in this case the activation of Ras followed by MEK is induced. MEK will phosphorylate the MAPK ERK1/2 which is able to induce multiple downstream signalling cascades. ERK1/2 is able to regulate protein translation via a downstream signalling pathway or gene transcription through activation of RSK or MSK thus regulating CREB phosphorylation. ERK1/2 has been shown to regulate gene transcription directly through CREB phosphorylation or via the transcription factor Elk1.* ***(3)*** *When the tyrosine residue, 816 is phosphorylated it will recruit and activate PLCγ1 which induces the release of intracellular calcium. The calcium ions will activate downstream CaMKs either CaMKII which is involved in synaptic plasticity and is translated upon LTP induction. The other CaMK involved is CaMKK which activates CaMKIV which localises principally to the nucleus and regulates CREB phosphorylation controlling gene transcription. The other pathway activated by PLCγ1 is PKC which is also involved in synaptic*

plasticity where it can modulate the phosphorylation of AMPAR and thus their trafficking. ***(4)*** *When TrkB is activated this promotes the association of Src family kinase (SFK) and TrkB in which the SFK activity mechanism has yet to be identified. Activated SRFKthen feedback and promote full activation of TrkB through facilitating phosphorylation of tyrosine residue 705/706 (Huang and McNamara, 2010). [Ras; Rat sarcoma protein, MEK; Mitogen-activated protein kinase kinase, ERK; Extracellular signal-regulated kinase, RSK; 90 kDa ribosomal S6 kinase, MSK; Mitogen-and stress-activated protein kinase, PLCγ1; Phospholipase Cγ1, CaMKK; Calcium/calmodulin-dependent protein kinase kinase, CaMK; Calcium/calmodulin-dependent protein kinase, BDNF; Brain-derived neurotrophic factor; TrkB; Tropomyosin receptor kinase, CT; C-terminus, PI3K; Phosphoinositide 3-kinase, PKC; Protein kinase C, AKT; Serine threonine kinase or protein kinase B, Elk1; E-26-like protein 1, CREB; Cyclic AMP response element-binding protein, SFK; Src family kinase, Shc; SH2-containing collagen-related proteins] [Adapted from (Finkbeiner et al., 1997; Bramham and Messaoudi, 2005; Minichiello, 2009)].*

1.5.2 BDNF-dependent transcriptional and translational control

When BDNF is applied to a population of neurones, the transcription factor CREB is rapidly phosphorylated at the residue S133 which is one of its transcriptional regulatory sites, as well as inducing CREB to bind to CRE allowing gene transcription (Finkbeiner et al., 1997). The majority of the transcriptional effects are modulated in an ERK-dependent fashion. The signalling pathway involved is ERK-Elk1 (E-26-like protein 1) which regulates transcription of plasticity-related genes (Bramham et al., 2010). Another important BDNF-dependent transcriptional regulatory site is the serum response factor (SRF)-mediated transcription (Kalita et al., 2006). An important property of BDNF is that it is able to regulate its own expression and release allowing hippocampal neurones to recycle BDNF so it can be released again (Santi et al., 2006).

The control of local translation of synaptic plasticity related genes has been shown to play a role in different forms of plasticity (Bramham and Messaoudi, 2005). BDNF stimulation induces an ERK signalling cascade which was demonstrated using a dominant negative MEK1 transgenic mouse which showed impaired ERK-dependent translational induction (Kelleher et al., 2004) (Figure 1.9). The BDNF-dependent translation regulates local mRNA such as αCaMKII, Arc (activity-regulated cytoskeleton-associated protein) and Homer 2 which are all involved in different forms of synaptic plasticity (Aakalu et al., 2001; Ying et al., 2002; Schratt et al., 2004).

1.5.3 Functional roles of BDNF

BDNF plays a role in synaptic plasticity and development which has been shown using BDNF homozygous KO mice who don't survive past 3 weeks of age (Ernfors et al., 1994). Using BDNF heterozygous KO mice allowed the mice to survive longer and to monitor their spatial learning using Morris water maze test in which they demonstrated impaired spatial learning (Linnarsson et al., 1997). The importance of BDNF during LTP was shown amongst many studies including the experiments using BDNF KO mice at P14, before their lethality at P21, showing impaired LTP induction in the CA1 region of the hippocampus (Patterson et al., 1996). The binding of BDNF to TrkB receptor is important as LTP induction was impaired in the presence of antibodies which inhibit the activation of the TrkB receptor (Figurov et al., 1996).

The activity-induced release of BDNF not only affects synaptic transmission but these changes are also observed as structural changes in dendritic spines. When BDNF was applied exogenously to organotypic hippocampal cultures it caused an upregulation of spine density in CA1 pyramidal neurones (Tyler and Pozzo-Miller, 2001) as well as changes in spine morphology (Tyler and Pozzo-Miller, 2003). The changes were shown to be ERK1/2- dependent were MEK inhibitors such as PD98059 and U0126 completely prevented BDNF-induced increase in spine density in hippocampal neurones (Alonso et al., 2004). These structural changes can be linked back to the direct effect of BDNF on the actin cytoskeleton. BDNF induces a signalling cascade which causes rapid phosphorylation of cofilin and therefore its inactivation allowing actin polymerisation to branch and cause spine enlargement often seen after LTP (Figure 1.9) (Messaoudi et al., 2007; Rex et al., 2007).

BDNF was one of the first molecules to be identified to play a potential role in homeostatic scaling (Rutherford et al., 1998). This was demonstrated in cortical neurones where exogenously applied BDNF prevented neurones from up-scaling their mEPSC amplitude in response to synaptic deprivation. Furthermore when a TrkB receptor scavenger was incubated with neuronal cultures, thus blocking activation of endogenous BDNF receptors, the neurones were unable to up-scale their synaptic strengths (Rutherford et al., 1998). This data suggests that one signalling pathway required to up-scale excitatory synaptic strengths in response to neuronal deprivation is a reduction in the release of BDNF by cortical pyramidal

neurones. Interestingly data has shown that reducing BDNF levels does not modulate homeostatic down-scaling and therefore its actions are limited to up-scaling. This was shown when blocking BDNF signalling using a TrkB-IgG scavenger so endogenous BDNF could not bind to its receptor, did not affect mEPSC down-scaling following chronic depolarisation in rat cortical neurones (Leslie et al., 2001).

BDNF can thus activate a range of intracellular signalling cascades upon binding to its TrkB receptor, regulating transcription of plasticity-related genes followed by their translation. Yet our understanding of many of these pathways is still incomplete. Identifying these pathways could reveal novel downstream mediators of gene transcription during different forms of synaptic plasticity.

1.6 Mitogen- and stress-activated protein kinase (MSK)

Mitogen-and stress-activated protein kinase (MSK) has two isoforms (1 and 2) which have 75% amino acid homology (Deak et al., 1998), where MSK1 is highly expressed in the whole brain and the hippocampus especially when compared to other organs such as liver and lungs (Arthur et al., 2004; Chwang et al., 2007). MSK is a nuclear serine/threonine protein kinase containing two kinase domains, one at the N-terminus (NT) belonging to the AGC (cAMP-dependent protein kinase/protein kinase G/protein kinase C) kinase family of which the RSK is also a member (Frodin and Gammeltoft, 1999). The other kinase domain is at the C-terminus (CT) belonging to the CaMK family (Arthur, 2008). MSK1 is a substrate for p38 MAPK since its activation is inhibited by a p38 inhibitor (SB 203580) as well as a substrate for ERK1/2 MAPK as it is inhibited by MEK inhibitor PD98059 (Deak et al., 1998; McCoy et al., 2007). However MSK1 appears to be more prominently activated by ERK1/2 than by p38 MAPK which could be associated with the type of stimulation used (Frenguelli and Corrêa, 2012). For example the neurotrophin, BDNF and the activation of NMDA receptors induces ERK1/2 phosphorylation and subsequent MSK1 phosphorylation in cortical neurones (Arthur et al., 2004). However the activation of NMDA receptors can induce ERK1/2 dependent-MSK1 phosphorylation in rat cortical neurones but has been shown to be affected by a p38 inhibitor SB203580 (Rakhit et al., 2005). The mechanism of activation is shown in Figure 1.10 where the upstream MAPK will phosphorylate the CT of MSK1 which then auto-phosphorylates its NT.

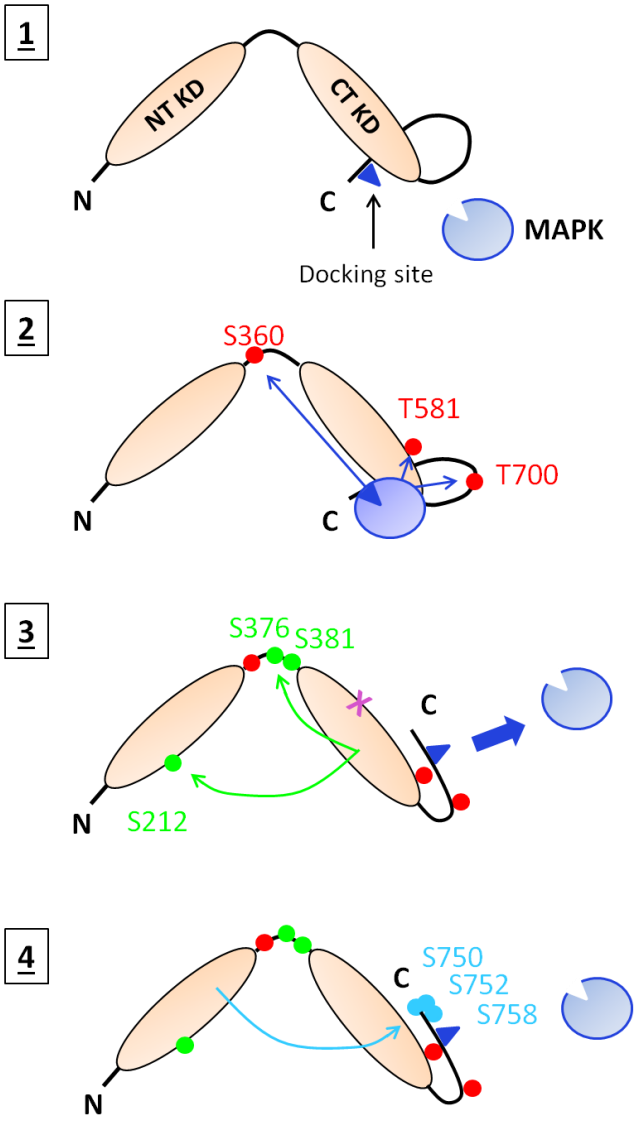

Figure 1.10; The activation and phosphorylation of MSK1 by MAPK. *MSK1 is comprised of an N-terminus kinase domain (NT KD) and a C-terminus kinase domain (CT KD) which is joined by a linker region.* ***(1)*** *When MSK1 is in an inactive form it is unphosphorylated and its C-terminus (CT) can fold back on itself acting as an inhibitor for the CT KD. A docking site (blue triangle) is available on the CT tail for the binding of MAPK.* ***(2)*** *When MSK1 is activated by MAPK the MAPK binds to the docking site and phosphorylates 3 residues, the S360 residue on the linker region, the T581 on the T loop of the CT KD which acts to stabilise the active conformation of the CT loop and the T700 on the CT tail. This residue functions to reduce the inhibition of the CT domain which is regulated by the autoinhibition CT sequence.* ***(3)*** *The phosphorylation of the T581 and T700 causes the activation of the CT KD which phosphorylates (green circles) 2 sites on the linker region (S376 and 381) as well as on the NT KD (S212) which activates the NT KD. The pink cross represents the domain in which 4 sites of MSK1 is phosphorylated by an unidentified kinase.* ***(4)*** *The active NT KD will then phosphorylate its substrates as well as autophosphorylating three resides on the CT tail (blue circles), S750, 752, 758. [MSK1; Mitogen-and stress-activated protein kinase 1; MAPK; Mitogen-activated protein kinase, NT KD; N-terminus kinase domain, CT KD; C-terminus kinase domain; S; Serine, T; Threonine] [Adapted from (McCoy et al., 2007; Arthur, 2008)]*

1.6.1 The regulation of CREB phosphorylation by MSK1

MSK1 will respond to external stimuli through the induction of an intracellular signalling cascade, predominantly via ERK1/2 allowing MSK1 to regulate gene transcription. There are two primary downstream targets which MSK1 phosphorylates, the first is the transcription factor CREB at S133 (Deak et al., 1998) and the second is histone H3 at S10 (Thomson et al., 1999) which allows the transcription of several genes including *c-fos, junB, nurr77* and *nor1 (Wiggin et al., 2002)*. *c-fos* is an immediate-early gene (IEG) which is extensively studied to use as a marker for neuronal activation. In cortical neurones CREB is phosphorylated upon BDNF stimulation and was shown to be ERK1/2 dependent (Arthur et al., 2004) (Figure 1.11). The role of MSK1 became more apparent when MSK1 KO mice showed significantly reduced levels of CREB phosphorylation. The expression of CREB- dependent genes *c-fos*, *Mkp1* and *nurr1* were also decreased in response to BDNF stimulation in the MSK1 KO mice (Arthur et al., 2004). There has been some controversy in the literature as to whether RSK also takes part in phosphorylating CREB. Nevertheless, work done in RSK2 KO mice has shown that RSK2 is not required for CREB phosphorylation via ERK1/2 (Bruning et al., 2000). It is worth noting that even though there are suggestive roles for ERK1/2-MSK1 signalling pathway that ERK1/2 is activated in many neuronal responses which can be independent of CREB phosphorylation and that CREB itself is a target of many different kinases.

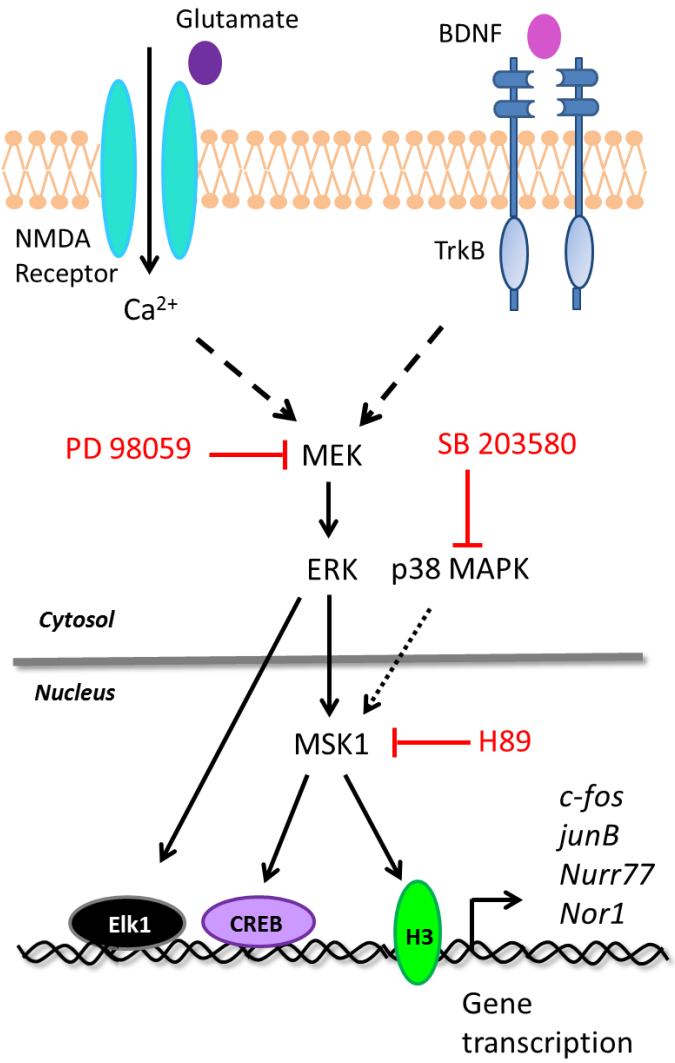

Figure 1.11; A simplified diagram of the signalling cascade regulating MSK activation. *There are a range of receptors in neurones which can be activated inducing a signalling cascade which overlaps with MSK1 (Frenguelli and Corrêa, 2012). In this diagram the activation of NMDA receptors by glutamate will open the channels allowing calcium ions to flow into the neurone. The other example is the BDNF binding to TrkB receptor inducing a range of intracellular signalling pathways shown in Figure 1.9. In both cases the upstream effectors will phosphorylate MEK which can be inhibited using PD98059. MEK will phosphorylate ERK1/2 which subsequently phosphorylates MSK1 in the nucleus. The p38 MAPK can also phosphorylate MSK1 but to a lesser degree (dotted line) and can also be inhibited using SB203580. MSK1 can be inhibited using the non-selective inhibitor H89. Gene transcription can occur where ERK1/2 is able to translocate into the nucleus to phosphorylate and activate the transcription factor Elk1. On the other hand, MSK1 can regulate gene transcription via phosphorylation of CREB as well as histone H3. Some examples of MSK1-dependent genes are shown in the diagram.[MEK; Mitogen-activated protein kinase kinase, ERK; Extracellular signal-regulated kinase, MSK; Mitogen- and stress-activated protein kinase, BDNF; Brain-derived neurotrophic factor; TrkB; Tropomyosin receptor kinase B, CREB; Cyclic AMP response element -binding protein, H3; Histone H3, Ca^{2+}; Calcium]. [Adapter from (Chwang et al., 2007)]*

1.6.2 The phosphorylation of histone H3 by MSK1

Gene transcription can be regulated by chromatin remodelling allowing direct access to the DNA. Histones are the structures holding/packaging the DNA together and which can be post-translationally modified by acetylation, methylation, ubiquitination and phosphorylation. These modifications can cause structural changes to the histone thus unravelling/tightening the DNA so affecting the binding of transcription factors to the DNA and altering subsequent gene transcription (Lee et al., 2010). There are four histones, histone H2A, H2B, H3 and H4 and the covalent changes occur at the histones' NT tail where histone H3 has many sites for epigenetic modulation via acetylation, methylation and phosphorylation (Roth and Sweatt, 2009). The effect of growth factors on the phosphorylation status of histone H3 was first discovered when mouse fibroblast cells were exposed to growth factors and rapid phosphorylation of histone H3 was observed (Mahadevan et al., 1991). It was later shown, using inhibitors to block upstream MEK and p38 MAPK activity in quiescent cells and mouse embryonic fibroblasts, that MSK1 could regulate the phosphorylation of histone H3 via both ERK1/2 and p38 MAPK (Figure 1.11) (Thomson et al., 1999; Soloaga et al., 2003). A non-selective MSK1 inhibitor (H89) was also used in these experiments to show a reduction in phosphorylation of histone H3. However, this was not conclusive due to the lack of specificity of the inhibitor. In order to confirm whether MSK1 does regulate chromatin remodelling via histone H3, experiments were conducted in mice that lacked MSK1 i.e. MSK1 KO mice. When a population of heterogeneous neurones known as striatal cells were cultured from MSK1 KO mice and stimulated with glutamate, histone H3 phosphorylation was abolished. This reduction in phosphorylation caused a reduction in the induction of IEGs such as *c-fos* when compared to the wild-type (WT) mice (Brami-Cherrier et al., 2007). The effect seen on histone H3 phosphorylation was due to MSK1 not RSK (Davie, 2003; Soloaga et al., 2003) as fibroblast cells lacking RSK2 still demonstrated phosphorylation of histone H3 in response to TPA (12-*O*-Tetradecanoyl-phorbol-13-acetate) a stimulus which is an oxidative stress inducer and an MSK1 activator (Soloaga et al., 2003).

1.6.3 The functional effects of MSK1

The functional effects of MSK1 in the mammalian brain have been studied and have revealed that MSK1 plays a crucial role in a range of cellular and cognitive

processes including: circadian clock gene expression (Butcher et al., 2005), visual cortex plasticity (Putignano et al., 2007), drug addiction (Brami-Cherrier et al., 2009), neurodegeneration (Roze et al., 2008), psychiatric conditions (Xu et al., 2010; Frenguelli and Corrêa, 2012) and learning and memory (Chwang et al., 2007).

MSK1 has become a kinase of interest as it could act to link activity with plasticity-related gene regulation. For example, visual cortex plasticity is at its most prominent during the 'critical period' of postnatal development which is thought to involve signalling cascades controlling gene expression. *In vivo* visual stimulation of juvenile mice induced both an ERK-CREB mediated signalling pathway as well as an ERK-MSK-histone H3 pathway (Putignano et al., 2007). This study also recorded visual evoked potentials as an electrophysiological read out. Following the pharmacological augmentation of histone acetylation using trichostatin (TSA) in the monocular deprived eye promotes ocular dominance plasticity, only in adult mice in contrast to juvenile mice. This indicates that experience-dependent plasticity may induce a signalling pathway dependent on the age of the animal.

It has been well established that ERK1/2 and CREB play important roles in IEG transcription involved in synaptic plasticity thought to underlie learning and memory (Thomas and Huganir, 2004). Some of the first studies revealing a potential role for MSK1 in hippocampal-dependent memories was shown by behavioural studies carried out in MSK1 KO mice (Chwang et al., 2007). Not only did the MSK1 KO mice show deficits in hippocampal-dependent forms of memories, but these were supported by the absence of changes in phosphorylation of CREB or phosphorylation and acetylation of histone H3. For example, fear conditioning stimuli induced an increase in phosphorylation of both CREB at residue S133 and histone H3 at S10 via ERK1/2 in the hippocampus. However these changes were absent in the MSK1 KO mice (Chwang et al., 2007). Similar changes were observed when mice were confronted with a psychological challenge such as forced swimming which activates NMDA-ERK signalling followed by MSK1 and Elk1 activation in the granule cells of the dentate gyrus (Reul et al., 2009; Gutierrez-Mecinas et al., 2011). The activation of MSK1 and Elk1 led to the phosphorylation of histone H3-S10 as well as its acetylation and the hyperacetylation of histone H4 which was associated with the induction of the IEG *c-fos* (Reul et al., 2009; Gutierrez-Mecinas et al., 2011). This signalling cascade, as well as others mentioned above have revealed that MSK1 can

epigenetically regulate gene transcription via histone modifications as well as CREB phosphorylation leading to the formation of memories.

1.7 Activity-regulated cytoskeleton-associated protein (Arc)

Arc, activity-regulated cytoskeleton-associated protein is an IEG which is induced upon neuronal activity (Link et al., 1995; Lyford et al., 1995; Bramham et al., 2010). In the past decade or so Arc has been proved to play a role in long lasting forms of synaptic plasticity as well as long term memory formation (Okuno, 2011).

Arc was discovered using cloning techniques used to identify its cDNA that was differentially screened from a cDNA library prepared from seizure-stimulated hippocampal extract (Lyford et al., 1995). In this study it was shown that Arc co-sediments with crude F-actin but not with highly purified actin (Lyford et al., 1995). This suggested that Arc requires other 'actin-binding' proteins that were present in the crude fraction in order to bind to F-actin i.e. Arc binds indirectly with F-actin. Interestingly the C-terminus of Arc possesses a domain which is a close homology to the cytoskeletal protein α-spectrin (Link et al., 1995; Lyford et al., 1995). This sequence could mediate potential interactions with spectrin-repeat-containing proteins, which still remain to be discovered.

The activity-induced upregulation of Arc mRNA was originally shown in various tissue and cultured PC12 cells in the presence of NMDA receptor antagonists (e.g. MK-8010), growth factors as well as synaptically stimulated using HFS of the perforant pathway (Link et al., 1995; Lyford et al., 1995). It was later discovered that several neuronal stimuli induced Arc mRNA transcription including both BDNF and HFS-induced LTP, learning experiences such as spatial learning and memory, as well as experience-induced stimuli such as environmental enrichment (EE) (Link et al., 1995; Steward et al., 1998; Guzowski et al., 1999; Ying et al., 2002; Plath et al., 2006; Kubik et al., 2007). Each of these stimuli will induce a range of intracellular signalling cascades which will contribute to the transcription of the Arc (Figure 1.12).

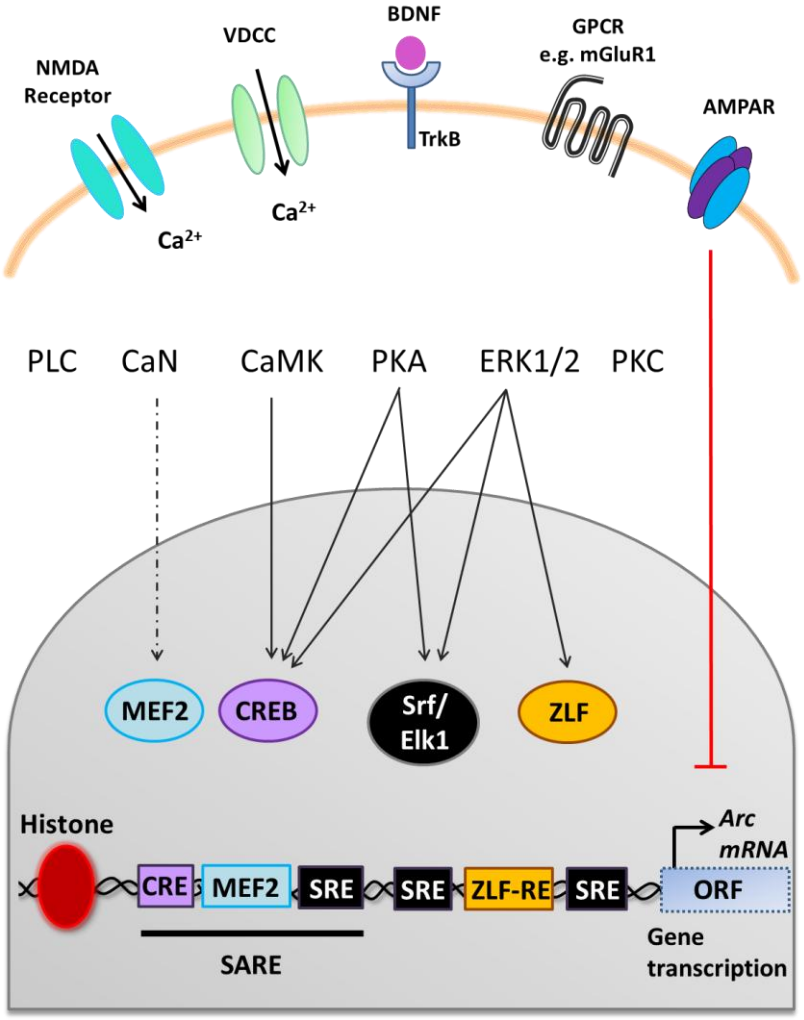

Figure 1.12; A simplified schematic diagram representing the transcriptional regulation of Arc mRNA. *The activation of NMDA receptor will initiate influx of calcium ions which can induce calcium-dependent signalling cascade including CaN and CaMKII. These effectors are also activated by the calcium influx through VDCC. Other kinases can also be activated by NMDA receptor activation via glutamate such as PKA, PKC and ERK1/2. TrkB-induced signalling induces a range of signalling cascades (Figure 1.9) affecting downstream kinases which control transcription factors involved in Arc transcription. The activation of the GPCR, group 1 metabotropic receptor has also been shown to regulate Arc transcription via CaMK, PLC and ERK1/2 MAPK pathways. AMPAR have an inhibitory role in regulating Arc gene transcription. Downstream to transcription factors are the regulatory elements of the Arc gene. CaN, as well as phosphatases that are not shown (dotted line) regulate MEF2. The transcription factor CREB binds to CRE which is controlled by CaMKs, ERK1/2 and PKA. The Srf/elk1 is activated by ERK1/2 and PKA allowing the regulation of the SRE on the Arc gene. Finally there is a ZLF which is activated by ERK1/2 which binds to the ZLF-RE on the Arc gene allowing the transcription of Arc. The SARE (synaptic activity-responsive element) consists of the binding sites for CREB, SRF and MEF2, all of which are necessary for Arc transcription. A recent finding has shown that Arc transcription could be modulated by post-translational modifications of histones (Xie et al., 2013). [CaN; Calcineurin, CaMK; Calcium/calmodulin-dependent protein kinase, ERK1/2; Extracellular signal- regulated kinase, BDNF; Brain- derived neurotrophic factor, PKA; Protein kinase A, PKC; Protein kinase C, PLCγ1; Phospholipase Cγ1, TrkB; Tropomyosin*

receptor kinase B, Ca^{2+}; Calcium, GPCR; G-coupled protein receptor, mGluR; Metabotropic glutamate receptors, AMPAR; α-amino-3-hydroxy-5-methyl-4-iso-xazolepropionic acid receptor, CREB; Cyclic AMP response element-binding protein, CRE; cAMP response element, Srf/Elk1; Serum response factor/E-26-like protein 1, SRE; Serum response element, ZLF; Zest-like factor; ZLF-RE; Zest-like factor response element, VDCC; Voltage-dependent calcium channel, Arc; Activity-regulated cytoskeleton-associated protein, SARE; Synaptic activity-responsive element; ORF, Open reading frame, MEF2; Myocyte enhancer factor 2] [Adapted from; (Wang et al., 2009; Bramham et al., 2010; Inoue et al., 2010; Korb and Finkbeiner, 2011; Okuno, 2011)]

1.7.1 Transcriptional regulation of Arc

Arc transcription can be regulated in a calcium-dependent manner (Waltereit et al., 2001; Adams et al., 2009) via NMDA activation (Steward et al., 1998; Steward, 2001) as well as through the stimulation of mGlu receptor in cortical neurones using the agonist, DHPG (3,5-Dihydroxyphenylglycine) (Park et al., 2008; Wang et al., 2009) (Figure 1.12).

In the presence of the synaptic mediator, BDNF, Arc mRNA levels are increased in rat cortical neurones which are occluded in the presence of a MAPK inhibitor, U0126 (Rao et al., 2006). Similarly when BDNF is administered into hippocampal slices by microinfusion to induce LTP, a selective upregulation of Arc mRNA and protein was observed, shown to be MEK-ERK1/2 dependent (Ying et al., 2002). Interestingly AMPAR inhibit BDNF-induced expression of Arc in hippocampal neurones and organotypic hippocampal slices cultures, shown using an AMPAR antagonist (Rao et al., 2006). This indicates a possible negative feedback mechanism in controlling Arc transcription. Further to this, a recent paper discovered that Arc has a role in 'inverse synaptic tagging' involving an interaction between Arc and CaMKIIβ which operate as a specific sensor for inactive synapses. This means that the interaction mediates the clearing of AMPAR in weaker synapses in potentiated neurones which prevents undesired enhancement of these synapses. This mechanism is thought to be essential for homeostatic scaling and thus for the reduction of surface AMPAR in stimulated neurones (Okuno et al., 2012).

All these intermediate signalling effectors integrate the signal from receptor activation to downstream transcription factors, which include cyclic AMP response element-binding protein (CREB), serum response factor/E-26-like protein 1 (SRF/Elk1), Zeste-like factor (ZLF) and myocyte enhancer factor 2 (MEF2) (Figure 1.12). The ZLF binds to zeste-like response element (ZL-RE) on the proximal site of

the Arc gene which enhances Arc transcription in response to synaptic activation and BDNF stimulation (Pintchovski et al., 2009). MEF2 is induced when calcium-dependent signalling cascades including CaMK, calcium dependent p38 activation and calcineurin phosphatase are activated in neurones (Lyons and West, 2011). BDNF, calcium and synaptic activity activate SRF via ERK1/2 which increases Arc transcription (Kawashima et al., 2009; Pintchovski et al., 2009). The SRF binds to an ERK1/2 dependent transcriptional cofactor known as Elk-1 forming the ternary complex allowing it to bind to the serum response element (SRE) promoter thus inducing the recruitment of basic transcriptional machinery to the DNA (Buchwalter et al., 2004). Arc appears to be the first IEG which is directly regulated by SRF/SRE that functions at the synapse and is required for learning and memory (Pintchovski et al., 2009). This is also reflected in the fact that mice lacking SRF have deficits in learning and memory (Etkin et al., 2006).

The final transcription factor which has been shown to regulate Arc transcription upon BDNF stimulation, calcium influx and other synaptic stimuli is CREB. CREB is activated by the phosphorylation at S133 residue by a range of intracellular effectors such as MAPK, CaMK and PKA. This transcription factor binds to cAMP response element (CRE) on the Arc gene. In the CA1 region of the hippocampus it was shown that ERK1/2 dependent activation of CREB induced a strong up-regulation of Arc mRNA and protein (Ying et al., 2002). The Arc promoter holds a unique activity-sensor element which has been named synaptic activity-responsive element (SARE) which consists of the binding sites for CREB, SRF and MEF2 all of which are necessary for Arc transcription and sufficient to allow rapid and synaptic activity-induced Arc expression in hippocampal neurones (Figure 1.12) (Kawashima et al., 2009; Bramham et al., 2010; Inoue et al., 2010). The activation of SARE was tested *in vivo* by injecting a SARE-reporter lentivirus in to embryonic mouse in utero (Kawashima et al., 2009) and after birth the mice were dark reared for 24 hours to bring the reporter expression to baseline. After exposing one eye to light for 2-3 hours, 60% of the infected neurones were GFP reporter positive indicating the need for experience-dependent activity for expression (Kawashima et al., 2009). More recently a paper has shown a correlation between increased histone H3 and H4 acetylation with elevated Arc expression in the mouse hippocampus in response to early life stress which involved maternal separation from P14-16 (Xie et al., 2013).

1.7.2 Transport of Arc mRNA and its local translation

Arc has a unique mechanism of mRNA induction and subsequent translation. It was first shown that when HFS was applied to the perforant pathway it caused newly synthesised Arc mRNA to localise selectively to activated dendritic segments (Steward et al., 1998; Steward, 2001) (Figure 1.13). Arc mRNA can be transported rapidly down dendrites at approximately 300 μm/hour after single electroconvulsive seizure was induced in dentate granule cells (Wallace et al., 1998). However Arc mRNA is also detected in dendrites under basal non-stimulated conditions, as low levels were detected in both synaptoneurosomes, which included both the postsynaptic and presynaptic terminals and in dendrites (Lyford et al., 1995; Steward, 2001; Yin et al., 2002; Rodriguez et al., 2005). There is evidence that the pre-existing stores of Arc mRNA in hippocampal neurones are locally translated during DHPG-induced LTD (Waung et al., 2008).

Later on it was shown that Arc mRNA could localise to the active dendritic segments via a 11 nucleotide response element within the Arc coding region and a 3' untranslated region (UTR) (Kobayashi et al., 2005; Gao et al., 2008) where it can be locally translated (Yin et al., 2002; Moga et al., 2004; Rodriguez et al., 2005). The role of actin polymerisation was highlighted when local inhibition of Rho kinases was shown to block HFS-induced actin polymerisation in the dentate gyrus which overlapped with the area in which Arc mRNA localises and thus was abolished in the presence of Rho kinases. Furthermore the application of a MEK inhibitor (U0126) not only blocked ERK phosphorylation but also the localisation of Arc mRNA, which was visualised using *in situ* hybridisation (Huang et al., 2007).

It was then suggested that Arc mRNA is transported from the nucleus along the dendrites via microtubules to the active synapse where F-actin dependent docking occurs (Figure 1.13). Arc is in fact required to stabilise F-actin at synapses and therefore suggests a possible positive feedback mechanism between Arc and F-actin (Messaoudi et al., 2007). Latrunculin B, an actin polymerisation inhibitor was applied and disrupted the Arc mRNA localisation but the band of polymerised actin was shown not to be sufficient to mediate localisation (Huang et al., 2007). Therefore another signalling effector was required, which was shown to be ERK1/2 as local injections of MEK inhibitor U0126 blocked Arc mRNA localisation (Huang et al., 2007).

A proteomic study was then carried out on protein extracted from mouse brain using mass spectrometry and pull-down assays of the NMDA receptor multiprotein complex where Arc was found to complexed with both PSD-95 and CaMKII (Husi et al., 2000) which were later shown to be concentrated at the postsynaptic density (Donai et al., 2003; Okuno et al., 2012). Arc mRNA is locally translated at the dendritic spines shown by evidence for polyribosomes and RNA trafficking to spines (Ostroff et al., 2002) (Figure 1.13). It appears that some forms of synaptic plasticity require enhanced protein synthesis to maintain synaptic plasticity. For example in the dentate gyrus, Arc synthesis is required within the first 10 minutes of HFS as well as 2-4 hours later for LTP consolidation (Messaoudi et al., 2007). In contrast to mGluR-LTD which requires *de novo* protein synthesis at postsynaptic CA1 pyramidal neurons, within the first 5-10 minutes post DHPG application in hippocampal slices (Huber et al., 2000). Arc mRNA undergoes a nonsense-mediated RNA decay (NMD) in the dendrites which consequently limits the translation of the protein from a single mRNA. The half-life of Arc mRNA in hippocampal neurones has been estimated to be 47 minutes (Rao et al., 2006). This characteristic as well as the tightly regulated transport of Arc mRNA and subsequent local translation at spines, would suggest that Arc is important for synaptic function and that any dysregulation in its expression could lead to severe physiological consequences.

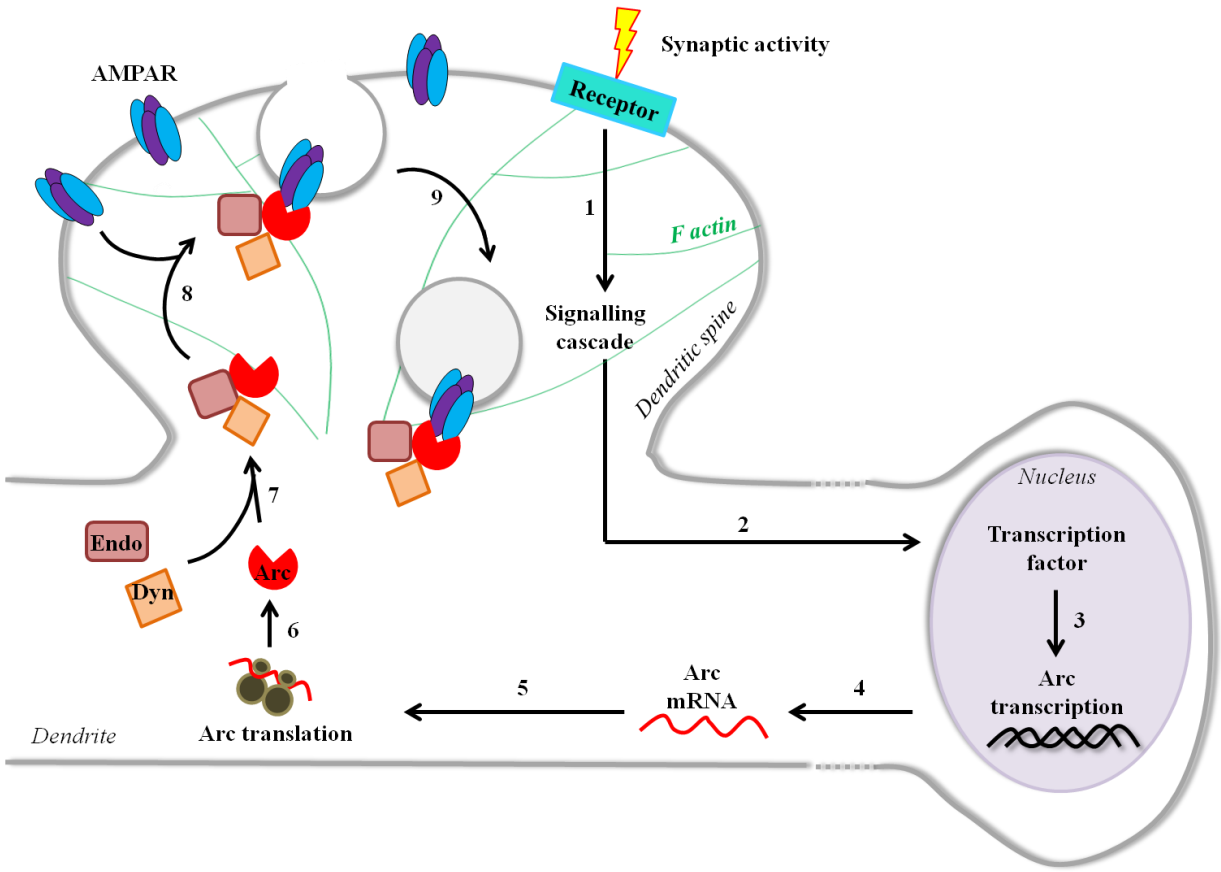

Figure 1.13; A schematic diagram representing the regulation of Arc synthesis upon neuronal activation. *Neuronal activation occurs when an appropriate receptor or channel is activated inducing a downstream intracellular signalling cascade* ***(1)***. *This activates transcription factors* ***(2)*** *which regulate the transcription of the Arc gene* ***(4)***. *The Arc mRNA is transcribed and transported out of the nucleus along the dendrites using the microtubule system* ***(5)***. *The Arc mRNA is docked at the dendritic spine with the aid the F-actin cytoskeleton. The mRNA is locally translated* ***(6)*** *and allowed to bind with the endocytotic machinery, dynamin (Dyn) and endophilin (Endo)****(7)***. *This interaction recruits surface AMPAR* ***(8)*** *which are then internalisaed through clathrin-mediated endocytosis* ***(9)***. *This occurs during different forms of synaptic plasticity [Arc; Activity-regulated cytoskeleton-associated protein, Dyn; Dynamin 2, Endo; Endophilin 3, AMPAR; α-amino-3-hydroxy-5-methyl-4-iso-xazolepropionic acid receptor.] [Adapted from; (Bramham et al., 2010)]*

It is important to note that Arc has also been shown to be expressed in glial cells where increased levels were seen in the potentiated dentate gyrus molecular cell layer when compared to un-stimulated conditions(Rodriguez et al., 2008b). However the role of glial-expressed Arc during synaptic plasticity has not yet been defined. There is evidence that astrocytes play an important role in glycogen breakdown and lactate release which has been shown to be important for long-term memory formation (Suzuki et al., 2011).

1.7.3 Arc interaction with endocytotic machinery

The mechanism by which Arc is able to alter synaptic transmission during different forms of synaptic plasticity is due to its function in AMPAR trafficking (Figure 1.13). The original work which elucidated its role in AMPAR trafficking was a yeast-two hybrid system as well as co-immunoprecipitation experiments in HEK293 cells, which demonstrated that Arc binds to both dynamin 2 and endophilin 3 which are both endocytotic proteins (Figure 1.13) (Chowdhury et al., 2006). The two clones shown to interact in yeast corresponded to the C-terminus half of dynamin 2 (amino acids 503-871) and C-terminus of the BAR (Bin-Amphiphysin-Rvs) domain of endophilin (amino acids 172-347). Arc interacts with dynamin and endophilin in association with endosomes in hippocampal neurones (Chowdhury et al., 2006). Its role in AMPAR trafficking was shown when Arc was overexpressed in hippocampal neurones which lead to a decrease in postsynaptic surface GluA1 expression (Chowdhury et al., 2006) as well as reducing the excitatory synaptic transmission onto hippocampal CA1 neurones (Rial Verde et al., 2006). Similarly when Arc KO hippocampal neurones were cultured and compared to WT neurones there was a significant increase in surface GluA1 expression (Shepherd et al., 2006). This characteristic has led to the suggestion that Arc is involved in the endocytosis of AMPAR during different forms of synaptic plasticity.

1.7.4 The functions of Arc

1.7.4.1 The role of Arc in memory and synaptic plasticity

Arc has been shown to play a role in a range of different functions in the brain including, neurogenesis, depression, drug addiction, memory and synaptic plasticity (LTP, LTD and homeostatic scaling) (Bramham et al., 2010). The temporal regulation of Arc transcription and translation determines its function in the processes mentioned above. For example, Arc is required for LTP consolidation, i.e. transferring short term memories to long term memories, thus stabilising memories, which was elegantly shown by using Arc antisense and Arc KO mice. In i*n vivo* studies using anaesthetised rats, an Arc antisense (AS) oligodeoxynucleotide was infused into the dentate gyrus which caused impairments in HFS-induced LTP maintenance but not induction (Messaoudi et al., 2007). The requirement for Arc during LTP consolidation but not induction was shown in behavioural training showing the importance of Arc for long-term memory formation. This was reflected

where mice needed Arc in order to form long- term spatial memory but not for short-term memory performance (Guzowski et al., 2000). This observation was demonstrated in Arc KO mice where their early phase of LTP was enhanced but late phase LTP was blocked in both the dentate gyrus *in vivo* and in the CA1 region of acute hippocampal slices (Plath et al., 2006). A possible explanation for the enhanced early LTP in the Arc KO animals might be that they have an altered metaplasticity (Abraham and Bear, 1996). This means that since the KO synapses can't consolidate prior to potentiation they are then constitutively in a more plastic state leading to an enhanced early LTP. The authors of the Plath et al., 2006 paper also claim that the enhanced early LTP could be a consequence of decreased activity-dependent AMPAR endocytosis. However LTP has been largely defined as an increase in AMPAR insertion rather than a reduction in endocyotis.

The later stages of LTP involves memory consolidation which may explain why the KO mice have severe deficits in spatial memory tasks. Interestingly these transgenic mice also have reduced LFS induced LTD at the Schaffer collateral/CA1 pyramidal cells synapses (Plath et al., 2006). The Arc-dependent mechanism involved during LTD was shown to involve its role in endocytosis of AMPAR. A study was carried out in hippocampal slices from WT and Arc KO mice where DHPG-induced LTD failed to decrease surface GluA1 expression thus preventing LTD in Arc KO mice (Park et al., 2008). Under homeostatic scaling conditions Arc KO hippocampal neurones were unable to scale either their mEPSC amplitude or GluA1 surface expression in the presence of either bicuculline or TTX (Shepherd et al., 2006).

Recent findings have shown that Arc can be post-translationally modified by a process known as SUMOylation. The small ubiquitin-like modifier (SUMO) protein is known to determine subcellular localisation of proteins. Arc has two SUMOylation sites that direct its expression to the dendrites and the cytoskeleton (Nair et al., 2009). LTP in the dentate gyrus of anesthetised rats induced an upregulation of SUMOylated Arc in the cytosol (Bramham et al., 2010). More recently SUMOylated Arc has been implicated in playing a role during TTX-induced homeostatic scaling (Craig and Henley, 2012). A construct was designed which mutated the two lysine residues which are SUMOylated in Arc. These neurones expressing the Arc double mutation were unable to up-scale their AMPAR expression in response to TTX when compared to control cells (Craig et al., 2012).

1.7.4.2 BDNF-dependent regulation of Arc

BDNF-induced LTP using BDNF infusion in the dentate gyrus results in an upregulation of Arc mRNA and protein, where *in situ* hybridisation showed that Arc transcripts were rapidly transported to granule cell dendrites (Ying et al., 2002). This mechanism was also shown to be MEK-ERK dependent as the U0126 MEK inhibitor blocked the upregulation of Arc upon BDNF-LTP. Interestingly this requirement for Arc transcription for synaptic strengthening was shown to be important during a specific time frame. When the transcription inhibitor, actinomycin D, was applied *in vivo* in the dentate gyrus, 1 hour or immediately before BDNF stimulation it blocked BDNF-LTP. However when actinomycin D was applied 2 hours after BDNF stimulation there was no effect (Messaoudi et al., 2002).

The role of Arc during LTP consolidation not only requires sustained Arc protein translation but Arc has also been shown to regulate actin dynamics. This was shown in a similar study where the inhibition of LTP consolidation using the Arc antisense was associated with rapid dephosphorylation of hyperphosphorylated cofilin (Messaoudi et al., 2007). Cofilin regulates F-actin dynamics where, when it is in a phosphorylated state, actin polymerisation is promoted. Therefore the rapid dephosphorylation is associated with the loss of F-actin. Furthermore the effect of Arc anti-dense (AS) on reversing LTP was blocked when an F-actin stabilising drug, jasplakinolide was applied to the dentate gyrus where LTP was maintained.

1.7.4.3 Arc and dendritic spine morphology

Arc dependent changes in actin cytoskeleton and AMPAR trafficking can influence structural changes in dendritic spines. Overexpressed Arc in hippocampal neurones increases the proportion of thin 'learning' spines containing reduced GluA1 expression (Peebles et al., 2010). By increasing the number of 'learning' spines the neurones are able to respond to changes in activity more readily. Arc has been implicated in regulating network excitability due to homeostatic regulation of AMPAR trafficking and spine morphology (Lyford et al., 1995). The network excitability was addressed by looking at the susceptibility of Arc KO neurones to convulsant drugs. The data showed that the loss of Arc expression *in vivo* lead to aberrant neuronal overexcitation. The loss of the homeostatic negative feedback could explain the epileptic-like state and the associated spine loss (Shepherd et al., 2006; Peebles et al., 2010).

1.8 Environmental enrichment (EE)

The concept of environmental enrichment (EE) was first suggested by Charles Darwin in 1874 when he observed a significant increase in the size of the brain in wild rabbits when compared to domesticated rabbits. He hypothesised that this reduction in brain size of domesticated rabbits, despite their larger size, could be attributed to them being closely confined during many generations which would restrict their 'intellect, instincts, senses and voluntary movements'. Genetic predisposition can also be affected by environmental factors whilst also influencing brain size (Darwin, 1871).

In the 1940s, a Canadian physiologist, Donald Olding Hebb first proposed EE as an experimental model in which one could compare laboratory kept rats to home kept pet rats (Hebb, 1947; Hebb, 1949). An experimental approach was to design the concept of EE into a testable scientific experimental model (Rosenzweig et al., 1962) which used the measurements of total brain weight, DNA/RNA content and protein (Rosenzweig and Bennett, 1969; Bennett et al., 1996). It was shown that rodents' brains which were exposed to environmentally enriched conditions weighed more than those in standard housing (SH) as well as having increased ratios of enzymes which hydrolyses the neurotransmitter acetylcholine (Rosenzweig et al., 1962). Later on high-density oligonucleotide microarrays were carried out to analyse the gene expression of the brain under EE conditions compared to SH which showed changes in gene expression following enrichment. For example the expression levels of PSD-95 protein increased 7 fold after 2 days of EE (Rampon et al., 2000b).

The experimental set up of EE involves larger cages, with toys, ladders, tunnels, running wheels, social groups as well as their standard requirements of nesting material, food pellets and water (Figure 1.14). This 'enriched' condition is then compared to animals in SH which include a smaller cage with just the standard required material mentioned above (Figure 1.14). EE is a form of experience and has been defined as 'a combination of complex inanimate and social stimulation' (Rosenzweig et al., 1978). This definition defines the fact that there are many contributing factors which cannot be easily isolated and are thought to interact with each other, stimulating the sensory, cognitive and motor areas of the brain (van Praag et al., 2000; Nithianantharajah and Hannan, 2006).

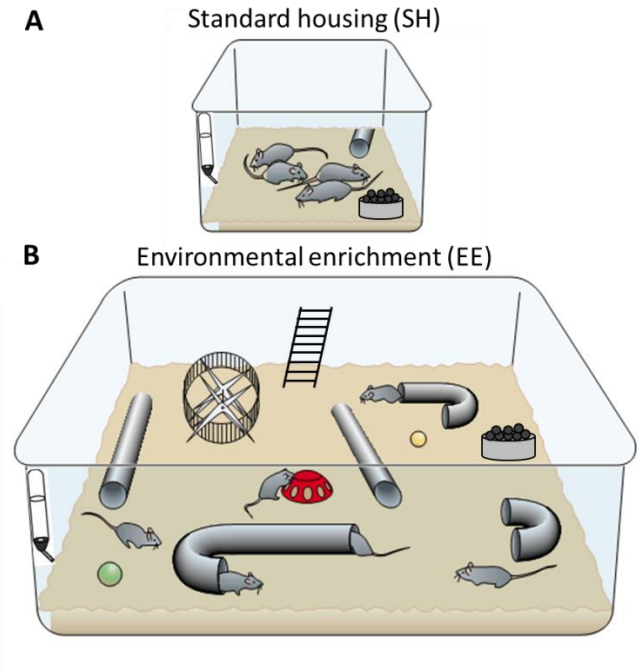

Figure 1.14; The experimental setup of standard housing (SH) compared to environmental enrichment (EE). ***(A)*** *The cage represents SH conditions in which the mice are housed in social groups with food pellets, water, a simple cardboard tube and bedding.* ***(B)*** *The EE cage is larger in size when compared to the SH where the mice are also in social groups in a cage with many tubes, toys, ladders and a running wheel as well as food pellets, water and bedding.*

1.8.1 The characteristics of environmental enrichment (EE)

Some of the consequences of enrichment in the intact brain include enhancements in spine density and morphology, the release of growth factors including BDNF, memory function and synaptic plasticity. These are addressed below in more detail.

1.8.1.1 Morphological changes in dendritic spines after environmental enrichment

Not only does EE increase brain weight and alter gene and protein expression but it has been shown that following EE there is increased dendritic branching in the rat visual cortex (Volkmar and Greenough, 1972) and pyramidal neurones in the hippocampus (Leggio et al., 2005) as well as dendritic spine density which can be visualised using Golgi staining (Globus et al., 1973; Rampon et al., 2000a; Leggio et al., 2005). Most EE studies involve male mice due to the effect of estrous cycle in female mice which affect spine density independently of their

environmental condition (Woolley et al., 1990). A study carried out in primates who either lived in standard laboratory cages or cages which were environmentally enriched for the duration of a month. The results showed that in CA1 pyramidal neurones, an increase in both spine density and dendritic branching was observed in primates after EE (Kozorovitskiy et al., 2005).

After environmentally enriching rats for 2 months, their spines in the dentate gyrus were visualised using Golgi staining where an increase in spine density was observed but the spines appeared longer and larger in morphology when compared to SH rat (Pham et al., 2002). The dynamics of spine density and morphological changes have been studied after 2 months of EE as well as after 60 minutes of exposure (Kitanishi et al., 2009). The effects seen on the spine reorganisation after 60 minutes of EE was reversed when the mice were placed back into their home cage (e.g. SH) thus spine dynamics are rapid and reversible. These structural changes are thought to contribute to the enhanced behavioural outcomes associated with EE such as improved, cognitive performance and learning (Alvarez and Sabatini, 2007).

1.8.1.2 The role of BDNF in environmental enrichment

BDNF mRNA was shown to be increased in CA1 hippocampal neurones post EE using *in situ* hybridisation which was associated with improved spatial memory using the Morris water maze test (Kuzumaki et al., 2011). It has been shown that mice exposed to environmentally enriched conditions have an enhanced number of newly generated neurones in the dentate gyrus of the hippocampus which was demonstrated using Brd-U (bromodeoxyuridine) a mitotic marker that labels newborn cells (Kempermann et al., 1997). Rossi et al., (2006) suggested that this may be dependent upon BDNF as $BDNF^{-/+}$ heterozygous mice did not show an enhancement of hippocampal neurogenesis after EE.

BDNF may also play a role in EE-dependent morphological changes as environmentally enriched heterozygous $BDNF^{-/+}$ mutant mice showed a delayed increase in spine density compared in WT in both CA1 and dentate gyrus neurones. The signalling mechanism involved in BDNF-dependent changes during EE has not yet been described.

The requirement for BDNF is consistent with the findings of Ickes et al., (2000) who reported that both BDNF and nerve growth factor (NGF) levels were elevated in the cerebral cortex, hippocampal formation (which contains the dentate gyrus and Subiculum), basal forebrain and the hind-brain of EE rats. It is clear that other neurotrophins are upregulated upon EE and are expressed in different areas of the brain. The time period of EE can also determine the type of neurotrophin released. For example, mice that were exposed to environmentally enriched conditions for 3-4 weeks showed a dramatic increase of BDNF mRNA in the hippocampus. But no changes were seen in many other neurotrophins including NGF (Kuzumaki et al., 2011). This study also showed that after 4 weeks of EE there was a significant increase in histone H3 methylation at the BDNF promoter suggesting that EE may increase BDNF expression via chromatin regulation in the mouse hippocampus.

1.8.1.3 The environmental enriched-induced epigenetic regulation

Epigenetic modifications can control gene transcription underlying the formation of long-term memories in response to experience-induced plasticity (e.g. EE) (Sweatt, 2009). The two main epigenetic mechanisms that play a role in gene-environment interface are DNA methylation and post-translational modifications of histones (Carulli et al., 2011). Post-translational modifications of histones have been shown to be regulated by an ERK-MSK1 dependent signalling pathway which has been characterised in the central nervous system (CNS) (Chwang et al., 2007). This cascade involves ERK1/2 which phosphorylates and activates MSK1 (Figure 1.11). The nuclear kinase then phosphorylates downstream CREB which recruits, CREB binding protein (CBP). CBP is a histone acetyltransferase (HAT) which regulates local chromatin structure via acetylation (Sweatt, 2009). This pathway has been alluded to using different experience-dependent stimuli such as contextual fear conditioning, which is a form of hippocampal-dependent learning. When mice were exposed to contextual fear conditioning stimuli *in vivo*, an increase in ERK-dependent histone H3 phosphorylation in CA1 area of the hippocampus was observed (Chwang et al., 2006). MSK1-independent chromatin modifications also occur which showed that in the hippocampus and cortex where an increase in acetylation of histone H3 and H4 resulted after different EE exposure times. This

was also linked to improved learning behaviour and was suggested to also involve HATs (Fischer et al., 2007).

1.8.1.4 Evidence for environmentally enriched-dependent induction of Arc expression

Arc mRNA expression has been shown, using *in situ* hybridisation, to be upregulated in the hippocampus in response to 3 weeks of daily EE sessions (Pinaud et al., 2001b). Using *in situ* hybridisation, increased levels of Arc mRNA were observed in the cortex, CA1, CA2, CA3 but less of an increase in the dentate gyrus after EE when compared to the SH groups. The conclusion was that Arc is upregulated after EE due to the greater complexity of the environment and that Arc is induced to permit/facilitate neuronal plasticity in order to process the complexity of sensory, motor and social inputs (Pinaud et al., 2001b). An EE-dependent increase in Arc synthesis was shown in acute form of EE, where rats were exposed to EE conditions for 2 hours. Using immunofluorescence, an upregulation of Arc protein was observed in the dentate gyrus granule cells after 1 and 2 hours of EE (Chotiner et al., 2010).

1.8.1.5 Evidence for a role of MSK1 during environmental enrichment

MSK1 has been shown to play a role in spinogenesis and dendritic branching in hippocampal neurones after EE. After 40 days of EE the associated cognitive enhancement which was measured using the Barnes maze and the novel objection recognition tests, was reduced in the MSK1 KO mice when compared to the WT. This cognitive deficit in the MSK1 KO mice was associated with reduced spine density and reduced dendritic branching in CA1 and CA3 compared to the WT (Karelina et al., 2012).

1.8.1.6 The effects of environmental enrichment on memory and synaptic plasticity

EE has been shown to enhance learning and memory in various behavioural tasks, such as spatial memory in the Morris water maze (Falkenberg et al., 1992; Kempermann et al., 1997), emotional memory in fear conditioning (Rampon et al., 2000a; Duffy et al., 2001) and recognition memory in novel object recognition task (Rampon et al., 2000a). The enhancement in these forms of learning and memory has been attributed to the structural and biochemical changes described above. It is

important to recognise that voluntary exercise in the running wheel in SH conditions has also been shown to enhance spatial learning (van Praag et al., 1999). Therefore it is worth noting that the type of objects/exercises available in the EE condition could affect the outcome observed. This among other variables have been discussed in the literature which can contribute to behavioural as well as biochemical changes seen after EE (Simpson and Kelly, 2011).

Whether EE promotes learning and memory via enhancing hippocampal LTP or LTD is controversial. The controversy has been driven principally by the varying experimental factors, some of which are age, sex, species and duration of EE. These have been highlighted in some studies shown in Table 1.1.

fEPSP	LTP (HFS)	LTD (LFS)	Area	Species	Sex	Age	EE Duration (weeks)	Reference
X	Enhanced	Enhanced	CA1	Rat	M	P50	5 cont	(Artola et al., 2006)
Enhanced	Decreased	X	DG	Rat	M	P40	4 per	(Foster et al., 1996)
NC	NC	Decreased	CA1	Rat	M	P28	12 cont	(Eckert and Abraham, 2010)
NC	Enhanced	X	CA1	Mouse	F	P28	8 cont	(Duffy et al., 2001)
X	Enhanced	X	CA1	Mouse	F	P21	10 cont	(Maggi et al., 2011)
NC	NC	X	DG	Mouse	M	Adult	2 per	(Feng et al., 2001)

Table 1.1; The range of electrophysiology findings from EE experiments and their variables. *This table represents the results for whether after EE, the fEPSP (field excitatory postsynaptic potential), LTP or LTD were enhanced, decreased, had no change (NC) or were not studied (X) from several studies. LTP was induced using high-frequency stimulation (HFS) and LTD was induced using low-frequency stimulation (LFS). The table also contains the area of the hippocampus from which electrophysiological recordings were taken as well as the animal species, sex (m; Male, F; Female) and age at which they were exposed to EE. The duration of EE is also specified in the number of weeks the animals were exposed to EE and whether it was continuous (cont) EE or periodic enrichment (per).[Adapted from (Eckert and Abraham, 2013)].*

The enhancement in LTP after EE seen in some conditions shown in Table 1.1 could be attributed to several factors. The first is an increase in neurogenesis in the dentate gyrus has been shown to contribute to HFS-induced LTP stimulated in the medial perforant path (Snyder et al., 2001). Therefore the increase in neurogenesis during EE could attribute to changes in plasticity. There are two common hypotheses (1) where EE promotes a learning-induced change in synaptic strength or (2) that EE contributes to a change in long-term plasticity mechanisms such as affecting the ability of neurones to strengthen or weaken their synapses. Changes in synaptic strength can be measured by monitoring basal synaptic transmission (i.e. fEPSP) (Table 1.1). Changes in LTP or LTD can be used to observe changes in plasticity after EE (Table 1.1) (Eckert and Abraham, 2013). If the mechanism for LTP and learning were similar then one would expect that if there were any changes in synaptic strength due to EE then this would occlude subsequent LTP induction i.e. LTP saturation occurs (Moser et al., 1998). On the other hand, an enhancement in LTP/LTD induction or maintenance might be observed in EE animals where plasticity mechanisms have changed due to enriched conditions. Lastly there may be no changes in plasticity post EE that are detectable during LTP or LTD which could be due to the EE protocol where the duration or complexity was not high enough to induce observable changes (Table 1.1).

Not much is known about the EE-dependent molecular signalling pathways involved in synaptic plasticity. However a signalling pathway was suggested when LTP-induced plasticity during EE was compared between adolescent and adult mice (Li et al., 2006a). When a protocol known as theta burst stimulation (TBS) was used to induce LTP in adolescent EE mice, the activation of p38 MAPK and cAMP-dependent signalling was observed. These signalling effectors were unaffected in the SH mice. To further detect a signalling pathway, Ras-GRF1 shown to be involved in NMDA-ERK dependent LTP and Ras-GRF2 known to activate NMDA-p38 dependent LTD were examined using Ras-GRF double KO mice (Li et al., 2006a). TBS-induced LTP in the Ras-GRF double KO mice was defective in adolescent mice but was rescued upon EE. Interestingly this EE-dependent signalling pathway was not observed in adult mice and therefore suggests the presence of multiple signalling cascades (Li et al., 2006b). Taking into account all the highlighted variables during EE it is clear that much is still unknown about the physiological and biochemical mechanisms involved during experience-dependent plasticity. However there are a

few key candidates, notably BDNF and signalling cascades, for example MAPK, which could contribute to the structural, biochemical and electrophysiological changes associated with EE.

1.9 Aims of thesis

There are a range of different signalling cascades that have been shown to underlie various forms of synaptic plasticity, which may be required for learning and memory. The aim of this thesis is to characterise the potential role of MSK1, which is known to be activated by BDNF in both activity and experience-dependent synaptic plasticity in the hippocampus. In order to address this, a MSK1 transgenic mutant mouse was used which contains a point mutation in the N-terminus kinase domain creating an inactive kinase i.e. kinase dead (MSK1 KD).

1. To investigate the effects of BDNF on the expression of plasticity related proteins such as Arc in dissociated hippocampal cultures from wild-type (WT) and MSK1 KD mice. The role of MSK1 will be determined in response to BDNF-induced synaptic changes of Arc expression during an acute time course of BDNF stimulation.
2. To establish whether a chronic form of synaptic plasticity known as homeostatic synaptic scaling requires MSK1. This will investigate the changes in Arc protein expression in response to 24 hours of synaptic deprivation in both WT and MSK1 KD hippocampal culture.
3. To establish the role of MSK1 in regulating structural changes in spine density and morphology during culture development. These changes can be characterised by visualising and measuring parameters of dendritic spines in both WT and MSK1 hippocampal neurones.
4. To investigate the role of MSK1 in experience-dependent synaptic plasticity such as environmental enrichment (EE). EE can influence the expression of activity-related proteins such as Arc, spine density as well as electrophysiological properties. These characteristics can be measured and compared between adult male WT and MSK1 KD mice in either EE or standard housing conditions.
5. To investigate the potential interaction between Arc and the cytoskeleton which could be regulating AMPAR trafficking. Arc can be immunoprecipitated from hippocampal lysate and run through mass spectrometry analysis to identify potential interacting partners which can be further validated using co-immunoprecipitation assays.

Chapter 2.

Materials and Methods

2.1 Generation of the MSK1 KD mouse

Mitogen-and stress-activated protein kinase 1 (MSK1) kinase dead (MSK1-KD) mutant mice were generated by mutating aspartic acid (D) 194 to an alanine in N-terminal kinase domain DFG motif of the endogenous MSK1 gene. The DFG motif consist of three amino acids, Aspartic acid (D), Glycine (F) and Phenylalanine (G) which form part of the catalytic activation domain of the kinase. C57/B16 mouse embryonic stem (ES) cells were modified with the target vector via homologous recombination. The target vector contained two selective markers a neomycin resistant cassette as well as a thymidine kinase cassette (Thomas and Capecchi, 1987; Correa et al., 2012). Successfully modified ES cells were confirmed using Southern Blotting. The targeted ES cells were injected into blastocysts to generate chimeric embryos. The chimeras that carried the target gene within their germline were crossed to Flp recombinase transgenic mice to excise the neomycin resistant cassette. The generation of MSK1 knock out (KO) mice has been previously described by (Wiggin et al., 2002).

2.1.1 Animal Use

All mice were maintained on a 12:12 light cycle in individually ventilated cages (IVC). All animals used were sacrificed in accordance with the UK Animal (Scientific Procedures) Act and local Ethical Review procedures.

2.2 Mouse primary hippocampal culture

Preparation of dissociated primary postnatal hippocampal culture was carried out as described by (Correa et al., 2009). Postnatal 0 (P0)-P1 mouse pups of both sexes were killed by decapitation (2.1.1). The brain was removed from the skull and placed in ice-cold DMEM (Dulbecco's Modified Eagle Medium). Using a dissecting microscope the cerebellum was removed using fine-curved scissors before cutting down the midline and exposing the thalamus of both hemispheres. This structure was

removed to reveal the hippocampi. The fine meshes of blood vessels coating the hippocampi as well as the fimbria were removed before excising the hippocampi from the brain.

The hippocampi were washed in DMEM and HBSS medium before trypsinating for 10 minutes at 37ºC [0.25% liquid trypsin]. The dissected hippocampi were then washed in HBSS and DMEM to remove excess trypsin before dissociating using DNase [2 mg]. The dissociated cells were centrifuged at 148 g for 10 minutes at 4ºC. The cells were seeded at ~0.2 x 10^6 cells per pre-treated poly-L-Lysine coated 22 mm coverslips (VWR, Leicestershire, UK) for immunocytochemical (ICC) experiments or at 0.8 x 10^6 cells in 60 mm x 15 mm petri dishes (BD Falcon, Oxford, UK) for protein extraction. The cells were seeded in plating medium consisting of Neurobasal A media, 0.2 % Gentamycin, 2 % B27, 0.5 % L-Glutamine and 5 % horse serum (HS) for 24 hours in a humidified atmosphere of 5% CO_2 at 37ºC. The medium was then replaced with feeding medium which is the same recipe as the plating medium except that it lacks HS. The neurones were cultured in a humidified atmosphere of 5% CO_2 at 37ºC for 14 – 21 days *in vitro* (DIV).

2.3 DNA manipulation

2.3.1 Constructs

A pEGFP-C2 Vector was used to study dendritic spine morphology in hippocampal cell culture (BD Biosciences Clontech, PT3051-5, Oxford, UK).

A pEGFP-C1 MSK1 plasmid was used to rescue the effect of MSK1 in MSK1 KD cultured hippocampal neurones (BD Biosciences Clontech, 6076-1, Oxford, UK).

2.3.2 Transformation of bacteria

The DNA was transformed into TOP10 *Escherichia coli* (Invitrogen, Paisley, UK) chemically competent cells according to the manufacturer's instructions.

Top 10 *Escherichia coli* genotype: *F-mcrA Δ(mrr-hsdRMS-mcrBC) φ80lacZΔM15 ΔlacX74 recA1 araD139 Δ(ara-leu) 7697 galU galK rpsL (StrR) endA1 nupG λ-*

Briefly, the chemically competent cells were mixed with 1 µl of DNA and left on ice for 30 minutes before heat shocking at 42ºC for 30 seconds. Following the heat shock, cells were placed on ice for 2 minutes before 250 µl of SOC (super-optima

broth with catabolite repression) medium was added. Cells were grown at 37ºC for 1 hour on a shaker.

After 1 hour of outgrowth the cells were plated on LB (lysogeny broth) agar plates supplemented with kanamycin [25 µg/ml] to select for the plasmid positive colonies. The plates were grown overnight (~14-16 hours) at 37ºC. Aseptic techniques were maintained throughout.

2.3.3 DNA preparation

2.3.3.1 Large scale

A single isolated colony was picked from a freshly streaked plate. A starter culture of 3 ml of LB media containing the selective antibiotic (i.e. 25 µg/ml of kanamycin) was inoculated and incubated for 8 hours at 37ºC in a shaker. The starter culture was then diluted 1/1000 into 200 ml of selective LB media. This culture was incubated overnight (~12-16 hours) at 37ºC in a shaker. Aseptic techniques were maintained throughout. Bacterial cells were harvested by centrifugation at 6000 g for 15 minutes at 4ºC and DNA was isolated using Hi-Speed Plasmid DNA maxi kit (Qiagen, West-Sussex, UK).

2.3.3.2 Determining DNA concentration

The concentration of the isolated DNA was measured using a NanoDrop ND-1000 spectrophotometer (Thermo Scientific, Loughborough, UK) and NanoDrop 1000 3.6.0 software. To measure the concentration of DNA accurately 1.5 µl of DNA was used. The NanoDrop calculated the concentrations in ng/ml as well as the purity of the DNA sample to ensure no contaminants were carried over from the Qiagen kit (Qiagen, West-Sussex). The ratio of absorbance at 260/280 nm was used to assess the purity of DNA. A ratio of ~1.8 is generally accepted as “pure” for DNA. The 260/230 nm ratio is used as a secondary measure of purity and was often higher ~2.0-2.2.

2.4 Immunocytochemistry (ICC) and Imaging

Cultured hippocampal neurones were washed twice with warm HEPES buffered saline solution (HBS, components in mM: NaCl, 119; KCL, 5; $CaCl_2$, 2; $MgCl_2$, 2; HEPES, 25; D-Glucose, 30; pH 7.2) and fixed in 4 % paraformaldehyde (PFA) in PBS (phosphate buffered saline) for 10 minutes at room temperature (RT). To quench the autofluorescence of the PFA, 0.1 M glycine in HBS was added for 5 minutes at RT. Permeabilisation using 0.1% Triton X-100 in PBS for 5 minutes at RT was required if the target protein was intracellular. The cells were washed with HBS solution before incubating with the primary antibody diluted in 5% bovine serum albumin (BSA) for 1 hour and 20 minutes at RT. The antibody table (Section 2.11) lists the antibodies used for ICC. The cells were washed with HBS before incubating with an Alexa-Fluor secondary antibody (Molecular Probes, UK) for 1 hour at 4ºC. After the incubation the cells were washed three times with ice-cold HBS and mounted on microscope slides (Thermo Scientific, Loughborough, UK) using 30 µl of Moviol (See Solution preparation).

Images were captured using an inverted Leica TCS SP5 laser scanning confocal system attached to a Leica DM RBE epifluorescence microscope. Immunofluorescent staining was observed using a 63x oil-immersion lens. Images were acquired as Z stacks (~0.2 µm step) and sequential scanning was used for co-staining to avoid bleed-through from one channel to another. Images were exported using Leica Microsystem LAS AF AF6000 software as a TIFF file and processed using Adobe Photoshop 8.0.

2.4.1 Transfection

A transfection mix was prepared 30 minutes beforehand to allow the DNA and the Lipofectamine 2000 (Invitrogen) to form a complex before adding them to the cultured hippocampal neurones (Correa et al. 2009). First, 2 µg of DNA was diluted in Neurobasal A medium and in a separate eppendorf tube 3 µl of Lipofectamine was diluted in Neurobasal A medium. These mixtures were centrifuged at 800 g for 2 seconds and incubated at RT for 15 minutes. Both the DNA and Lipofectamine were pooled together then centrifuged at 800 g for 2 seconds and incubated at RT for 15 minutes. The conditioned medium of the hippocampal culture was removed and retained. The DNA/Lipofectamine mixture was then added to the 22 mm coverslip of cultured hippocampal neurones for 1 hour

and 20 minutes at 5% CO_2 , 37ºC. The transfection mix was then aspirated and the cells were washed twice with warm Neurobasal A medium before adding the conditioned medium back to the cells for 14-16 hours at 5% CO_2, 37ºC. The transfected cells were then immunocytochemically stained following the protocol outlined in Section 2.4.

2.4.2 Dendritic spine analysis

Cultured hippocampal neurons were transfected with an eGFP construct using Lipofectamine 2000 (Invitrogen) as described in Section 2.4.1. After 15–18 h transfection, the cells were fixed using 4% PFA or for those that were TTX-treated, 1 µM was added into the conditioned media for 24 hours before being fixed along with their non-stimulated controls. The cells on the coverslips were mounted using Mowiol. These were then imaged on an inverted SP5 Leica confocal microscope using a 100x oil-immersion lens. Images of the dendrites were acquired as Z stacks (0.1 µm step) at a zoom of 2 and a resolution of 1024 x1024 pixels. Images saved on the Leica Microsystem LAS AF AF6000 software were exported using Image J as LIF files so that they could be saved as compressed Z stacks (i.e. TIFF files) as well as calibrating each image individually.

Spine morphology analysis was performed in NeuronStudio where all slides were blinded beforehand (Wearne et al., 2005; Rodriguez et al., 2008a). The confocal TIFF images were opened in NeuronStudio and calibrated according to the magnification parameters for spine and dendrite measurements. The spines were identified manually while the lengths of the dendrites were traced automatically. The spine volume (in cubic micrometers), spine head width (in micrometers), and spine length (in micrometers) were measured, as well as the spine density per 10 µm of dendrite (Figure 2.1).

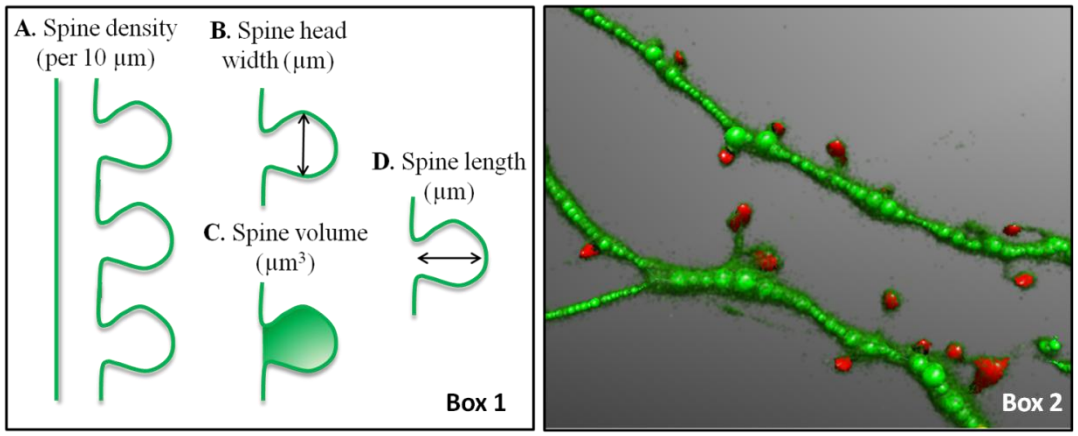

Figure 2.1; A schematic of the parameters measured for spine morphology using 3D reconstruction in NeuronStudio. ***Box 1:*** ***(A)*** *Spine density was calculated by counting the number of spines per 10 µm of dendrite* ***(B)*** *Spine head width was measured from the two furthest points away across the width of the spine (µm)* ***(C)*** *Spine volume was rendered from a 3D reconstruction of the compressed 0.1 µm z stacks. The volume consists of the shaded area up until the shaft of the dendrite (μm^3)* ***(D)*** *Spine length was measured from the shaft of the dendrite to the tip of the spine (µm).* ***Box 2:*** *A representation of a 3D reconstruction of a hippocampal dendrite and its protruding dendritic spines from a calibrated Tiff confocal image. The dendrites are traced shown by the green circles and the dendritic spines are selected and represented as 3D entities shown in the red.*

2.5 Culture treatment and protein extraction

Cultured hippocampal neurones were treated with the desired pharmacological agent which was added directly into the conditioned medium (See Table 2.1). The cells were then incubated in 5% CO_2 at 37ºC for the indicated incubation period. Once the incubation time was complete the cells were placed on ice where the medium was immediately removed and 200 µl of ice-cold lysis buffer (1 mM EDTA, 50 mM Tris-HCL pH7.5, 1% Triton X-100, 1 mM Na_3VO_4, 50 mM NaF, 5 mM $Na_4P_2O_7$, 0.27 M Sucrose, 20% NaN_3,0.1% β Mercaptoethanol and protease cocktail inhibitor tablet) was added to the cells. The cells were scrapped off the bottom of the dish and collected into an eppendorf tube. The cell lysate was placed on a rotating wheel for 1 hour at 4ºC to extract the protein from the cells followed by centrifuging at 13,800 g for 15 minutes at 4ºC. The supernatant was removed and a bicinchoninic acid protein assay (BCA) from Thermo Scientific, Northumberland, UK was carried out according to the manufacturer's instructions in order to measure the protein concentration of each sample in µg/µl.

Pharmacological agents	Target	Concentration		Source
		Stock	Final	
Brain-derived neurotrophic factor (BDNF)	Binds to surface TrkB receptor	50 ng/ml in dH_2O	50 µg/ml	Alomone Labs, Jerusalem, Israel
PD184352	ATP non-competitive MEK1/2 inhibitor	10 mM in DMSO	2 µM	Provided by Dr. Simon Arthur (University of Dundee, Scotland)
Bicuculline (Bic)	$GABA_A$ receptor antagonist	20 mM in dH_2O	20 µM	Ascent Scientific, Cambridge, UK
Tetrodotoxin (TTX)	Blocks voltage-gated sodium channels	1 mM in dH_2O	1 µM	Ascent Scientific, Cambridge, UK
TrkB inhibitor (SH722)	Inhibits TrkB receptor	10 mM in DMSO	0.5 µM	Provided by Dr. Simon Arthur (University of Dundee, Scotland)

Table 2.1*; Pharmacological agents used in treating cultured hippocampal neurones and their correlating final concentrations.*

2.5.1 SDS PAGE; Sodium dodecyl sulphate polyacrylamide gel electrophoresis

Polyacrylamide gels were made which consisted of a stacking gel and a lower gel (See 2.10). The protein samples were diluted in 5x loading buffer (See 2.10) and then heated at 95ºC for 5 minutes. Equal amounts of each protein sample were loaded in the gel (~20 µg protein) before running at 100 V using BioRad Western blot kit (Hertfordshire, UK). The gels were then transferred at 200 mA for 2 hours 30 minutes before blocking the membranes in 5% milk/PBS for an hour on a shaker at RT. Primary antibodies were prepared in 0.5% BSA, 0.1% Tween in PBS and incubated over night at 4ºC on the shaker (See 2.11). The secondary antibodies used were IgG peroxidase conjugated heavy/light chain specific, heavy chain specific or light chain specific (Jackson ImmunoResearch, Baltimore, USA). These were diluted 1/20,000 (for heavy/light chain) or 1/100,000 (for either heavy chain specific or light chain specific) in 0.1% Tween in PBS at RT for an hour. The membranes were washed in 0.1% Tween-PBS for 20 minutes and in PBS alone for 5 minutes. Enhanced chemiluminescence (ECL) solution from Thermo Scientific (Loughborough, UK) was incubated with the membrane and the exposed Fuji Film X-ray film RX (Fisher Scientific, Loughborough) was passed through a developer Curix 60 (AGFA, Mortsel, Belgium). The developed film was scanned and saved as

a TIFF to allow analysis with FIJI software which was based on the Image J software (NIH) with additional plugins. This software calculates the average peak intensity of the bands across a gel or across multiple gels which have been exposed for the same length of time.

2.6 RNA extraction and Q-PCR

RNA was extracted from both adult tissue as well as cultured hippocampal neurones. For adult tissue the hippocampus and frontal cortex were dissected from both hemispheres in ice-cold aCSF (artificial cerebrospinal fluid) containing in mM: 124 NaCl, 26 $NaHCO_3$, 10 D-Glucose, 1.3 NaH_2PO_4, 2 $CaCl_2$, 3 KCL and 1 $MgSO_4$ with an additional 10 mM $MgCl_2$. Once the aCSF was removed 350 µl of RLT buffer (Qiagen, Manchester, UK) was added which lyses the tissue and cultured cells. As opposed to cultured neurones where the 60 mm petri dishes were placed on ice, the media was removed before adding 350 µl of RLT buffer (Qiagen, Manchester, UK). The adult tissue however requires an additional step to dissociate the cells further by using a sterile manual pestle. These lysed samples were homogenised through a QiaShredder Column (Qiagen, Manchester, UK). The sample was centrifuged at 13,800 g for 2 minutes at 4ºC at which point the RNA containing flow through was frozen at -80 ºC. These samples were sent to our collaborator in Dundee, Dr. Simon Arthur, where he and a PhD student Kirsty Martin performed quantative-Polymerase Chain Reaction (Q-PCR) using Sybr Green Fastmix (VWR, Leicestershire, UK). The fold inductions of Arc mRNA levels was measured using 18S rRNA as the normalising gene.

2.7 Environmental enrichment (EE)

The experimental protocol was based and adapted from the work of Raphael Pinaud (Pinaud et al., 2001b). The mice were divided into two groups; an environmental enrichment (EE) group and a standard housing (SH) group. The mice were weaned at P21 and remained in their standard home cage for 7 days to recover from the weaning process. Wild-type (WT) and MSK1 KD mice were killed by cervical dislocation. At least two mice of the same litter were used for both the EE and SH experiments so social behaviour and interaction was retained. The EE group were exposed to environmentally enriched conditions for a specific period of time. These ranged from acute exposures from 1 hour to 6 hours as well chronic long term exposure of up to 2 weeks. The EE conditions included a large cage (39cm x 27cm x

55cm) with a variety of toys, including a running wheel, long and short plastic tubes and a climbing ladder as well as access to water, food pellets and bedding. The SH mice remained in their home cages (19cm x 29cm x 12cm) and were handled i.e. picked up and placed back into their cage and left for the same exposure time of EE group.

2.7.1 Golgi staining

Both WT and MSK1 KD mice from the age of P28 were either exposed to EE conditions for 2 weeks or remained in their SH cages (See Section 2.7 for further information). A complete FD Rapid GolgiStain Kit (FD Neuro Technologies, Columbia, U.S.A) was used and followed in according to the manufacturer's instructions to study the morphology of neurones in brain slices using a Golgi-Cox staining system.

The mice were killed by cervical dislocation where the brain was removed from the skull and washed in PBS before being placed in an A: B solution consisting of mercuric chloride, potassium dichromate and potassium chromate which impregnates the tissue. After 2 weeks incubation at RT protected from the light the brains were transferred to a C solution for 24 hours before replacing it with fresh C solution.

The impregnated fixed brains were cut down the midline into two hemispheres and then set in 5% agar in a petri dish overnight at 4ºC. Parasagittal 200 µm slices were prepared from the hemispheres set in agar on a Vibrotome (Microm, HM650V). The slices were mounted on gelatine-coated microscope slides. Gelatin-coated microscope slides were prepared (See 2.10) by immersing the slides in the gelatin solution 4 times for 4 seconds and allowing the slides to dry for 48 hours at RT. The mounted slides were left to dry overnight in the dark before processing them with solution D and E from the FD Rapid GolgiStain Kit.

The processing of slices involved a series of washing steps starting with distilled water, then solution D and E followed by another wash with distilled water. The brain slices were then dehydrated in successively higher ethanol concentrations starting at 50%, 75%, 95% and 100%. The final wash in Xylene allowed the slides to be cleared before mounting with Mowiol and square coverslips (VWR International, Leicestershire UK).

The slices were blinded before being visualised on a Zeiss Axioskop FS transmission light microscope and imaged using a Nikon DXM1200F digital camera. Using a 100x oil immersion lens the CA1 pyramidal cells in the hippocampus were located using their distinct structural features. A series of Z stacks were captured throughout the tissue using the software Screen Movie Studio (MandSoft, version 2.6.2). These videos were then used to visualise and count the number of spines along the secondary dendrites from the CA1 region of the hippocampus. In order to do this a Screen Tracing Paper programme (Iconico) was used to label and count all visible spines using each Z stack captured in the video. So that the length of the dendrite could be measured, the videos were compressed and converted to TIFF files and imported in Image J (NIH). These images were then calibrated accordingly to the scale bar. The spine density was calculated per 50 µm of dendrite and averaged to obtain an overall spine density value.

2.7.2 Electrophysiology

2.7.2.1 Hippocampal slice preparation and maintenance

4-6 week old WT and MSK1 KD mice exposed to enriched or standard housing conditions were used in these experiments. They were killed by cervical dislocation in accordance with the UK Animal (Scientific Procedures) Act and local Ethical Review procedures. The brain was removed from the skull and placed in oxygenated ice-cold aCSF cutting solution containing high magnesium (see 2.10). Using a razor blade a thin slice from the lateral aspect of each hemispheres was removed to provide a flat surface to glue the hemispheres to the cutting block. After this the brain was cut down the midline and both hemispheres were mounted onto a cold metal block using cyanoacrylate adhesive (RS Components, Corby, UK). The mounted hemispheres were submerged in oxygenated ice-cold aCSF cutting solution and fixed in the vibratome (Microm, HM650V) which was used to prepare 400 µm parasagittal hippocampal slices. The slices were then allowed to recover for an hour in standard aCSF solution (containing 1 mM Mg^{2+}) gassed with 95% O_2/5%CO_2 at 34ºC. This temperature has been shown to be vital in allowing the slice to recover energy parameters comparable to *in vivo* conditions.

2.7.2.2 Slice placement and stimulation protocol

A hippocampal slice was placed in a recording chamber which consisted of a mesh-like surface upon which the slice rested allowing oxygenated solution to perfuse both sides of the slice (Dale et al., 2000; Frenguelli et al., 2007). Slices were perfused with standard aCSF gassed with 95% O_2/5%CO_2 at a flow rate of 6-7 ml/minute at 32ºC. The Schaffer collateral-commissural pathway was stimulated in stratum radiatum with a bipolar Teflon-coated tungsten stimulating electrode (100 µm diameter) at 0.067 Hz using an isolated constant current stimulator DS3 (Digitimer, Ltd, UK) (Figure 2.2).

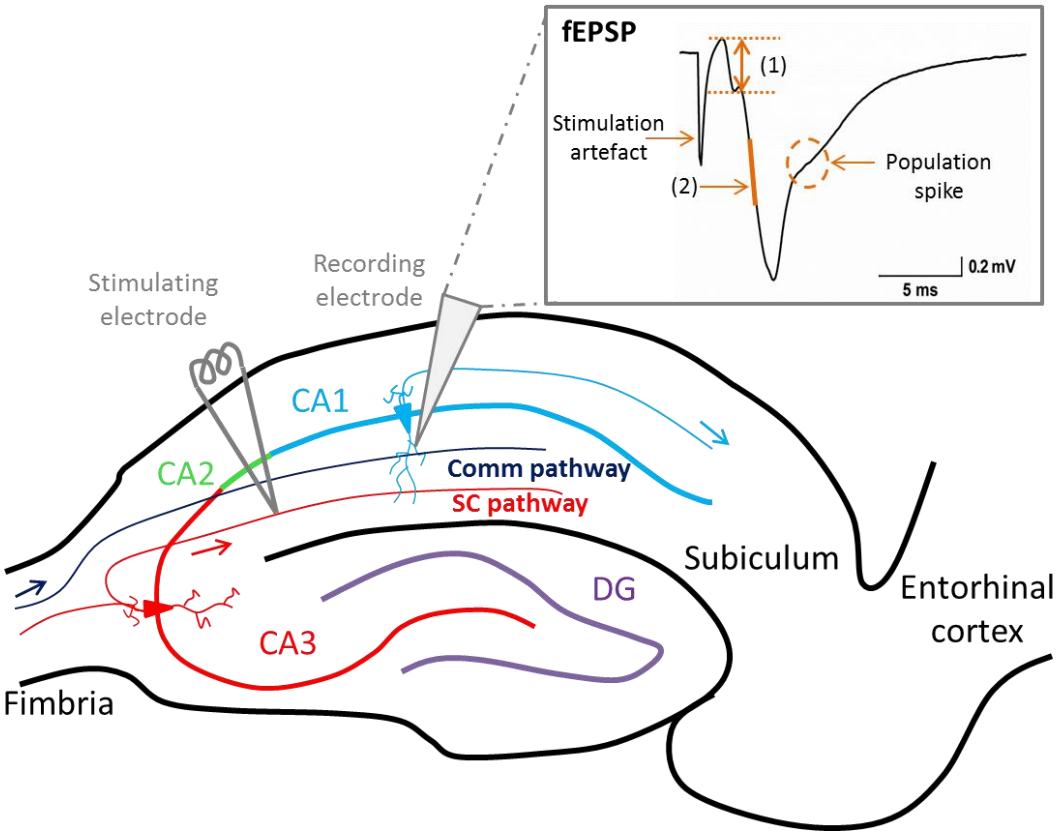

Figure 2.2; A schematic diagram representing where the stimulating and recording electrodes were placed on the hippocampal slice to obtain a field excitatory postsynaptic potential (fEPSP). *The hippocampal circuit includes the dentate gyrus (DG), the CA1 region and CA3 region. The pathway we stimulated is known as the Schaffer collateral (SC) pathway which comprises of the CA3 pyramidal cell axons (red) protruding to the CA1 region where they synapse with the CA1 pyramidal cells (blue). A bipolar Teflon-coated tungsten stimulating electrode was used. Using a glass microelectrode we recorded from the CA1 pyramidal cells in the stratum radiatum to obtain a fEPSP shown in the grey box. A typical fEPSP will have a spike representing the stimulation artefact followed by a fibre volley which represents the number of axons recruited upon stimulation. A functional readout for the size of a fEPSP is measuring* ***(1)*** *the pre-synaptic fibre volley amplitude (mV). The fEPSP slope* ***(2)*** *can also be measured as is most commonly used to represent the size of a fEPSP. A population spike can also occur when a high stimulation strength is used which corresponds to the population of cells firing action potentials.*

2.7.2.3 Basal synaptic transmission and paired-pulse experiments

Extracellular field excitatory postsynaptic potentials (fEPSP) were recorded from stratum radiatum in area CA1 with an aCSF-filled borosilicate glass microelectrode (Harvard Apparatus, Kent, UK) of ~1 MΩ resistance. The signal was collected at a sampling rate of 10 000 Hz and amplified on an Iso-Dam amplifier (WPI-Europe, UK), high-pass signal filtered at 1Hz and low-pass filtered at 3kHz.

The linear part of the fEPSP slope (Figure 2.2) was measured throughout the recording which usually measured over 1 ms range. A stable fEPSP was recorded using a stimulus which was 50% of maximal fEPSP slope before measuring an input/output (I/O) relationship curve using a range of stimuli (in µA) 10, 25, 50, 100, 150, 200, 250 and 300. The average of three values were collected per stimulation and plotted on a graph as average fEPSP slope (mV/ms) (Figure 2.2 (2)). The fibre volley (FV) was also measured (Figure 2.2 (1)) which was represented as an amplitude value (mV). The I/O traces were re-opened in the Win LTP programme (Bristol, UK).

The paired-pulse (PP) ratio was also calculated over an interpulse interval of 50 ms, 100 ms, 150 ms, 200 ms and 250 ms using fEPSP of ~50% of the maximal fEPSP slope .

2.7.2.4 Induction of long-term potentiation (LTP) protocol

Two different protocols were used to induce LTP in hippocampal slices. The first was a high-frequency stimulation (HFS) known as a tetanus consisting of 100 pulses at 100 Hz. The second was theta burst stimulation (TBS) which is thought to be a more physiological means of LTP induction. This stimulation involved 4 pulses at 100 Hz repeated 10 times with a 200 ms interval. This burst was repeated three times with a 20 second interval between bursts. The stimulation was applied after 10 minutes of stable baseline was collected at 0.067 Hz. The recordings continued for at least an hour after the induction of LTP.

2.8 Immunoprecipitation and proteomic study

An adult male C57/B16 mouse was sacrificed in accordance with the UK Animal (Scientific Procedures) Act and local Ethical Review procedures using anaesthetic overdose. The brain was removed from the skull and placed in oxygenated ice-cold standard aCSF. Using a microscope the hippocampi were dissected using the same technique outlined in Section 2.2. The hippocampi were manually dissociated in 400 µl HEPES/Sucrose solution (4 mM HEPES, 0.32 M sucrose and protease inhibitor tablet) using a pestle followed by brief sonication. The tissue was placed on a rotating wheel at 4ºC for 1 hour before centrifuging at 13,800 g at 4ºC for 15 minutes. The supernatant protein lysate was kept on ice and a small

sample was used to carry out a BCA Protein assay to determine the protein concentration of the sample extract.

In the mean time, Protein G agarose-fast flow beads (Merck Millipore, 16-266) were prepared for each immunoprecipitation reaction where they were washed in lysis buffer. For each immunoprecipitation reaction, 15 µl of beads was pipetted into an eppendorf. The washing step involved adding 800 µl of ice-cold lysis buffer without β-Mercaptoethanol or protease inhibitor tablet (Section 2.10) into the eppendorf containing the beads. As there is no protein present at this point there would be no need to add the β-Mercaptoethanol or protease inhibitor tablet. The eppendorf containing the beads and lysis buffer was inverted gently to mix the solutions followed by centrifugation at 64 g for 30 seconds at 4ºC to separate the beads (pellet) and lysis buffer (supernatant). The supernatant was aspirated and the washing process was repeated three times.

Once the protein concentration had been calculated and the beads had been washed the immunoprecipitation reactions were prepared using the following components shown in Table 2.2. The positive control involved adding Arc, 1 µg of Arc antibody (Synaptic systems, Germany, 156-003) to the eppendorf containing the beads as well as 500 µg of protein lysate diluted in a total volume of 500 µl of lysis buffer (Table 2.2; Arc IP column). The important negative control was the 1 µg anti-rabbit IgG IP (IgG control, Table 2.2) where the IgG acts a negative control for the IgG of the Arc antibody used in the Arc IP positive control. Some raw protein lysate was kept on ice to use as the positive control known as the input (approximately 10 µg loaded onto gel). The four negative controls are highlighted in Table 2.2.

Each IP tube was rotated gently for 3 hours at 4ºC. After the incubation time the IP were washed three times following the same protocol as before. Starting with centrifuging the eppendorfs at 64 g for 30 seconds at 4ºC followed by washing the beads with lysis buffer including β-Mercaptoethanol and protease inhibitor since there was protein present at this stage. After the last aspiration of lysis buffer washing step the beads were re-suspended in 20 µl of 5x loading buffer (See 2.10) before heating them at 95ºC for 5 minutes in a water bath. SDS PAGE was used to separate and detect the presence of specific proteins (See 2.5.1). The gels were transferred (BioRad western blot kit) for 2 hours and blocked in 5% milk/PBS for 1 hour before incubating overnight with primary antibodies. These included antibodies

against Arc as well as one of the following AP-2 μ, AP-2α, AP-1γ, AP-3σ and AP-4ε (See 2.11). Secondary antibodies used were either anti-rabbit or anti-mouse IgG peroxidase conjugated light-chain specific (Jackson ImmunoResearch Laboratories, Baltimore, USA). A light-chain specific secondary antibody was required because the heavy chain weighs ~50 kDa and ~100 kDa which is the molecular weight of Arc. Enhanced chemiluminescence was used to develop the immunoblots (Please see Section 2.5.1 for further details).

For the proteomic study, Arc was immunoprecipitated from hippocampal extracts as mentioned above. The IP extract was loaded into the gel and run for ~15 minutes at 80V. The gel was removed and placed into distilled water before cutting out the protein trace (which measured around 2 cm). This small trace of gel was placed into an eppendorf tube containing distilled water and sent to the Proteomics centre at Bristol University for mass spectrometry analysis.

IP components	Arc IP	Antibody control	Protein control	Lysis buffer control	IgG control
Protein G agarose-fast flow beads (15 µl)	✓	✓	✓	✓	✓
500 µg protein extract	✓		✓		
1 µg Antibody	✓	✓			
Lysis Buffer	✓	✓	✓	✓	✓
Anti-rabbit IgG (1 µg)					✓

Table 2.2; *A table highlighting the different components required for an IP (immunoprecipitation) experiment using Protein G agarose-fast flow beads. These include the 4 negative controls, antibody only, protein only, lysis buffer only and IgG control.*

2.9 Analysis and statistical tests

For all statistical tests carried out in this thesis the level of significance was set at $p<0.05$. The asteriks throughout this thesis represent * $p<0.05$, ** $p<0.01$ and *** $p<0.001$. In Chapter 3, in order to compare a non-stimulated condition to a stimulated condition for each genotype in one experiment multiple unpaired t tests were carried out using Holm-Sidak as a post hoc test for multiple comparisons. Multiple unpaired t tests were used as oppose to One Way ANOVA because in a One Way ANOVA all groups are compared, some of which are irrelevant and therefore one looses the power of significance. When there were only 2 groups of data to compare, a simple unpaired t test was used e.g. comparing basal RSK2 protien levels in WT and MSK1 KD hippocampal neurones.

In Chapter 4, percentage cumulative frequency distribution curves were created using a bin size of 0.005 for all spine parameters including volume, diameter and length as the number of values for each parameter were very high. The most appropriate statistical test to use on cumulative frequency data is a nonparametric Kolmogorov-Smirnov (KS) test which compares the distribution curves of two datasets. The bar graphs representing spine density were analysed using multiple unpaired t tests (Holm-Sidak as a post hoc test for multiple comparisons).

Finally, in Chapter 5, the bar graphs for mRNA, protein and spine density were analysed using multiple unpaired t tests (Holm-Sidak as a post hoc test for multiple comparisons).The electrophysiology data was analysed using Two Way ANOVA as there were two variables in each group which were being compared e.g. WT SH for each stimulus intensity or interpulse interval was compared to the WT EE at each stimulus internsity or interoulse interval. The LTP data was analysed within each group e.g. WT SH as the data from the begining of the LTP trace was compared to the end and therefore required a paired t test. However when the end of WT SH and WT EE LTP traces were compared, an unpaired t test was used as they were different conditions.

2.10 Solution preparation

Solution	Composition	Use
10 x aCSF (Artificial cerebrospinal fluid) [standard aCSF]	<u>To make 1 L:</u> NaCl 72.5 g (1.24 M), KCl 2.2 g (30 mM), $NaHCO_3$ 21.8 g (260 mM), NaH_2PO_4 1.7 g (13 mM). Dissovle in dH_2O. <u>To make 1 L of 1 x aCSF</u>; Dilute 1 in 10 in dH_2O and add 1.8 g Glucose (10 mM), 2 ml of 1M $CaCl_2$ (2 mM) and 1 ml 1M $MgSO_4$ (1 mM)	Stock solution (made weekly) Maintenance of acute hippocampal slices
aCSF high Mg^{2+} cutting solution	As above but add 10 ml of 1 M $MgCl_2$ (10 mM)	Acute hippocampal slice preparation
DMEM (Dulbecco's modified eagle medium)	*Prepared by Media Preparation Services* as per GIBCO (Invitrogen, Paisley, UK) recipe with phenol red	Preparation of hippocampal neuronal cell culture
LB (Lysogeny Broth)	*Prepared by media preparation services* For 1 L: 10 g tryptone, 5 g yeast extract, 10 g NaCl	DNA preparations
5x Loading buffer	100 mM Tris HCL pH 6.8, 20% glycerol, 10% SDS, 0.005% Bromophenol blue, 10 mM Dithiothreitol (DTT)	Gel electrophoresis
HBS (HEPES buffered saline)	<u>To make 10 x HBS in 100 ml dH_2O:</u> NaCl 6.95 g (1.2 M), KCL 0.37 g (50 mM), HEPES 5.9 g (250 mM), D-Glucose 6 g (330 mM), 2 ml of 1M $CaCl_2$ (20 mM) and 2 ml of 1 M $MgCl_2$ (20 mM). pH was adjusted to pH 7.2 using 5M NaOH	Immunocytochemistry (ICC)
PBS (Phosphate buffered saline)	*Prepared by media preparation services* as per GIBCO (Invitrogen, Paisley, UK) recipe	Gel electrophoresis
4% PFA (Paraformaldehyde)	<u>For 100 ml:</u> 4 g Paraformaldehyde dissolved in 1x PBS. pH adjusted to 7.4	ICC
Protein lysis buffer	1mM EDTA, 50 mM Tris-HCL pH7.5, 1% Triton X-100, 1 mM Na_3VO4, 50 mM NaF, 5 mM $Na_4P_2O_7$, 0.27 M Sucrose,	Protein extraction

	20% NaN_3, For 10 ml aliquot add:- 0.1% β Mercaptoethanol and 1/4 protease cocktail inhibitor tablet	
HEPES/Sucrose solution	4 mM HEPES, 0.32 M sucrose and protease inhibitor tablet. A ¼ of protease inhibitor tablet used per 10 ml of solution	Immunoprecipitation
Stacking gel (4%)	2.1 ml distilled water, 0.95 ml Upper buffer 0.5 mM Tris pH6.8, 0.6 ml 30% Acrylamide, 37.5 µl 10% Sodium dodecylsulphate (SDS), 37.5 µl TEMED and 4 µl Ammonium persulphate (APS)	Gel electrophoresis
Lower gel	For a 12% gel: 2.3 ml distilled water, 2.35 ml Lower buffer 1.5 mM Tris pH8.8, 3.35 ml 30% Acrylamide, 82.3 µl 10% SDS, 8.25 µl TEMED and 41.5 µl APS	Gel electrophoresis
SOC (super-optima broth with calabolite repression) medium	*Prepared by media preparation services* For 1 L: 20 g Bacto Tryptone, 5 g Bacto Yeast Extract, 2 ml of 5 M NaCl, 2.5 ml of 1M KCL, 10 ml of 1M $MgSO_4$, 20 ml of 1M glucose	Transformation of bacteria with DNA
Gelatin solution	2.5 g of gelatin is dissolved in 500 ml of distilled water. Then 0.25 g of chromium potassium sulphate is dissolved into the solution. Filter the solution.	To prepare gelatin for coating microscope slides for Golgi staining
10x SDS-PAGE Running Buffer	*Prepared by media preparation services* For 2 L: 288 g Glycine, 60.4 g Tris base, 20 g SDS and 1.8 L dH_2O	Gel electrophoresis
10x Tris based Transfer Buffer	*Prepared by media preparation services*	Gel electrophoresis

	For 2 L: 288g glycine, 60.4 g Tris base and 1.8 L of dH_2O For 1L of 1x transfer buffer: 100 ml of 10x transfer buffer, 200 ml of 100% methanol and 700 ml of dH_2O	
Mowiol	4.8g Mowiol, 12g glycerol,12ml dH2O, 24ml 0.2 M TrisHCL (pH8.5). Heat to 50ºC for 10 minutes. Centrifuge at 5000 g for 15 minutes	ICC

2.11 Antibodies

Antibodies	Company	Species	Molecular weight (kDa)	Use
α Adaptin 1/2 (C-8) [AP2-α2]	Santa cruz, Texas, UK	Mouse	100	ICC, WB
AP50 [AP2-μ2]	BD Transduction laboratories, Oxford, UK	Mouse	50	WB
AP-γ1	BD Transduction laboratories, Oxford, UK	Mouse	104	WB
AP-σ3	BD Transduction laboratories, Oxford, UK	Mouse	160	WB
AP-4ε	BD Transduction laboratories, Oxford, UK	Mouse	127	WB
Arc	Synaptic systems, Goettingen, Germany	Rabbit	50	WB, IP
Clathrin-heavy chain (CHC)	Cell signalling, Massachusetts, USA	Goat	180	ICC
C-terminus GluA1	Merk Millipore, Massachusetts, USA	Rabbit	100	WB
C-terminus GluA2	Zymed, Paisley, UK	Mouse	98	WB
GAPDH (Glyceraldehyde 3-phosphate dehydrogenase)	Abcam, Cambridge, UK	Mouse	37	WB
MSK1	Cell signalling, Massachusetts, USA	Rabbit	90	WB
N-terminus GluA1	Upstate, Massachusetts, USA	Rabbit	100	WB
Phospho H3 (S10)	Abcam, Cambridge, UK	Mouse	15	WB
Phospho p44/42 (ERK1/2)	New England-Biolabs, Herts, UK	Rabbit	42/44	WB

p44/42 (ERK1/2)	New England-Biolabs, Herts, UK	Mouse	42/44	WB
PSD-95	Abcam, Cambridge, UK	Mouse	95	ICC
RSK2	Cell signalling, Massachusetts, USA	Rabbit	90	WB

Key: WB; Western blot, ICC; Immunocytochemistry, IP; Immunoprecipitation

2.12 Materials and Chemicals

Material/ Chemical	Company
10% SDS	Melford (Suffolk, UK)
100% Ethanol	VWR International (Leicestershire, UK)
100% Methanol	VWR International (Leicestershire, UK)
Acrylamide	Sigma-Aldrich (Dorset, UK)
Agar	Sigma-Aldrich (Dorset, UK)
Ammonium persulphate (APS)	Fisher (Loughborough, UK)
Bromophenol blue	Sigma-Aldrich (Dorset, UK)
BSA	Sigma-Aldrich (Dorset, UK)
$CaCl_2$	Fisher (Loughborough, UK)
D-Glucose	Fisher (Loughborough, UK)
Dithiothreitol (DTT)	Melford (Suffolk, UK)
DNase	Sigma-Aldrich (Dorset, UK)
EDTA	VWR International (Leicestershire, UK)
Gelatin	Sigma-Aldrich (Dorset, UK)
Gentamyin	Melford (Suffolk, UK)
Glycerol	Fisher (Loughborough, UK)
Glycine	Sigma-Aldrich (Dorset, UK)
Hank's buffered salt solution	Fisher (Loughborough, UK)
HCL	Fisher (Loughborough, UK)
Heat inactivated horse serum	GIBCO (Paisley, UK)
HEPES	Sigma-Aldrich (Dorset, UK)
Kanamycin	Formedium (Norfolk, UK)
KCl	Fisher (Loughborough, UK)
L-Glutamine (150 mM)	Formedium (Norfolk, UK)
$MgCl_2$	VWR International (Leicestershire, UK)
$MgSO_4$	Fisher (Loughborough, UK)
Mowiol	Sigma-Aldrich (Dorset, UK)
Na_3VO4	Sigma-Aldrich (Dorset, UK)
NaCl	Fisher (Loughborough, UK)
NaF	Sigma-Aldrich (Dorset, UK)
NaH_2PO_4	Fisher (Loughborough, UK)
$NaHCO_3$	Fisher (Loughborough, UK)
NaN_3	Sigma-Aldrich (Dorset, UK)
NaOH	Fisher (Loughborough, UK)
Neurobasal A medium	GIBCO (Paisley, UK)
Poly-L-Lysine	Sigma-Aldrich (Dorset, UK)
Protease inhibitor tablets	Roche (West Sussex, UK)
SDS	Fisher (Loughborough, UK)
Sucrose	Fisher (Loughborough, UK)

Supplement B-27	GIBCO (Paisley, UK)
TEMED	Sigma-Aldrich (Dorset, UK)
Tris	Melford (Suffolk, UK)
Triton X-100	Fisher (Loughborough, UK)
Trypsin in Tris saline	BD Difco (New Jersey, USA)
Xylene	Fisher (Loughborough, UK)
β Mercaptoethanol	Gibco (Paisley, UK)

Chapter 3.

Characterisation of MSK1's role in hippocampal synaptic plasticity

3.1 Introduction

Brain-derived neurotrophic factor (BDNF) has emerged as being an important mediator in synaptic adaptation and plasticity, one of which is the induction and maintenance of LTP (Ying et al., 2002). LTP is a form of synaptic plasticity in which one of the molecular mechanism underlying the long lasting synaptic changes involves glutamate AMPAR (α-amino-3-hydroxy-5-methyl-4-iso-xazolepropionic acid receptor) trafficking (Collingridge et al., 2004; Anggono and Huganir, 2012). BDNF binds to TrkB receptor which initiates a mitogen-activated protein kinase (MAPK) dependent intracellular signalling cascade, including extracellular signal-regulated kinase 1/2 (ERK1/2) (Bramham and Messaoudi, 2005; Numakawa et al., 2010). More importantly acute BDNF application has shown to up-regulate the synthesis of an immediate-early gene (IEG) known as activity-regulated cytoskeleton-associated protein, Arc (Ying et al., 2002). Arc interacts with the endocytotic machinery including dynamin 2 and endophilin 3 (Chowdhury et al., 2006). Subsequently Arc has been shown to play an important role in the endocytosis of AMPAR at the postsynaptic membrane during different forms of synaptic plasticity. AMPAR are ionotropic transmembrane receptors for glutamate and can be made up of homodimers or heterodimers of 4 subunits, GluA1-4 (Palmer et al., 2005a; Anggono and Huganir, 2012).

The outstanding question which needs to be addressed is; what mediator is regulating the response between BDNF induced signalling and the expression of Arc protein? A potential candidate could be mitogen- and stress- activated protien kinase 1 (MSK1), as it is nuclear serine/threonine kinase which regulates gene transcription in a BDNF dependent manner.

MSK1 has two isoforms (1 and 2), in which MSK1 is more abundant in the hippocampus (Chwang et al., 2007; Arthur, 2008; Frenguelli and Corrêa, 2012). There are strong similarities in kinase domains between MSK and ribosomal s6 kinase (RSK) kinases. MSK1 is a substrate of ERK1/2 and to a lesser extent p38 MAPK (Mitogen activated protein kinases). These effectors are activated upon BDNF stimulation including upstream MAPK kinase, MEK1/2 which phosphorylates ERK1/2 (Ying et al., 2002; Bramham and Messaoudi, 2005). MSK1 is activated via a series of phosphorylation sites first of which are phosphorylated by ERK1/2 at the C-terminus which auto phosphorylates residues at the N-terminus kinase domain allowing MSK1 to phosphorylate downstream substrates (Figure 1.10) (Arthur, 2008). MSK1 regulates gene transcription by phosphorylation of CREB (cyclic AMP response element-binding protein) at serine-133 (S133) (Deak et al., 1998; Arthur and Cohen, 2000; Frenguelli and Corrêa, 2012) as well as phosphorylation of histone H3 at serine-10 (S10) allowing chromatin remodelling (Thomson et al., 1999; Chwang et al., 2007; Roth and Sweatt, 2009).

BDNF has also been implicated in another form of synaptic plasticity known as homeostatic scaling. This form of plasticity allows a population of neurones to maintain their synaptic activity within physiological limits especially when faced with chronic synaptic perturbations (Turrigiano, 2008). When neurones are incubated with TTX, a voltage gated sodium channel blocker which prevents action potentials, they respond by increasing their synaptic strength via the upregulation of their surface AMPAR expression (Turrigiano et al., 1998). The activity dependent IEG, Arc has been shown to be essential in regulating the trafficking of GluA1 AMPAR subunit during synaptic scaling in hippocampal neurones (Shepherd et al., 2006). The effects of suppression of neuronal activity via TTX application *in vitro* and *in vivo* have been attributed to a reduction in BDNF mRNA levels (Zafra et al., 1991; Bozzi et al., 1995; Rutherford et al., 1998). Therefore MSK1 could also be regulating the expression of Arc under TTX-induced synaptic scaling.

The aim of this Chapter is to characterise the role of MSK1 in regulating the expression of Arc protein in response to BDNF-ERK1/2 stimulation. As the regulation of Arc protein during synaptic plasticity has been shown to be BDNF-ERK dependent, it would be necessary to further depict if MSK1, as a nuclear kinase would be regulating the Arc expression via histone H3 (H3) phosphorylation under these conditions. In order to characterise the role of MSK1 a transgenic mouse line

was generated by Dr. Simon Arthur (University of Dundee, Scotland) known as MSK1 kinase dead (KD) (See Section 2.1 or (Correa et al., 2012).

The experiments required to investigate the role of MSK1 downstream to the BDNF-ERK1/2 signalling pathway would involve preparing dissociated hippocampal cultures from P0/1 MSK1 KD and wild-type (WT) mice. The three aims of this Chapter were to expose the hippocampal cultures to three agents (Figure 3.1); (1) exogenous BDNF, (2) a MEK1/2 inhibitor known as PD184352 and (3) a voltage gated sodium channel blocker, tetrodotoxin (TTX). A schematic diagram representing the hypotehsised pathway which would be manipulated using these three agents (Figure 3.1). The functional readout in response to thesis agents was to monitor whether the expression levels of phosphorylated ERK1/2, histone H3 (H3) and total Arc altered between WT and MSK1 KD neurones.

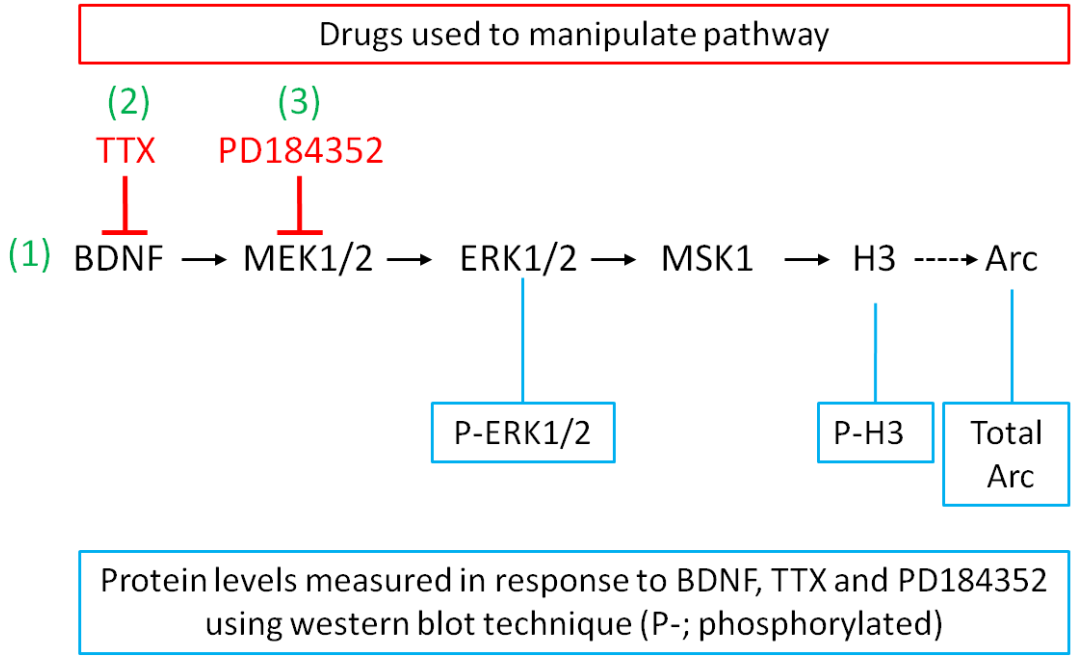

Figure 3.1; A BDNF-Arc pathway hypothesised to be MSK1 dependent*. This diagram represented the hypothesised pathway in which we had three aims to address. The pathway would be tested for its response to (1) exogenous BDNF, (2) PD184352, a MEK1/2 inhibitor and (3) TTX, a voltage gated sodium channel blocker. The dotted line represent the area of the pathway in which we would like to elucidate to using MSK1 KD mice as the aim is to characterise the potential role of MSK1 acting as a regulator in Arc protein expression via H3 phosphorylation. [BDNF; Brain-derived neurotrophic factor, MEK1/2; Mitogen-activated protein kinase kinase 1/2, ERK1/2; Extracellular signal-regulated kinase 1/2, MSK1; Mitogen-and stress-activated kinase 1, H3; Histone H3, Arc; Activity-regulated cytoskeleton-associated protein, TTX; Tetrodotoxin]*

3.2 Results

3.2.1 Characterisation of the endogenous Arc, GluA1 and RSK2 expression in MSK1 KD neurones

3.2.1.1 Endogenous expression of Arc and GluA1 in WT and MSK1 KD hippocampal culture

Primary dissociated hippocampal neurones from P0/1 WT and MSK1 KD mice were cultured for 14 DIV and 21 DIV in order to measure the total expression of Arc as well as the GluA1 AMPAR subunit. The data in Figure 3.2 demonstrates that there are no changes in total expression of neither Arc nor GluA1 under control conditions in 14 and 21 DIV hippocampal neurones.

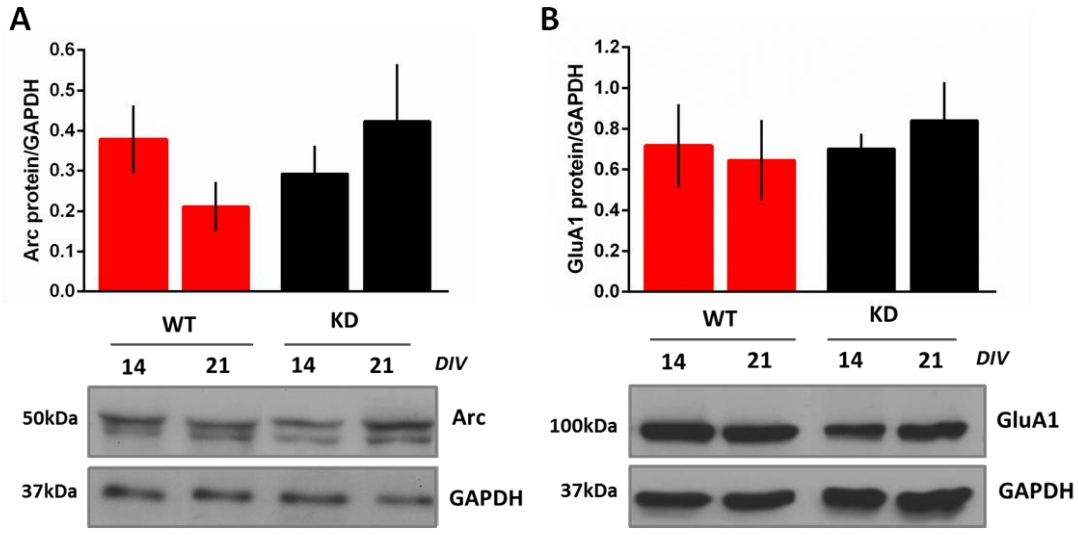

Figure 3.2; There were no developmental changes in total Arc and GluA1 protein in WT and MSK1 KD hippocampal culture. *Dissociated hippocampal neurones from WT and MSK1 KD mice were cultured for 14 and 21 DIV before being lysed and running the protein extract through SDS-PAGE. The membrane was incubated with* ***(A)*** *Anti-Arc and* ***(B)*** *Anti-GluA1 antibody overnight. GAPDH was used as a loading control. The band intensities were analysed using Fiji software. The bar graphs represent average ±SEM and the representative blots are shown below. Multiple unpaired t tests using the Holm-Sidak post hoc test which sets significance level at $p<0.05$. [n=7 for WT and MSK1 KD for Arc and n=3 for WT and MSK1 KD for GluA1]*

3.2.1.2 MSK1 KD neurones do not have compensatory increase in RSK2 protein expression

Another protein kinase located downstream to MAPK signalling is RSK (ribosomal S6 kinase) which is directly phosphorylated by ERK1/2. The RSK2 isoform has been shown to be important in neuronal function and development. So much so that in humans point mutations in the rsk2 gene causes Coffin-Lowry syndrome (CLS), an inherited condition characterised clinically by severe psycho-motor retardation (Thomas and Huganir, 2004). RSK2 has been shown to regulate phosphorylation of histone H3 (Sassone Corsi et al., 1999) just like MSK1 and therefore it was necessary to monitor the protein levels in the MSK1 KD neurones to see if RSK2 was up regulated in a compensatory manner.

Hippocampal tissue was prepared from P0 WT and MSK1 KD mice and the protein was extracted and separated using SDS PAGE. The membrane was probed against RSK2 and total ERK1/2 which was used as a loading control. Figure 3.3 showed that there were no differences observed in the total RSK2 protein expression in WT and MSK1 KD tissue.

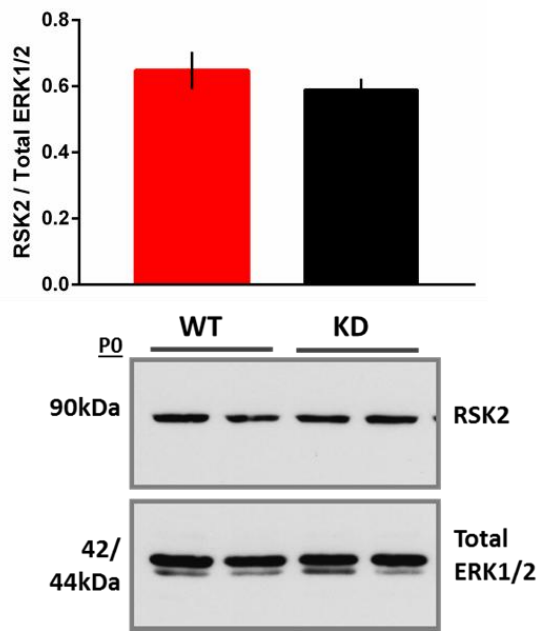

Figure 3.3; No up regulation of RSK2 protein in MSK1 KD postnatal hippocampal tissue. *Hippocampal tissue was dissected from P0 WT and MSK1 KD mice and the protein was extracted and separated through SDS-PAGE. The membrane was probed against anti-RSK2 and total ERK1/2 as a loading control where they were analysed using Fiji software. The bar graphs represent the average value ±SEM. An unpaired t test was carried out where there was no significant difference between WT and MSK1 KD. [n=5-6 for WT and MSK1 KD.]*

3.2.2 Probing a BDNF-MSK1-Arc dependent signalling pathway

3.2.2.1 The effects of a MEK1/2 inhibitor on phosphorylation levels of ERK1/2 and histone H3 as well as total levels of Arc protein in WT and MSK1 KD hippocampal neurones

In order to establish that the hippocampal neurones in culture are responsive to external manipulations we used the MEK1/2 inhibitor PD184352. MEK1/2 is a MAP kinase kinase (MAPKK) which directly phosphorylates the downstream MAPK ERK1/2 (Zassadowski et al., 2012) and therefore PD184352 should significantly reduce the phosphorylation of ERK1/2. This was tested in hippocampal neurones which were cultured for 18-21 DIV and treated with 2 μM of PD184352 for 3 hours at 37ºC, 5% CO_2. The cells were then lysed and then the protein was extracted and separated using SDS-PAGE. The phosphorylation levels of ERK1/2 were greatly reduced in response to the MEK1/2 inhibitor (Figure 3.4 A; multiple unpaired t tests, Holm-Sidak; ***$p<0.001$ and *$p<0.05$). This was apparent in both the WT and MSK1 KD neurones as ERK1/2 is located upstream to MSK1 and therefore should be unaffected in the MSK1 KD mice.

MSK1 can regulate gene transcription via chromatin remodelling through phosphorylation of histone H3 or via the phosphorylation of Ser133 residue on the transcription factor, CREB (Thomson et al., 1999; Wiggin et al., 2002). According to preliminary data received from Dr. Simon Arthur, MSK1 does not regulate the induction of Arc via CREB. Neurones were cultured from a S133 CREB mutant mouse mutant where the serine was mutated to an alanine. The neurones were cultured and stimulated with BDNF where the transcription of the CREB target gene, Nur77 was found to be greatly reduced. However the transcription of CREB-independent gene, c-jun was unaffected. However, Arc mRNA induction by BDNF was unchanged in the CREB S133Ala knock-in neurones. In knowing this we then investigated the levels of phosphorylated histone H3 after BDNF stimulation in WT and MSK1 KD neurones. Previous studies have shown that MSK1 is required for MAPK-induced histone H3 phosphorylation at S10 (Chwang et al., 2007; Roth and Sweatt, 2009). Interestinly both WT and MSK1 KD neurones showed a trend in reduced levels of histone H3 phosphorylation at S10 after incubation with MEK1/2 inhibitor. However only the MSK1 KD neurones showed this trend to be significant (Figure 3.4 B, * $p<0.05$, multiple unpaired t tests using Holmn Sidak post hoc).

Under basal conditions there appeared to be a reduced tone in phosphorylated histone H3 in the MSK1 when compared to WT but was not statistically significant. This suggests that MSK1 could be important in regulating histone H3 phosphorylation under basal conditions.

Our original hypothesis was that ERK1/2-dependent activation of MSK1 is regulating the phosphorylation of histone H3 at Ser10. This histone modification would subsequently control the gene transcription of the IEG Arc and therefore one would predict that the levels of Arc protein would also be reduced in the presence of PD 184352. The results shown in Figure 3.4 C suggests that this is not the case as the levels of total Arc protein expressed in the presence of the MEK1/2 inhibitor was unchanged when compared to the control, in both the WT and MSK1 KD.

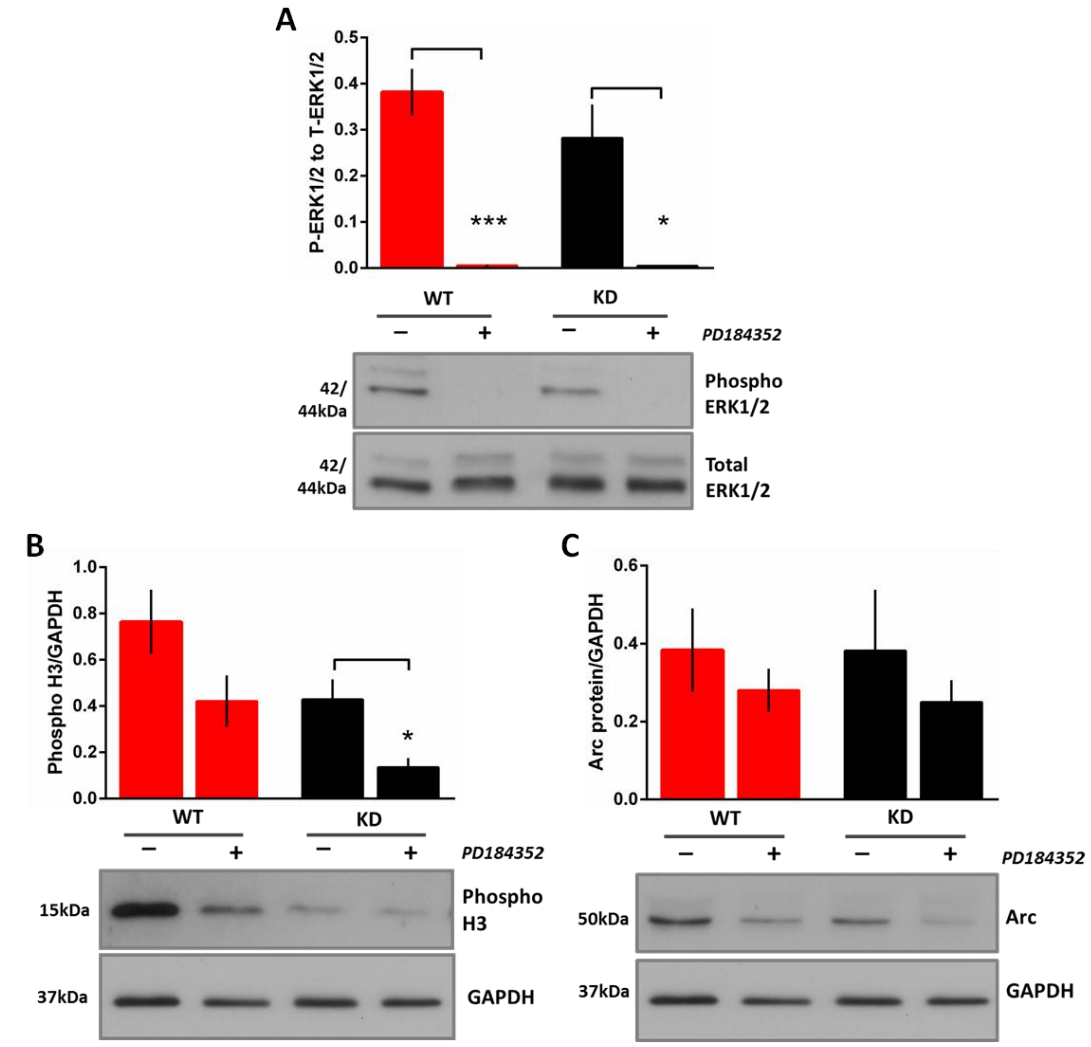

Figure 3.4; Characterisation of the ERK1/2-MSK1 dependent signalling pathway in hippocampal culture using a MEK1/2 inhibitor*. Dissociated hippocampal neurones from WT and MSK1 KD mice were cultured for 18-21 DIV before being treated (+) with 2 µM of PD 184352, a MEK1/2 inhibitor for 3 hours as well as a non-treated condition (-). The cells were then lysed and the proteins were separated using SDS-PAGE electrophoresis. Three target proteins, ERK1/2, Phospho H3 and Arc, were probed against in order to depict the signalling pathway. The bar graphs represent the average value ±SEM generated from measuring the intensity of the bands using Fiji software.* ***(A)*** *Anti-phospho ERK1/2 antibody was used with total ERK1/2 as a loading control.* ***(B)*** *The levels of phospho histone H3 (H3) at S10 was imaged using GAPDH as a loading control.* ***(C)*** *Using anti-Arc antibody the levels of Arc protein were analysed using GAPDH as a loading control. Multiple unpaired t tests using the Holm-Sidak post hoc test which sets significance level at * $p<0.05$ and *** $p<0.001$. [For (A) WT and MSK1 KD n=5, for (B) WT and MSK1 KD n=6 and for (C) WT and MSK1 KD control n=6 and for the treated n=3]*

3.2.2.2 Changes in phosphorylated ERK1/2 after BDNF stimulation in WT and MSK1 KD neurones

BDNF binds to its TrkB receptor which induces a MAPK dependent signalling pathway. It is therefore important to monitor the phosphorylated state of ERK1/2 in order to demonstrate ERK1/2 activation following BDNF stimulation. Figure 3.5 shows a significant increase in phosphorylated ERK1/2 after 1 hour and 3 hours of BDNF stimulation in WT and MSK1 KD neurones (using multiple unpaired t tests, Holm-Sidak post hoc) when compared to control levels. ERK1/2 is located upstream to MSK1 and therefore the levels of phosphorylation should be approximately the same in both genotypes which appeared to be the case.

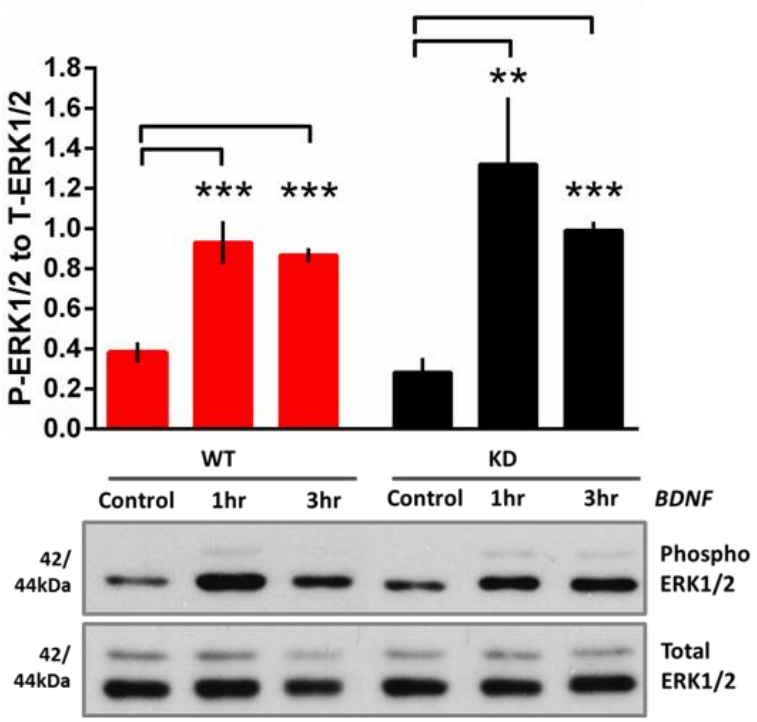

Figure 3.5; The BDNF-dependent increase in ERK1/2 phosphorylation in both WT and MSK1 KD hippocampal neurones. *Dissociated hippocampal neurones from WT and MSK1 KD mice were cultured for 18-21 DIV before being treated with 50 ng/ml of BDNF for 1 hour and 3 hours as well as a non-treated condition. The cells were then lysed and the proteins were separated using SDS-PAGE electrophoresis. The membrane was probed against phosphorylated and total ERK1/2. The intensity of the bands was analysed using Fiji software and the average values are represented in the bar graphs ±SEM. Multiple unpaired t tests using the Holm-Sidak post hoc test which sets significance level at **p<0.01 and ***p<0.001 (n=3 for WT and MSK1 KD 1hr and 3hr, n=6 for WT and MSK1 KD controls).*

3.2.2.3 Changes in Arc and phosphorylated histone H3 protein expression after BDNF application in WT and MSK1 KD hippocampal neurones

According to our hypothesis, MSK1 is regulating the phosphorylation of histone H3 and therefore one would hypothesis that in the presence of BDNF, WT neurones would increase their levels of phosphorylated histone H3. Interestingly we observed no signifcant trends or differences in response to BDNF in both WT and MSK1 KD neurones (Figure 3.6 A; multiple unpaired t test, Holm-Sidak post hoc). In saying this the protein extraction method may have not been optimal to exact histones which are firmly attached to the DNA. Therefore alternative methods such as chromatin immunoprecipitation (ChIP) should be tested before drawing any final conclusions.

It has been well documented that BDNF induces an up regulation of Arc protein expression (Messaoudi et al., 2002; Ying et al., 2002; Bramham and Messaoudi, 2005). Figure 3.6 B shows that in WT neurones there was approximately a 50% increase in total Arc expression after 1 hour of BDNF (* $p<0.05$ using multiple unpaired t test, Holm-Sidak post hoc). This increase was sustained even after 3 hours of BDNF incubation however did not render statistical significance. A similar response was observed in the MSK1 KD neurones because after 1 hour of BDNF there was a significant increase in Arc protein levels (Figure 3.6, * $p<0.05$). This data suggests that MSK1 may not be the sole mediator in regulating BDNF-dependent induction of Arc.

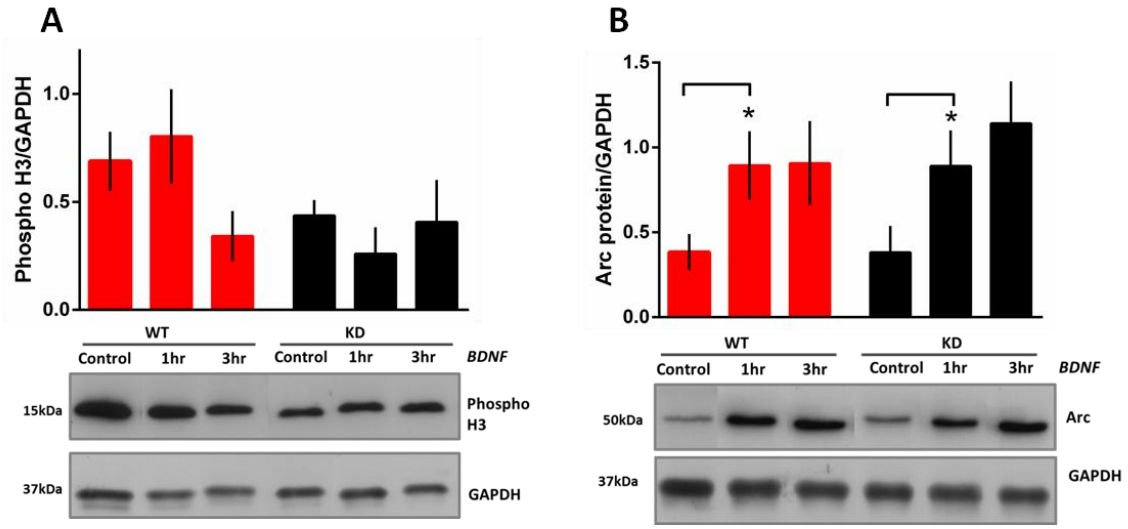

Figure 3.6; The effects of 1 and 3 hours BDNF stimulation on phosphorylated histone H3 and total Arc protein in WT and MSK1 KD hippocampal neurones. *Dissociated hippocampal neurones from WT and MSK1 KD mice were cultured for 18-21 DIV before being treated with 50 ng/ml of BDNF for 1 hour and 3 hours as well as a non-treated control. The cells were then lysed and the proteins were separated using SDS-PAGE electrophoresis. Two proteins were probed for, phosphorylated histone H3 (H3)* ***(A)*** and *Arc* ***(B)*** *where GAPDH was used as a loading control. The intensity of the bands were analysed using Fiji software and the average values are represented in the bar graphs ±SEM. Multiple unpaired t tests using the Holm-Sidak post hoc test which sets significance level at *p<0.05 (n=5 for MSK1 KD 3hr, n=6 for all other samples).*

The transcriptional regulation of IEG such as Arc occurs rapidly and transiently. It has been shown that the kinetics of S10 phosphorylation on histone H3 which regulates chromatin remodelling occurs in parallel to that of IEG transcription (Crosio et al., 2003). As mentioned before MSK1 regulates the phosphorylation of histone H3 (Thomson et al., 1999) and therefore we performed a short BDNF time course to monitor Arc and phosphorylated histone H3 protein levels in both WT and MSK1 KD neurones.

Hippocampal cultures were prepared from WT and MSK1 KD mice and cultured for 18-21 DIV. BDNF (50 ng/ml) was applied for 15, 30, 45 and 60 minutes before lysing and extracting the protein from the neurones. As observed before in Figure 3.6 there were no signifcant changes in the phosphorylated state of histone H3 in either WT or MSK1 KD after BDNF application (Figure 3.7 A). The expression of Arc protein demonstrated a time dependent increase in WT neurones after 45 minutes of BDNF (Figure 3.7 B, * $p<0.05$) and 60 minutes (** $p<0.01$ using multiple unpaired t test, Holm-Sidak post hoc). In contrast the MSK1 KD neurones showed no significant changes during the acute BDNF application but a time dependent trend is apparent. Interestingly in Figure 3.6, MSK1 KD neurones showed a small but significant increase in Arc protein (* $p<0.05$, multiple unpaired t test using Holm-Sidak post hoc). This shows that there is variation between samples from different experiments as Figure 3.7 confirms the increase in Arc protein after 1 hour of BDNF incubation in WT neurones.

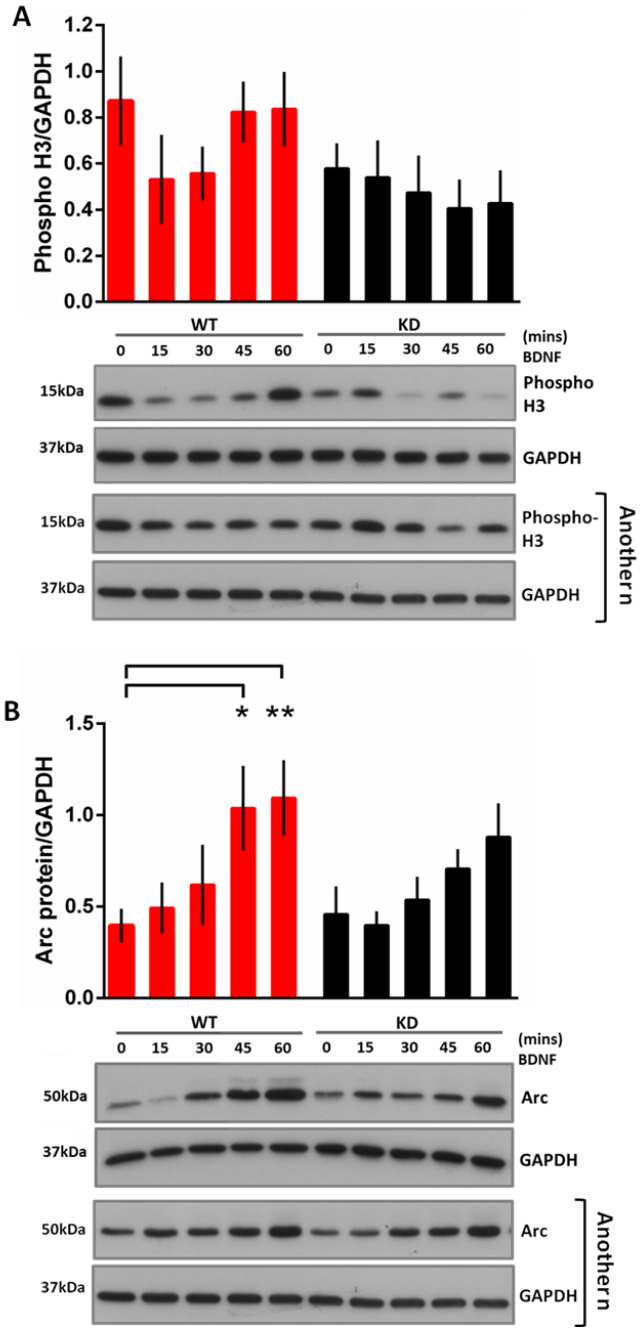

Figure 3.7; A time-dependent increase in Arc protein following acute BDNF stimulation in WT and MSK1 KD hippocampal culture. *Dissociated hippocampal neurones from WT and MSK1 KD mice were cultured for 18-21 DIV before being treated with 50 ng/ml of BDNF for 15, 30, 45 and 60 minutes as well as a non-treated control (represented as 0 minutes (mins) on the graph). The cells were then lysed and the proteins were separated using SDS-PAGE electrophoresis. An anti-phosphorylated histone H3 (H3) antibody was used in graph* ***(A)*** *where representative blots are shown below. As the sample variation was high, two representative blots are shown (another n)* ***(B)*** *The membrane was probed against total Arc and GAPDH which was also used as a loading control for both Arc and phospho H3. The band intensities were analysed using Fiji software and the average values are represented in the bar graphs ±SEM. Multiple unpaired t tests using the Holm-Sidak post hoc test which sets significance level at *p<0.05 and ** p<0.01). For WT and MSK1 KD control and 60 minutes n=7 and all other samples n=5.*

3.2.3 The role of MSK1 in regulating Arc protein expression during TTX-induced synaptic scaling

3.2.3.1 MSK1-dependent up regulation of Arc protein in response to 24 hours of TTX incubation

It has been shown that TTX-induced up-scaling is due to reduced levels of BDNF (Rutherford et al., 1998). To test whether a protracted decrease in activity was associated with BDNF/MSK1-dependent effects on Arc protein expression we incubated WT and MSK1 KD hippocampal neurones (14 DIV) with 1 μM TTX for 1 hour and 24 hours. The levels of phosphorylated ERK1/2 in the WT and MSK1 KD neurones were unchanged in the presence of TTX after 1 hour and 24 hours incubation (Figure 3.8 A). However there was a time dependent decrease in total Arc protein in the WT after 24 hours TTX incubation ($p<0.05$ multiple unpaired t test, Holm-Sidak post hoc) which was absent in MSK1 KD neurones (Figure 3.8 B).

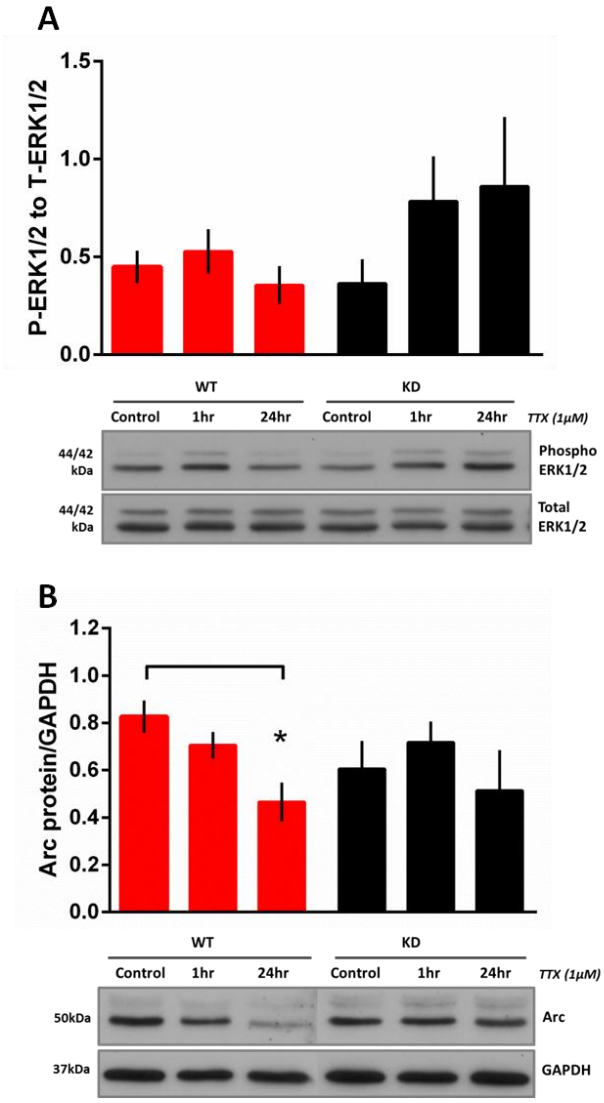

Figure 3.8; MSK1-dependent Arc induction after 24 hours of TTX incubation. *Dissociated hippocampal neurones from WT and MSK1 KD mice were cultured for 14 DIV before being treated with 1 µM of TTX for 1 hour and 24 hours as well as a non-treated control. The cells were then lysed and the proteins were separated using SDS-PAGE electrophoresis. The membranes were probed against phosphorylated ERK1/2 and total ERK1/2 as the loading control* ***(A)*** *as well as total Arc using GAPDH as the loading control* ***(B)****. The intensity of the bands was analysed using Fiji software and the average values are represented in the bar graphs ±SEM. Multiple unpaired t tests using the Holm-Sidak post hoc test which sets significance level at *p<0.05. For (A) n=3 for WT and MSK1 KD controls and n=5 for the other samples. For (B) n=3 for all samples. See Appendix 1 for (Correa et al., 2012).*

The reduced Arc protein expression after TTX stimulation has been shown to correlate with a reduction in Arc-dependent endocytosis of AMPAR GluA1 in hippocampal neurones and hence an increase in cell surface AMPAR expression (Shepherd et al., 2006). The (Shepherd et al., 2006) paper used immunocytochemistry to demonstrate an increase in surface GluA1 expression after

TTX incubation by using an N-terminus GluA1 antibody on fixed control and 48 hour TTX-treated WT hippocampal cultures.

Using the same technique, WT and MSK1 KD hippocampal neurones were cultured for 15-18 DIV under control and 24 hour TTX treated conditions before being immunocytochemically stained against N-terminus GluA1 and analysed using pixel intensity measurements in Image J (Correa et al., 2012). Interestingly, MSK1 KD neurones showed an increase in surface GluA1 expression under control conditions when compared to WT (Figure 3.9 C; $p<0.01$ One Way ANOVA). After 24 hours of TTX stimulation WT neurones demonstrated a higher expression of surface GluA1 ($p<0.01$). However in MSK1 KD neurones this increase was not seen (Figure 3.9). This observation correlates with the unchanged levels of total Arc expression between control and TTX conditions seen in Figure 3.8. This data has been published (Correa et al., 2012).

In the literature there is a discrepancy between which AMPAR subunits are trafficked during scaling which is dependent on the region of the brain. It appears that it is predominantly the GluA1 subunit which is trafficked in the hippocampal culture and the GluA2 subunit in cortical culture (Shepherd et al., 2006; Gainey et al., 2009). Therefore it was necessary to confirm that in hippocampal culture the trafficking of AMPAR in response to TTX was GluA1 specific. The WT and MSK1 KD neurones showed no differences in their levels of surface GluA2 expression under control and TTX-treated conditions (Figure 3.9 B and D).

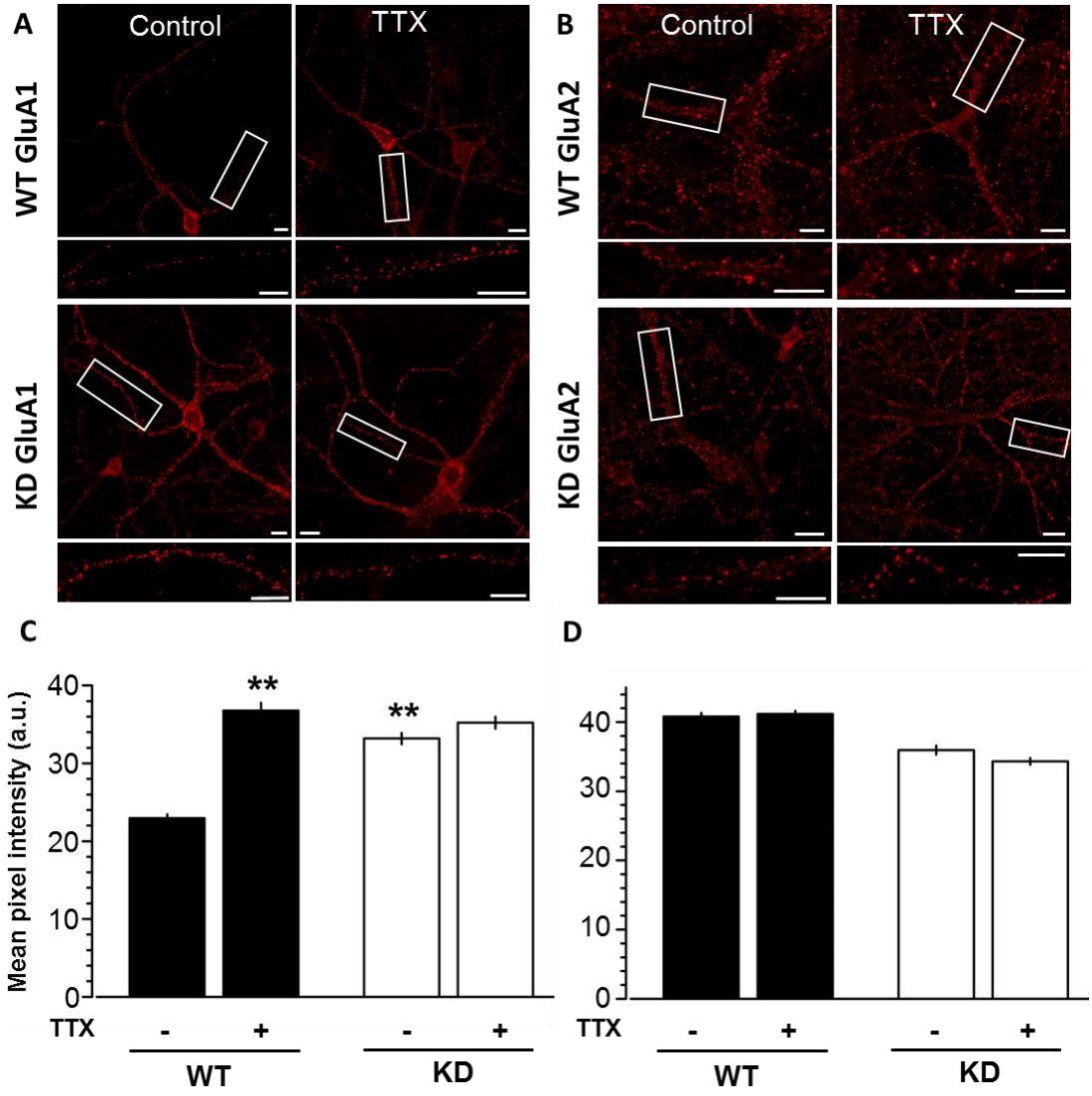

Figure 3.9; MSK1 regulates the trafficking of surface GluA1, not GluA2 expression during TTX-induced up-scaling. *Dissociated hippocampal neurones from WT and MSK1 KD mice were cultured for 15-18 DIV under control and 24 hours TTX (1 µM) incubation. The neurones were fixed and immunocytochemically stained using an anti-N-terminus GluA1 antibody and anti-N-terminus GluA2 followed by Alexa Fluor 568 secondary antibodies. Representative images are shown in* ***(A)*** *for GluA1 and* ***(B)*** *for GluA2, where the top panel demonstrates a pyramidal neurone and the bottom panels are an enlarged stretch of dendrite. Scale bars, 10 µm. The bar graphs represent the mean pixel intensity of* ***(C)*** *GluA1 staining and* ***(D)*** *GluA2 staining ±SEM which was measured in Image J. Three neurones from three different preps were analysed for both genotypes. A One Way ANOVA was used where ** $p<0.01$. This experiment was carried out by Dr. Sonia Correa and published in (Correa et al., 2012) (See Appendix 1) which is where this figure originates from.*

Another method to measure postsynaptic surface AMPAR expression was used in the (Correa et al., 2012) paper involving measuring miniature excitatory postsynaptic currents (mEPSC) amplitude which arise from random spontaneous release of presynaptic vesicles. It is a measure of the number of AMPAR at the

postsynaptic spine. In Figure 3.10, WT neurones showed a significant increase in mean mEPSC amplitude after 24 hours incubation with 1 µM of TTX ($p<0.001$, One Way ANOVA) which was absent in the MSK1 KD. These changes were also apparent in the traces shown in Figure 3.10 A. Interestingly the average mEPSC amplitude was significantly elevated under control conditions in the MSK1 KD when compared to the WT ($p<0.01$). These results correlated with the increased surface GluA1 expression data shown in Figure 3.9.

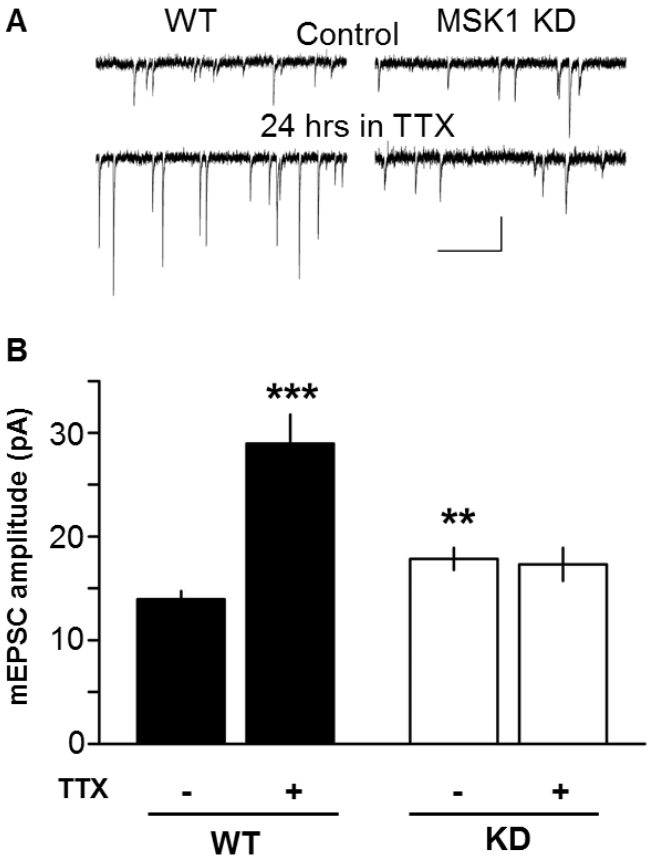

Figure 3.10; MSK1 regulates the mEPSC amplitude during TTX-induced up-scaling. *Dissociated hippocampal neurones from WT and MSK1 KD mice were cultured for 15-18 DIV under control and 24 hours TTX (1 µM) incubation.* ***(A)*** *Representative traces of mESPCs from WT and MSK1 KD hippocampal neurones under control and TTX-treatment. Calibration; 20 pA, 500 ms.* ***(B)*** *A bar graph representing the average mEPSC amplitude (pA) ±SEM in control (-) and TTX treated (+) conditions. A One Way ANOVA was used where ** $p<0.01$ and *** $p<0.005$ ($n=7$ to 21 cells from 3-5 independent preps for each genotype). This experiment was carried out by Dr. Yuriy Pankratrov and published in (Correa et al., 2012) (See Appendix 1) which is where this figure originates from.*

3.3 Discussion

In order to summarise the results of this Chapter, a table has been designed to represent the key findings for each aim which was highlighted in Figure 3.1; the application of BDNF, PD184352 and TTX (See Table 3.1). Each section will be discussed further in the following text.

3.3.1 MSK1 may influence the regulation of the BDNF-dependent Arc synthesis but does not necessarily involve the phosphorylation of histone H3

The MSK1 KD transgenic mice are viable and fertile with normal gross brain morphology which was observed using propidium iodide staining in parasagittal brain sections from both WT and MSK1 KD (Correa et al., 2012). The point mutation in the active MSK1 DFG motif rendered it inactive but was still able to be phosphorylated by ERK1/2. Despite MSK1 being part of the RSK family there was no up regulation of RSK2 protein in response to its inactivity.

In this study, MSK1 has been shown to be essential in TTX-induced homeostatic scaling in hippocampal neurones through a hypothesised signalling pathway shown in Table 3.1 (3). However its role in acute BDNF application was shown not to be as prominent and therefore demonstrated the presence of other paralleled intracellular signalling pathway (Table 3.1 (1)). When MEK1/2 inhibitor (PD184352) was applied to dissociated hippocampal neurones a reduction in phosphorylated ERK1/2 was observed, only a small decrease in phosphorylated histone H3 in MSK1 KD neurones but no such changes in Arc total protein expression (Table 3.1 (2)). The synthesis of Arc can also be induced by protein kinase A (PKA) via CREB phosphorylation and activation of a transcription factor known as serum response factor (SRF) (Waltereit et al., 2001; Bloomer et al., 2008; Pintchovski et al., 2009; Bramham et al., 2010). This pathway would be unaffected in the presence of the PD184352 and hence could contribute to the continued basal levels of Arc protein in both WT and MSK1 KD.

Summary of results		Conclusions represented in a diagram
(1) BDNF	BDNF induces the expression of Arc via ERK1/2. However this appears to be independent of MSK1 as both WT and MSK1 KD neurones showed an increase in ERK1/2 phosphorylation as well as total Arc protein. Histone H3 is most likely not involved as no changes in phosphorylation were observed in either of the genotypes.	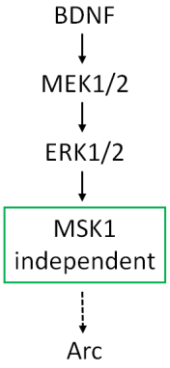
(2) PD 184352	The MEK1/2 inhibitor, PD184352 completely blocks phosphorylation of ERK1/2 which is located directly downstream to MEK1/2. This effect was observed in both genotypes as ERK1/2 is upstream to MSK1. Interestingly a small decrease in phosphorylated histone H3 was observed in the MSK1 KD neurones but no change in WT. However there was no change in total Arc protein in either of the genotypes, indicating a possible MSK1-H3 independent pathway in response to PD184352	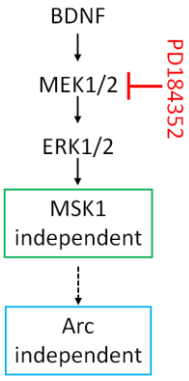
(3) TTX	After 24 hours of TTX, a reduction in Arc protein was observed in WT neurones indicating an up-scaling phenomenon. This decrease was not observe in the MSK1 KD neurones. There were no changes in phosphorylated ERK1/2 which may be indicative of the long term exposure of TTX where cells will homeostatic bring phosphorylated ERK1/2 back down to basal levels (dotted purple box). The involvement of histone H3 phosphorylation was not studied and therefore represented in a dotted box.	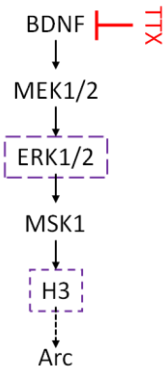

Table 3.1 A table representing the results obtained when characterising the role of MSK1 in BDNF-dependent signalling*. Each section has a summary column which is reflected in a simplified signalling cascade.*

The BDNF dependent increase in phosphorylated ERK1/2 levels which has been previously published was observed after 1 and 3 hours incubation in both WT and MSK1 KD neuronal culture (Ying et al., 2002). After a time course of acute

BDNF stimulation a time dependent increase in Arc protein was observed where an increased expression occurred after 45 minutes BDNF stimulation and then peaked further around 1 hour in WT neurones. The levels then plateaued at 3 hours of BDNF stimulation. Interestingly MSK1 KD cells did not show significant increase in total Arc protein after 45 minutes BDNF incubation nor at 60 minutes after the acute time course stimulation (Figure 3.7). From previous work in the literature it appears that the expression of Arc mRNA in the dentate gyrus is increased rapidly after 10 minutes of high-frequency stimulation (HFS) which is a protocol used to induce LTP (Ying et al., 2002; Messaoudi et al., 2007). Under these conditions there was also an increase in Arc protein expression but was much lower and had a slower transient increase compared to the mRNA levels. This observation supports the fact that the transcription of Arc mRNA is important immediately after neuronal activation and which may be why the effects post BDNF application was reduced slightly in the MSK1 KD neurones as they control transcription of Arc rather than translation (Figure 3.7 B).

However there was a small discrepancy in Arc protein expression after 1 hour in the MSK1 KD neurones as Figure 3.8 showed that the total levels of Arc had increased after 1 hour but not 3 hours, similarly to WT neurones ($p<0.05$ multiple t test, Hom-Sidak post hoc). This small discrepancy could be due to sample variation between experiments which meant that an increase in n numbers across both genotypes may further elucidate any obvious changes. Another limiting factor could be due to the statistical test carried out. The best stastical test to investigate our hypotheses was multiple t tests using Holm-Sidak post hoc to correct for the multiple comparisons where the significant level was set $p<0.05$. This test uses multiple unpaired t test to compare the difference between two groups of interest such as WT control versus WT 1 hour BDNF etc, without assuming a consistent standard deviation. The results generated by this statistical test were consistent with the trends observed in the graphs. A One Way ANOVA which compares all groups to eachother would dilute the statistical significance as there are groups in the experiments which were not relevant (e.g. WT 3 hours BDNF versus MSK1 KD 3 hours BDNF).

MSK1 regulates gene transcription through the phosphorylation of histone H3 (Thomson et al., 1999; Wiggin et al., 2002; Soloaga et al., 2003; Chwang et al., 2007; Correa et al., 2012; Frenguelli and Corrêa, 2012). However it is also known

that MSK1 controls gene transcription via the transcription factor, CREB (Wiggin et al., 2002). In saying that preliminary data from Dr. Simon Arthur (Dundee University, Scotland) showed that CREB phosphorylation was not involved in BDNF-dependent Arc induction using neurones from a CREB S133A knock-in mouse. Bearing this in mind we decided to study the phosphorylation of S10 on the N-terminus of histone H3 as this has been shown to be involved in regulation the transcription of the IEG c-fos after neuronal activation (Crosio et al., 2000; Crosio et al., 2003). When this phosphorylated serine was probed for in WT and MSK1 KD neuronal culture a slight reduction in basal levels (not significant) were observed in the mutant. MSK1 is the predominant kinase which is involved in phosphorylating histone H3 since MSK2 is less abundant in the hippocampus (Arthur, 2008) and therefore would explain a reduction in a basal phosphorylated histone H3. However it is not necessarily regulating the transcription of Arc because under stimulated conditions there were no differences in Arc protein expression between WT and MSK1 KD neurones. Another important aspect of the nature of these experiments is that in neuronal culture protein lysate is the study of a pool of total protein in which only a small fraction of the phosphorylation of histone H3 could be represented by the activation of the Arc promoter. This effect could be diluted by other genes which are controlled by phosphorylated histone H3 chromatin remodelling. A small proportion of primary hippocampal culture will be non-neuronal mitotic glial cells. As these cells are mitotic they will be undertaking DNA histone modifications during their cell cycle as well as the fact that they do express Arc protein (Nowak and Corces, 2004; Shepherd and Bear, 2011). However little is known about the function of glial-expressed Arc.

During acute BDNF stimulation histone H3 phosphorylation levels remain unchanged in both WT and MSK1 KD. Since the Arc protein levels increase in a time-dependent fashion one can speculate that the phosphorylation of histone H3 is not involved in regulating the expression of Arc. Interestingly after 3 hours of BDNF stimulation in WT neurones there was a slight reduction in the levels of phosphorylated histone H3 when compared to control conditions (Figure 3.6 A, but not significant). This could indicate that other histone modifications were possibly required for long term Arc gene transcription forcing a reduction in phosphorylated levels. The other possibility is that Arc transcription does not need to be maintained after 3 hours of stimulation as it is an IEG and required upon neuronal stimulation. In

the literature, BDNF-induced stimulation was shown to induce Arc synthesis up until 2 hours post induction and after 4 hours it was no longer necessary (Messaoudi et al., 2007). However another more refined technique to monitor histone modifications is chromatin immunoprecipitation (ChIP). This would allow the identification of the area of genome which contains a specific histone modification, under control and stimulated conditions. To summarise this section it is clear that Arc protein synthesis is induced in response to BDNF stimulation via ERK1/2 phosphorylation and that MSK1 may have a small role to play as the MSK1 KD showed a reduced response to BDNF. In terms of downstream chromatin remodelling via S10 histone H3 phosphorylation it is unclear whether this modification regulates the transcription of Arc as WT and MSK1 KD neurones showed varied results as well as technical issues in extracting purified histones and neuronal-glial culture.

3.3.2 MSK1 has a crucial role in TTX-induced up regulation of AMPAR via Arc

When TTX was added to primary WT and MSK1 KD hippocampal culture the levels of phosphorylated ERK1/2 remained unchanged across both genotypes. This was slightly unexpected as we would hypothesis according to Figure 3.11 that TTX would reduce the signalling pathway including the levels of phosphorylated ERK1/2. One could hypothesise that the levels of phosphorylated ERK1/2 may have been detected outside its peak optimum window which could be between1 hour and 24 hours.

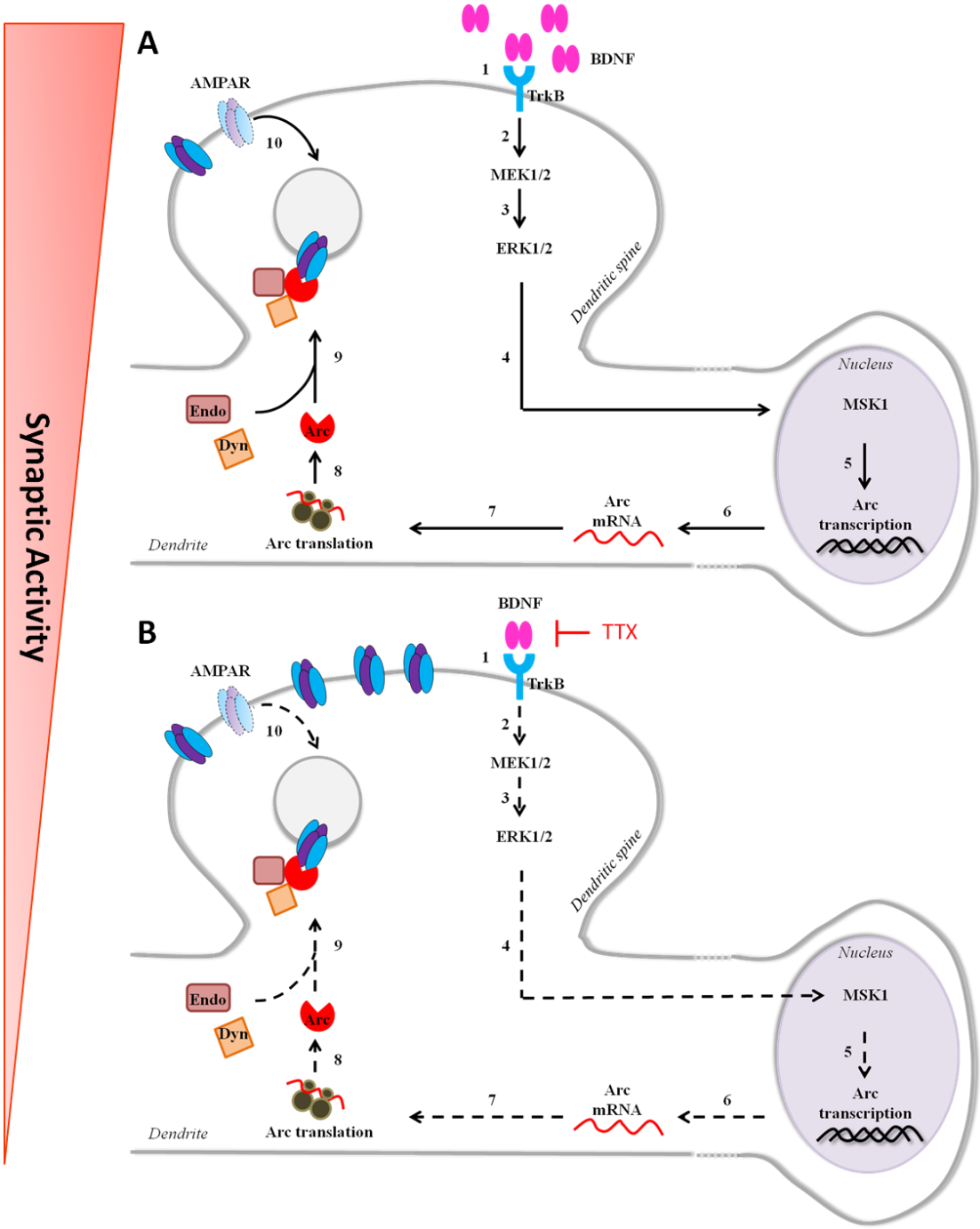

Figure 3.11; A schematic diagram of the MSK1-dependent regulation of Arc in AMPAR trafficking during TTX induced up-scaling. ***(A)*** *Represents a neurone under basal synaptic plasticity and therefore there are high levels of extracellular BDNF* ***(1)*** *BDNF binds to its TrkB tyrosine kinase receptor which induces signalling cascades via ERK1/2.* ***(2)*** *The binding of BDNF to TrkB induces the phosphorylation of MEK1/2 which can be inhibited by a PD184352.* ***(3)*** *ERK1/2 is then phosphorylated by MEK1/2 allowing ERK1/2 to* ***(4)*** *activate downstream MSK1.* ***(5)*** *MSK1 can regulate gene transcription by phosphorylating the transcription factor CREB and phosphorylating histone H3 at serine 10 residue.* ***(6)*** *Upon neuronal stimulation the Arc mRNA strands are transported from the nucleus along the dendrites to the spines.* ***(7 and 8)*** *At the spine the translation of Arc mRNA occurs where the* ***(9)*** *Arc protein binds to dynamin 2 and endophilin 3.* ***(10)*** *This forms a complex which internalises surface AMPAR.* ***(B)*** *Upon the addition of TTX, a voltage*

gated sodium channel blocker; the pathway will be reduced (dotted arrows) as it decreases BDNF release and thus increases surface AMPAR expression. [BDNF; Brain-derived neurotrophic factor, MEK1/2; Mitogen-activated protein kinase kinase 1/2, ERK1/2; Extracellular signal-regulated kinase 1/2, MSK1; Mitogen-and stress-activated protein kinase 1, CREB; Cyclic AMP response element-binding protein, Arc; Activity-regulated cytoskeleton-associated protein, Dyn; Dynamin 2, End; Endophilin 3, TTX; Tetrodotoxin, TrkB; Tropomyosin receptor kinase B]

MSK1 has been shown to play an important role in TTX-induced synaptic scaling which has been published and is represented in Figure 3.11 (Correa et al., 2012) (Appendix 1). In this Chapter I have shown using cultured hippocampal neurones from WT and MSK1 KD mice that 24 hours of TTX (1 µM) reduces the levels of Arc protein in WT. Which is in keeping with the data of others (Shepherd et al., 2006). The novel finding is that this process is MSK1-dependent as the MSK1 KD neurones did not show a TTX-induced reduction in Arc protein. The functional outcome of TTX-up scaling is the increase in surface GluA1 expression in response to decreased Arc levels (Shepherd et al., 2006). Arc has been shown to interact with the endocytotic machinery and therefore internalise GluA1 AMPAR (Chowdhury et al., 2006). These findings were repeated in our system using WT and MSK1 KD dissociated hippocampal neurones immunocytochemically stained for surface GluA1 receptors in response to 24 hours of TTX. WT neurones showed an increase in surface GluA1 expression after TTX incubation which was occluded in MSK1 KD neurones. The GluA2 surface expression remained unchanged in response to TTX which is in keeping with the theory that hippocampal neurones traffick GluA1 specific AMPAR during scaling as oppose to GluA2 receptors in cortical neurones. Measuring mEPSC amplitudes in culture is a functional read out for the surface AMPAR expression. In this case the increase in mEPSC amplitude in WT TTX-treated neurones complemented the increase in surface GluA1 expression. In terms of basal surface GluA1 expression, an increase was observed in the MSK1 KD neurones which was mirrored by an increase in mEPSC amplitude. One would hypothesis a reduction in basal Arc protein levels leading to a reduction in endocytosis and therefore an increase in surface GluA1 expression. However the western blots did not reveal any significant changes in basal Arc protein levels. This could be due to a MSK1-independent homeostatic mechanism which occurs under basal conditions, allowing the Arc protein levels to remain stable. Interestingly in cultured Arc KO neurones an increase in surface GluA1 and mEPSC amplitude was

observed. These observations correlated to the fact that Arc KO neurones were unable to up-scale their synaptic strength in response to TTX (Chowdhury et al., 2006).

Electrophysiological results have shown that MSK1 bidirectionally regulates BDNF-TrkB-ERK1/2 pathway during scaling (See Appendix 1). WT and MSK1 hippocampal neurones were cultured and incubated with BDNF, SH722 (TrkB inhibitor) or PD 184352 for 24 hours where mEPSC amplitudes were recorded. BDNF treated WT cells showed a decrease in mEPSC amplitude demonstrating a down-scaling phenomenon as oppose to the TrkB inhibitor and PD184352 which demonstrated up-scaling similar to the effects of TTX. The MSK1 KD neurones showed no scaling ability in response to the three drugs.

Finally in order to show that the electrophysiological results were due to the inactive form of MSK1 in the MSK1 KD neurones we performed a rescue experiment. The WT MSK1-GFP-tagged construct was transfected into the MSK1 KD neurones and the mEPSC amplitude was rescued back to WT levels (See Appendix 1). When the WT MSK1-GFP transfected MSK1 KD cells were incubated with TTX for 24 hours they were able to scale accordingly meaning that the mEPSC amplitude increased to WT-TTX treated levels revealing the importance of MSK1 in regulating homeostatic synaptic plasticity (Correa et al., 2012).

Chapter 4.

The role of MSK1 in regulating dendritic spine density and morphology

4.1 Introduction

Dendritic spines are small actin-rich protrusions that form the postsynaptic component of most excitatory synapses and are major sites of information processing (Bourne and Harris, 2008). Spines are formed by a protruding neck emerging from the dendritic shaft with a head at the end which contains the postsynaptic density (PSD) (Figure 1.6 B). The PSD will contain a cluster of glutamate receptors and accessory proteins which will orchestrate signalling cascades (Sheng and Hoogenraad, 2007). The neck length and diameter as well as the head width can alter to form a range of spine morphologies which have been categorised as illustrated in Figure 1.6 C (Peters and Kaiserman Abramof, 1969; Harris et al., 1992).

During synaptogenesis, long immature filopodia-like spines emerge from the shaft of the dendrite which have long flexible necks with a small head allowing them extend to form active synapses (Fiala et al., 2002; Von Bohlen and Halbach, 2009). These synapses will later give rise to stable and synaptically active spines during later development or the filopodia will retract (Fiala et al., 1998; Alvarez and Sabatini, 2007). These dynamic compartments respond to external stimuli through these morphological changes which dictate their synaptic output including different forms of synaptic plasticity. These mechanisms thought to contribute to the morphological changes range from (1) the trafficking of AMPAR (2) the compartmentalisation of calcium (Ca^{2+}) within the spine (3) the actin remodelling regulated by signalling molecules (Tada and Sheng, 2006; Bourne and Harris, 2007). For example mushroom shaped spines are thought to retain high levels of AMPAR in their heads and have been referred to as stable ‘memory spines' (Matsuzaki et al.,

2001; Kasai et al., 2003). As oppose to thinner spines which have been named as 'learning spines' due to their plasticity. Evidence has shown that these spines will preferentially undergo long-term potentiation (LTP) as they are more plastic in nature (Matsuzaki et al., 2004). LTP inducing stimulation increases actin polymerisation in spines which leads to branching of filamentous actin (F actin) forming mushroom shaped spines (Okamoto et al., 2004).

Homeostatic scaling of dendritic spines was observed after using manipulations in the visual environment, rats which were dark-reared revealed lower spine density as well as morphological changes in the visual cortex when compared to the light-reared control animals (Wallace and Bear, 2004). Chapter 3 highlighted the scaling phenomenon in neuronal culture in the presence of TTX and its MSK1-dependent role on Arc synthesis and AMPAR surface expression. In the light of these findings this following Chapter has been designed to characterise the possible role of MSK1 in regulating spine density and structure under basal and TTX stimulated conditions.

The aim of this Chapter is to visualise spine density and morphology using eGFP-transfected dissociated hippocampal neurones from WT and MSK1 KD postnatal mice. These pyramidal neurones will be cultured for 14 DIV and 21 DIV to see if MSK1 plays a role in regulating developmental changes in spine density and morphology. Spine density will be calculated as number of spines per 10 µm of dendrite and spine morphology will be analysed by measuring spine length, spine head width and spine volume using NeuronStudio software (Figure 2.1). Under synaptic up-scaling conditions hippocampal neurones will be incubated with TTX (1 µM) for 24 hours in parallel to a non-treated control in both WT and MSK1 KD cultures. These experiments were carried out in both 14 DIV and 21 DIV in order to determine if MSK1 dependent up-scaling was reliant on developmental mechanisms.

4.2 Results

4.2.1 eGFP-labelled hippocampal neurones used to verify spine-like structures with endogenous postsynaptic density protein 95 (PSD 95) staining

Primary hippocampal neurones were prepared from P0-P1 WT mice and were cultured in serum free media for 21 DIV. These neurones were then transfected with

an eGFP construct for 16 hours before fixing the neurones and immunocytochemically staining them with a PSD marker, PSD-95 (Figure 4.1). PSD-95 is a scaffold protein where it will cluster glutamate receptors on the postsynaptic membrane of excitatory synapses so to orchestrate signalling cascades (Sheng and Hoogenraad, 2007). This marker can be used to identify spines through their co-localisation with eGFP transfected spines in pyramidal neurones. Therefore eGFP labelled spine like structures were used as a proxy to identify and measure dendritic spine parameters highlighted in Figure 2.1.

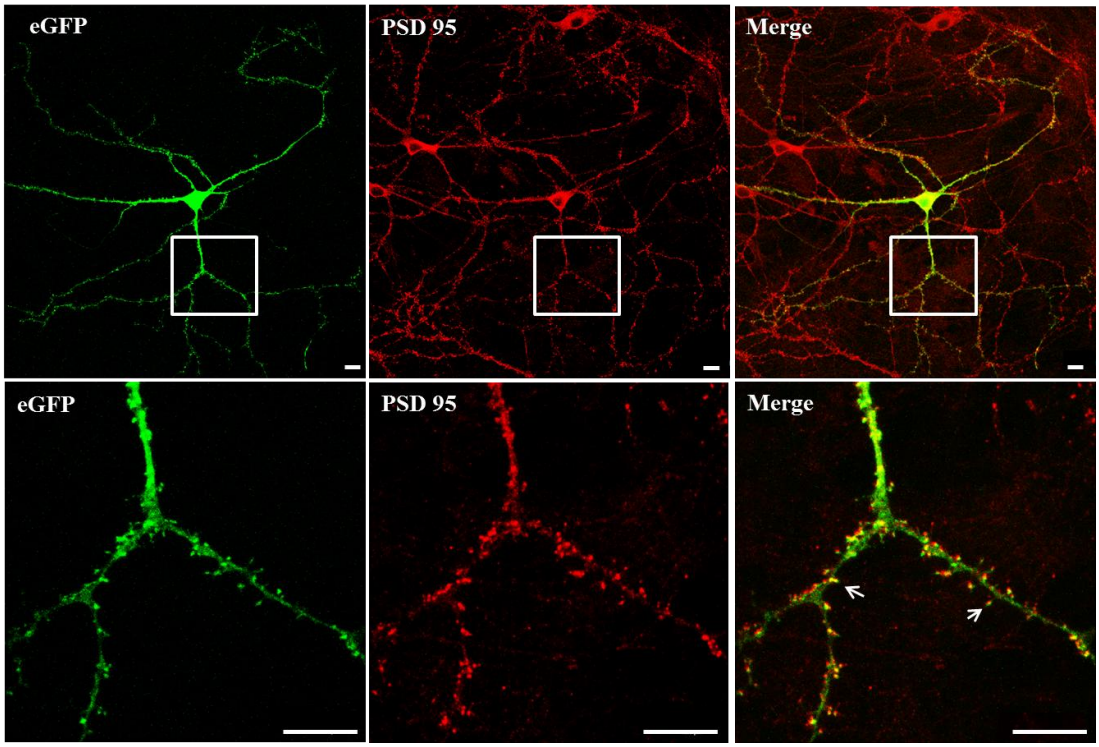

Figure 4.1; Hippocampal neurones transfected with eGFP co-stained with PSD 95. *Cultured hippocampal neurones (21 DIV) were transfected with eGFP construct for 16 hours, fixed, permeabilised and stained with PSD 95 (Abcam) which labels the postsynaptic density 95 protein using Alexa Fluor anti mouse 568. The white square is the area of dendrite enlarged in the bottom panels. Their co-localisation pattern (merged panel) highlights the PSD within a eGFP-labelled dendritic spine (white arrow). Scale bar; 10 µm*

4.2.2 Developmental changes in spine density and morphology in eGFP-transfected WT and MSK1 KD hippocampal neurones under basal conditions

Changes in spine density during development has been previously shown in hippocampal culture where from 1 to 3 weeks *in vitro* the spine density increases linearly (Papa et al., 1995). Hippocampal neurones were transfected with an eGFP construct for 16 hours before being fixed and imaged using confocal microscopy. After culturing WT and MSK1 KD hippocampal neurones for 14 DIV and 21 DIV we observed a developmental dependent increase in the number of spines per 10 µm of dendrite (Figure 4.2 A). However in WT neurones there was a two fold increase in spine density from 14 DIV containing 1.56 spines per 10 µm ±0.086 compared to 21 DIV which had 2.69 ±0.135 (Figure 4.2 B; $p<0.001$). In comparison the MSK1 KD neurones showed a reduced increase in density between 14 and 21 DIV which was statistically insignificant (multiple unpaired t test, Holm-Sidak post hoc). There appeared to be no significant differences between WT and MSK1 KD neurones after 14 DIV and 21 DIV (Figure 4.2 B).

During development there are morphological changes in dendritic spines as they mature and respond to external stimuli. Using eGFP transfected hippocampal neurones the following parameters were measured to reflect spine morphology which included spine volume (μm^3), spine head width (µm) and spine length (µm) (See Figure 2.1). The data showed that MSK1 KD neurones had increased spine volumes at 21 DIV when compared to WT (Figure 4.2 C; Table 4.1 $p<0.001$). However at 14 DIV the MSK1 KD showed a reduced spine volume ($p<0.01$) when compared to WT (Figure 4.2 C) and therefore the right-ward shift in distribution of voluminous spines after 21 DIV was much larger in the MSK1 KD. The spine head width developmentally increased in both WT and MSK1 KD neurones (Figure 4.2 D; $p<0.001$). It appeared that the enlarged spines observed after 21 DIV in the WT and MSK1 KD neurones could be associated with the increased spine head width.

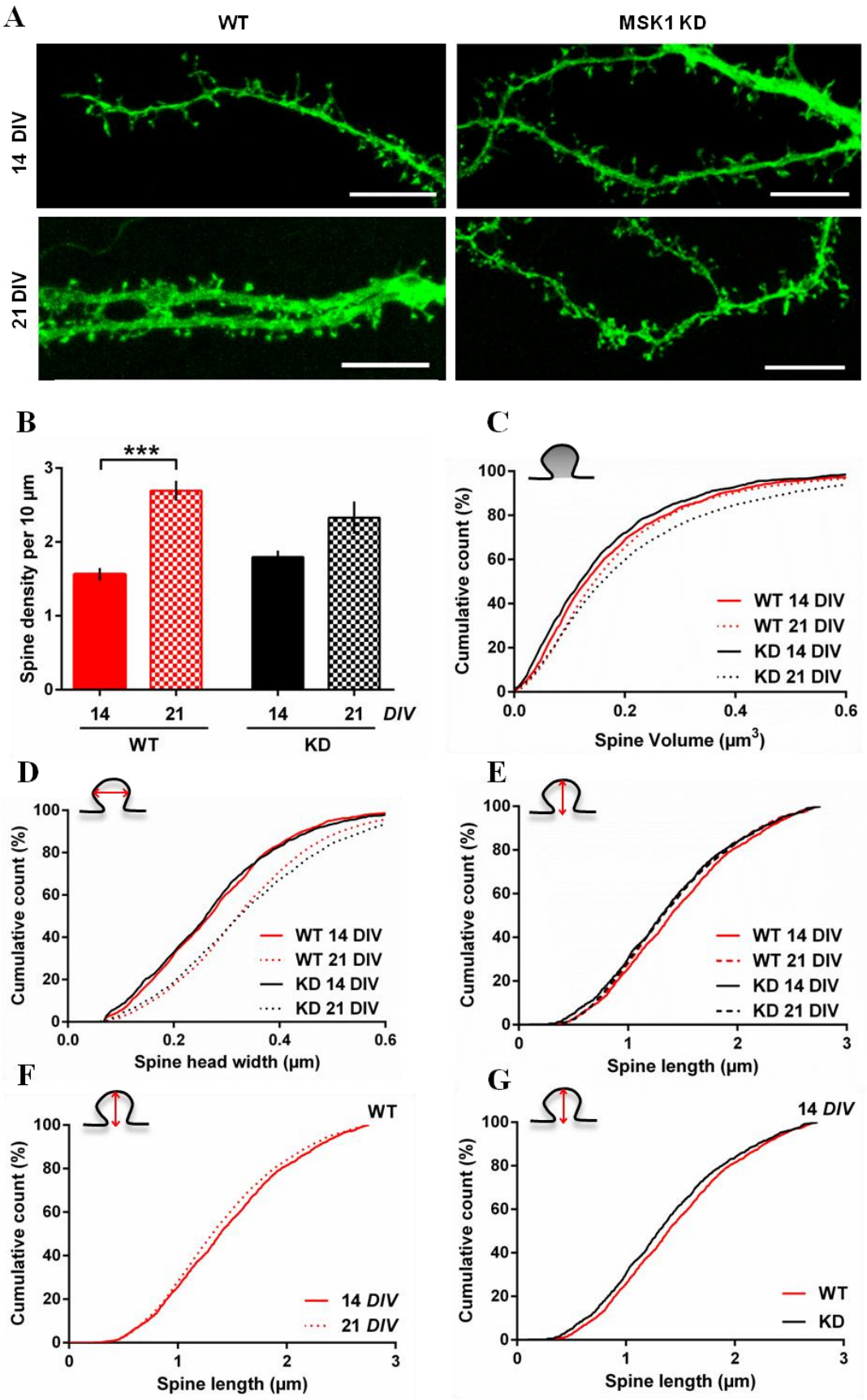
A
WT
MSK1 KD
14 DIV
21 DIV
B
***
Spine density per 10 µm
14
21
14
21
DIV
WT
KD
C
Cumulative count (%)
WT 14 DIV
WT 21 DIV
KD 14 DIV
KD 21 DIV
Spine Volume (µm3)
D
Cumulative count (%)
WT 14 DIV
WT 21 DIV
KD 14 DIV
KD 21 DIV
Spine head width (µm)
E
Cumulative count (%)
WT 14 DIV
WT 21 DIV
KD 14 DIV
KD 21 DIV
Spine length (µm)
F
WT
Cumulative count (%)
14 DIV
21 DIV
Spine length (µm)
G
14 DIV
Cumulative count (%)
WT
KD
Spine length (µm)

Figure 4.2; Developmental changes in spine density and morphology in hippocampal neurones from WT and MSK1 KD mice*. **(A)** A representative region of dendrite from eGFP transfected WT and MSK1 KD hippocampal neurones maintained for 14 and 21 DIV under control conditions. Scale bar 10 µm. **(B)** The bar graph represents the average spine density per 10 µm of dendrite ±SEM (*** p<0.001 using multiple unpaired t test using Holm-Sidak post hoc). Spine volume **(C)**, head width **(D)** and length **(E)** were measured and plotted as cumulative distribution curves using bin size of 0.005. The inset figures in each of the panels represent the measurements made for each. A Kolmogorov Smirnov (KS) test was used and the p values are given in Table 4.1. For spine length **(E)** the cumulative counts were calculated from spines measuring ≤ 2.75 µm which were classified as spines rather than filopodia-like spines (Park et al., 2006). **(F)** This cumulative graph just represents spine length of WT spines at 14 and 21 DIV so to visualise the difference more clearly **(G)** This cumulative graph just represents spine length at 14 DIV in WT and MSK1 KD spines so to visualise the difference more clearly. [n=3 WT and MSK1 KD preps, 5-9 neurones per prep and between 3000-6000 spines were analysed]*

Kolmogorov–Smirnov (KS) test			**Spine volume**	**Spine head width**	**Spine length**
WT 14 DIV	versus	KD 14 DIV	p<0.012 (**)	ns	p<0.001 (***)
WT 21 DIV	versus	KD 21 DIV	p<0.001 (***)	p<0.001 (***)	ns
WT 14 DIV	versus	WT 21 DIV	p<0.001 (***)	p<0.001 (***)	p<0.001 (***)
KD 14 DIV	versus	KD 21 DIV	p<0.001 (***)	p<0.001 (***)	ns

Table 4.1; Statistical p values from cumulative distribution curves comparing WT and MSK1 KD after 14 DIV and 21 DIV using a KS test. *This was performed using data collected from control conditions in WT and MSK1 KD as well as comparing different culture age for spine volume, head width and length. A p value was generated in which it either rendered not significant (ns) where p>0.05 or significant where p<0.01 (**) or p<0.001 (***) [n=3 WT and MSK1 KD preps, 5-9 neurones per prep and between 3000-6000 spines were analysed]*

During development dendritic spines will mature from long filopodia-like structures into stable mushroom shaped spines. Therefore spine maturity can be categorised according to their length. Immature filopodia-like spines can be classified as spines measuring over 2.75 µm long as opposed to normal spines measuring below 2.75 µm (Park et al., 2006). In Figure 4.1 E the spines measuring ≤2.75 µm in length are accounted for but the spines >2.75 µm were categorised as filopodia (according to (Park et al., 2006) and therefore not included in the

distribution curves. The WT spines appear to decrease in length after 21 DIV represented by the left-ward shift in the distribution curve (Figure 4.2 E and F, Table 4.1 $p<0.001$). However this shift was absent in the MSK1 KD neurones. Interestingly at 14 DIV the spines appeared to be longer in WT neurones than the MSK1 KD which could indicate lack of plasticity in the MSK1 KD spines curve (Figure 4.2 E and G, Table 4.1 $p<0.001$).

4.2.3 Changes in spine density and morphology in WT and MSK1 KD hippocampal neurones in response to TTX-induced scaling

4.2.3.1 The effects of TTX on spine morphology at 14 DIV

Spine density in both eGFP transfected WT and MSK1 KD neurones did not change after 24 hour TTX incubation (Figure 4.3). This was the case in both 14 and 21 DIV culture.

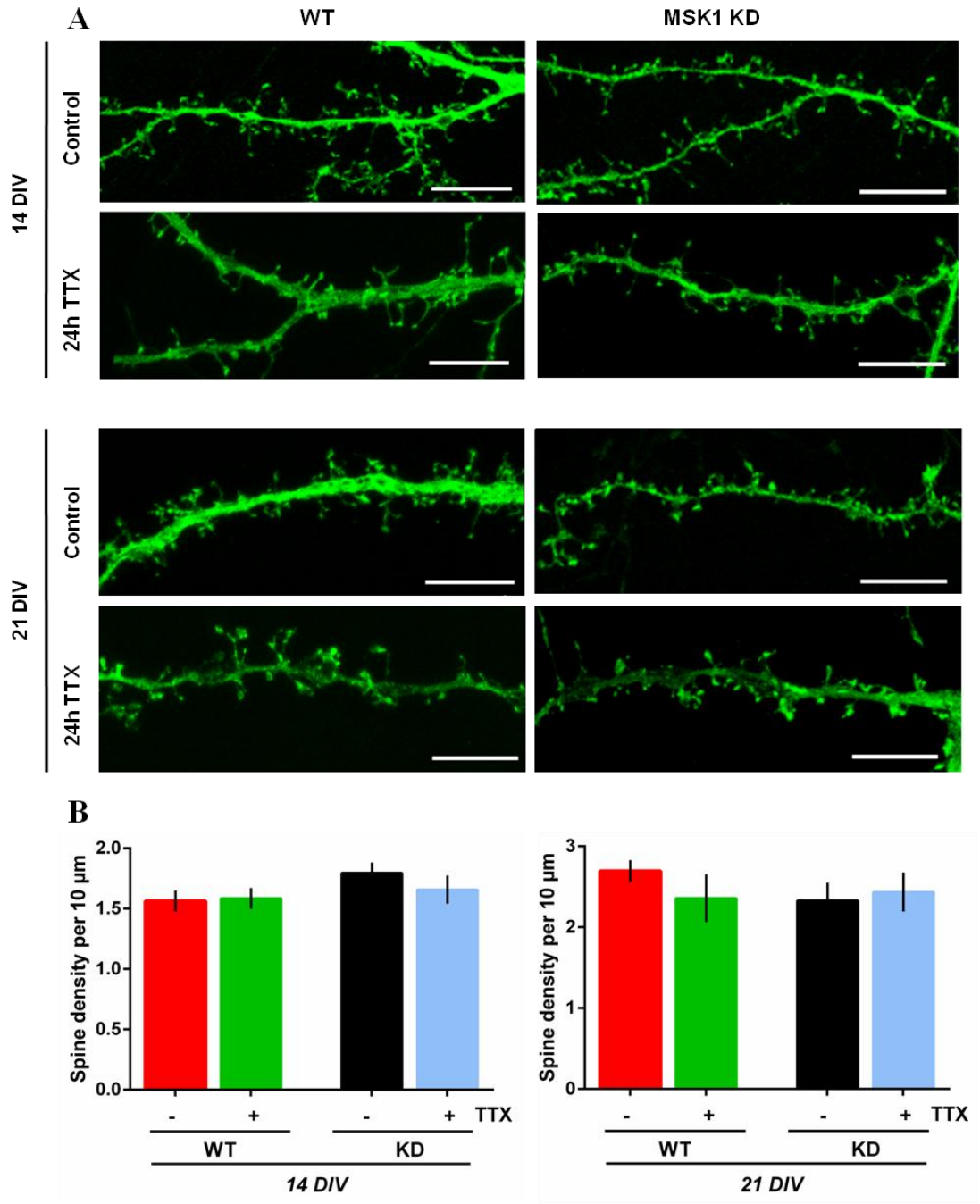

Figure 4.3; MSK1 has no effect on regulating dendritic spines in 14 DIV and 21 DIV hippocampal neurones. (A) *Representative dendrites of eGFP transfected neurones in control conditions and after 24 hours in TTX (1 µM) in both 14 and 21 DIV culture. Scale bar 10 µm.* ***(B)*** *These bar graphs demonstrate the average number of spines per 10 µm of dendrite ±SEM which were analysed using NeuronStudio software in 14 DIV and 21 DIV culture. WT and MSK1 KD-TTX treated neurones showed no significant changes in spine density in both 14 DIV and 21 DIV using multiple unpaired t test using Holm-Sidak post hoc. [n=3 WT and MSK1 KD preps, 5-9 neurones per prep and between 3000-6000 spines were analysed.]*

In contrast, the younger culture (14 DIV) showed morphological changes in the MSK1 KD spines after 24 hours of TTX incubation which were absent in the WT. The spines showed a reduced volume ($p<0.001$) as well as a reduction in spine head width ($p<0.001$) (Figure 4.4 A and B; D for p values). Along with the increased spine length (Figure 4.4 C; D for $p<0.001$) it appeared that the spines were adapting into immature shaped spines in the presence of TTX. The lack of active MSK1 could be impeding the signalling pathways required to maintain spine morphology when under synaptic deprivation. These signalling pathways will most likely include regulating the actin polymerisation so that spines elongate their necks.

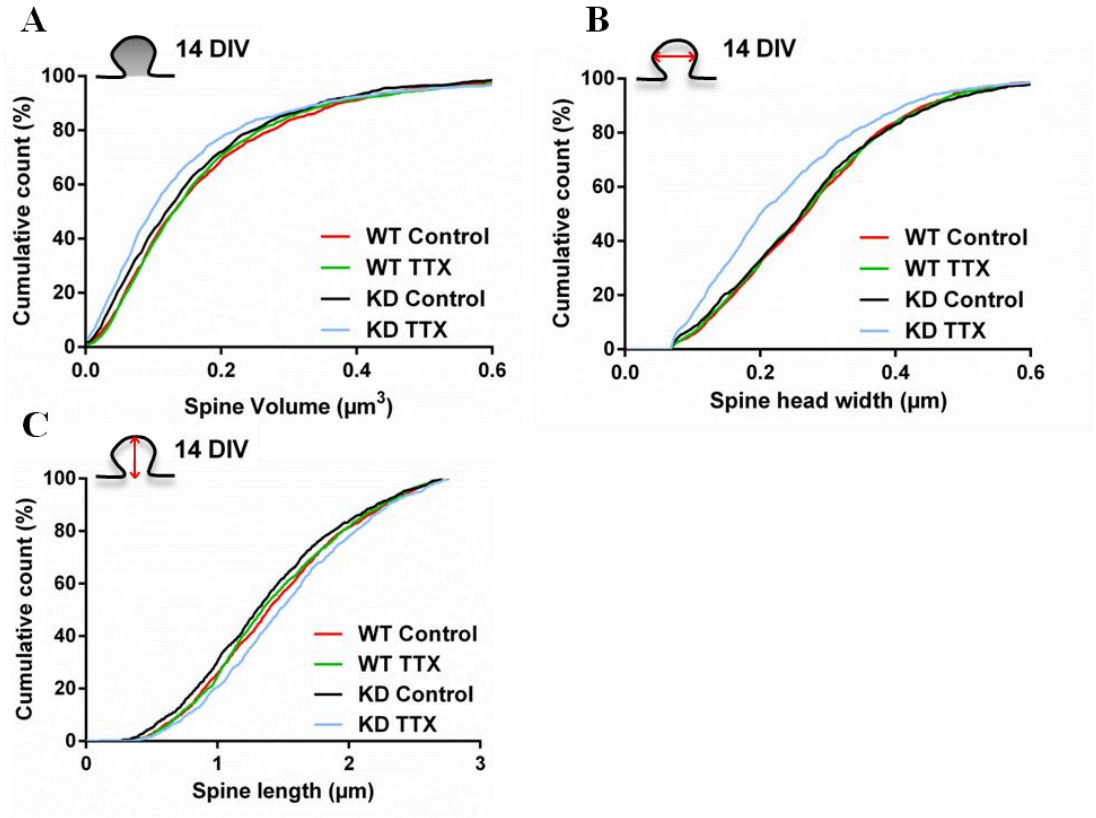

D

Kolmogorov–Smirnov (KS) test			Spine volume	Spine head width	Spine length
WT 14 DIV Control	versus	WT 14 DIV TTX	ns	ns	ns
KD 14 DIV Control	versus	KD 14 DIV TTX	p<0.0001 (***)	p<0.0001 (***)	p<0.0001 (***)

Figure 4.4; Changes in spine morphology following TTX-incubation for 24 hours in 14 DIV hippocampal culture from WT and MSK1 KD mice. *The eGFP-transfected neurones were incubated with TTX (1 µM; 24 hours) were fixed and imaged using confocal microscopy before being analysed using NeuronStudio software (Figure 2.1). The representative dendrites are shown in Figure 4.3 A. The cumulative distribution graphs were created using bin size of 0.005 for all measurements; spine volume* ***(A)****, spine head width* ***(B)*** *and spine length* ***(C)*** *and the inset figures represent the measurements made in each. A KS test was used to calculate the significance between the distributions of values for each parameter. For spine length* ***(C)*** *the cumulative counts were calculated from spines measuring ≤ 2.75 µm which are classified as spines rather than filopodia-like spines (Park et al., 2006) [n=3 WT and MSK1 KD preps, 5-9 neurones per prep and between 3000-6000 spines were analysed.]* ***(D)*** *Stastical p values from cumulative distribution curves comparing control and TTX induced WT and MSK1 KD conditions after 14 DIV using a KS test. A p value was generated in which it either rendered not significant (ns) where p>0.05 or significant where *** p<0.001 [n=3 WT and MSK1 KD preps, 5-9 neurones per prep and between 3000-6000 spines were analysed.]*

4.2.3.2 The effects of TTX on spine morphology at 21 DIV

WT neurones cultured for 21 DIV displayed reduced spine volume ($p<0.01$) and spine head width ($p<0.001$) in response to 24 hours of TTX (Figure 4.5 A and B; D for p values). In contrast, MSK1 KD neurones cultured for 21 DIV significantly increased their spine volume after 24 hours of TTX ($p<0.001$) represented by the right-ward shift in the cumulative distribution curve in Figure 4.5 A. However, the increase in spine volume did not correlate with the observed reduction in spine head width (Figure 4.5 B; D indicates $p<0.01$). Neither WT nor the MSK1 KD neurones altered their spine length (Figure 4.5 C).

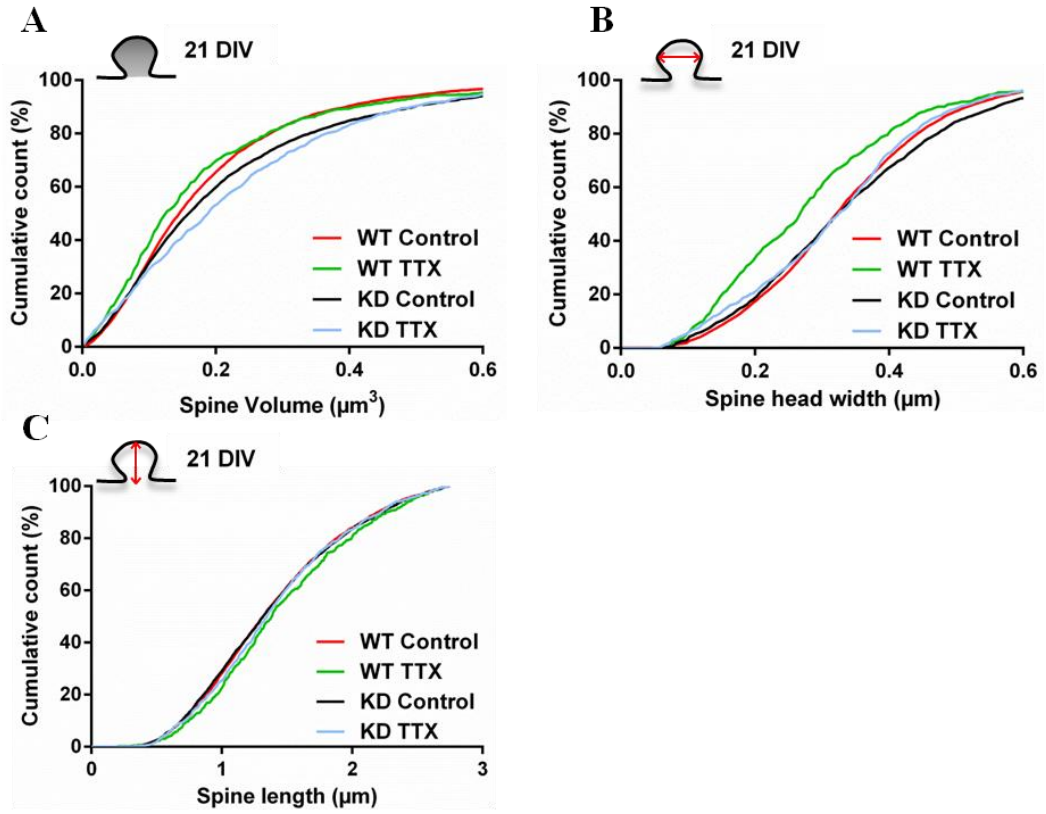

D

Kolmogorov–Smirnov (KS) test			Spine volume	Spine head width	Spine length
WT 21DIV Control	versus	WT 21DIV TTX	p<0.009 (**)	p<0.0001 (***)	ns
KD 21DIV Control	versus	KD 21DIV TTX	p<0.0001 (***)	p<0.002 (**)	ns

Figure 4.5; Changes in spine morphology following TTX-incubation for 24 hours in 21 DIV hippocampal cultures from WT and MSK1 KD mice. *The eGFP-transfected neurones were incubated with TTX (1 µM; 24 hours) after 16 hours of transfection then fixed and imaged using confocal microscopy before being analysed using NeuronStudio software (Figure 2.1). The representative dendrites are shown in Figure 3.4 The cumulative distribution graphs were created using bin size of 0.005 for all measurements; spine volume* ***(A)****, spine head width* ***(B)*** *and spine length* ***(C)*** *and the inset figures represent the measurements made in each. A KS test was used to calculate the significance between the distributions of values for each parameter. For spine length* ***(C)*** *the cumulative counts were calculated from spines measuring ≤ 2.75 µm which are classified as spines rather than filopodia-like spines (Park et al., 2006) [n=3 WT and MSK1 KD preps, 5-9 neurones per prep and between 3000-6000 spines were analysed.]* ***(D)*** *Statistical p values from cumulative distribution curves comparing control and TTX induced WT and MSK1 KD conditions after 21 DIV using a KS test. A p value was generated in which it either rendered not significant (ns) where p>0.05 or significant where or p<0.01(**) or p<0.001 (***) [n=3 WT and MSK1 KD preps, 5-9 neurones per prep and between 3000-6000 spines were analysed.]*

4.3 Discussion

During development an important neurotrophin is released known as BDNF which has been shown to play a crucial role in neuronal survival, growth and differentiation (Huang and Reichardt, 2001). Both BDNF and its receptor TrkB have been shown to be upregulated postnatally during development (Silhol et al., 2005). Furthermore the action of BDNF can be attributed to an increase in spine density shown when exogenous BDNF was applied to hippocampal slices and culture. (Alonso et al., 2004; Ji et al., 2010). The signalling pathway involved in regulating spine density may involve the BDNF dependent phosphorylation of ERK1/2 and subsequent MSK1 phosphorylation shown in Chapter 3. This may be the case as a delayed developmental increase in spine density in the MSK1 KD neurones from 14 DIV to 21 DIV was observed when compared to the WT (Figure 4.2 B). Therefore this BDNF-MSK1 pathway could be important in spinogenesis during development.

In terms of developmental control of spine morphology this Chapter's data has revealed that WT neurones mature in accordance to what is published in the literature (Fiala et al., 1998; Alvarez and Sabatini, 2007). This means that the long-filopodia like spines at 14 DIV retract in length and become more bulbous resembling mushroom shaped spines (Figure 4.6). Interestingly the MSK1 KD spines also become more bulbous meaning their spine volume and head width increase but these morphological changes are even more pronounced than the WT. It has been previously shown by (Correa et al., 2012) that MSK1 KD neurones express higher surface GluA1 receptors under basal conditions which correlated with an increase in mEPSC amplitude. Therefore one could hypothesise that this change in morphology could be due to the functional increase in surface AMPAR expression.

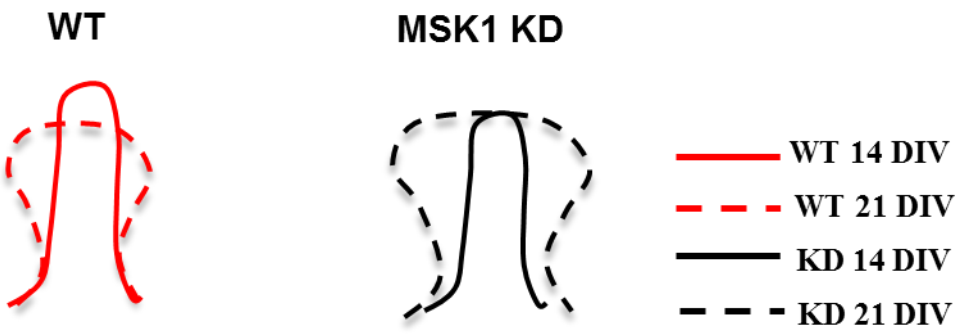

Figure 4.6; A schematic of the morphological changes observed under control conditions WT and MSK1 KD hippocampal neurones after 14 and 21 DIV *An illustration of the developmental changes in WT (red) and MSK1 KD (black) spines after 14 DIV (solid line) and 21 DIV (dotted line).*

The effects of TTX application on spine morphology have been studied in this Chapter in both young (14 DIV) and older (21 DIV) hippocampal neurones from WT and MSK1 KD mice. The application of TTX has been attributed to a reduction in the release of BDNF (Rutherford et al., 1998; Turrigiano et al., 1998) and therefore accordingly a reduction in the BDNF-ERK1/2-MSK1-Arc pathway outlined in Chapter 3 was observed. This would lead to a decrease in Arc protein followed by reduced GluA1 internalisation and therefore an increase in surface GluA1 expression in WT neurones (Correa et al., 2012). AMPAR trafficking has been shown to influence spine morphology in several studies demonstrating that chemically induced LTP rapidly enhances spine size with subsequent incorporation of GluA1 to the surface (Kopec et al., 2006). Further to this it has been suggested that both the increase in actin filaments and the synaptic incorporation of GluA1 can co-stabilise eachother during LTP thus balancing spine size and synaptic strength (Kopec et al., 2007). In contrast, another group have looked at the influence of GluA2 subunit where its over expression in hippocampal neurones increases spine size and density (Passafaro et al., 2003).

Thus in keeping with the data from Correa et al., 2012 and previous findings in the literature where spine morphology is influenced by AMPAR trafficking we would expect an increase in spine volume and head width after 24 hours of TTX in WT neurones. However this was not the case as the WT neurones at 14 DIV did not demonstrate any structural changes in spine morphology or changes in density after TTX stimulation (Figure 4.7 A). This illustrates that structural changes may not be

essential in shaping the functional outcome under these circumstances. However at 14 DIV in the MSK1 KD neurones there appeared to be morphological changes in the dendritic spines where they were elongated and narrower. This structural change mimics 'immature' filopodia-like spines. As these spines are unable to alter their GluA1 surface expression in response to TTX (Correa et al., 2012) they compensate in using a MSK1-independent structural mechanism. This structural change has previously been reported in a paper highlighting that spines extend out in order to increase their chances of making new synapses to compensate for the lack of synaptic activity (McKinney et al., 1999; Richards et al., 2005).

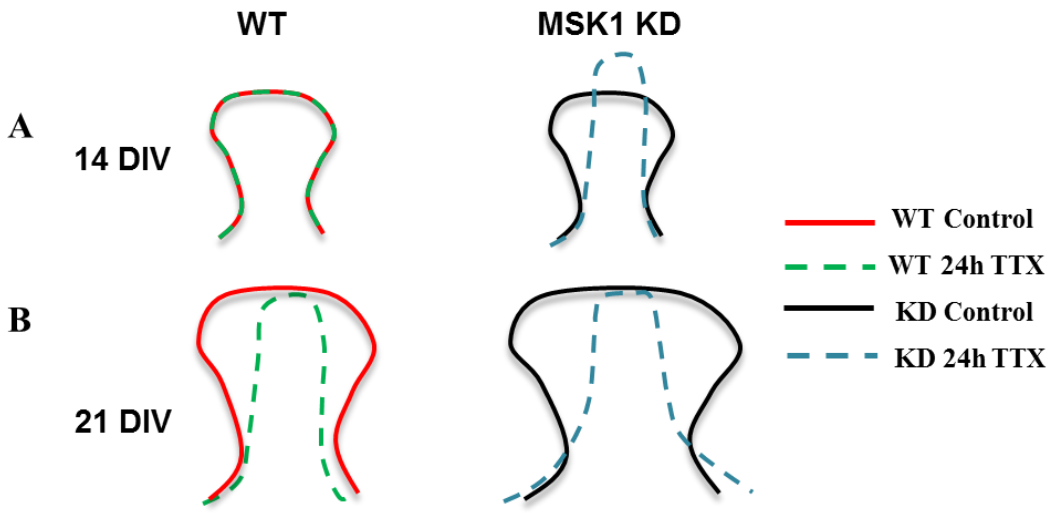

Figure 4.7; A schematic of the morphological changes observed in 14 and 21 DIV WT and MSK1 KD hippocampal neurones after 24 hour TTX treatment and in control conditions. *An illustration of the developmental changes in WT (red) and MSK1 KD (black) spines after 14 DIV (solid line) and 21 DIV (dotted line). The representative spines illustrate the changes in morphology after TTX treatment (dotted blue and green lines) compared to control conditions (solid red and black lines) in 14* ***(A)*** *and 21 DIV culture* ***(B)****.*

The application of TTX did not unalter the spine density in either WT or MSK1 KD neurones which was further supported by the unchanged mEPSC frequency data in the study published by (Correa et al., 2012). However spine morphology was significantly altered in older culture (21 DIV) after 24 hours TTX treatment in both WT and MSK1 KD neurones (Figure 4.7 B). WT spines have a significantly reduced volume and spine head width, which once again goes against the hypothesis where an increased surface AMPAR expression would suggest a spine volume enlargement (Turrigiano et al., 1998; Shepherd et al., 2006). However there

are other mechanisms shown to effect changes in spine morphology such as the compartmentalisation of Ca^{2+} (Harris and Kater, 1994; Yuste et al., 2000; Tada and Sheng, 2006). In the literature it has been shown that thinner spine necks are less 'leaky' to Ca^{2+} ions and therefore are able to compartmentalise intracellular calcium stores more efficiently (Nimchinsky et al., 2004; Noguchi et al., 2005). A drop in neuronal firing in the presence of TTX due to the reduction in glutamate receptor activation will occur and therefore reduce the influx of Ca^{2+} into the postsynaptic spine which would inhibit activating downstream effector proteins (Turrigiano, 2008). These will include those involved in regulating the actin cytoskeleton to alter spine morphology. Therefore the spine is best to compensate for the lack of synaptic activity by adopting a thinner spine neck in order to concentrate its intracellular calcium stores and remain synaptically active.

In comparison the MSK1 KD spines were unable to adapt to the TTX treatment as their spine volume increased whilst the spine head width decreased without changing the length of the spine. These spines almost resemble the 'stubby' spine which are most prominent during mid-developmental stages (Harris et al., 1992). Stubby spines are thought to have a transitory function between postnatal development as they will give rise to other spines such as mushroom or thin according to synaptic input (Harris et al., 1992). Therefore it appears that MSK1 has influenced spine morphology into an intermediate state and therefore could impede its potential to scale firing rate when faced with perturbations in synaptic transmission. In relation to our TTX-induced scaling model shown in Figure 3.11, the endocytic protein, Arc, can be regulated by MSK1 thus mediating AMPAR trafficking and subsequently influencing spine morphology. Arc is also thought to interact indirectly with the actin cytoskeleton, as illustrated in its abbreviation (Lyford et al., 1995; Bramham et al., 2010). This property could also involve a MSK1-Arc dependent mechanism in regulating spine morphology.

To summarise, this Chapter has shown that MSK1 could potentially play a role in regulating spine density during hippocampal neuronal development but has no such role during 24 hours TTX-incubation. Spines have been shown to transform from immature filopodia-like spines to mature and stable mushroom shaped spines during development. This natural transition did not occur in the MSK1 KD neurones as their spine length remained unaltered but was subsequently over compensated in the volume.

The presence of TTX did not affect the spine morphology of young WT neurones but forced MSK1 KD spines into more immature structures which could again indicate an ‘over compensatory’ mechanism due to the lack of the homeostatic regulator MSK1. At 21 DIV the neurones appear to respond differently to TTX where WT neurones adopt a thin shape to possibly compartmentalise intracellular calcium so as to remain synaptic active. However MSK1 KD mice are unable to respond accordingly. In conclusion MSK1 may be affecting the way dendritic spines are able to respond structurally to TTX-induced scaling and may be influenced by the maturity of the neurones.

Chapter 5.

Characterisation of MSK1's role in environmentally enriched conditions

5.1 Introduction

Environmental enrichment (EE) is described where 2 or more animals (e.g. mice or rats) are placed in a large 'enriched' cage with tunnels, running wheels, climbing ladders and toy blocks (Rosenzweig et al., 1962; Rosenzweig, 1966; Rosenzweig and Bennett, 1996) as opposed to standard housed animals in smaller cages containing only nesting material, food and water (Figure 5.1). The environmentally enriched conditions include a complex range of contributing factors ranging from social, sensory and motor stimuli.

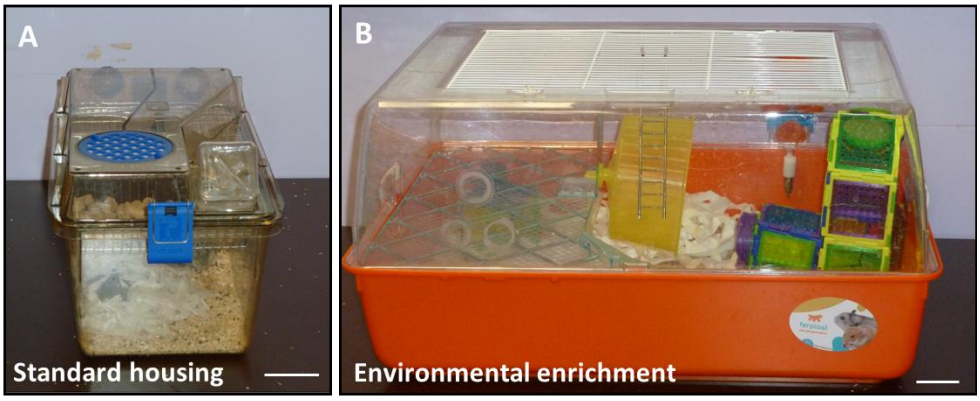

Figure 5.1; The experimental set up for environmental enrichment. *The experimental set up of standard housing (SH)* ***(A)*** *and environmental enrichment (EE)* ***(B)*** *cages. The SH cages (19cm x 29cm x 12cm) included water, food pellets and bedding and the EE cages (39cm x 27cm x 55cm) had a variety of toys, including a running wheel, long and short plastic tubes and a climbing ladder as well as access to water, food pellets and bedding. Both conditions had 2 or more mice during the experiment to allow social interaction. Scale bar; 4 cm.*

The consequences of enrichment in the intact brain includes enhancements in memory function, spine density and morphology, the release of growth factors including BDNF (brain-derived neurotrophic factor) (Falkenberg et al., 1992) and changes in synaptic plasticity, such as LTP and LTD (Artola et al., 2006). Enriched

mice show improved memory function in water-maze test illustrating enhanced spatial memory (Eckert and Abraham, 2010) and increased spine density in pyramidal neurones of the CA1 region (Globus et al., 1973; Rampon et al., 2000a). There are controversial studies in the literature on whether EE affects LTP or LTD which could be attributed to many factors such as the age and specie of the animal as well as the sex or the duration and protocol used for EE (Table 1.1) (Eckert and Abraham, 2013). BDNF has been shown previously to play a signalling role in synaptic plasticity. During EE BDNF mRNA is upregulated in the CA1 hippocampal neurones which was correlated with improved formation of spatial memory using Morris water maze test (Falkenberg et al., 1992; Kempermann et al., 1997). Accordingly the downstream IEG Arc was also shown to be upregulated in response to EE in the hippocampus (Guzowski et al., 1999; Pinaud et al., 2001b; Chotiner et al., 2010). We hypothesise a BDNF-MSK1-Arc pathway is involved in experience-dependent plasticity using EE model. The reason why we wanted to test whether MSK1 plays a role in EE-dependent phenotype is firstly because we have previously shown that MSK1 can regulate Arc protein expression during a form of synaptic plasticity e.g. TTX induced scaling (Figure 3.8), secondly the literature has shown that Arc expression is upregulated in response to EE and finally, EE can be influenced by an upregulation of released BDNF. Therefore the BDNF-Arc pathway is active in this model and we wanted to test whether MSK1 played a role in this model. This model represents yet another form of synaptic plasticity known as experience-dependent which is looking at whole animal rather than neuronal culture.

An important aspect of EE experiments is that the EE protocol heavily influences the functional output which is highlighted in many reviews and discussed further in my discussion (van Praag et al., 2000; Eckert and Abraham, 2013). Thus in keeping with this knowlege , it was necessary to test firstly if our protocol induced changes in (1) Arc mRNA and protein expression, (2) electrophysiological properties of the synapses and (3) changes in dendritic spine density. In parallel we wanted to characterise if there were EE-dependent changes, if these were MSK1-dependent.

The aim of this Chapter is to characterise the potential role of MSK1 in acute and chronic EE using WT and MSK1 KD adult mice. Acute EE consisted of one hour, 3 hours and 6 hours of exposure to enriched conditions at P28 whilst chronic EE is 2 weeks enrichment before being culled (Figure 5.2). It was important to only use male adult mice as female mice have hormonal cycles which strongly influences

spine density in the brain (Woolley et al., 1990). Samples were taken from both the anterior neocortex and hippocampus because these brain regions have shown changes in anatomical structure (Diamond et al., 1976) and spine density (Silva-Gomez et al., 2003) after EE as well as increased levels of BDNF (Ickes et al., 2000). Both RNA and protein were extracted from the acutely environmentally enriched mice to probe for Arc mRNA and protein levels. In chronically environmentally enriched mice, protein was extracted from one hemisphere and the other was prepared for *in vitro* electrophysiological recordings from the CA1 region of the hippocampus. In order to characterise the functional properties of hippocampal circuits and thus electrophysiological properties of synapses there are three standard electrophysiological techniques used as a functional readout (A-C shown below). Firstly extracellular field excitatorypostsynaptic potentials (fEPSP) were recorded from stratum radiatum in area CA1 (please see Figure 2.2 for more detailed information). fEPSP is when the postsynaptic membrane potential temporarily depolarises which is caused by the flow of positively charged ions into the postsynaptic cell via ligand-gated ion channels. Recording fEPSP allowed further electrophysiological measurements to be made. (A) The basal synaptic transmission of the pyramidal neurones was measured by recording an input/output curve. This was important as we wanted to see if EE changed the electrophysiological properties of the synapses under basal conditions before any stimulation was applied. (B) In order to see if EE caused any changes in the presynaptic properties of the synapses we measured paired pulse facilitation (PPF) recordings. It was important to establish if there were presynaptic changes which could be influencing any potential postsynaptic effects observed. (C) Changes in electrophysiological properties which could influence synaptic plasticity was measured by inducing LTP using two protocols known as tetanus and theta burst stimulation. From previous literature, EE can change synaptic properties which causes changes in synaptic plasticity expression (Eckert and Abraham, 2013). Finally, in order to correlate functional changes with structural changes the spine density in CA1 pyramidal neurones were measured.

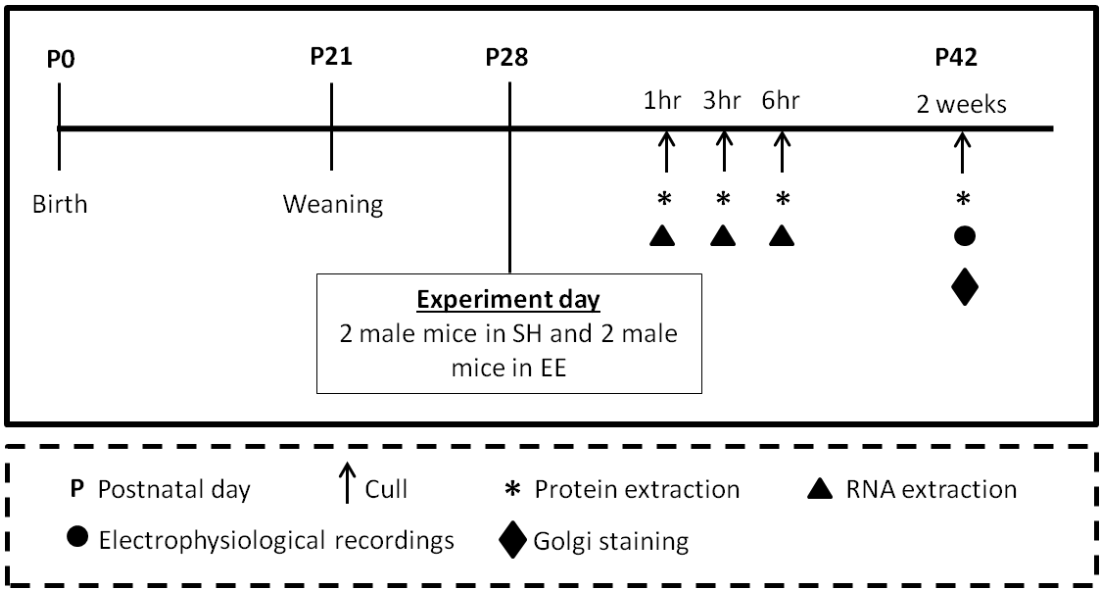

Figure 5.2; The experimental plan for environmental enrichment of WT and MSK1 KD mice*. The mice were born (P0), weaned at P21 and left a week in standard housing (SH) to recover from the weaning. At least two male mice (to retain social interaction) were either moved into the EE cages at P28 or remained in standard housing. The mice that remained in SH were picked up by the tail and placed back into their standard housed cage as a handling control, in order to maintain handling the same between both conditions. The mice were either SH or EE for 1 hour, 3 hours, 6 hours or 2 weeks before being culled. The brains were either used for RNA or protein extraction as well as electrophysiological recordings. Golgi staining was carried out in 2 week environmentally enriched mice and standard housed mice.*

5.2 Results

5.2.1 Arc mRNA and protein levels after acute environmental enrichment exposure in WT and MSK1 KD hippocampus and cortex

It has been shown that Arc mRNA is upregulated under environmentally enriched conditions in both the cortex and hippocampus (Pinaud et al., 2001b). In the following experiments both RNA and protein were extracted from the same animal. Both the hippocampus and cortex were dissected from the left hemisphere for RNA extraction and the right hemisphere for protein extraction (Figure 5.2).

RNA was extracted from the hippocampus and anterior neocortex of 4 week old male WT and MSK1 KD mice after exposure to environmentally enriched conditions for 1, 3 and 6 hours as well as a group of control standard housed mice.

When the time points were represented individually for Arc mRNA induction for both the hippocampus (Figure 5.3 A.1) and cortex (Figure 5.3 B.1) there didn't appear to be any striking differences at any of the time points. Therefore we pooled the data together to observe a general trend of EE after 1-6 hours of exposure in the hippocampus (Figure 5.3 A.2) and the cortex (Figure 5.3 B.2). Multiple unpaired t tests using Holm-Sidak post hoc was used to compare the SH and EE condition of WT which showed a significant increase in the hippocampus ($p<0.01$) and neocortex ($p<0.001$) after EE. However the MSK1 KD mice also showed a significant induction of Arc mRNA after EE. This was shown in both the hippocampus and the cortex ($p<0.01$).

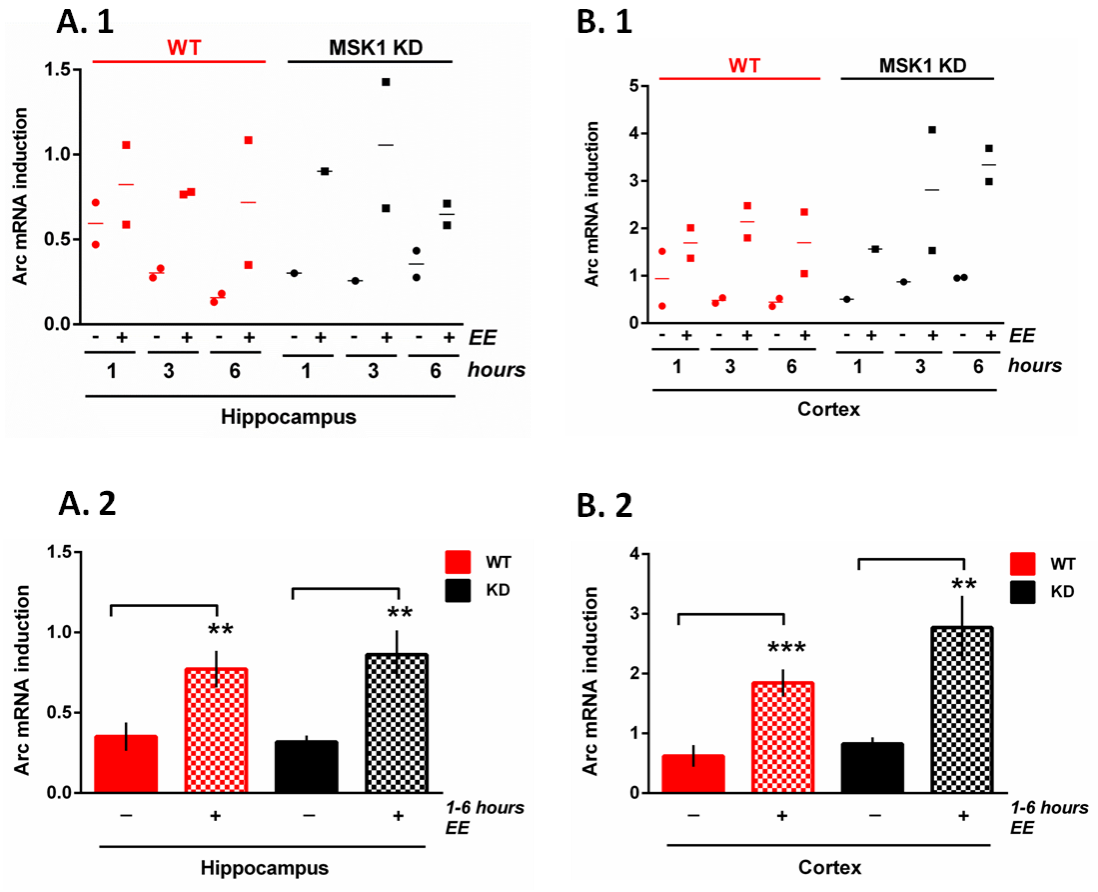

Figure 5.3; The induction of Arc mRNA following acute EE in WT and MSK1 KD adult mice in the hippocampus and cortex. *The mice were treated according to the experimental design shown in Figure 5.1 following 1, 3 and 6 hours of enrichment (+) or standard housing (-). The standard housed mice were handled briefly so to act as a handling control as the enriched mice were handled when placed in their new environment. After the time indicated the mice were culled and their brains removed followed by the dissection and RNA extraction of the hippocampus* ***(A)*** *and anterior neocortex* ***(B)*** *.The RNA was extracted from the tissue and sent to University of Dundee (Dr. Simon Arthur) where a Q-PCR was carried out using 18s rRNA as a control. Arc mRNA induction was visualised at each time point in the hippocampus (A. 1) and the cortex (B. 1). The graphs represent each individual sample where the bar represents the mean value since there was only 1-2 samples. In graphs* ***A. 2 and B. 2*** *the time points were pooled together representing the average Arc mRNA induction ±SEM including n=4 for KD SH and n=6 for KD EE, WT SH and WT EE (A. 2) and cortex (B. 2). Multiple unpaired t tests using the Holm-Sidak post hoc test which sets significance level at **p<0.01 and *** p<0.001.*

The Arc protein levels in the hippocampus and anterior neocortex were represented in same fashion as shown for Arc mRNA induction graphs. The 1, 3 and 6 hour time points were represented individually for both the hippocampus (Figure 5.4, 1.A) and cortex (Figure 5.4, 2.A) shown in the scatter graphs. There appeared to be an increase in Arc protein induction after 3 and 6 hours of EE but not necessarily

after 1 hour, so graphs were created pooling the 3 and 6 hour samples together (Figure 5.4, 1.B and 2.B). After 3-6 hours of EE there was a significant upregulation of Arc protein in both WT and MSK1 KD mice hippocampal samples (Figure 5.4, 1.B, multiple unpaired t test using Holm-Sidak $p<0.05$ and $p<0.001$). An increase in Arc protein was also observed in the cortex (Figure 5.4, 2.B) in both genotypes. The increase was more significant in the WT ($p<0.001$) when compared to the MSK1 KD ($p<0.05$). Lastly, for completeness all the data was pooled together to observe a general trend of EE after 1-6 hours of exposure in both the hippocampus (Figure 5.4, 1.C) and the cortex (Figure 5.4, 2.C). After EE a significant induction of Arc protein was observed in hippocampus of the WT mice ($p<0.05$) as well as the MSK1 KD mice ($p<0.001$) after using multiple unpaired t tests (Holm-Sidak post hoc) (Figure 5.3, 1.C). However in the cortex the WT mice showed increased levels of Arc protein after EE ($p<0.01$) but the Arc levels in the MSK1 KD mice remained unchanged. When the SH conditions were compared between the WT and MSK1 KD samples, elevated levels of Arc protein was demonstrated in the MSK1 KD mice (Figure 5.3, 2.C; $p<0.05$, multiple unpaired t tests-Holm Sidak post hoc).

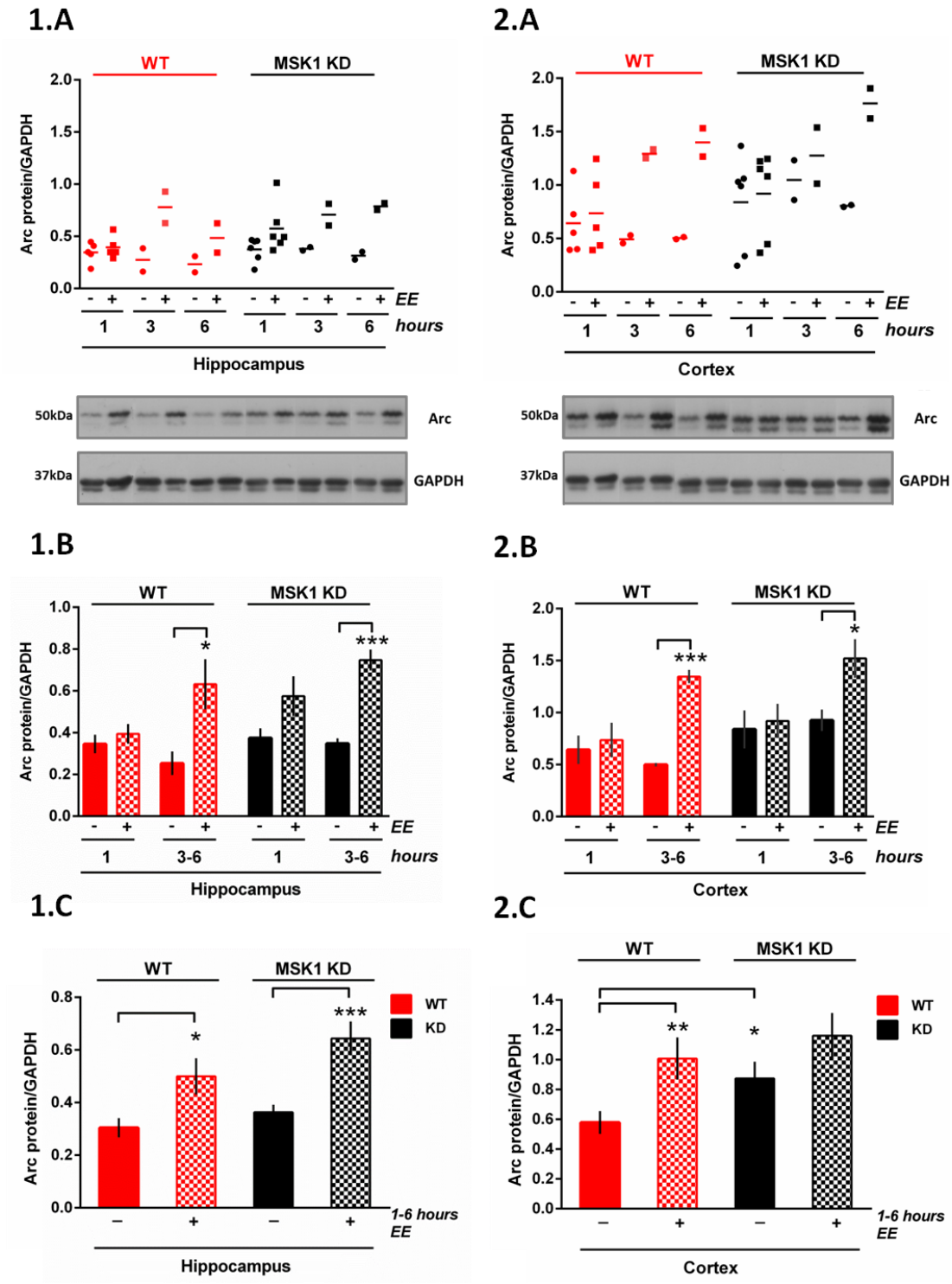

Figure 5.4; The effects of acute EE in WT and MSK1 KD adult mice on Arc protein in the hippocampus and cortex. *The mice were treated according to the experimental design shown in Figure 5.1 following 1, 3 and 6 hours of enrichment (+) or standard housing (-). After the time indicated the mice were culled and their brains removed followed by the dissection of the hippocampus and frontal cortex. Protein was extracted from the hippocampus* ***(1)*** *and anterior neocortex* ***(2)*** *where SDS-PAGE was carried out to separate the protein. The protein Arc was probed against using GAPDH as a loading control. The intensity of the bands were analysed using Fiji software which are represented as individual samples on a scatter graph where the line represents the mean value since there was only 2 samples in some*

*conditions for the hippocampus (1.A) and cortex (1.B). The representative western blots are shown below. The graphs **1.B** and **2.B** represent the average ±SEM for the hippocampal and cortical samples, respectively, where the 3-6 hour samples were pooled together and compared to 1 hour time point. Multiple unpaired t tests using the Holm-Sidak post hoc test which sets significance level at *p<0.05 and ***p<0.001. [WT SH and EE 1 hour n=5, KD SH and EE n=6 and 3- hours for both genotypes n=4]. In graphs **1.C** and **2.C** all the time points were pooled together representing the average Arc protein induction ±SEM including WT samples n=9 and KD samples n=10 from the hippocampus and cortex. Multiple unpaired t tests using the Holm-Sidak post hoc test which sets significance level at *p<0.05 **p<0.01 and ***p<0.001.*

5.2.2 The expression of Arc protein in the hippocampus and frontal cortex after 2 weeks of EE in both WT and MSK1 KD mice.

WT and MSK1 KD mice were transferred to EE conditions or handled and remained in SH conditions at P28 for 2 weeks (Figure 5.1 and 5.2). After those 2 weeks the mice were culled and the hippocampus and cortex were dissected. Protein was extracted from these tissues and separated using SDS-PAGE. There were no clear changes or trends in Arc protein expression after 2 weeks of EE in either WT or MSK1 KD, or the different parts of the brain (Figure 5.5, $p>0.05$ using multiple unpaired t tests-Holm Sidak post hoc).

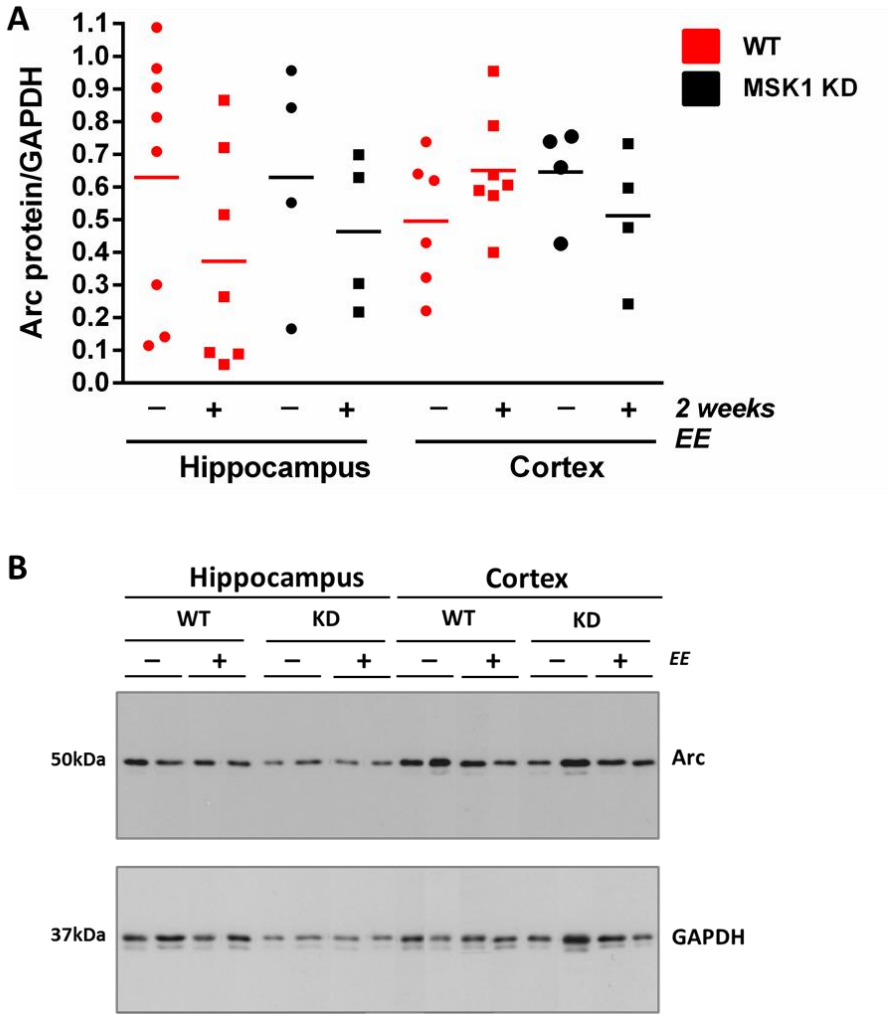

Figure 5.5; There were no changes in total Arc protein expression in the hippocampus or the cortex after 2 weeks of enrichment in both WT and MSK1 KD. *The mice were treated according to the experimental design shown in Figure 5.1 following 2 weeks of enrichment (+) or standard housing (-). After the time indicated the mice were culled and their brains removed followed by the dissection of the hippocampus and frontal cortex. Protein was extracted from the hippocampus and cortex where SDS-PAGE was carried out to separate the protein. The protein Arc was probed against using GAPDH as a loading control. The intensity of the bands were analysed using Fiji software which are represented as individual points in scatter plot with the line representing the average* ***(A)****. The representative blots are shown in* ***(B)*** *where each condition is shown as n=2. A multiple unpaired t tests using the Holm-Sidak post hoc test which sets significance level at $p<0.05$ where none of the groups were significantly different to each other (n=4-8 for both WT and MSK1 KD).*

5.2.3 Electrophysiological recordings in hippocampal slices from WT and MSK1 KD mice under SH and EE conditions

The CA1 Schaffer collateral/commissural pathway in the hippocampus was used to record a range of electrophysiological properties of synaptic transmission between CA3 and CA1 pyramidal neurones. The experimental setup is shown in Figure 2.2 (Section 2.7.2.2). The following parameters were measured in WT and MSK1 KD mice which had been in SH or EE conditions for 2 weeks (Figure 5.2).

(i) Input/output (I/O) curve which measures basal synaptic transmission (Section 5.2.3.1).

(ii) Paired-pulse (PP) facilitation which reflects the probability of transmitter release at the presynaptic terminal (Section 5.2.3.2).

(iii) Tetanus LTP (T-LTP) which induces synaptic potentiation in response to tetanic stimulation consisting of 100 pulses at 100 Hz. (Section 5.2.3.3)

(iv) Theta burst stimulation LTP (TBS-LTP) which induces synaptic potentiation in response to a TBS involving 4 pulses at 100 Hz repeated 10 times with a 200 ms interval. This burst was repeated three times with a 20 second interval between bursts (Section 5.2.3.4).

5.2.3.1 Electrophysiological recordings of basal synaptic transmission in WT and MSK1 KD CA1 region of the hippocampus after 2 weeks of EE.

Basal synaptic transmission was recorded from hippocampal slices prepared from WT and MSK1 KD mice following exposure to SH and EE conditions. This was represented by an I/O curve which involves recording the fEPSP slope and the presynaptic fibre volley (FV) amplitude after stimulating the Schaffer pathway at a range of stimuli intensities (in μA) 10, 25, 50, 100, 150, 200, 250 and 300 (Section 2.7.2.3). As the stimulus intensity increases the number of fibres recruited increases and therefore evokes larger fEPSP.

A plot of the relationship between the stimulus intensity and size of the evoked fEPSP is represented by two graphs. The first of which has the stimulus intensity along the x axis against the fEPSP slope (mV/ms) shown in Figure 5.6 (All A graphs) the second set of graphs show the stimulus intensity against FV amplitude (mV) along the y axis shown in Figure 5.6 (All B graphs). The FV amplitude is used as an index for the recruitment of presynaptic fibres and obviates confounds

associated with slice to slice variability in stimulus intensity. If there were to be a change in basal synaptic transmission there would be a shift in the I/O curve. A shift to the left would indicate an increase in basal synaptic transmission and a right-ward shift represents a decrease.

The comparison between WT SH and WT EE conditions is shown in Figure 5.6 (1 A and B). There appears to be no changes in fEPSP slope between SH and EE WT mice but the WT EE mice showed a slight left hand shift in the FV amplitude curve. This indicates that WT EE mice possibly have larger FV amplitude at the higher stimulus intensities or that the MSK1 KD mice have smaller FV amplitudes. However this was not significant using a two way ANOVA probably due to the sample variability. The MSK1 KD mice showed no EE-dependent changes in fEPSP slope or FV amplitude ($p>0.05$, Figure 5.6.2 A and B). This was also apparent when the SH conditions of both WT and MSK1 KD mice were compared (Figure 5.6.3 A and B). The fEPSP slope between WT EE and MSK1 KD EE showed no changes in the curves but the FV amplitude of the WT EE shifts slightly to the left when compared to the MSK1 KD EE. Nevertheless this was not statistically significant (a two way ANOVA (Figure 5.6.4 B, $p>0.05$). It is important to note that not every fEPSP has a FV which is measurable and therefore the n values will differ between fEPSP slope and FV amplitude as fewer FV were available to measure.

1.
WT SH versus WT EE

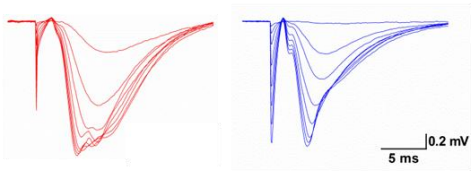

A

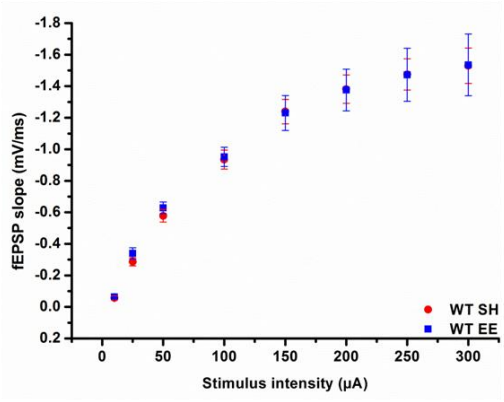

B

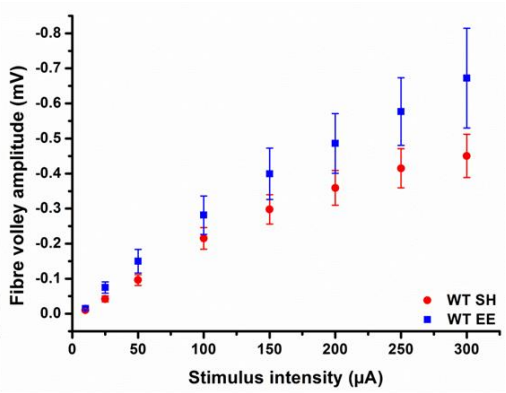

2.
KD SH versus KD EE

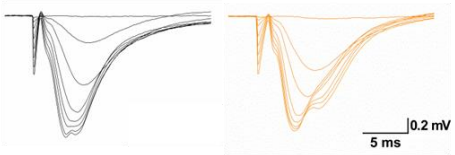

A

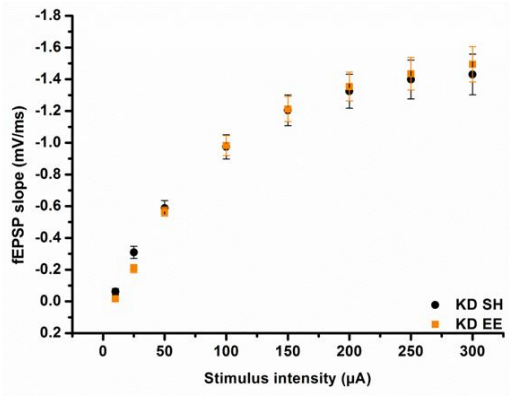

B

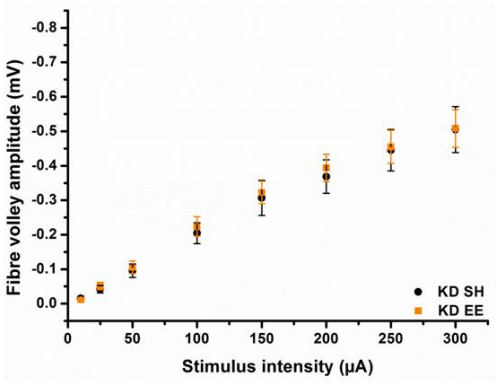

3.
WT SH versus KD SH

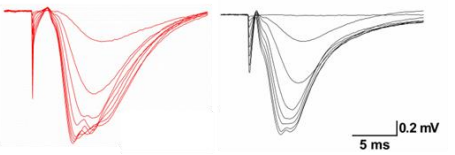

A

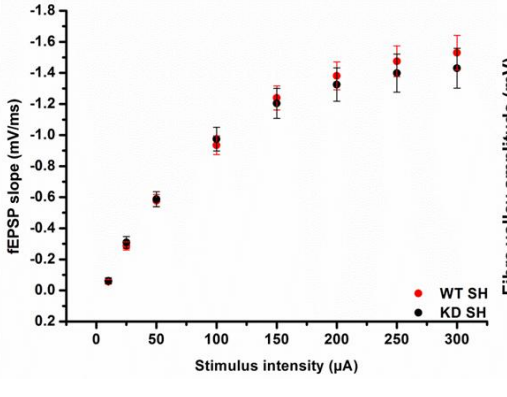

B

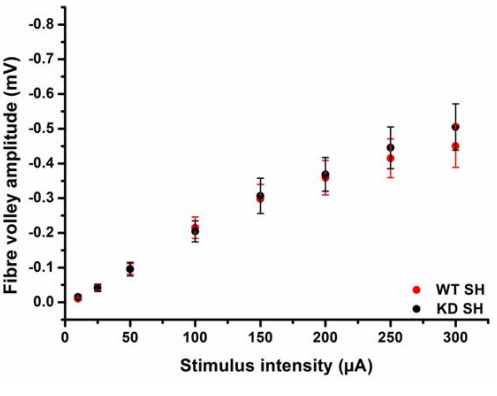

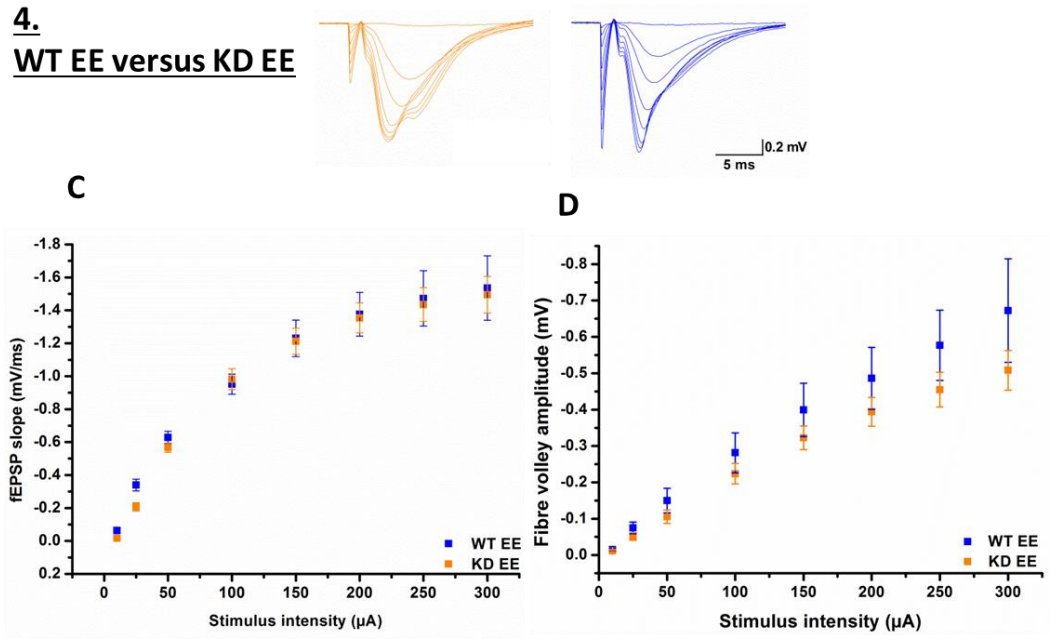

Figure 5.6; There were no changes in basal synaptic transmission in the CA1 region of the hippocampus after EE in either WT or MSK1 KD. *Parasagittal hippocampal slices (400 µm) were prepared from 6 week old male mice that had been exposed to SH or EE conditions for 2 weeks. Extracellular fEPSP were recorded from the stratum radiatum in the CA1 region. The linear part of the fEPSP slope was measured throughout the recording which usually measured over 1 ms range. A stable fEPSP was recorded using a stimulus which was 50% of maximal fEPSP slope before measuring an I/O relationship curve using a range of stimuli (units; in µA) 10, 25, 50, 100, 150, 200, 250 and 300. A representative fEPSP at each stimulus for each condition and genotype is shown above each corresponding graph. The graphs are labelled as* ***1.*** *WT SH versus WT EE,* ***2.*** *KD SH versus KD EE,* ***3.*** *WT SH versus KD SH and* ***4.*** *WT EE versus KD EE. All the graphs labelled* ***(A)*** *represent average fEPSP slope ± SEM and those labelled* ***(B)*** *represent the average FV amplitude ± SEM. A Two way ANOVA was carried out on each of the graphs and rendered all groups not significantly different to each other. (n numbers for fEPSP slope: WT SH= 39 slices, 11 mice; WT EE= 39 slices, 9 mice; KD SH=20 slice, 6 mice; KD EE=32 slices, 5 mice and n numbers for FV amplitude: WT SH= 13 slices, 6 mice; WT EE= 5 slices, 3 mice; KD SH=8 slice, 4 mice; KD EE=9 slices, 4 mice)*

In order to avoid grouping the values for fEPSP slope or the FV amplitude per stimulus intensity another graph was designed which represents the fEPSP slope (mV/ms) against FV amplitude (mV) shown in Figure 5.7. For each condition, e.g. WT SH and EE as well as MSK1 KD SH and EE, the average fEPSP slope was plotted against the FV amplitude ± SEM (Figure 5.7, A). Secondly another graph was designed to represent each data point as a scatter graph whilst adding a line of

best fit through the data (Figure 5.7, Bs). When WT SH and EE were compared the variation at the greater fEPSP slope and FV amplitude values was higher. The WT SH values appeared to be slightly shifted to the left indicating that more fEPSP average FV amplitude were smaller than the WT EE whilst retaining similar fEPSP slope average (Figure 5.7, 1. A). This pattern was replicated in the corresponding scatter graph shown below (Figure 5.7, 1. B) where the line of best fit for the WT EE was shifted right-ward to that of the WT SH. The MSK1 KD EE mice also showed a similar pattern in which it was also slightly shifted to the right in comparison to the SH condition (Figure 5.7, 2. A and B). There were no changes in the averaged or distribution of values for the WT SH when compared to the MSK1 KD SH (Figure 5.7, 3. A and B). This was also apparent when the WT and MSK1 KD EE mice were compared in Figure 5.7, 4. A and B. Although the MSK1 KD EE mice showed a very slight left-ward shift when compared to the WT EE which is highlighted in Figure 5.7, 4. B, where the line of best fit for MSK1 KD EE is marginally above the WT EE line.

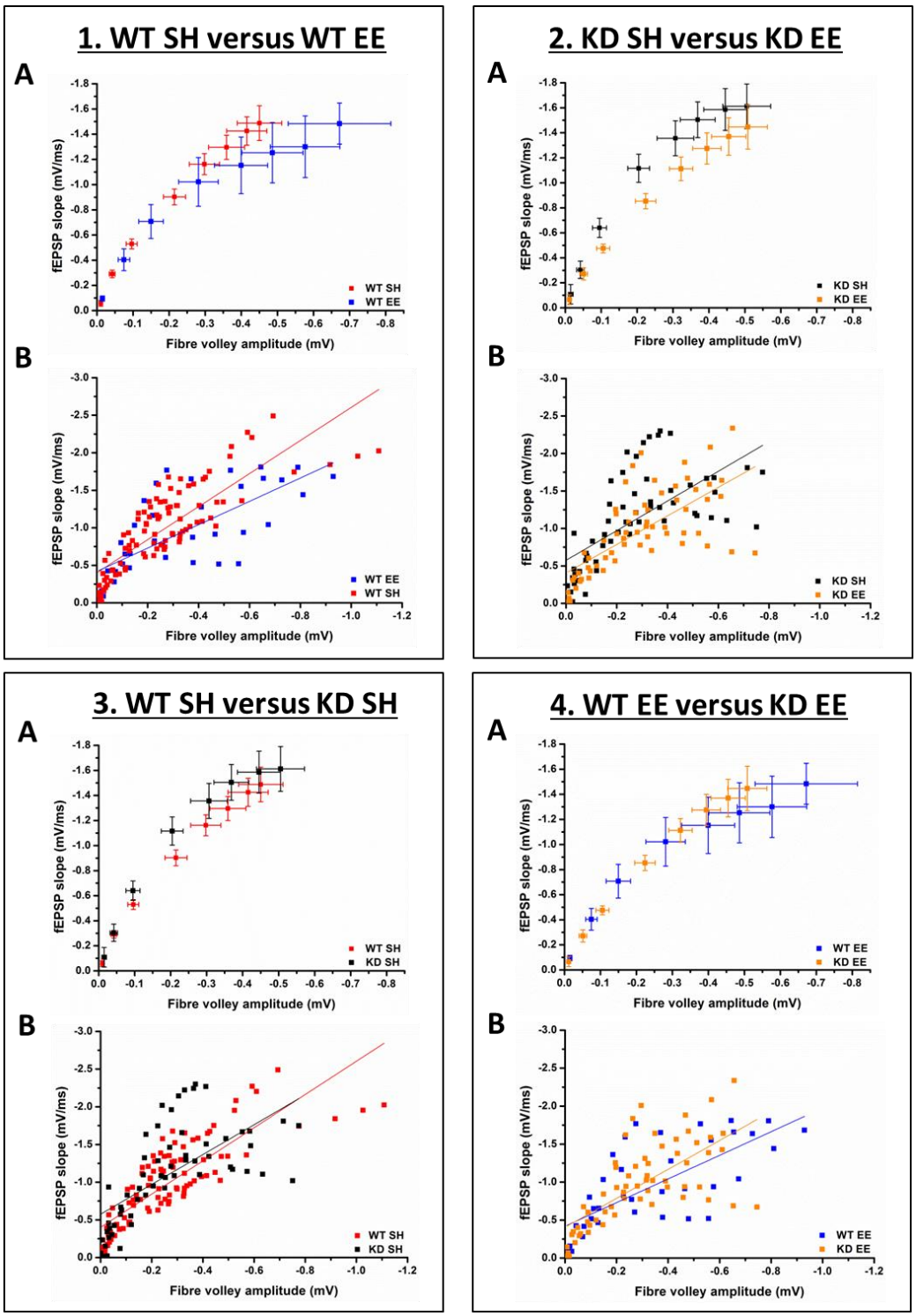

Figure 5.7; There were no striking differences in the relationship between FV amplitude and fEPSP slope in CA1 region of the hippocampus after EE in either WT or MSK1 KD. *Parasagittal hippocampal slices (400 µm) were prepared from 6 week old male mice that have been exposed to SH or EE conditions for 2 weeks. Extracellular fEPSP were recorded from the stratum radiatum in area CA1. The linear part of the fEPSP slope was measured throughout the recording which usually measured over 1 ms range. When a FV was observed in the fEPSP the amplitude of this FV was also measured. A stable fEPSP was recorded using a stimulus which was 50% of maximal fEPSP slope before measuring an I/O relationship curve using a range of stimuli (units; in µA) 10, 25, 50, 100, 150, 200, 250 and 300. The graphs*

*plots the average FV amplitude along the x axis against the average fEPSP slope ±SEM at each stimulus strength along the y axis for WT SH versus WT EE **(A)**, KD SH and KD EE **(B)**, WT SH and KD SH **(C)** and WT EE and KD EE **(D)**. Each data point of each condition was then plotted in a scatter graph represented in graphs **E-G**. A line of best fit was drawn across the scatter graphs represented by the coloured lines. (n numbers for fEPSP slope: WT SH= 39 slices, 11 mice; WT EE= 39 slices, 9 mice; KD SH=20 slice, 6 mice; KD EE=32 slices, 5 mice and n numbers for FV amplitude: WT SH= 13 slices, 6 mice; WT EE= 5 slices, 3 mice; KD SH=8 slice, 4 mice; KD EE=9 slices, 4 mice)*

5.2.3.2 The electrophysiological recording of the probability of release from the presynaptic terminal by measuring the paired pulse ratio in WT and MSK1 KD in the CA1 region of the hippocampus after 2 weeks of EE.

Paired pulse (PP) facilitation or depression is a form of short term synaptic plasticity reflecting the probability of release of neurotransmitter from the presynaptic terminal (Andersen, 2007). Experimentally this is measured by delivering two stimuli in close succession and the slope of the first and second synaptic responses are compared. The PP ratio is calculated by dividing the second fEPSP slope by the first fEPSP slope and is a reflection of the increase in the probability of transmitter release. The mechanism behind this phenomenon is due to the influx of calcium into the presynaptic terminal after the first stimuli which will still be present if the second stimulus is delivered in close succession. Therefore the second postsynaptic response will be larger as the calcium influx of the second stimuli will add to the residual calcium concentration from the first evoked fEPSP. Thus an enhanced calcium concentration will increase the probability of release as calcium is required for the fusion of the vesicle to the presynaptic membrane releasing neurotransmitter by exocytosis (Zucker and Regehr, 2002). Therefore differences in PP facilitation between treatments/genotypes will indicate that the probability of release will be different.

A PP ratio was calculated for all four groups in this study, WT SH, WT EE, MSK1 KD SH and MSK1 KD EE. The PP ratio was also calculated over an interpulse interval (IPI) of (units; ms) 50, 100, 150, 200 and 250 using fEPSP of ~50% of the maximal fEPSP slope. In all groups PP facilitation was observed as the ratio was above 1 at all IPI. However there were no significant shifts in the PP relationships between any of the conditions or genotypes ($p>0.05$, Two way ANOVA). Therefore there were no changes in the probability of release.

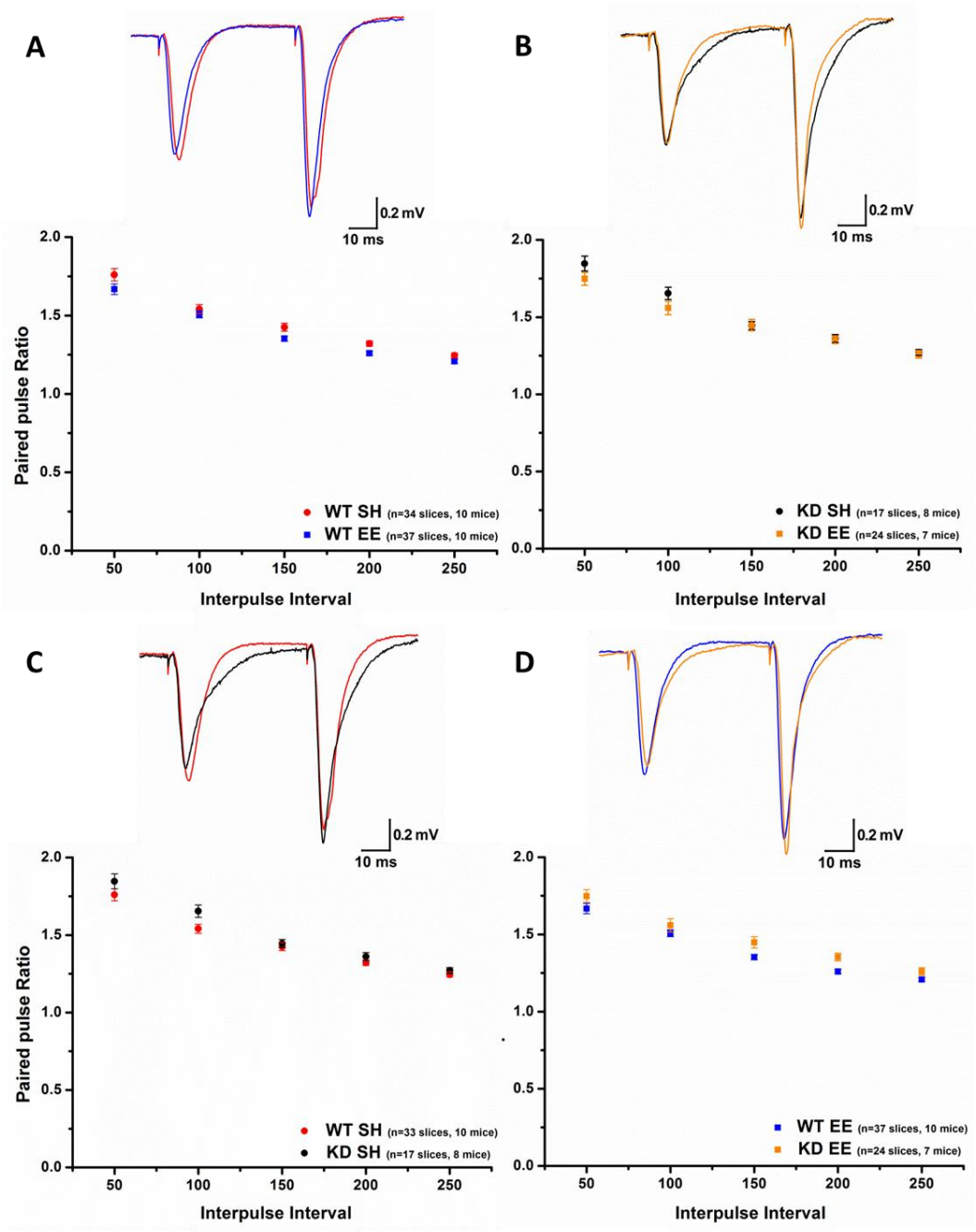

Figure 5.8; There were no changes in the general trend of the paired pulse (PP) ratios in CA1 region of the hippocampus after EE in either WT or MSK1 KD. *Parasagittal hippocampal slices (400 µm) were prepared from 6 week old male mice that had been exposed to SH or EE conditions for 2 weeks. Extracellular fEPSP were recorded from the stratum radiatum in the area CA1. The linear part of the fEPSP slope was measured throughout the recording which usually measured over a 1 ms range. The PP ratio was also calculated over an interpulse interval (IPI) of (units; ms) 50, 100, 150, 200 and 250 using fEPSPs of ~50% of the maximal fEPSP slope. The graphs represent the average PP ratio for each ISI ±SEM for WT SH versus WT EE* ***(A)****, MSK1 KD SH and EE* ***(B)*** *WT SH and KD SH* ***(C)*** *and WT EE and MSK1 KD EE* ***(D)****. A Two Way ANOVA was carried out for each coupled comparison in each graph which rendered all groups not significantly different to each other (p>0.05). (WT SH; n=33 slices from 10 mice, WT EE; n=37 slices from 10 mice, KD SH; 17 slices from 8 mice and KD EE; n=24 slices from 7 mice).*

5.2.3.3 Tetanus-induced LTP in WT and MSK1 KD CA1 region of the hippocampus after 2 weeks of EE.

Long-term potentiation (LTP) is a form of synaptic plasticity that can be initiated in hippocampal synapses through the delivery of a high-frequency stimulation (HFS) consisting of 100 pulses at 100 Hz, also known as a tetanus (T-LTP). The question that was addressed was whether EE of WT or MSK1 KD mice have changes in LTP expression in response to EE, and whether this response was MSK1-dependent.

T-LTP was successfully induced in all four groups, WT SH and EE as well as MSK1 KD SH and EE (Figure 5.9 A-D). This was confirmed after carrying out a paired t test on the average values prior to T-LTP (2 minutes prior to T-LTP) and at the end LTP (58^{th}-60^{th} minute post T-LTP) (Figure 5.9 E, ** $p<0.01$ and *** $p<0.001$ in the orange boxes). When the WT SH and WT EE LTP traces were compared after ~60 minutes of LTP there was no significant difference in LTP between the two groups (Figure 5.9 A and E; unpaired t test). Using the same analysis the MSK1 KD SH LTP showed no significant difference in LTP from the KD EE LTP trace (Figure 5.9 B and E). The SH condition in both WT and MSK1 KD showed no changes in LTP expression between 58^{th} -60^{th} minutes post T-LTP (Figure 5.9 C; unpaired t test shown in E). This was also the case for the EE condition in both WT and MSK1 KD (Figure 5.9 D, unpaired t test shown in E).

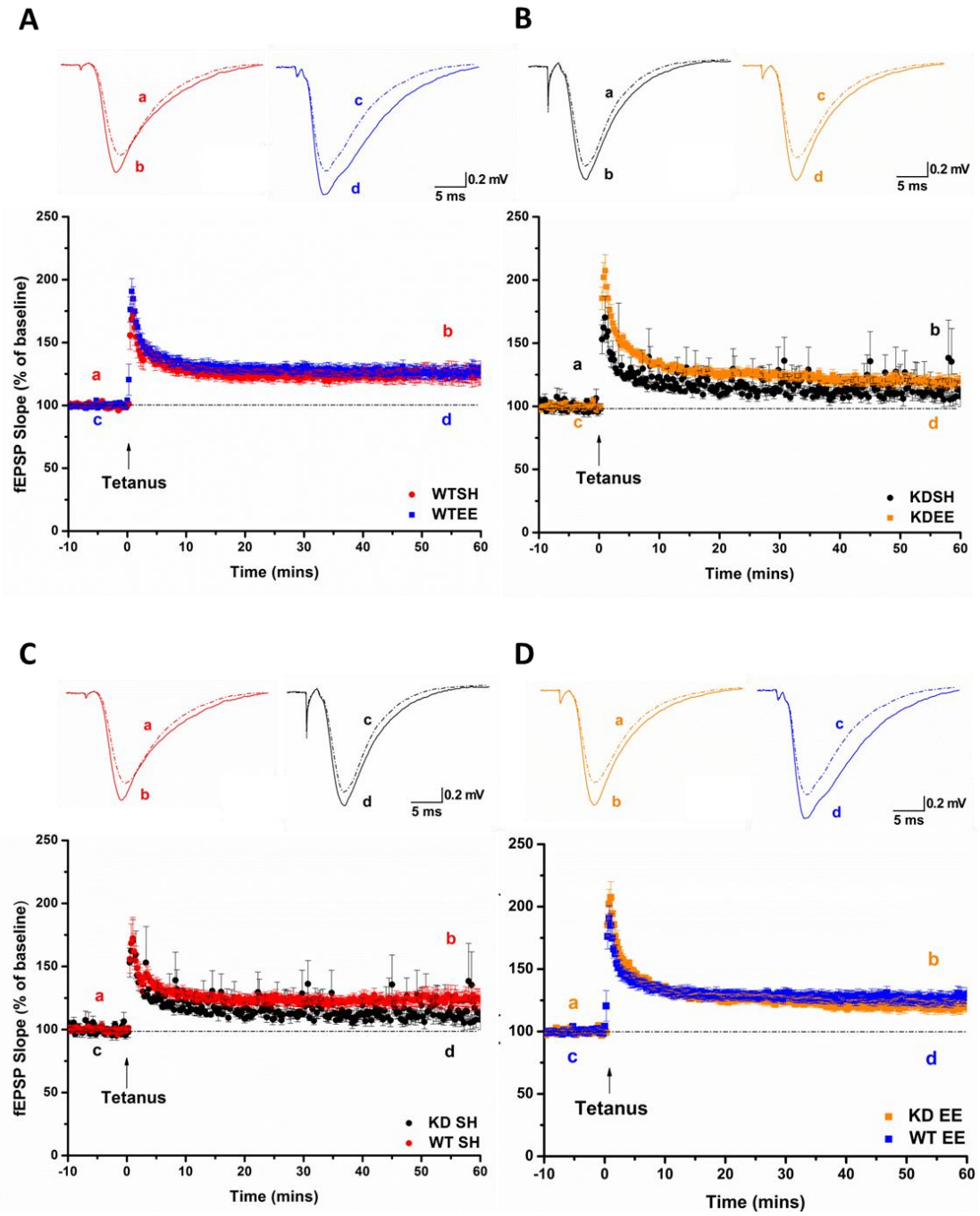

E

T-LTP	WT SH	WT EE	KD SH	KD EE
WT SH	***			
WT EE	ns	**		
KD SH	ns		***	
KD EE		ns	ns	***

Key

Was LTP induced in each condition? Using a paired t test (**p<0.01, ***p<0.001)

Were the LTP traces different across the four groups? Using an unpaired t test [ns= not significant]

Figure 5.9; There were no changes in tetanus induced LTP in CA1 region of the hippocampus after EE in either WT or MSK1 KD. *Parasagittal hippocampal slices (400 µm) were prepared from 6 week old male mice that had been exposed to SH or EE conditions for 2 weeks. Extracellular fEPSP were recorded from the stratum radiatum in area CA1 where the linear part of the fEPSP slope was measured. Tetanus LTP (T-LTP; 100 pulses at 100 Hz) was induced at the time indicated by the arrow. The stimulation was applied after 10 minutes of stable baseline was collected at 0.067 Hz (1 pulse per 15 sec). The recordings continued for at least an hour after the induction of LTP. Each graph represents the average fEPSP slope normalised to the baseline ± SEM for WT SH versus WT EE* ***(A)****, KD SH and KD EE* ***(B),*** *WT SH and KD SH* ***(C)*** *and WT EE and KD EE* ***(D)****. A representative fEPSP is shown above each of the graphs with a letter (a-d) which is indicative of the time at which the fEPSP was recorded shown on the graph. The fEPSP represented as a dotted line represents (a) and (c) pre-tetanus induction as oppose to (b) and (d) which are after LTP induction.* ***(E)*** *The statistical tests used to identify if LTP was successfully induced, compared 8 time points before LTP induction and the last 8 time points. The other test was to see if there were any differences in the traces between the groups which compared the last 8 time points (n numbers; WT SH= 11 slices, 5 mice; WT EE= 9 slices, 6 mice; KD SH=4 slices, 4 mice; KD EE=8 slices, 5 mice)*

5.2.3.4 Theta burst-induced LTP in WT and MSK1 KD CA1 region of the hippocampus after 2 weeks of EE.

Another protocol used to induce LTP is theta burst stimulation (TBS-LTP) which involved 4 pulses at 100 Hz repeated 10 times with a 200 ms interval. This burst was repeated three times with a 20 second interval between bursts. This form of LTP-induction is thought to be more physiological because these rhythmic bursts of activity mimic naturally-occurring theta rhythms recorded in the hippocampus during exploratory behaviour (Lynch, 2004). It also appears that the type of LTP stimulus used i.e. tetanus or theta burst, may induce different intracellular signalling cascades and therefore was worth studying both when characterising the role of a kinase in a mutant mouse (Minichiello et al., 2002). The magnitude of LTP is also affected by factors such as frequency, number of pulses, and stimulus intensity so it was necessary to use both the tetanus-induced and theta burst-induced LTP protocols as both differ in these factors (Hernandez et al., 2005). The questions to be answered are, after EE will the WT mice have enhanced TBS-LTP when compared to the SH condition? And will this pattern differ in the MSK1 KD EE mice?

Using TBS-LTP protocol in the experimental set up shown in Figure 2.2, LTP was successfully induced in all four groups, WT SH, WT EE, MSK1 KD SH and MSK1 KD EE using a paired t test to confirm the statistical significance (Figure

5.10 A-D and E). When the LTP traces were compared between groups, e.g. WT SH and WT EE there were no significant differences (Figure 5.10 A and E, unpaired t test). This meant that under our experimental conditions EE did not enhance TBS-LTP in the CA1 Schaffer collateral/commissural pathway. The same result was shown in the MSK1 KD EE mice as they did not show any difference in TBS-LTP expression when compared to SH (Figure 5.10 B; D shows unpaired t test results). WT and the MSK1 KD mice showed no difference in their SH or EE conditions when they were compared to each other which is represented in Figure 5.10 C and D respectively (E for statistical test).

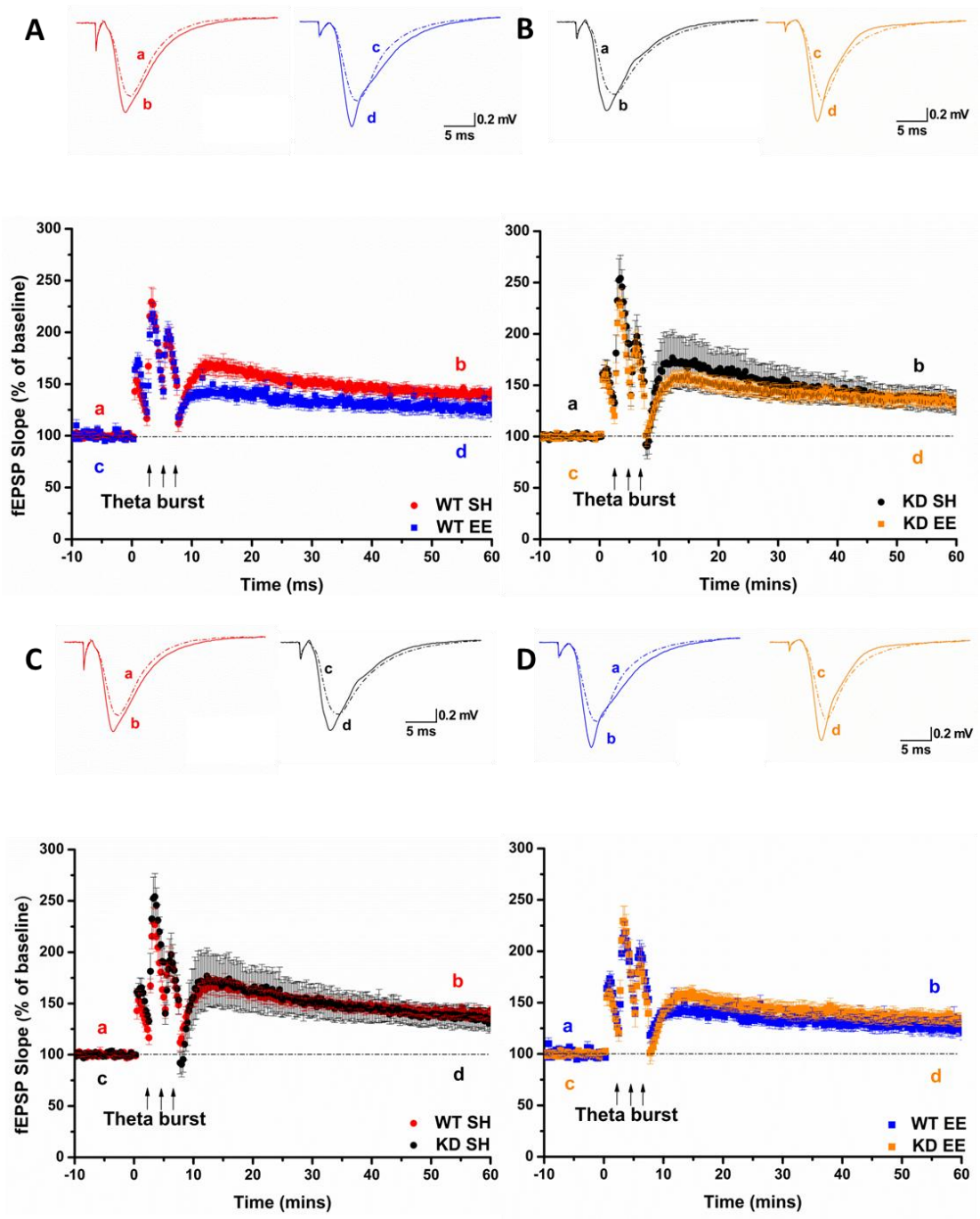

E

TBS-LTP	WT SH	WT EE	KD SH	KD EE
WT SH	***			
WT EE	ns	***		
KD SH	ns		**	
KD EE		ns	ns	***

Key
Was LTP induced in each condition? Using a paired t test (**p<0.01, ***p<0.001)
Were the LTP traces different across the four groups? Using an unpaired t test [ns= not significant]

Figure 5.10; There were no changes in theta burst-induced LTP in CA1 region of the hippocampus after EE in either WT or MSK1 KD. *Parasagittal hippocampal slices (400 µm) were prepared from 6 week old male mice that had been exposed to SH or EE conditions for 2 weeks. Extracellular fEPSP were recorded from the stratum radiatum in area CA1 where the linear part of the fEPSP slope was measured. Theta burst stimulation (TBS) involved a stimulation of 4 pulses at 100 Hz repeated 10 times with a 200 ms interval. This burst was repeated three times with a 20 second interval between bursts (represented by the arrows). The stimulation was applied after 10 minutes of stable baseline was collected at 0.067 Hz. The recordings continued for at least an hour after the induction of LTP. Each graph represents the average fEPSP slope normalised to the baseline ± SEM for WT SH versus WT EE* ***(A)****, KD SH and KD EE* ***(B),*** *WT SH and KD SH* ***(C)*** *and WT EE and KD EE* ***(D)****. A representative fEPSP is shown above each of the graphs with a letter (a-d) which is indicative of the time at which the fEPSP was recorded shown on the graph. The fEPSP represented as a dotted line represents (a) and (c) pre-tetanus induction as oppose to (b) and (d) which are after LTP induction.* ***(E)*** *The statistical tests used to identify if LTP was successfully induced which compared 8 time points before LTP induction and the last 8 time points. The other test was to see if there were any differences in the traces between the groups which compared the last 8 time points s (n numbers; WT SH= 12 slices, 4 mice; WT EE= 13 slices, 4 mice; KD SH=6 slice, 4 mice; KD EE=10 slices, 4 mice).*

5.2.4 The spine density and morphology in WT and MSK1 KD CA1 region of the hippocampus after 2 weeks of EE using Golgi-Cox staining system.

The Golgi staining system has been used extensively to visualise neurones in the brain. The exact staining mechanism is still largely unknown but it is achieved by impregnating fixed brain tissue with potassium dichromate and silver nitrate. The neurones stained in black are reflected by microcrystallisation of silver chromate. Thus using this technique hippocampal brain slices from WT EE, WT SH, MSK1 KD SH and MSK1 KD EE were stained and visualised via light microscopy (See Section 2.7.1 for further details). Representative primary dendrites from the CA1 region of the hippocampus are shown in Figure 5.11 A. The number of spines per 50 µm length of dendrite was analysed and showed no differences after 2 weeks of EE in neither the WT nor the MSK1 KD neurones (Figure 5.11 B, multiple unpaired t tests using Holm Sidak as post hoc). However there does appear to be a trend of increasing spine number in WT EE but this was not significant. The spine density for WT SH was 35.7 spines per 50 µm ±1.3 (SEM) i.e. 0.7 spines per µm. This number

is comparable with other studies such as Karelina et al., 2012 who observed ~0.8 spines per µm in the CA1 region but their EE WT mice had an increased spine density. However their EE protocol differed in that the mice were environmentally enriched for 40 days rather than the 2 weeks in our study.

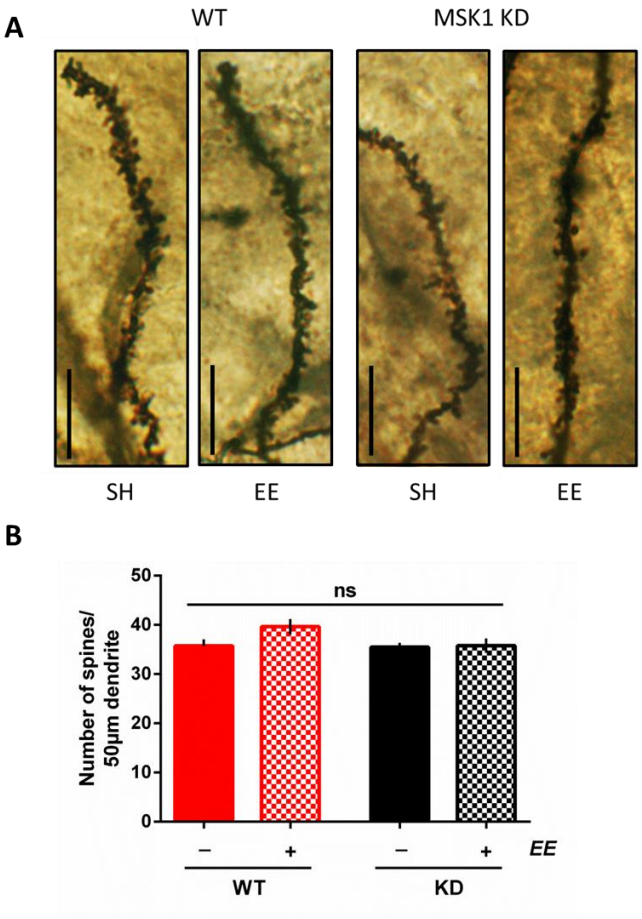

Figure 5.11; Spine density was unchanged in CA1 region of the hippocampus after EE in both WT and MSK1 KD. *Both WT and MSK1 KD mice from the age of P28 were either exposed to EE conditions for 2 weeks or remained in their SH cages. After the 2 weeks the mice were culled and their brains were removed and processed using the FD Rapid GolgiStain Kit to stain neurones. Parasagittal hippocampal slices (400 µm) were prepared from the processed brains and image under the 100x oil lens using a light microscope and analysed manually using Image J.* ***(A)*** *Representative primary dendrites from pyramidal cells in CA1 region from SH and EE conditions in WT and KD neurones. Scale bar, 10 µm.* ***(B)*** *A graph representing the average spine density per 50 µm of dendrite ±SEM. Multiple unpaired t tests using Holm-Sidak post hoc test where ns means not significant (p>0.05). [n=3 mice for both WT and KD in SH and EE, 143 neurones and 6321 spines analysed] Analysis was carried out by an undergraduate student, Stephanie von Kutsleben.*

5.3 Discussion

5.3.1 The role of Arc mRNA in EE

The results in this Chapter indicate that the protocol we used to induce acute and chronic EE did not show any changes in regulating Arc mRNA expression, protein, electrophysiological properties or dendritic spine density. The acute EE experiments included environmentally enriching WT and MSK1 KD mice for 1, 3 and 6 hours before being culled to extract RNA and protein. These three individual time points for EE were used as a pilot study and therefore only a small sample number of mice were used. This study was carried out to confirm that under our EE protocol we were able to see an upregulation of Arc mRNA in response to EE, as well as characterising the response of EE in the MSK1 KD mutants. We were unable to see clear changes in Arc mRNA levels at each individual time point in both WT and MSK1 KD mice. In order to reduce the variability within each time point as well as to increase the n numbers per condition for statistical tests of significance, the 3 time points were pooled together. These results showed that during acute EE of between 1 and 6 hours, Arc mRNA was significantly upregulated in WT mice within the hippocampus and cortex. The induction of Arc mRNA after acute environmental enrichment has been observed by other labs using *in situ* hybridisation technique (Guzowski et al., 1999; Chotiner et al., 2010). Nevertheless this increase in Arc mRNA after EE was not MSK1-dependent as the MSK1 KD mice also showed increase mRNA levels in both hippocampus and cortex. This could be due to the fact there are many known signalling pathways to induced Arc mRNA transcription (See Figure 1.12) which are MSK1-independent (Figure 1.11) (Bramham et al., 2010). MSK1 is activated by ERK1/2 and subsequently phosphorylates its downstream effectors such as histone H3 and CREB in order to activate Arc gene transcription (Chwang et al., 2007). However, ERK1/2 can activate gene transcription directly by translocating into the nucleus and regulating the serum response element (SRE) on the gene promoter (Pintchovski et al., 2009). There are other BDNF-induced TrkB signalling pathways which are independent of MSK1 these include calcium-dependent pathways such as those involving CaMKs which can regulate gene transcription via the transcription factor CREB (Figure 1.9). However Dr. Simon Arthur used CREB Ser133Ala knock-in mice which showed that the phosphorylation of CREB downstream of BDNF is not rate limiting for Arc transcription (unpublished).

5.3.2 The role of Arc protein in EE

When looking at Arc protein induction there was no clear EE-dependent induction after 1 hour of EE in neither genotypes across both areas of the brain. When the 3 and 6 hour time points were pooled together there was an increase in Arc protein within the hippocampus for both WT and MSK1 KD mice ($p<0.05$). This effect was conserved when all three time points were pooled together. Thus the upregulation of Arc mRNA correlated with an increase in Arc protein in the hippocampus and remained unaffected in the MSK1 KD mice. However there may be an MSK1-dependent mechanism present in the cortex as the MSK1 KD mice did not show an increase in EE-dependent Arc protein induction whilst the WT mice did. This was observed in both graphs representing the 3 time points together as well as separating the 3 and 6 hours in another graph. Interestingly the MSK1 KD mice had elevated levels of Arc protein in SH conditions compared to the WT SH mice within the cortex. This increased basal expression could have delayed a further significant increase after EE. Interestingly this elevated basal cortical Arc expression in MSK1 KD mice was not observed in the mice culled after 2 week of SH at P28. This could be due to an age-dependent mechanism as the mice were 2 weeks older than those used in the acute EE experiments.

There could be a limited time frame to detect and measure Arc protein induction which may be why no obvious changes were seen after 2 weeks of EE. The time difference between 6 hours and 2 weeks of EE is large and therefore the dynamics of Arc protein expression could have changed in that period of time. There is no literature which has monitored the expression of Arc protein in relation to EE as oppose to the literature available on Arc mRNA induction patterns. It appears from the results in this Chapter that Arc protein induction occurs at least between 3 and 6 hours of EE but after 2 weeks of EE there appears to be no need for Arc protein induction in either WT or MSK1 KD hippocampus or cortex. Notably the samples collected after 2 weeks of EE were variable in nature.

It is also important to note that in some samples the western blot showed a double band for Arc protein detection. This could be due to a post translational modification such as SUMOylation which has recently been implicated in playing a role in TTX-induced synaptic scaling (Craig et al., 2012).

5.3.3 The variables involved in EE experiments

Across the literature it is well known that the effects observed after EE are highly dependent on the experimental method used (van Praag et al., 2000; Nithianantharajah and Hannan, 2006). There are many factors contributing to EE which can subtly change the effects observed, some of which include (1) social or isolated housing (2) novelty aspect of EE and (3) protocol of EE.

(1) An important factor of EE is the social housing (Rosenzweig et al., 1978). The mice used in our study always had 2-4 mice per condition across both genotypes. However if the SH mice are also socially housed rather than being isolated this may reduce the EE effect. Housing mice in isolation for a long period of time requires a Project Licenses from the Home Office and therefore was not used in our lab. Other labs have successfully seen increased spine density after EE of mice when compared to isolated mice in SH conditions (Silva-Gomez et al., 2003). (2) The novelty aspect of EE comes from the new and complex environment in which the mice can be exposed to. However if that mouse remains in this environment for a length of time the novelty aspect will wear off unless toys are replaced every day (Nithianantharajah and Hannan, 2006). This method has been used in some labs. (3) The protocol of EE can vary enormously for example some labs keep the mice in SH but are exposed to EE for a given period of time daily (Pinaud et al., 2001b). Others chronically enrich the mice such as the experiments used in this Chapter as well as others (Duffy et al., 2001; Artola et al., 2006). Published data from our lab Correa et al., 2012 used another method where mice were born in the EE cage and kept there for 6 weeks before being culled. The spine density was increased in WT EE when compared to WT SH but this increase was somewhat blunted in the MSK1 KD neurones (See Appendix 1). Due to this technical difference as well as the method of labelling the spines, the spine density observed in this Chapter did not change significantly. In order to see changes in the turnover of spine numbers a longer EE time frame may have been required.

5.3.4 The electrophysiological properties after EE compared in WT and MSK1 KD mice

5.3.4.1 The properties of tetanus and theta burst induced LTP after EE between WT and MSK1 KD mice

Considerable interest in LTP has been generated due to its characteristics suggesting a possible link to learning and memory. These characteristics include the rapid, associative and persistent changes seen in LTP (Abraham and Williams, 2008). Not only is it important to study the changes in synaptic plasticity in response to EE but these forms of synaptic plasticity involve different signalling cascades which can regulate gene transcription and protein translation.

In the CA1, LTP is dependent on NMDA receptor activation which causes the postsynaptic membrane to depolarise thus relieving the voltage-dependent magnesium block allowing the influx of calcium ions (Purves et al., 2012). This will in turn activate a range of signalling cascades involved in the expression of LTP. These signalling cascades can involve the activation of protein kinases such as, protein kinase C (PKC) and PKA, CaMKII and MAPK (Sweatt, 1999; Thomas and Huganir, 2004). ERK, a MAPK, was shown to be involved in the signalling pathway required for LTP induction in the hippocampus (English and Sweatt, 1997). This ERK dependence was later shown to be reliant on the LTP-induction protocol used. For example in the CA1 of mouse hippocampal slice tetanus-induced LTP does not require ERK activation but TBS -induced LTP uses an ERK-dependent pathway (Selcher et al., 2003). This was why it was important to use both tetanus and TBS-induced LTP.

BDNF is released upon neuronal stimulation and therefore upon LTP-induction. BDNF will bind to its TrkB receptor and induce a range of signalling cascades (Figure 1.9) (Bramham and Messaoudi, 2005; Minichiello, 2009). There were no changes in WT and MSK1 KD SH LTP-induction for either tetanus or TBS which was consistent with the observation that TrkB-phospholipase C γ (PLC γ) signalling is required rather than TrkB-ERK1/2 pathway (Minichiello et al., 2002). Since MSK1 is dependent on the upstream activation of ERK1/2, one might have expected that the MSK1 KD mice would have had impaired LTP if they depended on LTP-induced TrkB-ERK1/2 signalling cascade.

TBS-induced LTP is the most physiologically relevant form of inducing LTP because of the similar theta rhythm in the brain (Lynch, 2004). There were no changes in the maintenance of LTP i.e. after 60 minutes of potentiation in either the WT or MSK1 KD and neither was TBS-induced LTP affected by chronic EE conditions. Tetanus (T)-induced LTP is the most commonly used in the literature for EE experiments. There were no changes in the maintenance of T-LTP after 60 minutes of potentiation in neither the WT nor MSK1 KD mice and neither was this affected by EE. Therefore each LTP induction protocol appeared to have similar effects in WT and MSK1 KD mice whether they were EE or kept in SH conditions. The aspect of the effect of EE on LTP expression has also been controversial in the literature and consequently it is not unusual that LTP was not enhanced or diminished after EE in WT animals (Table 1.1) (Eckert and Abraham, 2013).

5.3.4.2 Other electrophysiological properties after EE between WT and MSK1 KD mice

However in the literature there appears to be region-specific changes in synaptic plasticity in the hippocampus after EE using T-induced LTP. In the dentate gyrus there was a decrease in T-induced LTP after EE which was associated with an increase in basal synaptic transmission but not changes in PP ratio (Foster et al., 1996). But in the CA1 region an enhancement of T-induced LTP was observed after 8 weeks of EE but not after 2 weeks of EE without changes in neither basal synaptic transmission or PP ratio (Duffy et al., 2001). In our study there were no changes in basal synaptic transmission after EE in WT or MSK1 KD. Neither were there changes in basal synaptic transmission under SH conditions between the two genotypes. It is important to remember that the downstream targets of MSK1 are CREB as well as histone-H3 which are both phosphorylated directly by MSK1 to control gene expression. However CREB is also activated and phosphorylated by other protein kinases such as PKA and CaMK including CaMKIV (Figure 1.9) (Shaywitz and Greenberg, 1999). Histone H3 is also activated by other kinases which could also be compensating for the loss of MSK1 activity in the MSK1 KD mutant but most of these kinases have not been studied in neuronal cells (Bode and Dong, 2005). The Ikappa B kinase α (IKKα) has been shown to directly phosphorylate histone H3 *in vitro* using mouse embryo fibroblast cells (MEF) in response to tumor necrosis factor alpha (TNF-α) (Yamamoto et al., 2003). TNF-α has been shown to be released from astrocytes (Stellwagen and Malenka, 2006) and therefore could

contribute to histone H3 modifications. Another kinase known to phosphorylate histone H3 in NIH 3T3 fibroblasts is RSK2 (Sassone Corsi et al., 1999). In saying this, RSK2 should not be compensating as the basal protein levels were measured in the MSK1 KD compared to the WT and no significant changes were observed (Figure 3.3).

There was a trend in which the fibre volley (FV) amplitude of the fEPSP in the WT EE showed a left-ward shift in the curve representing stimulus intensity versus FV amplitude when compared to the WT SH. This slight increase, but not significant, indicates that more presynaptic fibres were recruited at the higher stimulus intensities. The effect of EE could have activated more presynaptic axons which could be contributing to the increased FV amplitude. The other possibility is the BDNF has been shown to induce axon arborisation and remodelling *in vivo* in dissociated retinal cells from *Xenopus laevis* (Cohen-Cory and Fraser, 1995). As BDNF levels have been shown to increase in response to EE (Ickes et al., 2000) then this arborisation could lead to enhanced axonal excitability thus leading to an increase in FV amplitude. The linear regression graphs demonstrate the relationship between fEPSP slope and FV amplitude without taking into account stimulus intensity showing that the relationship does not change depending on whether the mouse was EE or its genotype. The lack of changes in basal synaptic transmission after EE has been published before and therefore is not an unusual phenomenon (Table 1.1).

In our study there were no changes in PP facilitation in either genotypes when exposed to 2 weeks of chronic EE. This again is a controversial subject as there has been many studies in the literature which have looked at PP ratio after EE in mice and rats at different ages as well as using different EE protocols in different areas of the hippocampus (Eckert and Abraham, 2013). A study by (Eckert and Abraham, 2010) showed that after chronic EE of rats there were no changes in PP facilitation in either CA1 or the dentate gyrus.

In conclusion MSK1 has been shown to play a potential role in regulating cortex specific Arc protein induction after 3-6 hours. However Arc mRNA induction between 1-6 hours of EE in the cortex was equally upregulated in both WT and MSK1 KD mice. EE-dependent increase in Arc protein was observed in the hippocampus after 3-6 hours of EE in both WT and MSK1 KD but no significant

changes were seen in Arc mRNA regulation. Interestingly after 2 weeks of EE in adult male mice the levels of Arc protein remained unchanged in the hippocampus and cortex after EE for both genotypes. This then correlated with the electrophysiological properties and dendritic spine density measured in WT and MSK1 KD mice under SH and EE conditions which remained unaffected by EE as well as MSK1-independent.

All in all as the results in this Chapter have been principally negative, it is fair to say that the EE protocol plays a crucial role in determining the functional output. Especially when the results in Arc protein induction in this Chapter is compared to those in the literature (Guzowski et al., 1999; Pinaud et al., 2001b; Chotiner et al., 2010). As discussed in Section 5.3.3. there are many variables involved in EE as it is a phenomenon of a combination of complex inanimate and social stimulation (Rosenzweig et al., 1978) . If we were to repeat these experiments another control would be of great value. This control would be an 'unhandled control' where a group of mice were left unhandled during the time of the EE experiment (Pinaud et al., 2001b). Using this control may have shown a larger increase in Arc mRNA and protein changes after EE as the basal levels of Arc would have been lower in the unhandled mice as they would have not been exposed to the stress of handling. However the handled SH control is also important to eliminate the element of stress when comparing to EE conditions. The other aspect shown in this paper which we could have chosen was daily EE exposure rather than the chronic EE exposure. The effects of EE could have been more pronounced as chronic exposure may have been exacerbated earlier in the 2 week time frame and therefore returned back to basal levels when the mice were culled for the experiments. Following the results from these EE experiments fellow colleagues decided to take another approach and try another EE protocol where the mice were born and maintained in EE conditions for up to 6 weeks before performing electrophysiological recordings (mEPSC) and spine density measurements (See Appendix 1). These showed positive EE results as well as a functional role for MSK1.

Chapter 6.

The novel interaction between Arc and adaptor-protein 2 (AP-2)

6.1 Introduction

Activity-regulated cytoskeleton-associated protein, Arc is an IEG which is transcribed upon neuronal activity such as seizures, learning experiences, following HFS or BDNF induced LTP as well as mGluR-LTD (Bramham et al., 2010). Upon neuronal activity Arc mRNA is transcribed in response to a signalling cascade of protein kinases and transcription factors. These transcription factors will bind to the *Arc* gene at regulatory elements such as synaptic activity-responsive element (SARE) allowing the transcription of the Arc mRNA (Figure 1.12). The mRNA strand is transported out of the nucleus along the dendrites where it is localised at the active dendritic spine for translation (Bramham et al., 2010). Arc protein has been shown to interact directly with dynamin 2 and endophilin 3 which are part of the endocytotic machinery (Chowdhury et al., 2006). The role of Arc in endocytosis of AMPAR has been shown in different forms of synaptic plasticity such as mGluR-LTD, LTP and homeostatic scaling (Plath et al., 2006; Shepherd et al., 2006; Waung et al., 2008).

mGluR-LTD can be induced pharmacologically in the hippocampus by adding a specific Group I mGluR agonist known as DHPG (Palmer et al., 1997). It was shown that dendritic Arc mRNA was very rapidly (~3 -5 min) translated into protein after DHPG exposure and was responsible for the internalisation of GluA1/2 AMPAR via the endocytosis machinery (Waung et al., 2008).

The role of Arc in AMPAR endocytosis has been shown to play an important role in homeostatic scaling. This was demonstrated when Arc KO hippocampal neurones were incubated with either bicuculline (10 µM) or TTX (1 µM) for 48 hours and they were unable to scale their surface GluA1 AMPAR expression (Shepherd et al., 2006). In our lab we have shown that MSK1 KD mice showed

impaired TTX-induced scaling of mEPSC amplitude as well as surface GluA1 expression which was shown to be due to the inability of MSK1 KD neurones to down regulate total Arc protein (Correa et al., 2012).

Whilst Arc has been shown to be important in AMPAR endocytosis it has also been shown to regulate spine morphology. In cultured Arc KO hippocampal neurones an increase in the number of larger, mushroom shaped spines was observed (Peebles et al., 2010) which was consistent with the data shown in Chapter 4 where MSK1 KD hippocampal neurones harboured more voluminous spines than WT neurones. Morphological changes in dendritic spines have been associated with different forms of synaptic plasticity such as LTP and LTD (Tada and Sheng, 2006). During LTP dendritic spines enlarge in shape whilst harbouring increased levels of surface AMPAR. The opposite occurs during LTD where spines shrink according to the smaller surface AMPAR pool. These changes have been associated with changes in actin polymerisation and cytoskeleton (Hanley, 2008). Interestingly when Arc was first discovered in 1995 it was shown to co-precipitate with F actin through an indirect interaction (Lyford et al., 1995). However, the link between the actin cytoskeleton and Arc in trafficking of AMPAR remains unknown.

The aim of this Chapter is to look for new interacting partners of Arc potentially involved in endocytosis. Interestingly we found a member of the adaptor protein family as a potential hit. Adaptor proteins (AP) mediate sorting of membrane proteins in the secretory and endocytotic pathways. There are five AP complexes (AP-1 to 5) that have been identified but AP-1 and AP-3 have two isoforms, AP-1A/B and AP-3A/B (Boehm and Bonifacino, 2001; Hirst et al., 2011). AP-2 is ubiquitously expressed in mammals and is involved in the formation of clathrin-coated vesicles (CCV) by recruiting the scaffold proteins and clathrin (Pearse et al., 2000) to internalise transmembrane receptors.

All AP complexes are cytosolic heterotetramers composed of 2 large (~100-140 kDa), 1 medium (50 kDa) and 1 small subunit (20 kDa) each tailored with a unique function to play in the sorting pathway. The large subunit for AP-2 is known as the α subunit which localises the AP-2 complex to the plasma membrane in collaboration with the µ2 subunit. The N terminus of the α2 subunit in the core domain has a binding site for phosphoionsitides (e.g. PIP_2) (Gaidarov et al., 1996) which most likely initiates its recruitment to the membrane (Gaidarov and Keen,

1999). The C terminus appendage domain acts as a scaffoling platform for endocyotic accessory proteins (Ohno, 2006).The second large subunit is β2 is largely responsible for recruiting clathrin through the clathrin specific sequence known as the clathrin box in the hinge region (Brodsky et al., 2001; Owen et al., 2004). The β2 appendage also contains an additional clathrin-binding site which also binds to accessory proteins such as AP-180, epsin and eps15 at the same site (Owen et al., 2000). Clathrin-mediated endocytosis occurs when AP-2 recruits clathrin via the hinge region of β2 subunit (and possibly α subunit too (Prasad and Keen, 1991; Pearse et al., 2000) (Figure 6.1) which forms a 'clathrin coated pit' at the inner cell plasma membrane surface. This pit invaginates/endocytoses and buds off into the cell to form a CCV with the target membrane protein inside (da Costa et al., 2003). The small subunit σ2 has a close sequence similarity with the medium sized μ2 subunit and therefore it is thought to stabilise the complex (Traub, 1997; Boehm and Bonifacino, 2001; Ohno, 2006; Jackson et al., 2010). The σ2 subunit also harbous a commonly observed dileucine sorting signal ([DE]xxxL[LI]) which interacts with the core (Owen et al., 2004; Doray et al., 2007).

The medium subunit is referred to as μ2 plays two important roles; one is binding to the plasma membrane via PIP_2 and the other is recognising the target cargo through a tyrosine based sorting signal at the cytosolic domain (YXXΦ) where Φ is a bulky hydrophobic residue (Bonifacino and Traub, 2003). It appears that the AP-2 complex undergoes a conformational change allowing it to crosslink the endocytotic clathrin scaffold to PIP_2-containing membranes and transmembrane protein cargo. When AP-2 is in a 'locked' conformation the tyrosine based sorting signal at the C terminus (CT) domain of the μ2 subunit as well as the dileucine motif on the σ2 subunit are hidden, by parts of the β2 subunit. Upon a conformational change the CT-μ2 relocates thus unblocking the PIP2 and endocytotic sorting signal motifs and allowing the simultaneuous interaction with PIP_2/cargo-containing membranes (Collins et al., 2002; Jackson et al., 2010).

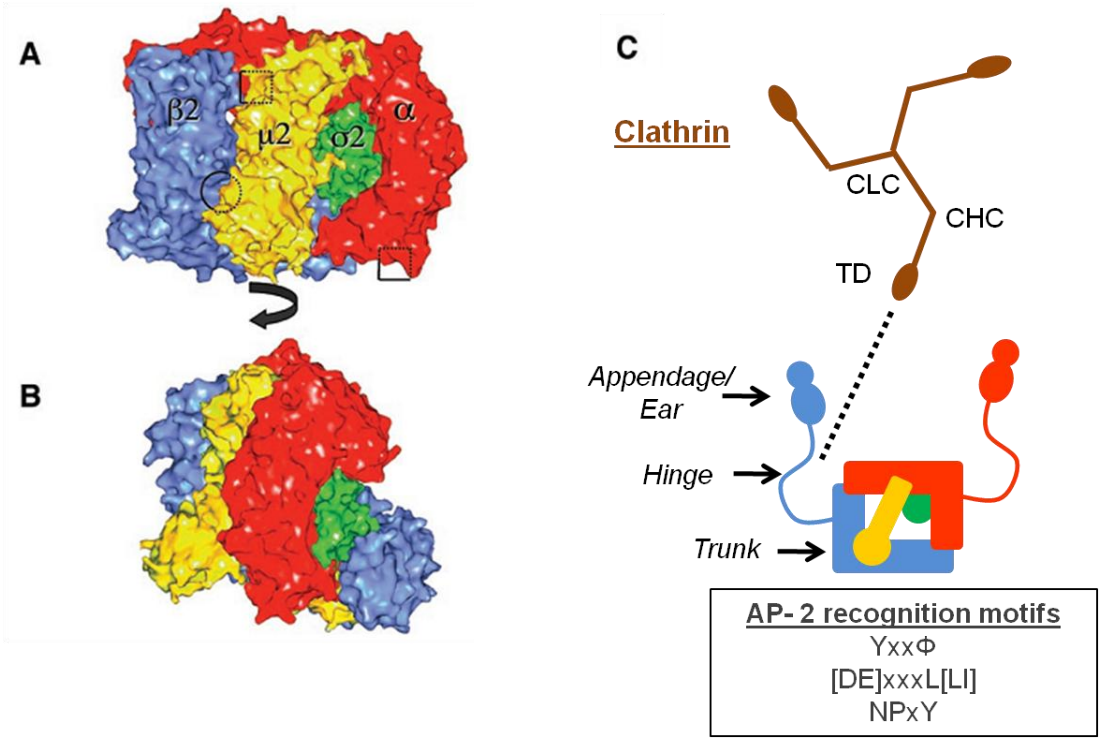

Figure 6.1; The structure of AP-2. ***(A)*** *A surface representation of AP-2 core where the four subunits are represented in different colours; α in red, β2 in blue, σ2 in green and μ2 in yellow. The squares indicate the PIP_2 (or PIP_3) binding sites, one on the μ2 subunit and one on the α. The circle represents the YxxØ-binding site on the μ2 which is partially occluded in the 'locked' conformational form.* ***(B)*** *A rotated view of the structure shown in A.* ***(C)*** *AP-2 is a heterotetramer comprised of a trunk domain made up of the two large subunits α and β2, a medium sized μ2 and a small σ2. There are two hinge domains that connect the core to two appendages/ear domains. The canonical recognition sites for sorting of the cargo are represented in the amino acid (aa) sequences shown below AP-2, YxxΦ, [DE]xxxL[LI] and NPxY. Clathrin binds to AP-2 via its globular terminal domain (TD) (dotted line) which is attached to clathrin-heavy chain (CHC) and then to the clathrin-light chain (CLC). The TD domain binds to the hinge domain of the β2 subunit (and possibly also α). [PIP_2; Phosphatidylinositol-4,5-bisphosphate, PIP_3; Phosphatidylinositol-4,5-triphosphate, CHC; Clathrin-heavy chain, TD; Terminal domain, CLC; Clathrin-light chain] Figure adapted from (Bonifacino and Traub, 2003).*

Interestingly the AP-2μ subunit has been shown to bind to the AMPAR GluA2 subunit via a basic motif found in the C-terminus (Lee et al., 2002; Kastning et al., 2007) as well as the presynaptic synaptotagmin protein (Grass et al., 2004) and the inhibitory postsynaptic $GABA_A$ receptors (Kittler et al., 2005). Further work is needed to clarify Arc's precise role in determining the specificity of AMPAR subunit endocytosis and whether it is dependent on the form of synaptic plasticity induced.

6.2 Results

6.2.1 Identification of interaction between endogenous AP-2 and Arc protein using immunoprecipitation assay combined with mass spectrometry analysis.

The whole hippocampus was extracted from an adult mouse brain, homogenised and assayed for protein concentration. For one immunoprecipitation reaction, 500 µg of protein was incubated with anti-Arc antibody and protein G agarose-fast flow beads and for the other immunoprecipitation reaction the same protein concentration was used with the beads but without the anti-Arc antibody, used as a negative control (See Section 2.8). The immunoprecipitation reaction was incubated for 3 hours at 4ºC before separating the beads with the bound antibody and protein from the unbound supernatant lysate which was discarded. The beads were heated at 95 ºC for 5 minutes in loading buffer to separate the protein from the beads so that the protein could be loaded into a SDS-polyacrylamide gel and run for around 15 minutes using electrophoresis. The lanes containing the separated protein were cut from the gel and sent to Bristol University for mass spectrometry analysis (Table 6.1). The mass spectrometry analysis involved subjecting each gel piece to tryptic digestion and then the resulting peptides were fractionated. The peptides were ionised and then passed through tandem mass spectrometry analysis.

Protein	Accession Number	Peptides	Peptide recovery (%)
Adaptor protein 2- α1	NP_031484.1	19	22.31
Adaptor protein 2- α2	NP_031485.2	10	11.19
Adaptor protein 2- β2	NP_082191.1	12	13.45
Adaptor protein 2- µ2	NP_033809.1	9	20.69
Clathrin- heavy chain	NP_001003908.1	31	20.54
GluA2	NP_001034284.1	2	3.52

Table 6.1; A table showing AP-2 peptides recovered from one Arc immunoprecipitation experiment. *Arc was immunoprecipitated (IP) from whole adult hippocampal lysate using protein-G agarose-fast flow beads and anti-Arc antibody incubated with the lysate. The negative control contained the hippocampal lysate and the beads but no anti-Arc antibody. Here we show some proteins (hits) that bound to Arc but were not present in the negative control. The table includes the four subunits from the adaptor protein-2 (α1, α2, β2 and µ2), clathrin-heavy chain and the AMPAR GluA2 which were found amongst other proteins. The number of peptides and their % recovery are shown in the columns above. The amino acid sequence of the protein can be accessed through the given accession number.*

The AP-2 subunits that form part of the AP-2 complex that were identified as binding partners with Arc protein were the two α adaptin isoforms α1 (also known as αA) and α2 (also known as αC) (Table 6.1). Both the α1 and α2 proteins are encoded by two separate genes but they share 85% amino acid sequence homology (Robinson, 1989). The expression pattern of α2 appears to be more ubiquitous across different tissue. However the expression of α1 protein has been shown to be more neuronal specific. Both these isoforms may be detected in brain lysate when using western blot technique (Ball et al., 1995). The other AP-2 subunits found were β2 and μ2 (Table 6.1). Clathrin is involved in the endocytosis of GluA2 AMPAR subunits (Kastning et al., 2007).

6.2.2 Validation of the interaction between Arc and AP-2 subunits using hippocampal lysate

After analysing the mass spectrometry results it was necessary to validate the interaction between Arc and AP-2 using endogenous mouse hippocampal lysate. Both the α and μ2 subunits were probed against after immunoprecipitating Arc. The same concentration of hippocampal lysate protein (500 μg) was incubated with the protein G agarose-fast flow beads with the anti-Arc antibody for the Arc immunoprecipitation. The negative controls all contained the beads as well as; one immunoprecipitation reaction containing lysis buffer and the Arc primary antibody, another just containing lysis buffer, and the last reaction contained just the protein lysate (500 μg) diluted in lysis buffer. These were run on a SDS-PAGE system and immunoblotted against Arc, α and μ2 (Figure 6.2). Arc protein was successfully co-immunoprecipitated (IP) with both α and μ2 subunits from endogenous hippocampal protein lysate.

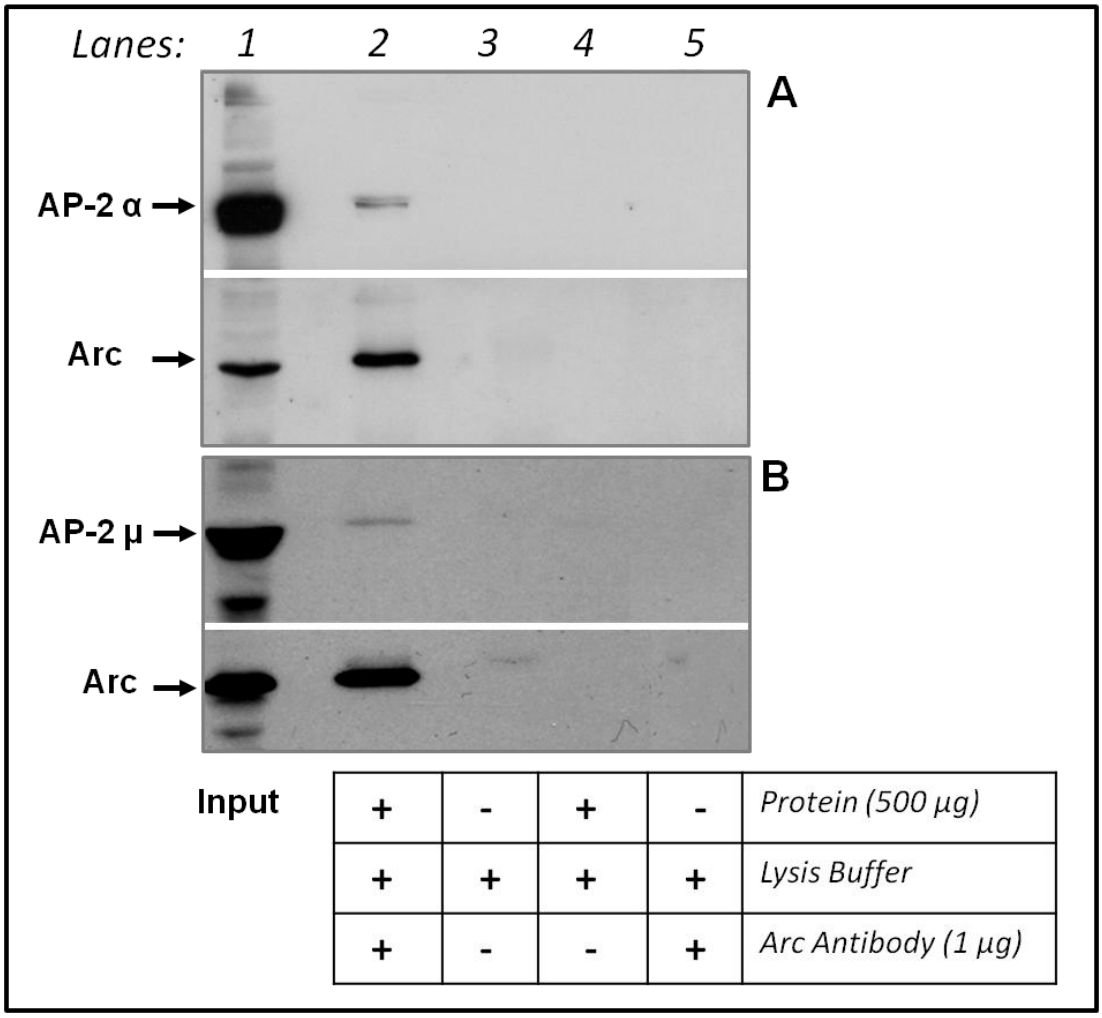

Figure 6.2; Arc co-immunoprecipitates with AP-2 α and μ2 subunit in hippocampal lysate. *Representative blots showing endogenous IP Arc from hippocampal lysate and blots probed for* ***(A)*** *anti-α adaptin 2 (anti-mouse; sc-17771) at 100 kDa which recognises both α1 and α2 isoforms hence the double band and* ***(B)*** *anti-μ adaptin 2 (anti-mouse; BD 611350.) at 50 kDa. Both blots were also probed for anti-Arc (anti-rabbit; Synaptic systems 156-003) found at 50 kDa. The input (lane 1) shows the Arc protein is expressed in the hippocampal lysate (10 μg) used to perform the immunoprecipitations. Lane 2 shows that Arc binds specifically to the beads as well as the interacting partners α and μ2 subunits. The negative controls are shown in the table with lysis buffer (lane 3), protein (lane 4), and Arc antibody (lane 5) which were all shown to be negative (n=4).*

In order to confirm that the co-immunoprecipitation between Arc and AP-2α was specific to the Arc binding site of the IgG antibody rather than the immunoglobulin domains, an IgG negative control was required. As the Arc antibody (Synaptic systems; 156-003) was raised against rabbit an anti-rabbit IgG antibody was required (R&D systems; AB-105-C). The same concentration of antibody (1 μg) was added in the immunoprecipitation tube containing protein-G agarose beads and

protein lysate (500 µg) diluted in lysis buffer (Figure 6.3). The immunoblot was probed against AP-2α and Arc in which we observed that AP-2 co-IP with Arc (lane 2, Figure 6.3) and didn't with the IgG negative control (lane 3, Figure 6.3). The input protein lysate (lane 1) was used as a positive control.

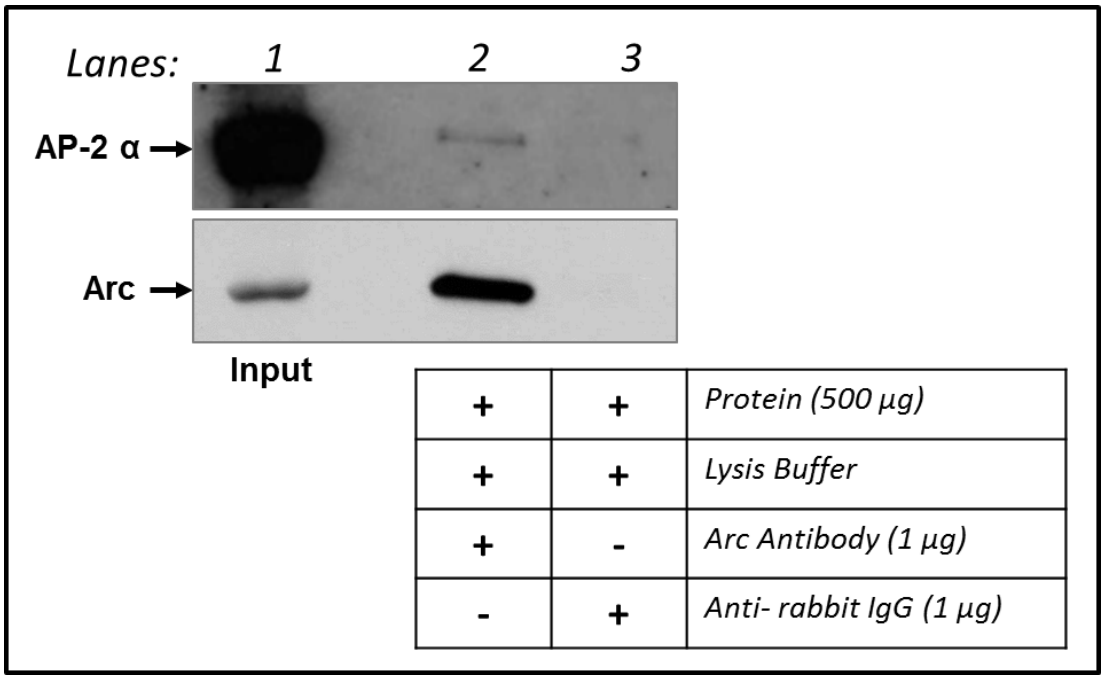

Figure 6.3; Arc co-immunoprecipitates with AP-2 α in hippocampal lysate not with an IgG negative control. *Representative blots showing endogenous IP Arc from hippocampal lysate and blots probed for anti-α adaptin 2 (anti-mouse; sc-17771) at 100 kDa. The blot was also probed for anti-Arc (anti-rabbit; Synaptic systems 156-003) found at 50 kDa. The input (lane 1) is the raw protein lysate (10 µg) that was extracted from the hippocampus used as a positive control. The Arc IP in lane 2 shows a positive band for immunoprecipitation Arc as well as a band for AP-2α. The negative control containing the polyclonal anti-rabbit IgG (R&D systems AB-105-C) instead of the Arc antibody (lane 3) which was shown to be negative.*

6.2.3 The co-immunoprecipitation of endogenous Arc with AP-1, AP-3 and AP-4 from hippocampal lysate

To show if the interaction between Arc and APs was specific to AP-2, endogenous Arc immunoprecipitation experiments were performed against other AP proteins such as AP-1, AP-3 and AP-4 in order to see the specificity of this interaction to adaptor proteins. Interestingly, Arc co-IP with AP-4 ε but not with AP-1 γ or AP-3 δ (Figure 6.4). There are no commercially available antibodies against AP-5 which is why this assay was not performed. AP-3δ basal expression levels appeared to be lower in hippocampal lysate when comapred to AP-1γ. Equal

amounts of protein was loaded (10µg) but the maximum film exposure appeared to show reduced AP-3δ protein levels when comapred to AP-1γ (Figure 6.4).

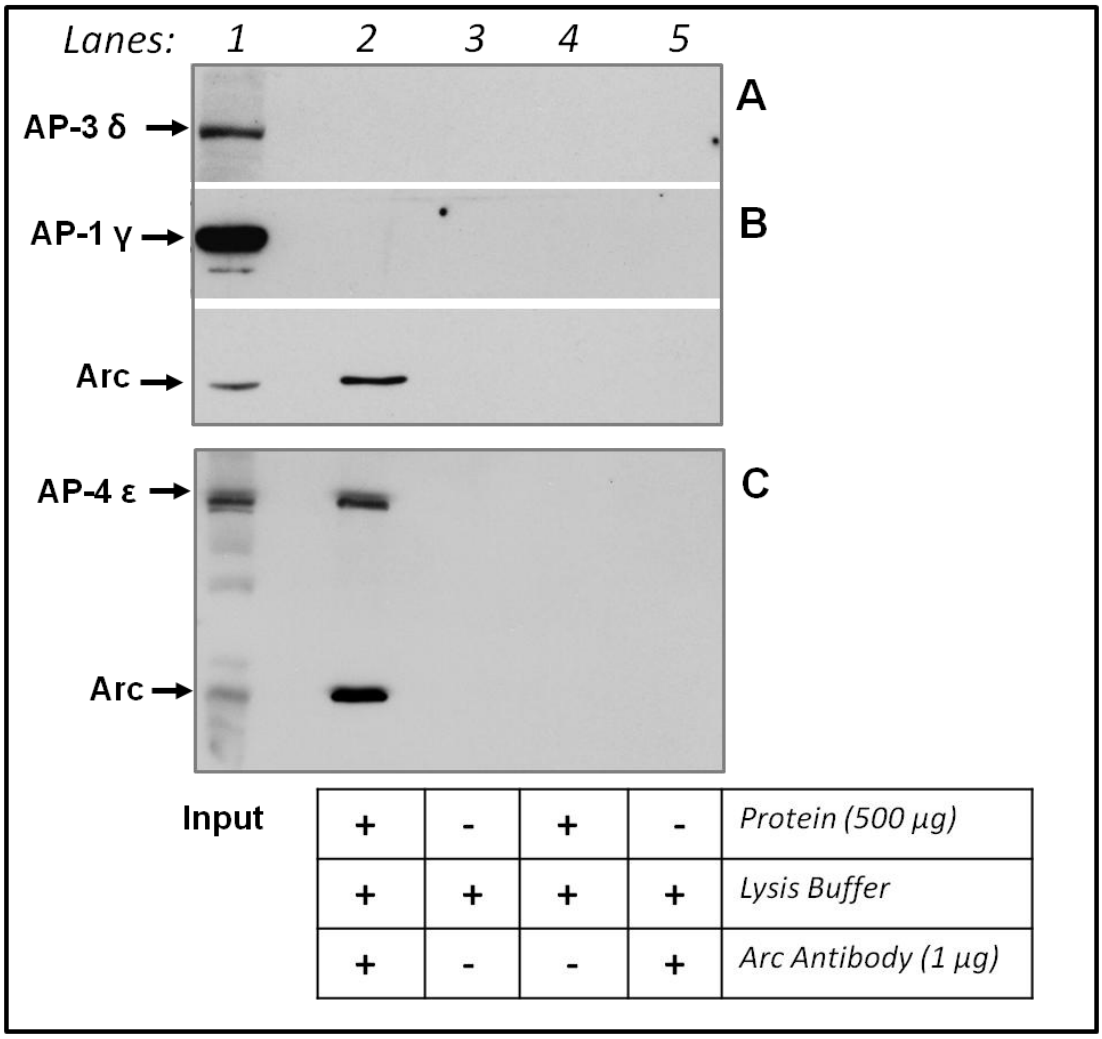

Figure 6.4; Arc co-immunoprecipitates with AP-4 ε but not with AP-1 γ or AP-3 δ in hippocampal lysate. *Representative blots showing endogenous IP Arc from hippocampal lysate and blots probed for* ***(A)*** *anti-δ adaptin 3 (anti-mouse; BD 611328) at 160 kDa and* ***(B)*** *anti-γ adaptin 1 (anti-mouse; BD610386.) at 104 kDa.* ***(C)*** *anti-ε adaptin 4 (anti-mouse; BD 612019) at 127 kDa. All three blots were also probed for anti-Arc (anti-rabbit; Synaptic systems 156-003) found at 50 kDa. The input (lane 1) is the raw protein lysate (10 µg) that was extracted from the hippocampus used as a positive control. The Arc IP in lane 2 shows a positive band for IP Arc as well as a band for AP-4 ε. The negative controls are shown in the table with lysis buffer (lane 3), protein (lane 4), and Arc antibody (lane 5) which were all shown to be negative (n=2 for AP-1 and AP-3, n=5 for AP-4).*

Using the anti-rabbit IgG antibody as a negative control for the Arc immunoprecipitation we showed that the interaction between Arc and AP-4-ε was specific to Arc and not the IgG of the antibody (Figure 6.5). The input lane (lane 1,

Figure 6.5) was positive for the expression of both Arc and AP-4-ε from the hippocampal lysate and Arc co-IP with AP-4-ε shown in lane 2. Lastly the IgG control was negative shown in lane 3 (Figure 6.5).

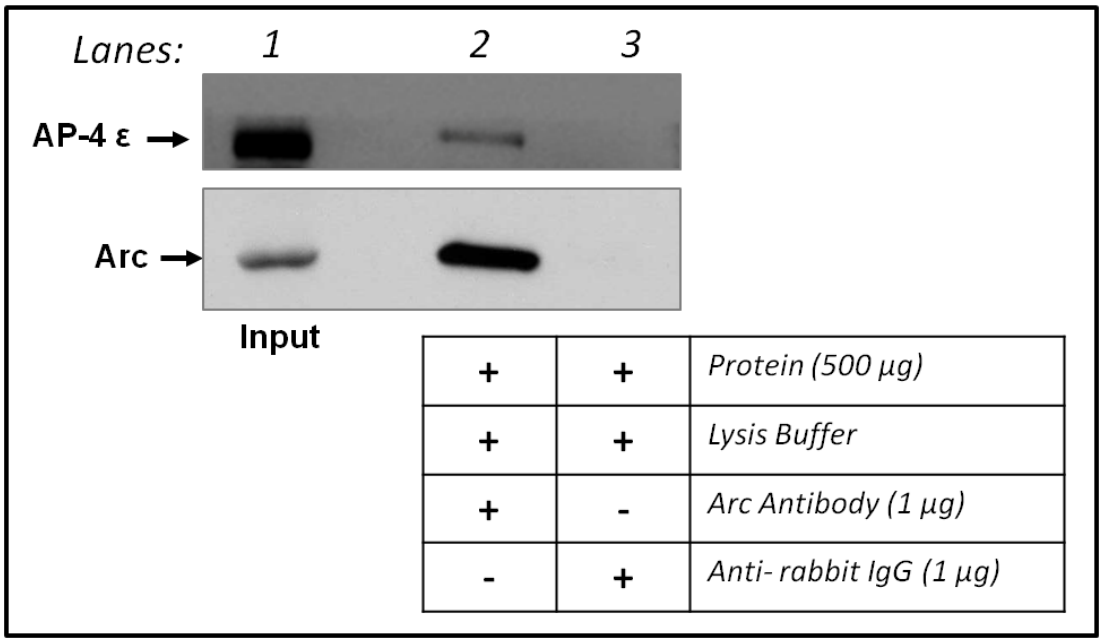

Figure 6.5; Arc co-immunoprecipitates with AP-4 ε in hippocampal lysate but not with IgG antibody used as a negative control. *Representative blots showing endogenous IP Arc from hippocampal lysate and blots probed for anti-ε adaptin 4 (anti-mouse; BD 612019) at 127 kDa. The blot was also probed for anti-Arc (anti-rabbit; Synaptic systems 156-003) found at 50 kDa. The input (lane 1) is the raw protein lysate (10 µg) that was extracted from the hippocampus used as a positive control. The Arc IP in lane 2 shows a positive band for immunoprecipitated Arc as well as a band for AP-4 ε. The negative control containing the polyclonal anti-rabbit IgG (R&D systems AB-105-C) instead of the Arc antibody is shown in lane 3 which was shown to be negative.*

6.2.4 Endogenous expression and co-localisation of Arc and AP-2 in non-stimulated hippocampal neurones using immunocytochemistry

Dissociated WT hippocampal neurones were cultured for 28 DIV before being fixed in 4% PFA under basal conditions. The neurones were permeabilised and incubated with AP-2 α and Arc primary antibodies. Fluorescent secondary antibodies were used to stain AP-2 α with anti-mouse Alexa 488 (green panel in Figure 6.6) and anti-rabbit Alexa 568 was used to localise Arc (red panel in Figure 6.6). Pyramidal hippocampal neurones were imaged using a sequential scan under the confocal

microscope and the images were exported as Tif files as represented in Figure 6.6. The expression pattern of AP-2 α is more punctate as opposed to Arc staining which is more diffuse and concentrated along the dendrites. The 'merge' panel represents the Arc and AP-2 α staining panels merged on top of together. This expression pattern could be due to the experiemtal variables, such as the gain used on the confocal microscope and the selection of primary antibody used, especially when it is compared to other immunocytochemical staining in the literature (See 6.3 Discussion).

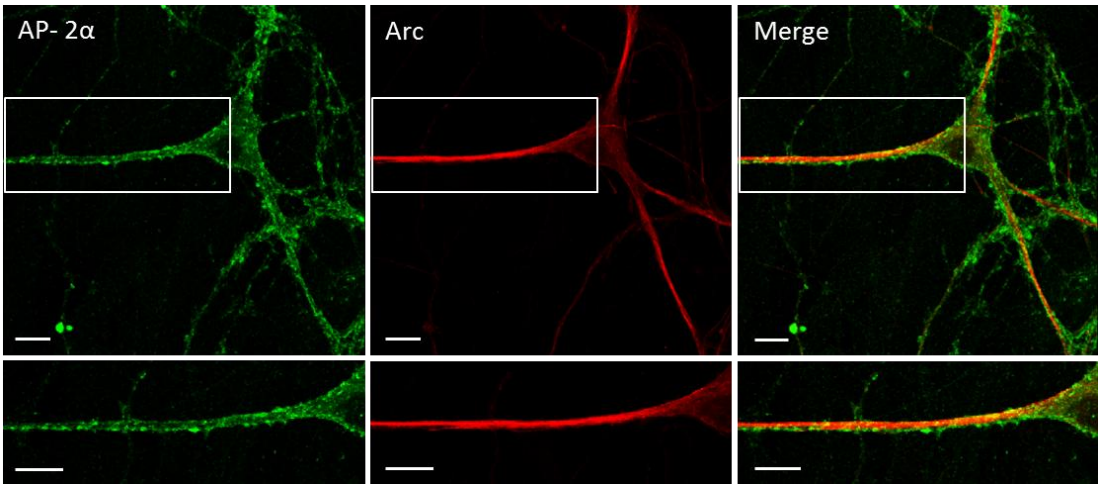

Figure 6.6; Immunocytochemical staining of endogenous AP-2 α and Arc protein in pyramidal hippocampal neurones cultured for 28 DIV. *Hippocampal WT neurones were cultured for 28 DIV and fixed and stained with anti-Arc (Synaptic systems 156-003) and anti-AP-2 α primary antibodies (sc-17771). Alexa Fluor secondary antibodies were used to fluorescently label AP-2α using mouse-488 (green) and Arc using rabbit-568 (red). The merged panel (yellow) represents the AP-2α and Arc staining merged together. Scale bar; 10 µm.*

6.2.5 Using Bimolecular Fluorescence Complementation (BiFC) technique to confirm the Arc and µ2 interaction and localisation in H4 neuroglioma cells

The BiFC technique involves the co-expression of Arc-fused to yellow fluorescence protein 1 (YFP1) including amino acids (aa) 1-158 and µ2-fused to YFP2 fragment including aa 159-239 (constructs generated by Dr. Jürgen Muller, University of Warwick). The interaction between the proteins, Arc and µ2 fused to the fragments will bring the two non-fluorescent fragments of YFP into closer proximity to each other allowing the fragments to associate together to form a functional complex (Kerppola, 2008). The functional readout of this association is the formation of the full length YFP sequence allowing the emission of the yellow

fluorescence when excited at 514 nm (Figure 6.7). This BiFC technique is very useful as you can visualise direct protein interactions with minimal disruption of their normal environment as well as determining subcellular locations of their interaction.

The YFP fragments used are better known as 'Venus' sequences as they are a more stable and improved version of the normal YFP. The normal YFP are relatively pH-sensitive and uniquely quenched by chloride ions (Cl^-). Therefore the 'Venus' sequences have mutations that decrease sensitivity to both pH and Cl^- (Nagai et al., 2002). These sequences will be referred to as V1 for YFP1 and V2 for YFP2.

The two vectors were transfected into and H4 neuroglioma cells using Lipofectamine 2000 and after 15 hours the cells were fixed in 4% PFA and mounted on microscope slides. The co-expression of these two constructs resulted in the subcellular punctea pattern of YFP.

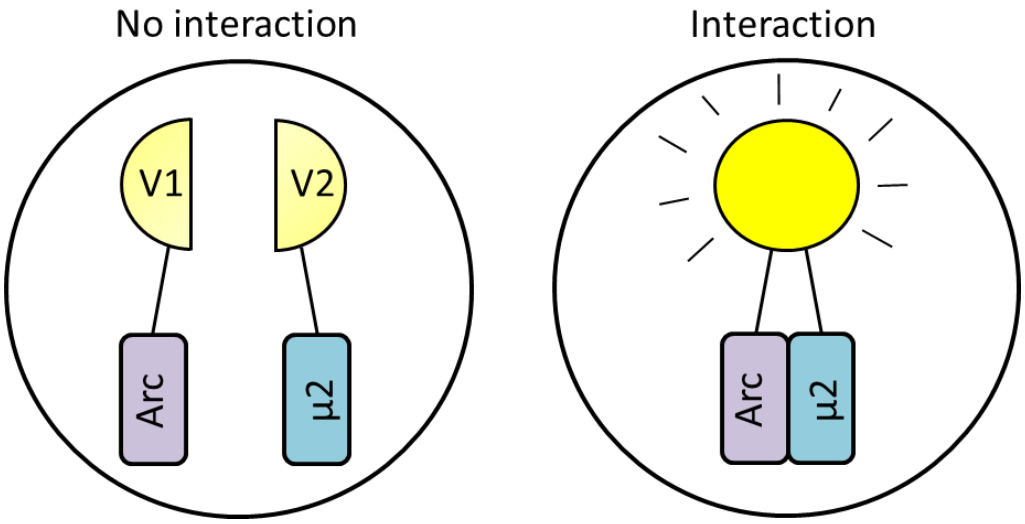

Figure 6.7; A schematic diagram representing the BiFC technique. *Two constructs were used; the first construct is vector known as pcDNA3_Arc_Venus [part 1] (V1). This contains the Arc sequence and half of the Venus sequence (V1) which codes for yellow fluorescent protein (YFP) and the second construct 2 was pcDNA3_µ2_Venus [part 2] (V2) containing the µ2 sequence and the other half of the Venus sequence (V2) which codes for yellow fluorescent protein (YFP). If Arc and AP-2µ interact the fragments will associate where the V1 and V2 will form the full length YFP sequence and fluoresces.*

6.2.5.1 Using BiFC in H4 neuroglioma cells with the negative controls and endogenous clathrin-heavy chain staining

H4 neuroglioma cells were used to test the BiFC technique using the co-expression of Arc-V1 and µ2-V2 vectors (Figure 6.7). The reason why H4 neuroglioma cells were used was because they were the closest cell line to neurones which Dr. Luis da Silva (São Paulo University) had culturing in his lab. However two negative controls were required to prove that it is the interaction between Arc and µ2 protein that was producing the fluorescence rather than the V1 and V2 proteins interacting non-specifically. Therefore two extra constructs were designed, one with only the V2 sequence and no µ2 which was co-expressed with the Arc-V1 vector and one with V1 sequence and no Arc sequence which was co-expressed with the µ2-V2 vector which should not emit fluorescence (Figure 6.8 A). This was successfully shown in H4 neuroglioma cells where the Arc-V1 and µ2-V2 pair emitted fluorescence, seen in green in Figure 6.8 B. The red staining represents endogenous clathrin-heavy chain (CHC) expression which was merged with the YFP transfected panel. The negative controls with Arc-V1 vector co-transfected with a vector only containing the V2 sequence did not fluoresce (Figure 6.8 C). The same occurred when the vector containing V1 sequence without the Arc which was co-transfected with the µ2-V2 vector (Figure 6.8 D). Therefore the Venus sequences required the presence of both the Arc sequence and the µ2 sequence to fluoresce and therefore was specific to the Arc-AP-2 interaction. These cells were immunocytochemically stained against endogenous CHC using an anti-CHC primary antibody and an Alexa fluor 568 for the secondary (Figure 6.8).

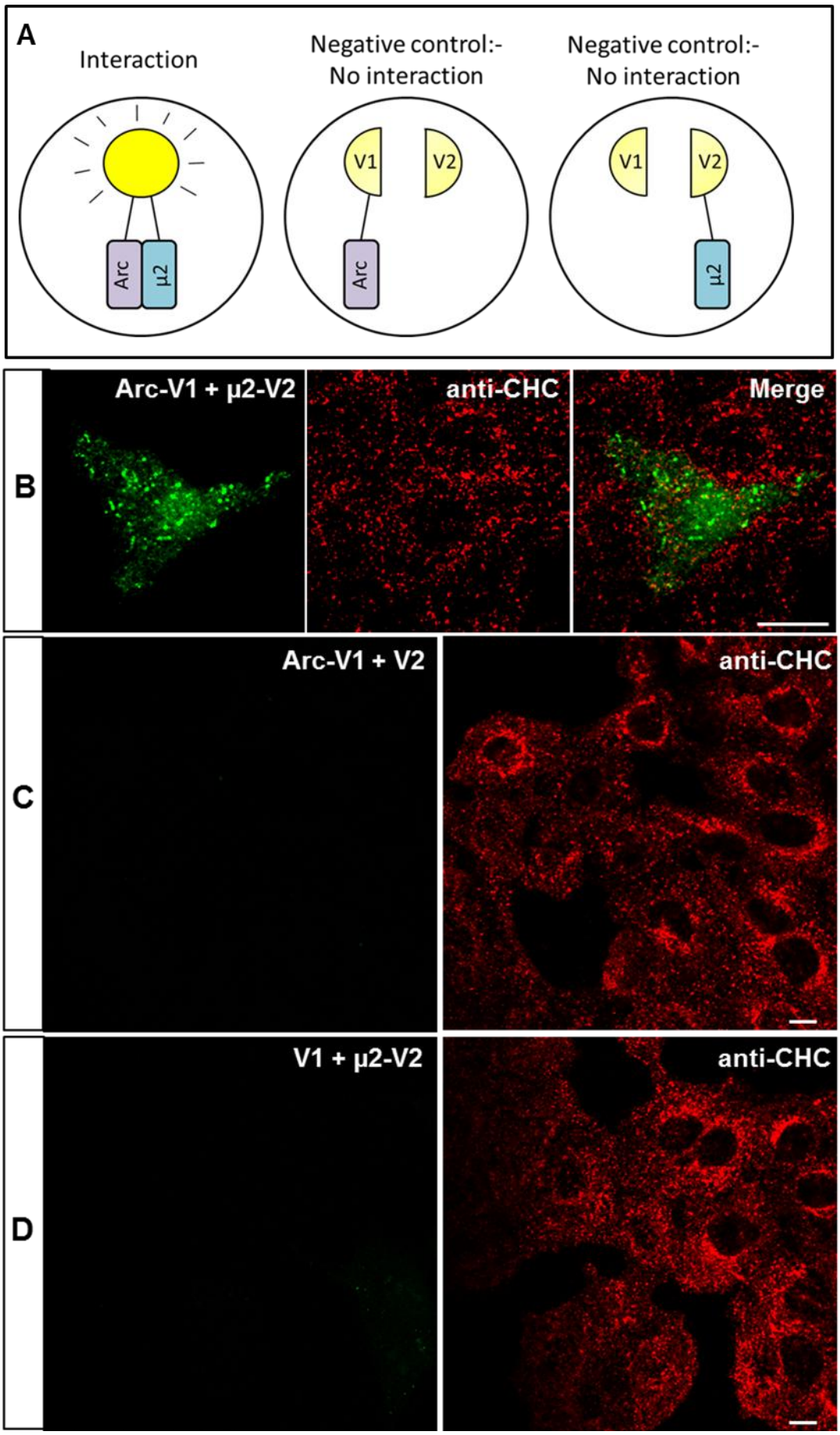
A
Interaction
Negative control:-
No interaction
Negative control:-
No interaction
Arc
μ2
V1
V2
Arc
V1
V2
μ2
B
Arc-V1 + μ2-V2
anti-CHC
Merge
C
Arc-V1 + V2
anti-CHC
D
V1 + μ2-V2
anti-CHC

Figure 6.8; Confirmation of Arc and μ2 interaction using BiFC technique using negative controls as well as endogenous co-staining of clathrin-heavy chain (CHC) in H4 cells (A) *A schematic diagram representing how the BiFC technique works with two negative controls. The Arc-V1 and μ2-V2 association is the positive control with both Arc and μ2 sequences resulting in fluorescence. The first negative control includes the co-expression of Arc-V1 and Venus 2 sequence without the μ2. This should not fluoresce as the fluorescence is only attainable when both Arc and μ2 sequences are present in each co-expressed vector. The second negative control involves the co-expression of the μ2-V2 construct with the construct containing only the Venus 1 sequence without the Arc sequence which should not fluorescence as it is the opposing negative control. H4 Neuroglioma cells were co-transfected with* ***(B)*** *Arc-V1 and μ2-YFP-V2* ***(C)*** *Arc-V1 and V2 and* ***(D)*** *V1 and μ2-V2. The green fluoresence represents the YFP signal as the colour was manually changed for better clarity after the image was taken. These cells were stained with goat anti- CHC antibody (sc-6579) followed by anti-goat-Alexa 594 secondary antibody (Invitrogen) shown in red. The 'merged' panel represents both the YFP and the anti-CHC image. Scale bar; 10 μm*

6.3 Discussion

Here we demonstrate a novel interaction between Arc and the AP-2 complex as Arc pulls down α and the μ2 subunits in hippocampal lysate. This was also alluded to in the proteomic study carried out in hippocampal tissue. The mass spectrometry analysis was a primary indicator that the AP-2 subunits, α1, α2, β2 and μ2 were found to interact with Arc. These binding partners were found in the hippocampal lysate which had IP Arc and was not present in the negative control. The μ2 subunit was of prime interest as this is the subunit which binds to the 'cargo', in this case we hypothesised it was Arc. In terms of the larger subunit the α or β, we chose to validate the Arc interaction with the α1/2 as this binds to the target membrane and therefore could also be playing a role in determining the sorting pathway in which Arc might take part.

From the immunoprecipitation experiments, both AP-2 α and μ2 subunit co-IP with Arc. The μ2 subunit is responsible for binding to the cargo via a conserved recognition sequence. There are two canonical tyrosine based AP binding motifs found on the protein cargo which are either YxxΦ or [DE]xxxL[LI] (Figure 6.1). The motif YxxΦ represents a tyrosine (Y) residue followed by preferably two hydrophilic amino acids (x) and finishes with a bulky hydrophobic amino acid (Φ). This motif, which is found on membrane-bound receptors, is essential for rapid internalisation (Bonifacino and Traub, 2003). Figure 6.9 shows the full sequence of Arc protein and

the possible YxxΦ motif sequence found at position 309-312 (*purple) where the sequence consists of the following amino acids, YQTL. The glutamine (Q) and threonine (T) are both considered to be hydrophilic whilst the final reside is a bulky hydrophobic leucine (L) amino acid which fits with the motif's profile. The second motif [DE]xxxL[LI] where x represents any amino acid works much like the YxxΦ motif as it is the sorting motif for the endocytosis of cargo receptors. The LL or LI pairs are very important for binding as well as the acidic residues found at position -4 or -5 after the first leucine. Figure 6.9 shows a potential [DE]xxxL[LI] site found at position 315-322, DAEEEEII (* purple). Importantly these two canonical sites do not compete with each other and therefore indicates that both motif signals don't bind to the same site on the μ2 subunit (Bonifacino and Traub, 2003). The site found in the Arc sequence where Arc binds with dynamin 2 and endophilin 3 is highlighted in blue in Figure 6.9 (Chowdhury et al., 2006). Dynamin 2 is a large GTPase involved in clathrin-mediated endocytosis and endophilin 3 plays a role in vesicle formation and therefore will regulate Arc-dependent endocytosis of AMPAR following neuronal activity (Chowdhury et al., 2006). Due to the nature of these endocytotic proteins it was shown that their interaction with Arc occurs in endosomes during internalisation (Chowdhury et al., 2006). An important question to ask is where Arc-AP-2 complex interaction occurs? And could the localisation of this interaction depend on whether the neuron is activated? Interestingly when hippocampal neurons were cultured for 28 DIV and stained for endogenous Arc and AP-2α there was no clear co-localisation between the two proteins. The expression pattern of AP-2 α is more punctate as it most likely be localised at the dendritic spines were AMPAR endocytosis primarily takes place. The Arc staining is more diffuse and concentrated along the dendrites. This observation could be due to the fact that the neurones were under basal conditions rather than undergoing synaptic plasticity such as mGluR-LTD or homeostatic scaling.

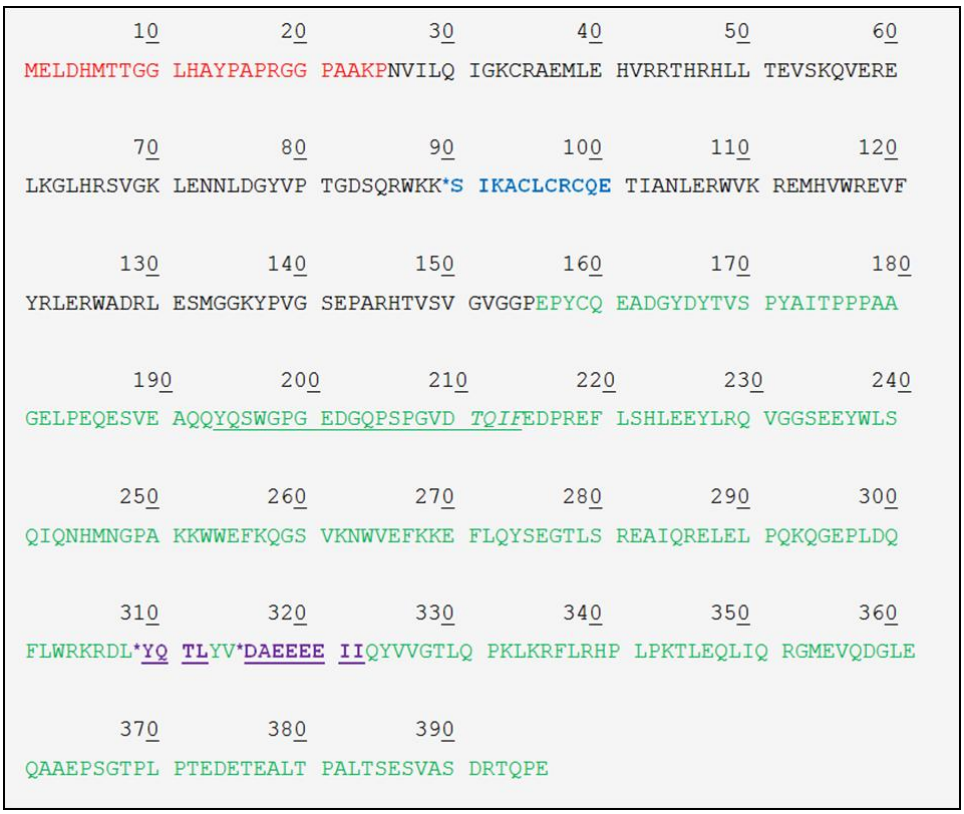

Figure 6.9; The amino acid sequence of Arc (Mus musculus) annotated with potential AP-2 binding sites (Accession number; NM-018790). *The N-terminus consists of 1-25 aa, a coil-coiled domain stretching from 26-154 aa and finally the C-terminus (155-396 aa). The dynamin 2 and endophilin 3 interacting motif is highlighted in *blue (aa 90-100) and the two potential AP-2 binding domains are highlighted in *purple (designed by our collaborator Prof. Luis da Silva)*

The expression of AP-2 in hippocampal neurones using immunocytochemical techniques has been observed by other groups which show a similar punctate pattern of expression (Palmer et al., 2005b). Interestingly the expression pattern of Arc may be influenced by the primary antibody used (Figure 6.6). In the Chowdhury et al., 2006 and Shepherd et al., 2006 papers they used a monoclonal antibody from Santa Cruz. In contrast we used an anti-Arc polyclonal antibody (Synaptic Systems, 156-003) raised against the full length protein, in which the representative images are shown in Figure 6.6 (also see paper (Niere et al., 2012) as they used the same antibody in neurones). The pattern of Arc expression is more diffuse throughout the dendrites. Therefore the recognition sequence used to raise the anitbody may influence its specificity and expression pattern.

When Arc-V1 and µ2-V2 were co-expressed in H4 neuroglioma cells a punctate like pattern of subcellular expression was observed. The H4 neuroglioma cells were immunocytochemically stained to monitor the expression of endogenous

clathrin-heavy chain (CHC). The interaction of Arc and μ2 did not co-localise with the CHC staining. It is known that β2 subunit binds to CHC (Shih et al., 1995) but in these experiments we were over-expressing μ2 subunit and the other subunits of the AP-2 complex may be required to localise the interacting complex to its site of function. AP-2 is thought to be localised in the cytosol until it becomes activated to take part in the sorting pathway (Ohno, 2006). It is recruited to the plasma membrane where it mediates the formation of clathrin coated vesicles (CCV) to internalise plasma membrane proteins (Owen et al., 2004; Ohno, 2006). These CCV are destined to fuse with early endosomes as well as other sorting organelles which could be a potential location for the interaction between Arc and AP-2 depending on the role of this interaction. In the future it would be important to co-localise the BiFC interaction with an organelle marker. As it is known that AP-2 will bind to the CCV to fuse with the early endosomes and therefore early endosome antigen 1 (EEA1) maker could be used.

An important property of Arc's endocytic role is that it is 'activity-dependent' and thus has been characterised in many synaptic plasticity models, such as LTD (Waung et al., 2008). Furthermore, the interaction between AP-2 and GluA2 has also been shown to play an important role under LTD inducing conditions (Lee et al., 2002). Thus it is fair to hypothesis that our novel Arc-AP-2 interaction is most likely to be functional upon neuronal activity, e.g. LTD. A model representing a possible mechanism for this interaction is shown in Figure 6.10. The first objective after validating this novel Arc-AP-2 interaction is to establish if AP-2 is required for endocytosis of AMPAR during synaptic plasticity. In order to answer this question a synaptic plasticity model would be necessary. This model would ideally increase the synthesis of Arc which would induce internalisation of AMPAR. Therefore this could include mGluR-LTD or bicuculline-induced down scaling, where bicuculline is a $GABA_A$ antagonist and consequently will inhibit an inhibitory pathway thus causing neuronal activation and up regulation of Arc synthesis. Both GluA1 and GluA2 subunits would have to be monitored as GluA1 has been shown to be endocytosed by Arc/dynamin 2/endophilin 3 complex (Chowdhury et al., 2006; Shepherd et al., 2006) and GluA2 has been shown to interact with AP-2 (Kastning et al., 2007). If AP-2 is required for the endocytosis of GluA1/2 AMPAR then the next important question is whether the interaction between Arc and AP-2 is required during AMPAR endocytosis. The interacting motif within the Arc sequence would

have to be identified and mutated so that the surface GluA1/2 expression could be monitored in cells expressing the mutant compared to the Arc-WT.

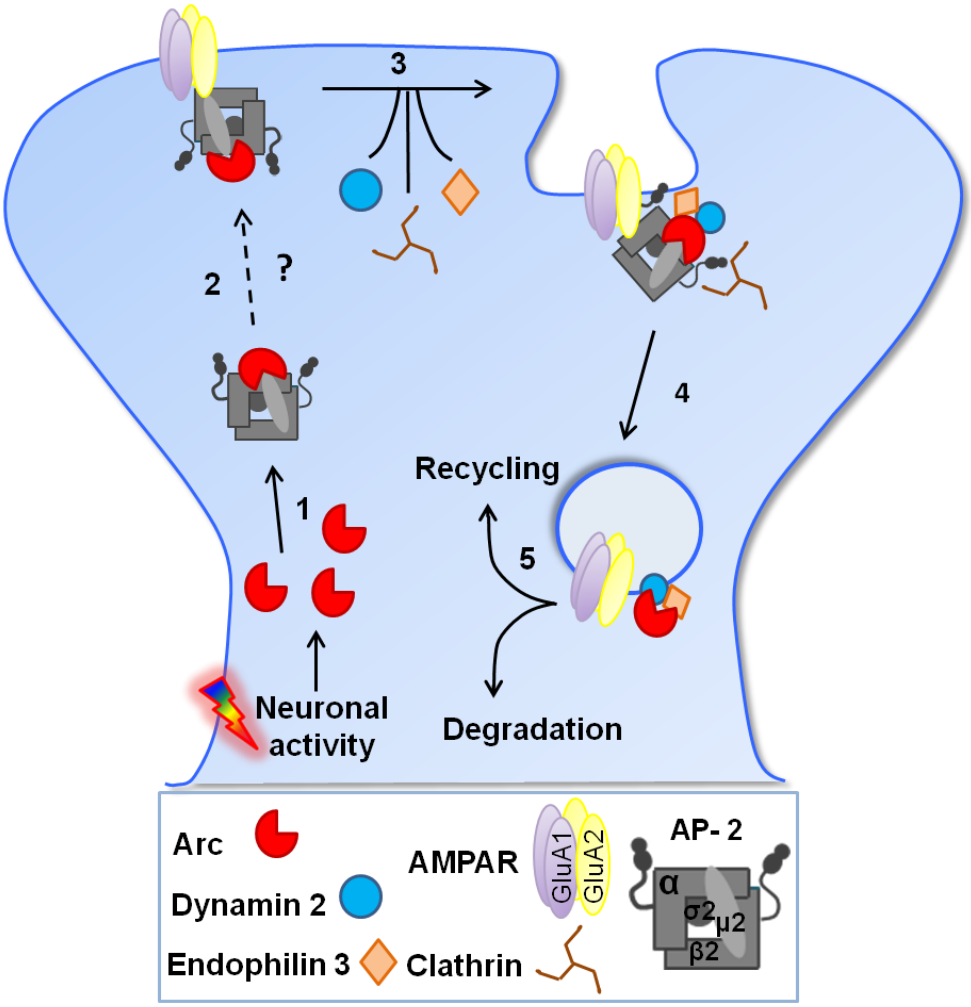

Figure 6.10; Working model of Arc-AP-2 interaction controlling activity dependent AMPAR trafficking ***(1)*** *Upon neuronal activity Arc synthesis is upregulated.* ***(2)*** *Arc binds to the μ2 subunit and possibly overlapping with the α subunit which is recruited to the plasma membrane. The μ2 subunit will bind to the cytoplasmic tail of the GluA2 AMPAR which may be found as a heterodimer with GluA1.* ***(3)*** *The endocytotic machinery are recruited to the complex, including dynamin 2, endophilin 3 and clathrin where they bind to Arc to initiate internalisation of the AMPAR* ***(4)*** *The invagination of the plasma membrane occurs when clathrin polymerises around the vesicle to initiated clathrin-mediated endocytosis of AMPAR.* ***(5)*** *The AP-2 complex dissociates from the endosome and the AMPAR are then either recycled or degraded. [Arc; Activity-regulated cytoskeleton-associated protein, AP-2; Adaptor protein-2, AMPAR; α-amino-3-hydroxy-5-methyl-4-iso-xazolepropionic acid receptor]*

Out of the other adaptor proteins it appeared that AP-4 ε binds to Arc in hippocampal lysate but AP-1 γ and AP-3 δ do not interact. AP-1 γ has been shown to interact with synaptophysin, a protein that participates in fusion pore formation

during neurotransmitter release and therefore serves as a docking site for AP-1 during clathrin-dependent vesicle budding (Horikawa et al., 2002). Therefore AP-1 appears to be more involved in the presynaptic membrane whilst Arc activity occurs in the postsynaptic membrane (Chowdhury et al., 2006). AP-3 is expressed in neuronal tissue and is involved in the biogenesis of a synaptic-like microvesicle from endosomes (Blumstein et al., 2001) and therefore does not necessarily overlap with any of Arc's functions. Interestingly the interaction between Arc and AP-4 could potentially have a significant role to play in the pathology of β-amyloid. Amyloid precursor protein (APP), the precursor of the β-amyloid (Aβ), is a ubiquitously expressed transmembrane protein that undergoes differential proteolytic processing depending on its itinerary through the secretory and endocytotic pathways (Thinakaran and Koo, 2008). AP-4 interacts with APP at the trans-Golgi network and mediates recruitment of APP into specific transport carriers directed to the plasma membrane (Burgos et al., 2010). Depletion of AP-4 or impairment of its interaction with APP promotes 'amyloidogenic' processing enhancing cleavage by γ-secretase. Recently, Arc has been shown to interact with presenilin 1, a component of the γ secretase complex and regulate activity-dependent generation of Aβ peptides (Wu et al., 2011). Here we could hypothesis that the Arc-AP-4 interaction controls activity-dependent amyloidogenic processing of APP by promoting recruitment of APP to γ-secretase enriched membranes and/or vesicles.

To summarise the results of this Chapter, it is clear that a novel interaction between endogenous Arc and AP-2 and AP-4 has been identified in the hippocampus. The μ2 subunit and Arc interaction has been confirmed using BiFC. The localisation of this interaction needs to be identified as well as the function under stimulated conditions. A working model has been designed to potentially address functional importance of this interaction regulating endocytosis of AMPAR in synaptic plasticity.

Chapter 7.

General Discussion

Neurones have a remarkable property in which they are able to modify their synaptic strength according to changes in synaptic activity. This process is known as synaptic plasticity which is the basis of information storage in the brain. There are different forms of synaptic plasticity such as LTP, LTD and homeostatic scaling. Each of these processes will entail their own cellular and molecular mechanisms regulating their functional output.

Long-lasting forms of synaptic plasticity require protein synthesis and gene transcription which are orchestrated by a range of intracellular signalling pathways. Depicting the signalling pathway involved in regulating plasticity-related genes, such as transcription regulators have been of interest to neuroscientists. The nuclear serine/threonine kinase, MSK1 has been shown to regulate gene transcription via phosphorylation of histone H3 as well as CREB in a BDNF-MAPK dependent manner. Using MSK1 KD transgenic mice we were able to depict such signalling pathways in response to different stimuli whilst monitoring the regulation of plasticity-related proteins, such as Arc.

Acute BDNF stimulation of cultured hippocampal neurones showed the well-established increase in downstream ERK1/2 phosphorylation in both WT and MSK1 KD neurones. However MSK1 was not shown to play a prominent role in BDNF-dependent increase in Arc synthesis. Interestingly there was a delayed increase in Arc protein levels after 45 minutes of BDNF stimulation in the MSK1 KD neurones indicating a potential role for MSK1 during the early stages of BDNF-dependent Arc synthesis. The levels of phosphorylated histone H3 was also monitored using western blot technique which showed that histone H3 phosphorylation was unaffected in the presence of BDNF. These observations would support the fact that Arc induction can be regulated by a range of signalling cascades including via NMDA receptors, muscarinic acetylcholine receptors as well as BDNF, which can signal to PKA, ERK1/2 and PKC. In terms of transcriptional regulation, MSK1 would certainly not

be the only upstream regulator as others have been indentified such as CREB, MEF2, ZLF and SRF/Elk1(Bramham et al., 2010).

During synaptic scaling, which is a more chronic form of synaptic plasticity, a MSK1-dependent mechanism was observed (Appendix 1; (Correa et al., 2012)). The hypothesis was that during synaptic deprivation i.e. incubation with TTX there is a correlating reduction in BDNF release (Rutherford et al., 1998). Thus this would downregulate a BDNF-Arc dependent pathway which may or may not require MSK1. Arc interacts with the endocytotic machinery which regulates GluA1 endocytosis (Chowdhury et al., 2006) which was characterised during homeostatic scaling where Arc KO hippocampal neurones were unable to up-scale their surface GluA1 expression and mEPSC amplitude in response to TTX-incubation (Rial Verde et al., 2006; Shepherd et al., 2006). In our lab we demonstrated that MSK1 KD hippocampal neurones were unable to up-scale their mEPSC amplitude or their surface GluA1 AMPAR. TTX-induced scaling causes a downregulation of Arc protein thus reducing the endocytosis of AMPAR. However MSK1 KD neurones have a deficit in scaling Arc protein levels. The role of MSK1 during TTX-induced up-scaling was also shown when WT-MSK1 was transfected back into MSK1 KD neurones which rescued their ability to scale in response to TTX.

As MSK1 showed functional effects in response to synaptic deprivation using TTX incubation for 24 hours it was of interest to see if these synaptic changes were coupled to structural changes. These structural changes would be observed in the dendritic spines which form the postsynaptic component of most excitatory synapses and can vary in density and morphology. The spine density and morphology of the MSK1 KD hippocampal neurones were analysed under basal conditions at either 14 DIV or 21 DIV which was compared to WT neurones. It is known that during development the number of spines will increase and their morphology will evolve from immature long-like filopodia spines to mature mushroom-shaped spines (Papa et al., 1995; Fiala et al., 1998). These characteristics were observed in WT hippocampal neurones but the increase in spine density during development was stunted in the MSK1 KD neurones. The morphology changes at 21 DIV in the MSK1 KD neurones were more exaggerated as the spines were larger mushroom shaped than the WT. It was hypothesised that this increase in spine volume at 21 DIV in the MSK1 KD neurones was due to the elevated GluA1 surface expression seen under basal conditions (Correa et al., 2012). Interestingly when TTX was applied to WT

neurones the spines become thinner as oppose to MSK1 KD neurones which become stubbier in shape. The longer thinner spines are thought to be able to effectively compartmentalise calcium. However MSK1 KD spines resemble an 'intermediate' morphological state which is found during transition of function. This could mean that the lack of MSK1 may have stunted morphological changes in response to TTX.

So far the role of MSK1 on Arc synthesis has been shown in dissociated primary hippocampal cell culture in response to acute BDNF stimulation and chronic synaptic deprivation. Could MSK1 play a role in experience-dependent synaptic plasticity in adult mice? The model used was environmental enrichment (EE) of post weaned male mice in social groups for either 1-6 hours or 2 weeks. The biochemical, structural and electrophysiological properties were analysed in both WT and MSK1 KD mice to depict a potential signalling pathway. Arc mRNA has been shown to be upregulated upon EE in the hippocampus following EE (Guzowski et al., 1999; Pinaud et al., 2001a; Chotiner et al., 2010). In our experimental conditions, Arc mRNA levels were elevated following acute (i.e. 1-6 hours) EE in both WT and MSK1 KD mice hippocampus and cortex. This subsequently correlated with an increase in Arc protein in both genotypes in the hippocampus. However the EE-dependent upregulation of Arc protein in the cortex was deficient in the MSK1 KD mice. This indicated a possible role for MSK1 in regulating Arc synthesis in the cortex during acute EE and hence tissue specific signalling pathways. The signalling cascades may also be reliant on the time period of EE as neither WT nor MSK1 KD mice showed significant changes in Arc protein levels after 2 weeks of EE. This may be due to the dynamics of Arc expression which is confined to a small timeframe during development. This was followed up with electrophysiological experiments monitoring basal synaptic transmission, presynaptic changes and alterations in synaptic plasticity after 2 weeks EE. Interestingly neither WT nor MSK1 KD mice showed changes in any of these parameters including the expression of LTP induced by both, tetanus and theta burst stimulation (TBS) protocols. Both tetanus and TBS-induced LTP were tested as both protocols may involve different signalling pathways thus implying that MSK1 may play a role in one but not the other. The unchanging electrophysiological properties of WT and MSK1 KD mice upon EE were also reflected in the spine density of the CA1 pyramidal cells which remain unaltered.

Finally the importance of Arc in synaptic plasticity in its role in endocytosis has been elucidated to by its interaction with dynamin 2 and endophilin 3 which are

involved in clathrin-mediated endocytosis of membrane bound receptors (Chowdhury et al., 2006). However its indirect interaction with the cytoskeleton remains a mystery (Lyford et al., 1995). Thus our novel finding that Arc pulls down with AP-2 α and μ subunit from hippocampal lysate may be a piece of the puzzle linking Arc with the cytoskeleton. AP-2 is known to bind to clathrin (Shih et al., 1995; Pearse et al., 2000) and to GluA2 AMPAR (Kastning et al., 2007) thus making it a candidate in mediating Arc-dependent AMPAR endocytosis during different forms of synaptic plasticity such as homeostatic downscaling or mGluR-LTD.

To summarise, the role of MSK1 in synaptic plasticity appears to be dependent on a few factors. These include the type of stimulant, the incubation time of the stimulation and age of the hippocampal culture. The most prominent effect of MSK1 was shown during TTX-induced up-scaling which regulated Arc synthesis and AMPAR trafficking accompanied changes in synaptic transmission (mEPSC). These synaptic changes were also reflected in MSK1-dependent structural changes in spine morphology. During experience-dependent synaptic plasticity there appeared to be no role for MSK1 during chronic EE from a biochemical, structural and electrophysiological point of view. All in all one must remember that MSK1 is regulated by a range of kinases depending on the stimulation which subsequently effects gene transcription via CREB or histone H3. Whether MSK1 regulates Arc gene transcription directly, this remains unknown. However it is clear that Arc is also regulated by many upstream signalling cascades as well as transcription factors and thus narrowing one specific pathway may be unlikely as it is a prime mediator of many cellular processes. Understanding further the role of Arc in clathrin-mediated endocytosis of receptors is of prime importance for the further understanding of the mechanisms underlying learning and memory.

8.

References

Aakalu G, Smith WB, Nguyen N, Jiang CG, Schuman EM (2001) Dynamic visualization of local protein synthesis in hippocampal neurons. Neuron 30:489-502.

Abraham WC, Bear MF (1996) Metaplasticity: The plasticity of synaptic plasticity. Trends in Neurosciences 19:126-130.

Abraham WC, Williams JM (2008) LTP maintenance and its protein synthesis-dependence. Neurobiology of Learning and Memory 89:260-268.

Adams JP, Robinson RA, Hudgins ED, Wissink EM, Dudek SM (2009) NMDA receptor independent control of transcription factors and gene expression. Neuroreport 20:1429-1433.

Allison DW, Gelfand VI, Spector I, Craig AM (1998) Role of actin in anchoring postsynaptic receptors in cultured hippocampal neurons: Differential attachment of NMDA versus AMPA receptors. Journal of Neuroscience 18:2423-2436.

Alonso M, Medina JH, Pozzo-Miller L (2004) ERK1/2 activation is necessary for BDNF to increase dendritic spine density in hippocampal CA1 pyramidal neurons. Learning & Memory 11:172-178.

Altimimi HF, Stellwagen D (2013) Persistent Synaptic Scaling Independent of AMPA Receptor Subunit Composition. Journal of Neuroscience 33:11763-11767.

Alvarez VA, Sabatini BL (2007) Anatomical and physiological plasticity of dendritic spines. Annual Review of Neuroscience 30:79-97.

Andersen P, Morris. R, Amaral. D, Bliss. T, O'Keefe. J (2007) The Hippocampus Book: Oxford University Press.

Anggono V, Huganir RL (2012) Regulation of AMPA receptor trafficking and synaptic plasticity. Current Opinion in Neurobiology 22:461-469.

Anggono V, Clem RL, Huganir RL (2011) PICK1 Loss of Function Occludes Homeostatic Synaptic Scaling. Journal of Neuroscience 31:2188-2196.

Aoto J, Nam CI, Poon MM, Ting P, Chen L (2008) Synaptic Signaling by All-Trans Retinoic Acid in Homeostatic Synaptic Plasticity. Neuron 60:308-320.

Arikkath J (2010) N-cadherin: stabilizing synapses. Journal of Cell Biology 189:395-396.

Arthur JS (2008) MSK activation and physiological roles. Front Biosci 13:5866-5879.

Arthur JS, Cohen P (2000) MSK1 is required for CREB phosphorylation in response to mitogens in mouse embryonic stem cells. FEBS Lett 482:44-48.

Arthur JSC, Fong AL, Dwyer JM, Davare M, Reese E, Obrietan K, Impey S (2004) Mitogen- and stress-activated protein kinase 1 mediates cAMP response element-binding protein phosphorylation and activation by neurotrophins. Journal of Neuroscience 24:4324-4332.

Artola A, von Frijtag JC, Fermont PCJ, Gispen WH, Schrama LH, Kamal A, Spruijt BM (2006) Long-lasting modulation of the induction of LTD and LTP in rat hippocampal CA1 by behavioural stress and environmental enrichment. European Journal of Neuroscience 23:261-272.

Ascoli GA et al. (2008) Petilla terminology: nomenclature of features of GABAergic interneurons of the cerebral cortex. Nature Reviews Neuroscience 9:557-568.
Ball CL, Hunt SP, Robinson MS (1995) Expression and localization of α-adaptin isoforms. Journal of Cell Science 108:2865-2875.
Barria A, Derkach V, Soderling T (1997a) Identification of the Ca2+/calmodulin-dependent protein kinase II regulatory phosphorylation site in the alpha-amino-3-hydroxyl-5-methyl-4-isoxazole-propionate-type glutamate receptor. Journal of Biological Chemistry 272:32727-32730.
Barria A, Muller D, Derkach V, Griffith LC, Soderling TR (1997b) Regulatory phosphorylation of AMPA-type glutamate receptors by CaM-KII during long-term potentiation. Science 276:2042-2045.
Beattie EC, Carroll RC, Yu X, Morishita W, Yasuda H, von Zastrow M, Malenka RC (2000) Regulation of AMPA receptor endocytosis by a signaling mechanism shared with LTD. Nature Neuroscience 3:1291-1300.
Beltran JQ, Gutierrez R (2012) Co-release of glutamate and GABA from single, identified mossy fibre giant boutons. Journal of Physiology-London 590:4789-4800.
Benke TA, Luthi A, Isaac JTR, Collingridge GL (1998) Modulation of AMPA receptor unitary conductance by synaptic activity. Nature 393:793-797.
Bennett EL, Diamond MC, Krech D, Rosenzweig MR (1996) Chemical and anatomical plasticity of brain (Reprinted from Science, vol 146, pg 610-619, 1964). Journal of Neuropsychiatry and Clinical Neurosciences 8:459-470.
Blanpied TA, Scott DB, Ehlers MD (2002) Dynamics and regulation of clathrin coats at specialized endocytic zones of dendrites and spines. Neuron 36:435-449.
Bliss TV, Collingridge GL (1993) A synaptic model of memory: long-term potentiation in the hippocampus. Nature 361:31-39.
Bliss TVP, Lomo T (1973) Long- lasting potentiation of synaptic transmission in dentate are of anesthetized rabbit following stimulation of perforant path. Journal of Physiology-London 232:331-356.
Bloomer WAC, VanDongen HMA, VanDongen AMJ (2008) Arc/Arg3.1 translation is controlled by convergent N methyl D aspartate and G(s) coupled receptor signaling pathways. Journal of Biological Chemistry 283:582-592.
Blumstein J, Faundez V, Nakatsu F, Saito T, Ohno H, Kelly RB (2001) The neuronal form of adaptor protein-3 is required for synaptic vesicle formation from endosomes. Journal of Neuroscience 21:8034-8042.
Bode AM, Dong Z (2005) Inducible covalent posttranslational modification of histone H3. Science's STKE : signal transduction knowledge environment 2005:re4-re4.
Boehm M, Bonifacino JS (2001) Adaptins - The final recount. Molecular Biology of the Cell 12:2907-2920.
Bonifacino JS, Traub LM (2003) Signals for sorting of transmembrane proteins to endosomes and lysosomes. Annual Review of Biochemistry 72:395-447.
Bourne J, Harris KM (2007) Do thin spines learn to be mushroom spines that remember? In, pp 381–386. Current Opinion in Neurobiology.
Bourne JN, Harris KM (2008) Balancing structure and function at hippocampal dendritic spines. Annu Rev Neurosci 31:47-67.
Bozzi Y, Pizzorusso T, Cremisi F, Rossi FM, Barsacchi G, Maffei L (1995) Monocular deprivation decreases the expression of messenger- RNA for Brain- derived neurotrophic factor in the rat visual cortex. Neuroscience 69:1133-1144.
Braak H, Braak E (1991) Neuropathological staging of Alzheimer- related changes. Acta Neuropathologica 82:239-259.

Bramham CR, Messaoudi E (2005) BDNF function in adult synaptic plasticity: The synaptic consolidation hypothesis. Progress in Neurobiology 76:99-125.

Bramham CR, Alme MN, Bittins M, Kuipers SD, Nair RR, Pai B, Panja D, Schubert M, Soule J, Tiron A, Wibrand K (2010) The Arc of synaptic memory. Exp Brain Res 200:125-140.

Brami-Cherrier K, Lavaur J, Pages C, Arthur JSC, Caboche J (2007) Glutamate induces histone H3 phosphorylation but not acetylation in striatal neurons: role of mitogen- and stress-activated kinase-1. Journal of Neurochemistry 101:697-708.

Brami-Cherrier K, Roze E, Girault JA, Betuing S, Caboche J (2009) Role of the ERK/MSK1 signalling pathway in chromatin remodelling and brain responses to drugs of abuse. J Neurochem 108:1323-1335.

Bredt DS, Nicoll RA (2003) AMPA receptor trafficking at excitatory synapses. Neuron 40:361-379.

Brodsky FM, Chen CY, Knuehl C, Towler MC, Wakeham DE (2001) Biological basket weaving: Formation and function of clathrin-coated vesicles. Annual Review of Cell and Developmental Biology 17:517-568.

Brown TC, Tran IC, Backos DS, Esteban JA (2005) NMDA receptor-dependent activation of the small GTPase Rab5 drives the removal of synaptic AMPA receptors during hippocampal LTD. Neuron 45:81-94.

Bruning JC, Gillette JA, Bjoerbaeck C, Kotzka J, Knebel B, Avci H, Wilhelm K, Muller-Wieland D (2000) Ribosomal subunit kinase (Rsk)-2 is required for growth factor-stimulated transcription of the c-Fos gene. Diabetes 49:A326-A326.

Bryan B, Kumar V, Stafford LJ, Cai Y, Wu GY, Liu MY (2004) GEFT, a Rho family guanine nucleotide exchange factor, regulates neurite outgrowth and dendritic spine formation. Journal of Biological Chemistry 279:45824-45832.

Buchwalter G, Gross C, Wasylyk B (2004) Ets ternary complex transcription factors. Gene 324:1-14.

Burgos PV, Mardones GA, Rojas AL, daSilva LLP, Prabhu Y, Hurley JH, Bonifacino JS (2010) Sorting of the Alzheimer's Disease Amyloid Precursor Protein Mediated by the AP-4 Complex. Developmental Cell 18:425-436.

Butcher GQ, Lee B, Cheng HY, Obrietan K (2005) Light stimulates MSK1 activation in the suprachiasmatic nucleus via a PACAP-ERK/MAP kinase-dependent mechanism. J Neurosci 25:5305-5313.

Carroll RC, Lissin DV, von Zastrow M, Nicoll RA, Malenka RC (1999a) Rapid redistribution of glutamate receptors contributes to long-term depression in hippocampal cultures. Nature Neuroscience 2:454-460.

Carroll RC, Beattie EC, Xia HH, Luscher C, Altschuler Y, Nicoli RA, Malenka RC, von Zastrow M (1999b) Dynamin-dependent endocytosis of ionotropic glutamate receptors. Proceedings of the National Academy of Sciences of the United States of America 96:14112-14117.

Carulli D, Foscarin S, Rossi F (2011) Activity-dependent plasticity and gene expression modifications in the adult CNS. Frontiers in molecular neuroscience 4:50.

Chao MV, Bothwell M (2002) Neurotrophins: To cleave or not to cleave. Neuron 33:9-12.

Chotiner JK, Nielson J, Farris S, Lewandowski G, Huang F, Banos K, de Leon R, Steward O (2010) Assessment of the role of MAP kinase in mediating activity-dependent transcriptional activation of the immediate early gene Arc/Arg3.1 in the dentate gyrus in vivo. Learn Mem 17:117-129.

Chowdhury S, Shepherd JD, Okuno H, Lyford G, Petralia RS, Plath N, Kuhl D, Huganir RL, Worley PF (2006) Arc/Arg3.1 interacts with the endocytic machinery to regulate AMPA receptor trafficking. Neuron 52:445-459.

Chwang WB, O'Riordan KJ, Levenson JM, Sweatt JD (2006) ERK/MAPK regulates hippocampal histone phosphorylation following contextual fear conditioning. Learning & Memory 13:322-328.

Chwang WB, Arthur JS, Schumacher A, Sweatt JD (2007) The nuclear kinase mitogen- and stress-activated protein kinase 1 regulates hippocampal chromatin remodeling in memory formation. J Neurosci 27:12732-12742.

Cingolani LA, Thalhammer A, Yu LMY, Catalano M, Ramos T, Colicos MA, Goda Y (2008) Activity-dependent regulation of synaptic AMPA receptor composition and abundance by beta 3 integrins. Neuron 58:749-762.

Cohen-Cory S, Fraser SE (1995) Effects of brain-derived neurotrophic factor on optic axon branching and remodelling in-vivo. Nature 378:192-196.

Collingridge GL, Isaac JT, Wang YT (2004) Receptor trafficking and synaptic plasticity. Nat Rev Neurosci 5:952-962.

Collins BM, McCoy AJ, Kent HM, Evans PR, Owen DJ (2002) Molecular architecture and functional model of the endocytic AP2 complex. Cell 109:523-535.

Contractor A, Heinemann SF (2002) Glutamate receptor trafficking in synaptic plasticity. Sci STKE 2002:RE14.

Correa SAL, Mueller J, Collingridge GL, Marrion NV (2009) Rapid endocytosis provides restricted somatic expression of a K+ channel in central neurons. Journal of Cell Science 122:4186-4194.

Correa SAL, Hunter CJ, Palygin O, Wauters SC, Martin KJ, McKenzie C, McKelvey K, Morris RGM, Pankratov Y, Arthur JSC, Frenguelli BG (2012) MSK1 Regulates Homeostatic and Experience-Dependent Synaptic Plasticity. Journal of Neuroscience 32:13039-13051.

Craig TJ, Henley JM (2012) SUMOylation, Arc and the regulation homeostatic synaptic scaling: Implications in health and disease. Communicative & integrative biology 5:634-636.

Craig TJ, Jaafari N, Petrovic MM, Rubin PP, Mellor JR, Henley JM (2012) Homeostatic Synaptic Scaling Is Regulated by Protein SUMOylation. Journal of Biological Chemistry 287:22781-22788.

Crosio C, Cermakian N, Allis CD, Sassone-Corsi P (2000) Light induces chromatin modification in cells of the mammalian circadian clock. Nature Neuroscience 3:1241-1247.

Crosio C, Heitz E, Allis CD, Borrelli E, Sassone-Corsi P (2003) Chromatin remodeling and neuronal response: multiple signaling pathways induce specific histone H3 modifications and early gene expression in hippocampal neurons. Journal of Cell Science 116:4905-4914.

da Costa SR, Okamoto CT, Hamm-Alvarez SF (2003) Actin microfilaments et al. - the many components, effectors and regulators of epithelial cell endocytosis. Advanced Drug Delivery Reviews 55:1359-1383.

Dailey ME, Smith SJ (1996) The dynamics of dendritic structure in developing hippocampal slices. Journal of Neuroscience 16:2983-2994.

Dale N, Pearson T, Frenguelli BG (2000) Direct measurement of adenosine release during hypoxia in the CA1 region of the rat hippocampal slice. Journal of Physiology-London 526:143-155.

Darwin C (1871) The Descent of Man, and selection in relation to sex: John Murray.

Davie JR (2003) MSK1 and MSK2 mediate mitogen- and stress-induced phosphorylation of histone H3: a controversy resolved. Science's STKE : signal transduction knowledge environment 2003:PE33-PE33.

Deak M, Clifton AD, Lucocq LM, Alessi DR (1998) Mitogen- and stress-activated protein kinase-1 (MSK1) is directly activated by MAPK and SAPK2/p38, and may mediate activation of CREB. Embo J 17:4426-4441.

DeFelipe J (2011) The evolution of the brain, the human nature of cortical circuits, and intellectual creativity. Frontiers in Neuroanatomy 5.

Derkach V, Barria A, Soderling TR (1999) Ca2+/calmodulin-kinase II enhances channel conductance of alpha-amino-3-hydroxy-5-methyl-4-isoxazolepropionate type glutamate receptors. Proceedings of the National Academy of Sciences of the United States of America 96:3269-3274.

Diamond MC, Ingham CA, Johnson RE, Bennett EL, Rosenzweig MR (1976) Effects of environment on morphology of rat cerebral- cortex and hippocampus. Journal of Neurobiology 7:75-85.

Donai H, Sugiura H, Ara D, Yoshimura Y, Yamagata K, Yamauchi T (2003) Interaction of Arc with CaM kinase II and stimulation of neurite extension by Arc in neuroblastoma cells expressing CaM kinase II. Neuroscience Research 47:399-408.

Doray B, Lee I, Knisely J, Bu G, Kornfeld S (2007) The gamma/sigma 1 and alpha/sigma 2 hemicomplexes of clathrin adaptors AP-1 and AP-2 harbor the dileucine recognition site. Molecular Biology of the Cell 18:1887-1896.

Duffy SN, Craddock KJ, Abel T, Nguyen PV (2001) Environmental enrichment modifies the PKA-dependence of hippocampal LTP and improves hippocampus-dependent memory. Learning & Memory 8:26-34.

Dunah AW, Hueske E, Wyszynski M, Hoogenraad CC, Jaworski J, Pak DT, Simonetta A, Liu GS, Sheng M (2005) LAR receptor protein tyrosine phosphatases in the development and maintenance of excitatory synapses. Nature Neuroscience 8:458-467.

Eckert MJ, Abraham WC (2010) Physiological effects of enriched environment exposure and LTP induction in the hippocampus in vivo do not transfer faithfully to in vitro slices. Learning & Memory 17:480-484.

Eckert MJ, Abraham WC (2013) Effects of environmental enrichment exposure on synaptic transmission and plasticity in the hippocampus. Current topics in behavioral neurosciences 15:165-187.

Ehlers MD (2000) Reinsertion or degradation of AMPA receptors determined by activity-dependent endocytic sorting. Neuron 28:511-525.

Ehrlich I, Malinow R (2004) Postsynaptic density 95 controls AMPA receptor incorporation during long-term potentiation and experience-driven synaptic plasticity. Journal of Neuroscience 24:916-927.

Eichenbaum H, Cohen N (2001) From Conditioning to conscious recollection.

Engert F, Bonhoeffer T (1999) Dendritic spine changes associated with hippocampal long-term synaptic plasticity. Nature 399:66-70.

English JD, Sweatt JD (1997) A requirement for the mitogen-activated protein kinase cascade in hippocampal long term potentiation. Journal of Biological Chemistry 272:19103-19106.

Ernfors P, Lee KF, Jaenisch R (1994) Mice lacking Brain- derived neurotrophic factor develop with sensory deficits. Nature 368:147-150.

Etkin A, Alarcon JM, Weisberg SP, Touzani K, Huang YY, Nordheim A, Kandel ER (2006) A role in learning for SRF: Deletion in the adult forebrain disrupts LTD and the formation of an immediate memory of a novel context. Neuron 50:127-143.

Faherty CJ, Kerley D, Smeyne RJ (2003) A Golgi-Cox morphological analysis of neuronal changes induced by environmental enrichment. Brain research Developmental brain research 141:55-61.

Falkenberg T, Mohammed AK, Henriksson B, Persson H, Winblad B, Lindefors N (1992) Increased expression of Brain-Derived neurotrophic factor messenger-RNA in rat hippocampus is associated with improved spatial memory and enriched environment. Neuroscience Letters 138:153-156.

Fayard B, Loeffler S, Weis J, Vogelin E, Kruttgen A (2005) The secreted brain-derived neurotrophic factor precursor pro-BDNF binds to TrkB and p75NTR but not to TrkA or TrkC. Journal of Neuroscience Research 80:18-28.

Feng RB, Rampon C, Tang YP, Shrom D, Jin J, Kim M, Sopher B, Martin GM, Kim SH, Langdon RB, Sisodia SS, Tsien JZ (2001) Deficient neurogenesis in forebrain-specific presenilin-1 knockout mice is associated with reduced clearance of hippocampal memory traces. Neuron 32:911-926.

Fiala JC, Spacek J, Harris KM (2002) Dendritic spine pathology: Cause or consequence of neurological disorders? Brain Research Reviews 39:29-54.

Fiala JC, Feinberg M, Popov V, Harris KM (1998) Synaptogenesis via dendritic filopodia in developing hippocampal area CA1. Journal of Neuroscience 18:8900-8911.

Figurov A, PozzoMiller LD, Olafsson P, Wang T, Lu B (1996) Regulation of synaptic responses to high-frequency stimulation and LTP by neurotrophins in the hippocampus. Nature 381:706-709.

Finkbeiner S, Tavazoie SF, Maloratsky A, Jacobs KM, Harris KM, Greenberg ME (1997) CREB: A major mediator of neuronal neurotrophin responses. Neuron 19:1031-1047.

Fischer A, Sananbenesi F, Wang X, Dobbin M, Tsai L-H (2007) Recovery of learning and memory is associated with chromatin remodelling. Nature 447:178-U172.

Fleming JJ, England PM (2010) AMPA receptors and synaptic plasticity: a chemist's perspective. Nature Chemical Biology 6:89-97.

Ford MGJ, Pearse BMF, Higgins MK, Vallis Y, Owen DJ, Gibson A, Hopkins CR, Evans PR, McMahon HT (2001) Simultaneous binding of PtdIns(4,5)P-2 and clathrin by AP180 in the nucleation of clathrin lattices on membranes. Science 291:1051-1055.

Foster TC, Gagne J, Massicotte G (1996) Mechanism of altered synaptic strength due to experience: Relation to long-term potentiation. Brain Research 736:243-250.

Frenguelli B, Corrêa S (2012) Regulation and role of MSK in the mammalian brain. Landes Bioscience.

Frenguelli BG, Wigmore G, Llaudet E, Dale N (2007) Temporal and mechanistic dissociation of ATP and adenosine release during ischaemia in the mammalian hippocampus. Journal of Neurochemistry 101:1400-1413.

Frodin M, Gammeltoft S (1999) Role and regulation of 90 kDa ribosomal S6 kinase (RSK) in signal transduction. Molecular and Cellular Endocrinology 151:65-77.

Fukazawa Y, Saitoh Y, Ozawa F, Ohta Y, Mizuno K, Inokuchi K (2003) Hippocampal LTP is accompanied by enhanced F actin content within the dendritic spine that is essential for late LTP maintenance in vivo. Neuron 38:447-460.

Gaidarov I, Keen JH (1999) Phosphoinositide-AP-2 interactions required for targeting to plasma membrane clathrin-coated pits. Journal of Cell Biology 146:755-764.

Gaidarov I, Chen Q, Falck JR, Reddy KK, Keen JH (1996) A functional phosphatidylinositol 3,4,5-trisphosphate/phosphoinositide binding domain in the clathrin adaptor AP-2 alpha subunit (vol 271, pg 20922, 1996). Journal of Biological Chemistry 271:27188-27188.

Gainey MA, Hurvitz-Wolff JR, Lambo ME, Turrigiano GG (2009) Synaptic scaling requires the GluR2 subunit of the AMPA receptor. J Neurosci 29:6479-6489.

Gao Y, Tatavarty V, Korza G, Levin MK, Carson JH (2008) Multiplexed dendritic targeting of alpha calcium calmodulin-dependent protein kinase II, neurogranin, and activity-regulated cytoskeleton-associated protein RNAs by the A2 pathway. Molecular Biology of the Cell 19:2311-2327.

Garcia-Lopez P, Garcia-Marin V, Freire M (2007) The discovery of dendritic spines by Cajal in 1888 and its relevance in the present neuroscience. Progress in Neurobiology 83:110-130.

Gerges NZ, Backos DS, Rupasinghe CN, Spaller MR, Esteban JA (2006) Dual role of the exocyst in AMPA receptor targeting and insertion into the postsynaptic membrane. Embo Journal 25:1623-1634.

Giese KP, Fedorov NB, Filipkowski RK, Silva AJ (1998) Autophosphorylation at Thr(286) of the alpha calcium-calmodulin kinase II in LTP and learning. Science 279:870-873.

Gladding CM, Fitzjohn SM, Molnar E (2009) Metabotropic Glutamate Receptor-Mediated Long-Term Depression: Molecular Mechanisms. Pharmacological Reviews 61:395-412.

Globus A, Rosenzwe.Mr, Bennett EL, Diamond MC (1973) Effects of differential experience on dendritic spine counts in rat cerebral- cortex. Journal of Comparative and Physiological Psychology 82:175-181.

Goley ED, Welch MD (2006) The ARP2/3 complex: an actin nucleator comes of age. Nature Reviews Molecular Cell Biology 7:713-726.

Granger AJ, Shi Y, Lu W, Cerpas M, Nicoll RA (2013) LTP requires a reserve pool of glutamate receptors independent of subunit type. Nature 493:495-+.

Grass I, Thiel S, Honing S, Haucke V (2004) Recognition of a basic AP-2 binding motif within the C2B domain of synaptotagmin is dependent on multimerization. Journal of Biological Chemistry 279:54872-54880.

Grober E, Dickson D, Sliwinski MJ, Buschke H, Katz M, Crystal H, Lipton RB (1999) Memory and mental status correlates of modified Braak staging. Neurobiology of Aging 20:573-579.

Guichet A, Wucherpfenning T, Dudu V, Etter S, Wilsch-Brauniger M, Hellwig A, Gonzalez-Gaitan M, Huttner WB, Schmidt AA (2002) Essential role of endophilin A in synaptic vesicle budding at the Drosophila neuromuscular junction. Embo Journal 21:1661-1672.

Gutierrez-Mecinas M, Trollope AF, Collins A, Morfett H, Hesketh SA, Kersante F, Reul JMHM (2011) Long-lasting behavioral responses to stress involve a direct interaction of glucocorticoid receptors with ERK1/2-MSK1-Elk-1 signaling. Proceedings of the National Academy of Sciences of the United States of America 108:13806-13811.

Guzowski JF, McNaughton BL, Barnes CA, Worley PF (1999) Environment-specific expression of the immediate-early gene Arc in hippocampal neuronal ensembles. Nature Neuroscience 2:1120-1124.

Guzowski JF, Lyford GL, Stevenson GD, Houston FP, McGaugh JL, Worley PF, Barnes CA (2000) Inhibition of activity-dependent arc protein expression in the rat hippocampus impairs the maintenance of long-term potentiation and the consolidation of long-term memory. Journal of Neuroscience 20:3993-4001.

Haapasalo A, Sipola L, Larsson K, Akerman KEO, Stoilov P, Stamm S, Wong G, Castren E (2002) Regulation of TRKB surface expression by brain-derived neurotrophic factor and truncated TRIM Isoforms. Journal of Biological Chemistry 277:43160-43167.

Hanley JG (2008) AMPA receptor trafficking pathways and links to dendritic spine morphogenesis. Cell Adh Migr 2:276-282.

Hanley JG (2010) Endosomal sorting of AMPA receptors in hippocampal neurons. Biochemical Society Transactions 38:460-465.

Hao WH, Luo Z, Zheng L, Prasad K, Lafer EM (1999) AP180 and AP-2 interact directly in a complex that cooperatively assembles clathrin. Journal of Biological Chemistry 274:22785-22794.

Harris KM, Kater SB (1994) Dendritic spines: Cellular specializations imparting both stability and flexibility to synaptic function. Annual Review of Neuroscience 17:341-371.

Harris KM, Jensen FE, Tsao B (1992) 3D Structure of dendritic spines and synapses in rat Hippocampus (CA1) at postnatal day 15 and adult ages. Implications for the maturation of synpatic physiology and long term potentiation. Journal of Neuroscience 12:2685-2705.

Hassinger TD, Atkinson PB, Strecker GJ, Whalen LR, Dudek FE, Kossel AH, Kater SB (1995) Evidence for glutamate- mediated activation of hippocampal-neurons by glial calcium waves. Journal of Neurobiology 28:159-170.

Haydon PG (2001) Glia: Listening and talking to the synapse. Nature Reviews Neuroscience 2:185-193.

Hebb D (1949) The organization of behavior: a neuropsychological theory.

Hebb DO (1947) The effects of early experience on problem solving at maturity. Am Psychol 2:306–307.

Henley JM, Barker EA, Glebov OO (2011) Routes, destinations and delays: recent advances in AMPA receptor trafficking. Trends in Neurosciences 34:258-268.

Hering H, Sheng M (2003) Activity-dependent redistribution and essential role of cortactin in dendritic spine morphogenesis. Journal of Neuroscience 23:11759-11769.

Hernandez RV, Navarro MM, Rodriguez WA, Martinez JL, LeBaron RG (2005) Differences in the magnitude of long-term potentiation produced by theta burst and high frequency stimulation protocols matched in stimulus number. Brain Research Protocols 15:6-13.

Hinds HL, Tonegawa S, Malinow R (1998) CA1 long-term potentiation is diminished but present in hippocampal slices from alpha-CaMKII mutant mice. Learning & Memory 5:344-354.

Hirst J, Barlow LD, Francisco GC, Sahlender DA, Seaman MNJ, Dacks JB, Robinson MS (2011) The Fifth Adaptor Protein Complex. Plos Biology 9.

Hollmann M, Heinemann S (1994) Cloned glutamate receptors. Annual Review of Neuroscience 17:31-108.

Honing S, Ricotta D, Krauss M, Spate K, Spolaore B, Motley A, Robinson M, Robinson C, Haucke V, Owen DJ (2005) Phosphatidylinositol-(4,5)-bisphosphate regulates sorting signal recognition by the clathrin-associated adaptor complex AP2. Molecular Cell 18:519-531.

Horikawa HPM, Kneussel M, El Far O, Betz H (2002) Interaction of synaptophysin with the AP-1 adaptor protein gamma-adaptin. Molecular and Cellular Neuroscience 21:454-462.

Hotulainen P, Hoogenraad CC (2010) Actin in dendritic spines: connecting dynamics to function. Journal of Cell Biology 189:619-629.

Hotulainen P, Paunola E, Vartiainen MK, Lappalainen P (2005) Actin-depolymerizing factor and cofilin-1 play overlapping roles in promoting rapid F-actin depolymerization in mammalian nonmuscle cells. Molecular Biology of the Cell 16:649-664.

Hou Q, Zhang D, Jarzylo L, Huganir RL, Man HY (2008) Homeostatic regulation of AMPA receptor expression at single hippocampal synapses. Proc Natl Acad Sci U S A 105:775-780.

Huang EJ, Reichardt LF (2001) Neurotrophins: Roles in neuronal development and function. Annual Review of Neuroscience 24:677-736.

Huang EJ, Reichardt LF (2003) Trk receptors: Roles in neuronal signal transduction. Annual Review of Biochemistry 72:609-642.

Huang F, Chotiner JK, Steward O (2007) Actin polymerization and ERK phosphorylation are required for Arc/Arg3.1 mRNA targeting to activated synaptic sites on dendrites. Journal of Neuroscience 27:9054-9067.

Huang YZ, McNamara JO (2010) Mutual Regulation of Src Family Kinases and the Neurotrophin Receptor TrkB. Journal of Biological Chemistry 285:8207-8217.

Hubel DH, Wiesel TN (1970) Period of susceptibility to physiological effects of unilateral eye closure in kittens. Journal of Physiology-London 206:419-436.

Huber KM, Kayser MS, Bear MF (2000) Role for rapid dendritic protein synthesis in hippocampal mGluR-dependent long-term depression. Science 288:1254-1257.

Hughes JR (1958) Post-tetanic potentiation. Physiological reviews 38:91-113.

Husi H, Ward MA, Choudhary JS, Blackstock WP, Grant SGN (2000) Proteomic analysis of NMDA receptor-adhesion protein signaling complexes. Nature Neuroscience 3:661-669.

Ibanez CF (2002) Jekyll-Hyde neurotrophins: the story of proNGF. Trends in Neurosciences 25:284-286.

Ibata K, Sun Q, Turrigiano GG (2008) Rapid synaptic scaling induced by changes in postsynaptic firing. Neuron 57:819-826.

Ickes BR, Pham TM, Sanders LA, Albeck DS, Mohammed AH, Granholm AC (2000) Long-term environmental enrichment leads to regional increases in neurotrophin levels in rat brain. Experimental Neurology 164:45-52.

Inoue M, Yagishita-Kyo N, Nonaka M, Kawashima T, Okuno H, Bito H (2010) Synaptic activity-responsive element (SARE): A unique genomic structure with an unusual sensitivity to neuronal activity. Communicative & integrative biology 3:443-446.

Isaac JTR, Ashby M, McBain CJ (2007) The role of the GluR2 subunit in AMPA receptor function and synaptic plasticity. Neuron 54:859-871.

Jackson LP, Kelly BT, McCoy AJ, Gaffry T, James LC, Collins BM, Hoening S, Evans PR, Owen DJ (2010) A Large-Scale Conformational Change Couples Membrane Recruitment to Cargo Binding in the AP2 Clathrin Adaptor Complex. Cell 141:1220-U1213.

Ji Y, Lu Y, Yang F, Shen W, Tang TTT, Feng L, Duan S, Lu B (2010) Acute and gradual increases in BDNF concentration elicit distinct signaling and functions in neurons. Nature Neuroscience 13:302-309.

Jung N, Haucke V (2007) Clathrin-mediated endocytosis at synapses. Traffic 8:1129-1136.

Kalita K, Kharebava G, Zheng J-J, Hetman M (2006) Role of megakaryoblastic acute leukemia-1 in ERK1/2-dependent stimulation of serum response factor-driven transcription by BDNF or increased synaptic activity. Journal of Neuroscience 26:10020-10032.

Karelina K, Hansen KF, Choi Y-S, DeVries AC, Arthur JSC, Obrietan K (2012) MSK1 regulates environmental enrichment-induced hippocampal plasticity and cognitive enhancement. Learning & Memory 19:550-560.

Kasai H, Matsuzaki M, Noguchi J, Yasumatsu N, Nakahara H (2003) Structure-stability-function relationships of dendritic spines. Trends in Neurosciences 26:360-368.

Kastning K, Kukhtina V, Kittler JT, Chen G, Pechstein A, Enders S, Lee SH, Sheng M, Yan Z, Haucke V (2007) Molecular determinants for the interaction between AMPA receptors and the clathrin adaptor complex AP-2. Proceedings of the National Academy of Sciences of the United States of America 104:2991-2996.

Kawashima T, Okuno H, Nonaka M, Adachi-Morishima A, Kyo N, Okamura M, Takemoto-Kimura S, Worley PF, Bito H (2009) Synaptic activity-responsive element in the Arc/Arg3.1 promoter essential for synapse-to-nucleus signaling in activated neurons. Proceedings of the National Academy of Sciences of the United States of America 106:316-321.

Kelleher RJ, Govindarajan A, Jung HY, Kang H, Tonegawa S (2004) Translational control by MAPK signaling in long-term synaptic plasticity and memory. Journal of Neurochemistry 90:30-30.

Kelly BT, McCoy AJ, Spaete K, Miller SE, Evans PR, Hoening S, Owen DJ (2008) A structural explanation for the binding of endocytic dileucine motifs by the AP2 complex. Nature 456:976-U981.

Kempermann G, Kuhn HG, Gage FH (1997) More hippocampal neurons in adult mice living in an enriched environment. Nature 386:493-495.

Kerchner GA, Nicoll RA (2008) Silent synapses and the emergence of a postsynaptic mechanism for LTP. Nature Reviews Neuroscience 9:813-825.

Kerppola TK (2008) Biomolecular fluorescence complementation (BiFC) analysis as a probe of protein interactions in living cells. Annual Review of Biophysics 37:465-487.

Kitanishi T, Ikegaya Y, Matsuki N (2009) Behaviorally evoked transient reorganization of hippocampal spines. European Journal of Neuroscience 30:560-566.

Kittler JT, Chen GJ, Honing S, Bogdanov Y, McAinsh K, Arancibia-Carcamo IL, Jovanovic JN, Pangalos MN, Haucke V, Yan Z, Moss SJ (2005) Phospho-dependent binding of the clathrin AP2 adaptor complex to GABA(A) receptors regulates the efficacy of inhibitory synaptic transmission. Proceedings of the National Academy of Sciences of the United States of America 102:14871-14876.

Kobayashi H, Yamamoto S, Maruo T, Murakami F (2005) Identification of a cis-acting element required for dendritic targeting of activity-regulated cytoskeleton-associated protein mRNA. European Journal of Neuroscience 22:2977-2984.

Kopec CD, Real E, Kessels HW, Malinow R (2007) GluR1 links structural and functional plasticity at excitatory synapses. Journal of Neuroscience 27:13706-13718.

Kopec CD, Li B, Wei W, Boehm J, Malinow R (2006) Glutamate receptor exocytosis and spine enlargement during chemically induced long-term potentiation. Journal of Neuroscience 26:2000-2009.

Korb E, Finkbeiner S (2011) Arc in synaptic plasticity: from gene to behavior. Trends in Neurosciences 34:591-598.

Korobova F, Svitkina T (2010) Molecular Architecture of Synaptic Actin Cytoskeleton in Hippocampal Neurons Reveals a Mechanism of Dendritic Spine Morphogenesis. Molecular Biology of the Cell 21:165-176.

Kozorovitskiy Y, Gross CG, Kopil C, Battaglia L, McBreen M, Stranahan AM, Gould E (2005) Experience induces structural and biochemical changes in the adult primate brain. Proceedings of the National Academy of Sciences of the United States of America 102:17478-17482.

Kubik S, Miyashita T, Guzowski JF (2007) Using immediate-early genes to map hippocampal subregional functions. Learning & Memory 14:758-770.

Kuzumaki N, Ikegami D, Tamura R, Hareyama N, Imai S, Narita M, Torigoe K, Niikura K, Takeshima H, Ando T, Igarashi K, Kanno J, Ushijima T, Suzuki T, Narita M (2011) Hippocampal Epigenetic Modification at the Brain-Derived Neurotrophic Factor Gene Induced by an Enriched Environment. Hippocampus 21:127-132.

Lee HK, Takamiya K, He K, Song L, Huganir RL (2009) Specific roles of AMPA receptor subunit GluR1 (GluA1) phosphorylation sites in regulating synaptic plasticity in the CA1 region of hippocampus. J Neurophysiol.

Lee J-S, Smith E, Shilatifard A (2010) The Language of Histone Crosstalk. Cell 142:682-685.

Lee S, Liu L, Wang Y, Sheng M (2002) Clathrin adaptor AP2 and NSF interact with overlapping sites of GluR2 and play distinct roles in AMPA receptor trafficking and hippocampal LTD. Neuron 36:661-674.

Lee SH, Simonetta A, Sheng M (2004) Subunit rules governing the sorting of internalized AMPA receptors in hippocampal neurons. Neuron 43:221-236.

Leggio MG, Mandolesi L, Federico F, Spirito F, Ricci B, Gelfo F, Petrosini L (2005) Environmental enrichment promotes improved spatial abilities and enhanced dendritic growth in the rat. Behavioural Brain Research 163:78-90.

Leslie KR, Nelson SB, Turrigiano GG (2001) Postsynaptic depolarization scales quantal amplitude in cortical pyramidal neurons. Journal of Neuroscience 21:art. no.-RC170.

Lessmann V, Brigadski T (2009) Mechanisms, locations, and kinetics of synaptic BDNF secretion: An update (vol 65, pg 11, 2009). Neuroscience Research 65:316-317.

Li F, Tsien JZ (2009) Memory and the NMDA receptors. N Engl J Med 361:302-303.

Li S, Tian X, Hartley DM, Feig LA (2006a) The environment versus genetics in controlling the contribution of MAP kinases to synaptic plasticity. Current Biology 16:2303-2313.

Li SM, Tian XJ, Hartley DM, Feig LA (2006b) Distinct roles for Ras-guanine nucleotide-releasing factor 1 (Ras-GRF1) and Ras-GRF2 in the induction of long-term potentiation and long-term depression. Journal of Neuroscience 26:1721-1729.

Liao DZ, Scannevin RH, Huganir R (2001) Activation of silent synapses by rapid activity-dependent synaptic recruitment of AMPA receptors. Journal of Neuroscience 21:6008-6017.

Lin D-T, Huganir RL (2007) PICK1 and phosphorylation of the glutamate receptor 2 (GluR2) AMPA receptor subunit regulates GluR2 recycling after NMDA receptor-induced internalization. Journal of Neuroscience 27:13903-13908.

Link W, Konietzko U, Kauselmann G, Krug M, Schwanke B, Frey U, Kuhl D (1995) Somatodendritic expression of an immediate- early gene is regulated by synaptic activity. Proceedings of the National Academy of Sciences of the United States of America 92:5734-5738.

Linnarsson S, Bjorklund A, Ernfors P (1997) Learning deficit in BDNF mutant mice. European Journal of Neuroscience 9:2581-2587.
Lisman J, Raghavachari S (2006) A unified model of the presynaptic and postsynaptic changes during LTP at CA1 synapses. Science's STKE : signal transduction knowledge environment 2006:re11-re11.
Lissin DV, Gomperts SN, Carroll RC, Christine CW, Kalman D, Kitamura M, Hardy S, Nicoll RA, Malenka RC, von Zastrow M (1998) Activity differentially regulates the surface expression of synaptic AMPA and NMDA glutamate receptors. Proc Natl Acad Sci U S A 95:7097-7102.
Lledo PM, Zhang XY, Sudhof TC, Malenka RC, Nicoll RA (1998) Postsynaptic membrane fusion and long-term potentiation. Science 279:399-403.
Lu W, Shi Y, Jackson AC, Bjorgan K, During MJ, Sprengel R, Seeburg PH, Nicoll RA (2009) Subunit Composition of Synaptic AMPA Receptors Revealed by a Single-Cell Genetic Approach. Neuron 62:254-268.
Lu WY, Man HY, Ju W, Trimble WS, MacDonald JF, Wang YT (2001) Activation of synaptic NMDA receptors induces membrane insertion of new AMPA receptors and LTP in cultured hippocampal neurons. Neuron 29:243-254.
Lyford GL, Yamagata K, Kaufmann WE, Barnes CA, Sanders LK, Copeland NG, Gilbert DJ, Jenkins NA, Lanahan AA, Worley PF (1995) Arc, a growth-factor and activity- regulated gene, encodes a novel cytoskeleton- associated protein that is enriched in neuronal dendrites. Neuron 14:433-445.
Lynch G, Rex CS, Gall CM (2007) LTP consolidation: Substrates, explanatory power, and functional significance. Neuropharmacology 52:12-23.
Lynch MA (2004) Long-term potentiation and memory. Physiological Reviews 84:87-136.
Lyons MR, West AE (2011) Mechanisms of specificity in neuronal activity-regulated gene transcription. Progress in Neurobiology 94:259-295.
Maffei A, Turrigiano G (2008) The age of plasticity: developmental regulation of synaptic plasticity in neocortical microcircuits. In: Essence of Memory (Sossin WSLJCCVFBS, ed), pp 211-223.
Maggi L, Scianni M, Branchi I, D'Andrea I, Lauro C, Limatola C (2011) CX(3)CR1 deficiency alters hippocampal-dependent plasticity phenomena blunting the effects of enriched environment. Frontiers in Cellular Neuroscience 5.
Mahadevan LC, Willis AC, Barratt MJ (1991) Rapid histone H3 phosphorylation in response to growth factors, phorbol esters, okadaic acid, and protein synthesis inhibitors. Cell 65:775-783.
Malenka RC (2003) Opinion - The long-term potential of LTP. Nature Reviews Neuroscience 4:923-926.
Malenka RC, Bear MF (2004) LTP and LTD: an embarrassment of riches. Neuron 44:5-21.
Maletic-Savatic M, Malinow R, Svoboda K (1999) Rapid dendritic morphogenesis in CA1 hippocampal dendrites induced by synaptic activity. Science 283:1923-1927.
Malinow R, Malenka RC (2002) AMPA receptor trafficking and synaptic plasticity. Annu Rev Neurosci 25:103-126.
Man HY, Lin JW, Ju WH, Ahmadian G, Liu LD, Becker LE, Sheng M, Wang YT (2000) Regulation of AMPA receptor-mediated synaptic transmission by clathrin-dependent receptor internalization. Neuron 25:649-662.
Martina JA, Bonangelino CJ, Aguilar RC, Bonifacino JS (2001) Stonin 2: An adaptor-like protein that interacts with components of the endocytic machinery. Journal of Cell Biology 153:1111-1120.

Mataga N, Mizuguchi Y, Hensch TK (2004) Experience-dependent pruning of dendritic spines in visual cortex by tissue plasminogen activator. Neuron 44:1031-1041.
Matsuzaki M, Honkura N, Ellis-Davies GC, Kasai H (2004) Structural basis of long-term potentiation in single dendritic spines. Nature 429:761-766.
Matsuzaki M, Ellis-Davies GCR, Nemoto T, Miyashita Y, Iino M, Kasai H (2001) Dendritic spine geometry is critical for AMPA receptor expression in hippocampal CA1 pyramidal neurons. Nature Neuroscience 4:1086-1092.
McCoy CE, MacDonald A, Morrice NA, Campbell DG, Deak M, Toth R, McIlrath J, Arthur JSC (2007) Identification of novel phosphorylation sites in MSK1 by precursor ion scanning MS. Biochemical Journal 402:491-501.
McCutchen ME, Bramham CR, Pozzo-Miller LD (2002) Modulation of neuronal calcium signaling by neurotrophic factors. Int J Dev Neurosci 20:199-207.
McKinney RA, Capogna M, Durr R, Gahwiler BH, Thompson SM (1999) Miniature synaptic events maintain dendritic spines via AMPA receptor activation. Nature Neuroscience 2:44-49.
McMahon HT, Boucrot E (2011) Molecular mechanism and physiological functions of clathrin-mediated endocytosis. Nature Reviews Molecular Cell Biology 12:517-533.
Mendez P, De Roo M, Poglia L, Klauser P, Muller D (2010) N-cadherin mediates plasticity-induced long-term spine stabilization. Journal of Cell Biology 189:589-600.
Messaoudi E, Ying SW, Kanhema T, Croll SD, Bramham CR (2002) Brain-derived neurotrophic factor triggers transcription-dependent, late phase long-term potentiation in vivo. Journal of Neuroscience 22:7453-7461.
Messaoudi E, Kanhema T, Soule J, Tiron A, Dagyte G, da Silva B, Bramham CR (2007) Sustained Arc/Arg3.1 synthesis controls long-term potentiation consolidation through regulation of local actin polymerization in the dentate gyrus in vivo. J Neurosci 27:10445-10455.
Minichiello L (2009) TrkB signalling pathways in LTP and learning. Nature Reviews Neuroscience 10:850-860.
Minichiello L, Calella AM, Medina DL, Bonhoeffer T, Klein R, Korte M (2002) Mechanism of TrkB-mediated hippocampal long-term potentiation. Neuron 36:121-137.
Moga DE, Calhoun ME, Chowdhury A, Worley P, Morrison JH, Shapiro ML (2004) Activity-regulated cytoskeletal-associated protein is localized to recently activated excitatory synapses. Neuroscience 125:7-11.
Morris RGM, Garrud P, Rawlins JNP, Okeefe J (1982) Place navigation impaired in rats with hippocampal lesions. Nature 297:681-683.
Moser E, Moser MB, Andersen P (1993) Spatial- learning impairment parallels the magnitude of dorsal hippocampal- lesions, but is hardly present following ventral lesions. Journal of Neuroscience 13:3916-3925.
Moser EI, Krobert KA, Moser MB, Morris RGM (1998) Impaired spatial learning after saturation of long-term potentiation. Science 281:2038-2042.
Mousavi SA, Malerod L, Berg T, Kjeken R (2004) Clathrin-dependent endocytosis. Biochemical Journal 377:1-16.
Murer MG, Yan Q, Raisman-Vozari R (2001) Brain-derived neurotrophic factor in the control human brain, and in Alzheimer's disease and Parkinson's disease. Progress in Neurobiology 63:71-124.
Nagai T, Ibata K, Park ES, Kubota M, Mikoshiba K, Miyawaki A (2002) A variant of yellow fluorescent protein with fast and efficient maturation for cell-biological applications. Nature Biotechnology 20:87-90.

Nagappan G, Lu B (2005) Activity-dependent modulation of the BDNF receptor TrkB: mechanisms and implications. Trends in Neurosciences 28:464-471.
Nagerl UV, Eberhorn N, Cambridge SB, Bonhoeffer T (2004) Bidirectional activity-dependent morphological plasticity in hippocampal neurons. Neuron 44:759-767.
Nair RR, Tiron A, Bramham CR (2009) SUMOylation-dependent subcellular localization of Arc/Arg3.1 in hippocampal neurons. Society for Neuroscience Abstract Viewer and Itinerary Planner 39.
Neves G, Cooke S, Bliss T (2008) Synaptic plasticity, memory and the hippocampus. Nat Rev Neurosci 1:65-75.
Newey SE, Velamoor V, Govek EE, Van Aelst L (2005) Rho GTPases, dendritic structure, and mental retardation. Journal of Neurobiology 64:58-74.
Nicoll RA (2003) Expression mechanisms underlying long-term potentiation: a postsynaptic view. Philos Trans R Soc Lond B Biol Sci 358:721-726.
Niere F, Wilkerson JR, Huber KM (2012) Evidence for a Fragile X Mental Retardation Protein-Mediated Translational Switch in Metabotropic Glutamate Receptor-Triggered Arc Translation and Long-Term Depression. Journal of Neuroscience 32:5924-5936.
Nimchinsky EA, Yasuda R, Oertner TG, Svoboda K (2004) The number of glutamate receptors opened by synaptic stimulation in single hippocampal spines. Journal of Neuroscience 24:2054-2064.
Nithianantharajah J, Hannan AJ (2006) Enriched environments, experience-dependent plasticity and disorders of the nervous system. Nat Rev Neurosci 7:697-709.
Noguchi J, Matsuzaki M, Ellis-Davies GCR, Kasai H (2005) Spine-neck geometry determines NMDA receptor-dependent Ca2+ signaling in dendrites. Neuron 46:609-622.
Nowak SJ, Corces VG (2004) Phosphorylation of histone H3: a balancing act between chromosome condensation and transcriptional activation. Trends in Genetics 20:214-220.
Numakawa T, Suzuki S, Kumamaru E, Adachi N, Richards M, Kunugi H (2010) BDNF function and intracellular signaling in neurons. Histology and Histopathology 25:237-258.
O'Keefe J, Dostrovs J (1971) Hippocampus as a spatial map- Preliminary evidence from unit activity in freely- moving rat. Brain Research 34:171-&.
OBrien RJ, Kamboj S, Ehlers MD, Rosen KR, Fischbach GD, Huganir RL (1998) Activity dependent modulation of synaptic AMPA receptor accumulation. Neuron 21:1067-1078.
Ohno H (2006) Clathrin-associated adaptor protein complexes. Journal of Cell Science 119:3719-3721.
Ohno H, Stewart J, Fournier MC, Bosshart H, Rhee I, Miyatake S, Saito T, Gallusser A, Kirchhausen T, Bonifacino JS (1995) Interaction of tyrosine‐based sorting signals with clathrin‐associated proteins. Science 269:1872-1875.
Okamoto KI, Nagai T, Miyawaki A, Hayashi Y (2004) Rapid and persistent modulation of actin dynamics regulates postsynaptic reorganization underlying bidirectional plasticity. Nature Neuroscience 7:1104-1112.
Okamura K, Tanaka H, Yagita Y, Saekl Y, Taguchi A, Hiraoka Y, Zeng LH, Colman DR, Miki N (2004) Cadherin activity is required for activity-induced spine remodeling. Journal of Cell Biology 167:961-972.
Okuno H (2011) Regulation and function of immediate-early genes in the brain: Beyond neuronal activity markers. Neuroscience Research 69:175-186.

Okuno H, Akashi K, Ishii Y, Yagishita-Kyo N, Suzuki K, Nonaka M, Kawashima T, Fujii H, Takemoto-Kimura S, Abe M, Natsume R, Chowdhury S, Sakimura K, Worley PF, Bito H (2012) Inverse Synaptic Tagging of Inactive Synapses via Dynamic Interaction of Arc/Arg3.1 with CaMKII beta. Cell 149:886-898.

Oray S, Majewska A, Sur M (2004) Dendritic spine dynamics are regulated by monocular deprivation and extracellular matrix degradation. Neuron 44:1021-1030.

Osterweil E, Wells DG, Mooseker MS (2005) A role for myosin VI in postsynaptic structure and glutamate receptor endocytosis. Journal of Cell Biology 168:329-338.

Ostroff LE, Fiala JC, Allwardt B, Harris KM (2002) Polyribosomes redistribute from dendritic shafts into spines with enlarged synapses during LTP in developing rat hippocampal slices. Neuron 35:535-545.

Owen DJ, Collins BM, Evans PR (2004) Adaptors for clathrin coats: Structure and function. Annual Review of Cell and Developmental Biology 20:153-191.

Owen DJ, Vallis Y, Pearse BMF, McMahon HT, Evans PR (2000) The structure and function of the beta 2-adaptin appendage domain. Embo Journal 19:4216-4227.

Palmer CL, Cotton L, Henley JM (2005a) The molecular pharmacology and cell biology of alpha-amino-3-hydroxy-5-methyl-4-isoxazolepropionic acid receptors. Pharmacological Reviews 57:253-277.

Palmer CL, Lim W, Hastie PGR, Toward M, Korolchuk VI, Burbidge SA, Banting G, Collingridge GL, Isaac JTR, Henley JM (2005b) Hippocalcin functions as a calcium sensor in hippocampal LTD. Neuron 47:487-494.

Palmer MJ, Irving AJ, Seabrook GR, Jane DE, Collingridge GL (1997) The group I mGlu receptor agonist DHPG induces a novel form of LTD in the CA1 region of the hippocampus. Neuropharmacology 36:1517-1532.

Papa M, Bundman MC, Greenberger V, Segal M (1995) Morphological analysis of dendritic spine development in primary cultures of hippocampal- neurons. Journal of Neuroscience 15:1-11.

Park M, Penick EC, Edwards JG, Kauer JA, Ehlers MD (2004) Recycling endosomes supply AMPA receptors for LTP. Science 305:1972-1975.

Park M, Salgado JM, Ostroff L, Helton TD, Robinson CG, Harris KM, Ehlers MD (2006) Plasticity-induced growth of dendritic spines by exocytic trafficking from recycling endosomes. Neuron 52:817-830.

Park S, Park JM, Kim S, Kim JA, Shepherd JD, Smith-Hicks CL, Chowdhury S, Kaufmann W, Kuhl D, Ryazanov AG, Huganir RL, Linden DJ, Worley PF (2008) Elongation factor 2 and fragile X mental retardation protein control the dynamic translation of Arc/Arg3.1 essential for mGluR-LTD. Neuron 59:70-83.

Passafaro M, Nakagawa T, Sala C, Sheng M (2003) Induction of dendritic spines by an extracellular domain of AMPA receptor subunit GluR2. Nature 424:677-681.

Patterson MA, Szatmari EM, Yasuda R (2010) AMPA receptors are exocytosed in stimulated spines and adjacent dendrites in a Ras-ERK-dependent manner during long-term potentiation. Proceedings of the National Academy of Sciences of the United States of America 107:15951-15956.

Patterson SL, Abel T, Deuel TAS, Martin KC, Rose JC, Kandel ER (1996) Recombinant BDNF rescues deficits in basal synaptic transmission and hippocampal LTP in BDNF knockout mice. Neuron 16:1137-1145.

Pearse BMF, Smith CJ, Owen DJ (2000) Clathrin coat construction in endocytosis. Current Opinion in Structural Biology 10:220-228.

Peebles CL, Yoo J, Thwin MT, Palop JJ, Noebels JL, Finkbeiner S (2010) Arc regulates spine morphology and maintains network stability in vivo. Proceedings of the National Academy of Sciences of the United States of America 107:18173-18178.

Perestenko P, Ashby MC, Henley JM (2003) Real-time imaging of alpha-amino-3-hydroxy-5methyl-4-isoxazolepropionic acid receptor (AMPA receptor) movements in neurons. Biochemical Society Transactions 31:880-884.

Peters A, Kaiserman Abramof IR (1969) The small pyramidal neuron of the rat cerebral cortex. The synapses upon dendritic spines. Zeitschrift fur Zellforschung und mikroskopische Anatomie (Vienna, Austria : 1948) 100:487-506.

Peters A, Kaiserma I (1970) Small pyramidal neuron of rat cerebral cortex. Perikaryon, dendrites and spines. American Journal of Anatomy 127:604-619.

Pham TM, Winblad B, Granholm AC, Mohammed AH (2002) Environmental influences on brain neurotrophins in rats. Pharmacology Biochemistry and Behavior 73:167-175.

Pinaud E, Khamlichi AA, Le Morvan C, Drouet M, Nalesso V, Le Bert M, Cogne M (2001a) Localization of the 3' IgH locus elements that effect long-distance regulation of class switch recombination. Immunity 15:187-199.

Pinaud R, Penner MR, Robertson HA, Currie RW (2001b) Upregulation of the immediate early gene arc in the brains of rats exposed to environmental enrichment: implications for molecular plasticity. Brain Res Mol Brain Res 91:50-56.

Pintchovski SA, Peebles CL, Kim HJ, Verdin E, Finkbeiner S (2009) The Serum Response Factor and a Putative Novel Transcription Factor Regulate Expression of the Immediate-Early Gene Arc/Arg3.1 in Neurons. Journal of Neuroscience 29:1525-1537.

Plath N et al. (2006) Arc/Arg3.1 is essential for the consolidation of synaptic plasticity and memories. Neuron 52:437-444.

Pozo K, Goda Y (2010) Unraveling Mechanisms of Homeostatic Synaptic Plasticity. Neuron 66:337-351.

Prasad K, Keen JH (1991) Interaction of Assembly Protein AP-2 and Its Isolated Subunits with Clathrin. Biochemistry 30:5590-5597.

Purves D, Augustine GJ, Fitzpatrick D, Hall WC, LaMantia A-S, White LE (2012) Neuroscience, Fifth Edition: Sinauer Associates, Inc.

Putignano E, Lonetti G, Cancedda L, Ratto G, Costa M, Maffei L, Pizzorusso T (2007) Developmental downregulation of histone posttranslational modifications regulates visual cortical plasticity. Neuron 53:747-759.

Rakhit S, Clark CJ, O'Shaughnessy CT, Morris BJ (2005) N-methyl-D-aspartate and brain-derived neurotrophic factor induce distinct profiles of extracellular signal-regulated kinase, mitogen- and stress-activated kinase, and ribosomal S6 kinase phosphorylation in cortical neurons. Molecular Pharmacology 67:1158-1165.

Ramon y Cajal S (1888) Estructura de los centros nerviosos de las aves. 1:1-10.

Rampon C, Tang YP, Goodhouse J, Shimizu E, Kyin M, Tsien JZ (2000a) Enrichment induces structural changes and recovery from nonspatial memory deficits in CA1 NMDAR1-knockout mice. Nature Neuroscience 3:238-244.

Rampon C, Jiang CH, Dong H, Tang YP, Lockhart DJ, Schultz PG, Tsien JZ, Hu YH (2000b) Effects of environmental enrichment on gene expression in the brain. Proceedings of the National Academy of Sciences of the United States of America 97:12880-12884.

Ramón y Cajal S (1909) Histologie du Système nerveux de l'Homme et des Vertébrés. A Maloine.
Rao VR, Pintchovski SA, Chin J, Peebles CL, Mitra S, Finkbeiner S (2006) AMPA receptors regulate transcription of the plasticity-related immediate-early gene Arc. Nature Neuroscience 9:887-895.
Reul JMHM, Hesketh SA, Collins A, Mecinas MG (2009) Epigenetic mechanisms in the dentate gyrus act as a molecular switch in hippocampus-associated memory formation. Epigenetics 4:434-439.
Rex CS, Lin C-Y, Kramar EA, Chen LY, Gall CM, Lynch G (2007) Brain-derived neurotrophic factor promotes long-term potentiation-related cytoskeletal changes in adult hippocampus. Journal of Neuroscience 27:3017-3029.
Rial Verde EM, Lee-Osbourne J, Worley PF, Malinow R, Cline HT (2006) Increased expression of the immediate-early gene arc/arg3.1 reduces AMPA receptor-mediated synaptic transmission. Neuron 52:461-474.
Richards DA, Mateos JM, Hugel S, de Paola V, Caroni P, Gahwiler BH, McKinney RA (2005) Glutamate induces the rapid formation of spine head protrusions in hippocampal slice cultures. Proceedings of the National Academy of Sciences of the United States of America 102:6166-6171.
Robinson MS (1989) Cloning of cDNAs Encoding Two Related 100-kD Coated Vesicle Proteins (c -Adaptins). Journal of Cell Biology 108:833-842.
Rodriguez A, Ehlenberger DB, Dickstein DL, Hof PR, Wearne SL (2008a) Automated three-dimensional detection and shape classification of dendritic spines from fluorescence microscopy images. PLoS One 3:e1997.
Rodriguez JJ, Davies HA, Errington ML, Verkhratsky A, Bliss TVP, Stewart MG (2008b) ARG3.1/ARC expression in hippocampal dentate gyrus astrocytes: ultrastructural evidence and co-localization with glial fibrillary acidic protein. Journal of Cellular and Molecular Medicine 12:671-678.
Rodriguez JJ, Davies HA, Silva AT, De Souza IEJ, Peddie CJ, Colyer FM, Lancashire CL, Fine A, Errington ML, Bliss TVP, Stewart MG (2005) Long-term potentiation in the rat dentate gyrus is associated with enhanced Arc/Arg3.1 protein expression in spines, dendrites and glia (vol 21, pg 2384, 2005). European Journal of Neuroscience 22:1264-1264.
Rosenzweig MR (1966) Environmental complexity cerebral change and behaviour. American Psychologist 21:321-&.
Rosenzweig MR, Bennett EL (1969) Effects of differential environments on brain weights and enzyme activities in gerbils, rats, and mice. Developmental Psychobiology 2:87-95.
Rosenzweig MR, Bennett EL (1996) Psychobiology of plasticity: Effects of training and experience on brain and behavior. Behavioural Brain Research 78:57-65.
Rosenzweig MR, Krech D, Bennett EL, Diamond MC (1962) Effects of environmental complexity and training on brain chemistry and anatomy: a replication and extension. Journal of comparative and physiological psychology 55:429-437.
Rosenzweig MR, Bennett EL, Hebert M, Morimoto H (1978) Social grouping cannot account for cerebral effects of enriched environments. Brain Res 153:563-576.
Roth TL, Sweatt JD (2009) Regulation of chromatin structure in memory formation. Curr Opin Neurobiol 19:336-342.
Roussignol G, Ango F, Romorini S, Tu JC, Sala C, Worley PF, Bockaert JRL, Fagni L (2005) Shank expression is sufficient to induce functional dendritic spine synapses in aspiny neurons. Journal of Neuroscience 25:3560-3570.

Roze E, Betuing S, Deyts C, Marcon E, Brami-Cherrier K, Pages C, Humbert S, Merienne K, Caboche J (2008) Mitogen- and stress-activated protein kinase-1 deficiency is involved in expanded-huntingtin-induced transcriptional dysregulation and striatal death. FASEB J 22:1083-1093.

Rutherford LC, Nelson SB, Turrigiano GG (1998) BDNF has opposite effects on the quantal amplitude of pyramidal neuron and interneuron excitatory synapses. Neuron 21:521-530.

Santi S, Cappello S, Riccio M, Bergami M, Aicardi G, Schenk U, Matteoli M, Canossa M (2006) Hippocampal neurons recycle BDNF for activity-dependent secretion and LTP maintenance. Embo Journal 25:4372-4380.

Sassone Corsi P, Mizzen CA, Cheung P, Crosio C, Monaco L, Jacquot S, Hanauer A, Allis CD (1999) Requirement of Rsk 2 for epidermal growth factor-activated phosphorylation of histone H3. Science 285:886-891.

Schratt GM, Nigh EA, Chen WG, Hu L, Greenberg ME (2004) BDNF regulates the translation of a select group of mRNAs by a mammalian target of rapamycin-phosphatidylinositol 3-kinase-dependent pathway during neuronal development. Journal of Neuroscience 24:9-Couldn't find page 9.

Scoville WB, Milner B (1957) Loss of recent memory after bilateral hippocampal lesions. Journal of neurology, neurosurgery, and psychiatry 20:11-21.

Selcher JC, Weeber EJ, Christian J, Nekrasova T, Landreth GE, Sweatt JD (2003) A role for ERK MAP kinase in physiologic temporal integration in hippocampal area CA1. Learning & Memory 10:26-39.

Shaywitz AJ, Greenberg ME (1999) CREB: A stimulus-induced transcription factor activated by a diverse array of extracellular signals. Annual Review of Biochemistry 68:821-861.

Shen L, Liang F, Walensky LD, Huganir RL (2000) Regulation of AMPA receptor GluR1 subunit surface expression by a 4.1N-linked actin cytoskeletal association. Journal of Neuroscience 20:7932-7940.

Sheng M, Kim E (2000) The Shank family of scaffold proteins. Journal of Cell Science 113:1851-1856.

Sheng M, Sala C (2001) PDZ domains and the organization of supramolecular complexes. Annual Review of Neuroscience 24:1-29.

Sheng M, Hoogenraad CC (2007) The postsynaptic architecture of excitatory synapses: A more quantitative view. Annual Review of Biochemistry 76:823-847.

Shepherd JD, Huganir RL (2007) The cell biology of synaptic plasticity: AMPA receptor trafficking. Annu Rev Cell Dev Biol 23:613-643.

Shepherd JD, Bear MF (2011) New views of Arc, a master regulator of synaptic plasticity. Nature Neuroscience 14:279-284.

Shepherd JD, Rumbaugh G, Wu J, Chowdhury S, Plath N, Kuhl D, Huganir RL, Worley PF (2006) Arc/Arg3.1 mediates homeostatic synaptic scaling of AMPA receptors. Neuron 52:475-484.

Shi SH, Hayashi Y, Esteban JA, Malinow R (2001) Subunit-specific rules governing AMPA receptor trafficking to synapses in hippocampal pyramidal neurons. Cell 105:331-343.

Shi SH, Hayashi Y, Petralia RS, Zaman SH, Wenthold RJ, Svoboda K, Malinow R (1999) Rapid spine delivery and redistribution of AMPA receptors after synaptic NMDA receptor activation. Science 284:1811-1816.

Shih W, Gallusser A, Kirchhausen T (1995) A clathrin binding site in the hinge of the beta 2 chain of mammalian AP 2 complexes. Journal of Biological Chemistry 270:31083-31090.

Siddoway B, Hou H, Xia H (2013) Molecular mechanisms of homeostatic synaptic downscaling. In, pp 1-7. Neuropharmacology.
Silhol M, Bonnichon V, Rage F, Tapia-Arancibia L (2005) Age-related changes in brain-derived neurotrophic factor and tyrosine kinase receptor isoforms in the hippocampus and hypothalamus in male rats. Neuroscience 132:613-624.
Silva AJ, Stevens CF, Tonegawa S, Wang YY (1992) Deficient hippocampal long-term potentiation in alpha- calcium- calmodulin kinase- II mutant mice. Science 257:201-206.
Silva-Gomez AB, Rojas D, Juarez I, Flores G (2003) Decreased dendritic spine density on prefrontal cortical and hippocampal pyramidal neurons in postweaning social isolation rats. Brain Research 983:128-136.
Simpson J, Kelly JP (2011) The impact of environmental enrichment in laboratory rats-Behavioural and neurochemical aspects. Behavioural Brain Research 222:246-264.
Snyder JS, Kee N, Wojtowicz JM (2001) Effects of adult neurogenesis on synaptic plasticity in the rat dentate gyrus. Journal of Neurophysiology 85:2423-2431.
Soares C, Lee KFH, Nassrallah W, Beique J-C (2013) Differential Subcellular Targeting of Glutamate Receptor Subtypes during Homeostatic Synaptic Plasticity. Journal of Neuroscience 33:13547-13559.
Soloaga A, Thomson S, Wiggin GR, Rampersaud N, Dyson MH, Hazzalin CA, Mahadevan LC, Arthur JSC (2003) MSK2 and MSK1 mediate the mitogen- and stress-induced phosphorylation of histone H3 and HMG-14. Embo Journal 22:2788-2797.
Song I, Huganir RL (2002) Regulation of AMPA receptors during synaptic plasticity. Trends in Neurosciences 25:578-588.
Sorra KE, Harris KM (2000) Overview on the structure, composition, function, development, and plasticity of hippocampal dendritic spines. Hippocampus 10:501-511.
Stein V, House DRC, Bredt DS, Nicoll RA (2003) Postsynaptic density-95 mimics and occludes hippocampal long-term potentiation and enhances long-term depression. Journal of Neuroscience 23:5503-5506.
Stellwagen D, Malenka RC (2006) Synaptic scaling mediated by glial TNF-alpha. Nature 440:1054-1059.
Steward O, Wallace CS, Lyford GL, Worley PF (1998) Synaptic activation causes the mRNA for the IEG Arc to localise selectively near activated postsynaptic sites on dendrites. Neuron 21:741-751.
Steward O, Worley, PF (2001) Selective targetting of newly synthesised Arc mRNA to active synapses requires NMDA receptor activation. Neuron 30:227-240.
Sun Q, Turrigiano GG (2011) PSD-95 and PSD-93 Play Critical But Distinct Roles in Synaptic Scaling Up and Down. Journal of Neuroscience 31:6800-6808.
Sutton MA, Schuman EM (2006) Dendritic protein synthesis, synaptic plasticity, and memory. Cell 127:49-58.
Suzuki A, Stern SA, Bozdagi O, Huntley GW, Walker RH, Magistretti PJ, Alberini CM (2011) Astrocyte-Neuron Lactate Transport Is Required for Long-Term Memory Formation. Cell 144:810-823.
Sweatt JD (1999) Toward a molecular explanation for long-term potentiation. Learning & Memory 6:399-416.
Sweatt JD (2009) Experience-Dependent Epigenetic Modifications in the Central Nervous System. Biological Psychiatry 65:191-197.
Tada T, Sheng M (2006) Molecular mechanisms of dendritic spine morphogenesis. Current Opinion in Neurobiology 16:95-101.

Takei K, Slepnev VI, Haucke V, De Camilli P (1999) Functional partnership between amphiphysin and dynamin in clathrin-mediated endocytosis. Nature Cell Biology 1:33-39.
Tanaka J-i, Horiike Y, Matsuzaki M, Miyazaki T, Ellis-Davies GCR, Kasai H (2008) Protein synthesis and neurotrophin-dependent structural plasticity of single dendritic spines. Science 319:1683-1687.
Tashiro A, Minden A, Yuste R (2000) Regulation of dendritic spine morphology by the Rho family of small GTPases: Antagonistic roles of Rac and Rho. Cerebral Cortex 10:927-938.
Tavosanis G (2011) Dendritic Structural Plasticity. Wiley Periodicals, Inc.
Terashima A, Pelkey KA, Rah J-C, Suh YH, Roche KW, Collingridge GL, McBain CJ, Isaac JTR (2008) An essential role for PICK1 in NMDA receptor-dependent bidirectional synaptic plasticity. Neuron 57:872-882.
Thiagarajan TC, Lindskog M, Tsien RW (2005) Adaptation to synaptic inactivity in hippocampal neurons. Neuron 47:725-737.
Thinakaran G, Koo EH (2008) Amyloid Precursor Protein Trafficking, Processing, and Function. Journal of Biological Chemistry 283:29615-29619.
Thomas GM, Huganir RL (2004) MAPK cascade signalling and synaptic plasticity. Nat Rev Neurosci 5:173-183.
Thomas KR, Capecchi MR (1987) Site directed mutagenesis by gene targeting in mouse embryo derived stem cells. Cell 51:503-512.
Thomson S, Clayton AL, Hazzalin CA, Rose S, Barratt MJ, Mahadevan LC (1999) The nucleosomal response associated with immediate-early gene induction is mediated via alternative MAP kinase cascades: MSK1 as a potential histone H3/HMG-14 kinase. Embo Journal 18:4779-4793.
Tomita S, Chen L, Kawasaki Y, Petralia RS, Wenthold RJ, Nicoll RA, Bredt DS (2003) Functional studies and distribution define a family of transmembrane AMPA receptor regulatory proteins. Journal of Cell Biology 161:805-816.
Traub LM (1997) Clathrin-associated adaptor proteins putting it all together. Trends in Cell Biology 7:43-46.
Turrigiano G (2012) Homeostatic Synaptic Plasticity: Local and Global Mechanisms for Stabilizing Neuronal Function. Cold Spring Harbor Perspectives in Biology 4.
Turrigiano GG (2008) The self-tuning neuron: synaptic scaling of excitatory synapses. Cell 135:422-435.
Turrigiano GG, Nelson SB (2004) Homeostatic plasticity in the developing nervous system. Nat Rev Neurosci 5:97-107.
Turrigiano GG, Leslie KR, Desai NS, Rutherford LC, Nelson SB (1998) Activity-dependent scaling of quantal amplitude in neocortical neurons. Nature 391:892-896.
Tyler WJ, Pozzo-Miller LD (2001) BDNF enhances quantal neurotransmitter release and increases the number of docked vesicles at the active zones of hippocampal excitatory synapses. Journal of Neuroscience 21:4249-4258.
Tyler WJ, Pozzo-Miller L (2003) Miniature synaptic transmission and BDNF modulate dendritic spine growth and form in rat CA1 neurones. Journal of Physiology-London 553:497-509.
Tyler WJ, Alonso M, Bramham CR, Pozzo-Miller LD (2002) From acquisition to consolidation: On the role of brain-derived neurotrophic factor signaling in hippocampal-dependent learning. Learning & Memory 9:224-237.
van Praag H, Kempermann G, Gage FH (2000) Neural consequences of environmental enrichment. Nature Reviews Neuroscience 1:191-198.

van Praag H, Christie BR, Sejnowski TJ, Gage FH (1999) Running enhances neurogenesis, learning, and long term potentiation in mice. Proceedings of the National Academy of Sciences of the United States of America 96:13427-13431.
Verstreken P, Kjaerulff O, Lloyd TE, Atkinson R, Zhou Y, Meinertzhagen IA, Bellen HJ (2002) Endophilin mutations block clathrin-mediated endocytosis but not neurotransmitter release. Cell 109:101-112.
Volkmar FR, Greenough (1972) Rearing complexity affects branching of dendrites in the visual cortex of the rat. Science 176:1445-&.
Von Bohlen O, Halbach O (2009) Structure and function of dendritic spines within the hippocampus. In, p 518—531. Annals of anatomy.
Wallace CS, Lyford GL, Worley PF, Steward O (1998) Differential intracellular sorting of immediate early gene mRNAs depends on signals in the mRNA sequence. Journal of Neuroscience 18:26-35.
Wallace W, Bear MF (2004) A morphological correlate of synaptic scaling in visual cortex. Journal of Neuroscience 24:6928-6938.
Waltereit R, Dammermann B, Wulff P, Scafidi J, Staubli U, Kauselmann G, Bundman M, Kuhl D (2001) Arg3.1/Arc mRNA induction by Ca2+ and cAMP requires protein kinase A and mitogen activated protein kinase/extracellular regulated kinase activation. Journal of Neuroscience 21:5484-5493.
Wang G, Gilbert J, Man H-Y (2012) AMPA Receptor Trafficking in Homeostatic Synaptic Plasticity: Functional Molecules and Signaling Cascades. Neural Plasticity.
Wang Y, Zheng F, Zhou X, Sun Z, Wang H (2009) Converging signal on ERK1/2 activity regulates group I mGluR-mediated Arc transcription. Neurosci Lett 460:36-40.
Wang YT, Linden DJ (2000) Expression of cerebellar long-term depression requires postsynaptic clathrin-mediated endocytosis. Neuron 25:635-647.
Waung MW, Pfeiffer BE, Nosyreva ED, Ronesi JA, Huber KM (2008) Rapid translation of Arc/Arg3.1 selectively mediates mGluR-dependent LTD through persistent increases in AMPAR endocytosis rate. Neuron 59:84-97.
Wearne SL, Rodriguez A, Ehlenberger DB, Rocher AB, Henderson SC, Hof PR (2005) New techniques for imaging, digitization and analysis of three-dimensional neural morphology on multiple scales. Neuroscience 136:661-680.
Wenthold RJ, Petralia RS, Blahos J, Niedzielski AS (1996) Evidence for multiple AMPA receptor complexes in hippocampal CA1/CA2 neurons. Journal of Neuroscience 16:1982-1989.
Wierenga CJ, Ibata K, Turrigiano GG (2005) Postsynaptic expression of homeostatic plasticity at neocortical synapses. J Neurosci 25:2895-2905.
Wigge P, McMahon HT (1998) The amphiphysin family of proteins and their role in endocytosis at the synapse. Trends in Neurosciences 21:339-344.
Wiggin GR, Soloaga A, Foster JM, Murray-Tait V, Cohen P, Arthur JSC (2002) MSK1 and MSK2 are required for the mitogen-and stress-induced phosphorylation of CREB and ATF1 in fibroblasts. Molecular and Cellular Biology 22.
Woolley CS, Gould E, Frankfurt M, McEwen BS (1990) Naturally- occurring fluctuation in dendritic spine density on adult hippocampal pyramidal neurons. Journal of Neuroscience 10:4035-4039.
Wu J, Petralia RS, Kurushima H, Patel H, Jung M-y, Volk L, Chowdhury S, Shepherd JD, Dehoff M, Li Y, Kuhl D, Huganir RL, Price DL, Scannevin R,

Troncoso JC, Wong PC, Worley PF (2011) Arc/Arg3.1 regulates an endosomal pathway essential for activity-dependent β-amyloid generation. Cell 28:615-628.
Xie L, Korkmaz KS, Braun K, Bock J (2013) Early life stress-induced histone acetylations correlate with activation of the synaptic plasticity genes Arc and Egr1 in the mouse hippocampus. Journal of Neurochemistry 125:457-464.
Xie Z, Huganir RL, Penzes P (2005) Activity-dependent dendritic spine structural plasticity is regulated by small GTPase Rap1 and its target AF-6. Neuron 48:605-618.
Xu B, Karayiorgou M, Gogos JA (2010) MicroRNAs in psychiatric and neurodevelopmental disorders. Brain Research 1338:78-88.
Yamamoto Y, Verma UN, Prajapati S, Kwak YT, Gaynor RB (2003) Histone H3 phosphorylation by IKK-alpha is critical for cytokine-induced gene expression. Nature 423:655-659.
Yamazaki M, Ohno-Shosaku T, Fukaya M, Kano M, Watanabe M, Sakimura K (2004) A novel action of stargazin as an enhancer of AMPA receptor activity. Neuroscience Research 50:369-374.
Yin Y, Edelman GM, Vanderklish PW (2002) The brain-derived neurotrophic factor enhances synthesis of Arc in synaptoneurosomes. Proceedings of the National Academy of Sciences of the United States of America 99:2368-2373.
Ying SW, Futter M, Rosenblum K, Webber MJ, Hunt SP, Bliss TV, Bramham CR (2002) Brain-derived neurotrophic factor induces long-term potentiation in intact adult hippocampus: requirement for ERK activation coupled to CREB and upregulation of Arc synthesis. J Neurosci 22:1532-1540.
Yudowski GA, Puthenveedu MA, Leonoudakis D, Panicker S, Thorn KS, Beattie EC, von Zastrow M (2007) Real-time imaging of discrete exocytic events mediating surface delivery of AMPA receptors. Journal of Neuroscience 27:11112-11121.
Yuste R, Bonhoeffer T (2001) Morphological changes in dendritic spines associated with long-term synaptic plasticity. Annual Review of Neuroscience 24:1071-1089.
Yuste R, Majewska A, Holthoff K (2000) From form to function: calcium compartmentalization in dendritic spines. Nature Neuroscience 3:653-659.
Zafra F, Castrén E, Thoenen H, Lindholm D (1991) Interplay between glutamate and y-aminobutyric acid transmitter systems in the physiological regulation of brain- derived neurotrophic factor and nerve growth factor synthesis in hippocampal neurons. Proc Natl Acad Sci USA 88:10037-10041.
Zassadowski F, Rochette-Egly C, Chomienne C, Cassinat B (2012) Regulation of the transcriptional activity of nuclear receptors by the MEK/ERK1/2 pathway. Cellular Signalling 24:2369-2377.
Zhang B, Zelhof AC (2002) Amphiphysins: Raising the BAR for synaptic vesicle recycling and membrane dynamics. Traffic 3:452-460.
Zhang HY, Webb DJ, Asmussen H, Niu S, Horwitz AF (2005) A GIT1/PIX/Rac/PAK signaling module regulates spine morphogenesis and synapse formation through MLC. Journal of Neuroscience 25:3379-3388.
Zhou Q, Homma KJ, Poo MM (2004) Shrinkage of dendritic spines associated with long-term depression of hippocampal synapses. Neuron 44:749-757.
Zhu JJ, Qin Y, Zhao M, Van Aelst L, Malinow R (2002) Ras and Rap control AMPA receptor trafficking during synaptic plasticity. Cell 110:443-455.
Zhu YH, Pak D, Qin Y, McCormack SG, Kim MJ, Baumgart JP, Velamoor V, Auberson YR, Osten P, van Aelst L, Sheng M, Zhu JJ (2005) Rap2-JNK

removes synaptic AMPA receptors during depotentiation. Neuron 46:905-916.
Ziff EB (2007) TARPs and the AMPA receptor trafficking paradox. Neuron 53:627-633.
Zucker RS, Regehr WG (2002) Short-term synaptic plasticity. Annual Review of Physiology 64:355-405.

9.

Appendix 1

See pages 228-240 for attached paper.